INFORMATION TO USERS

This manuscript has been reproduced from the microfilm master. UMI films the text directly from the original or copy submitted. Thus, some thesis and dissertation copies are in typewriter face, while others may be from any type of computer printer.

The quality of this reproduction is dependent upon the quality of the copy submitted. Broken or indistinct print, colored or poor quality illustrations and photographs, print bleedthrough, substandard margins, and improper alignment can adversely affect reproduction.

In the unlikely event that the author did not send UMI a complete manuscript and there are missing pages, these will be noted. Also, if unauthorized copyright material had to be removed, a note will indicate the deletion.

Oversize materials (e.g., maps, drawings, charts) are reproduced by sectioning the original, beginning at the upper left-hand corner and continuing from left to right in equal sections with small overlaps.

ProQuest Information and Learning
300 North Zeeb Road, Ann Arbor, MI 48106-1346 USA
800-521-0600

THE 1996 ERUPTION OF KARYMSKY VOLCANO, KAMCHATKA: DETAILED PETROLOGICAL STUDY OF A SINGLE BASALT-TRIGGERED ERUPTION CYCLE

A

THESIS

Presented to the Faculty

of the University of Alaska Fairbanks

in Partial Fulfillment of the Requirements

for the Degree of

DOCTOR OF PHILOSOPHY

By

Pavel Edgarovich Izbekov

Fairbanks, Alaska

December 2002

THE 1996 ERUPTION OF KARYMSKY VOLCANO, KAMCHATKA: DETAILED PETROLOGICAL STUDY OF A SINGLE BASALT-TRIGGERED ERUPTION CYCLE

By

Pavel Edgarovich Izbekov

RECOMMENDED:

Advisory Committee Chair

Department Head

APPROVED:

Dean, College of Science, Engineering and Mathematics

Dean of the Graduate School

12-12-02

Date

Abstract

The current activity at Karymsky Volcano, Kamchatka, began on January 2, 1996, with simultaneous eruptions from two vents located 6 km apart: Karymsky summit vent, which erupted andesite, and a newly formed vent within Academy Nauk caldera, which erupted basalt. Detailed petrologic study of volcanic ash, bombs, and lavas of Karymsky erupted during 1996-1999 provides evidence for basaltic replenishment at the beginning of the eruptive cycle, as well as a record of compositional variations within the Karymsky magma reservoir induced by basaltic recharge.

Shortly after the beginning of eruption the composition of matrix glasses of Karymsky tephra became more mafic, and then, within two months, gradually returned to its original state and remained almost constant the following three years. Further evidence for basaltic replenishment includes the presence of xenocrysts of basaltic origin in andesites erupted from Karymsky. A conspicuous portion of plagioclase phenocrysts in Karymsky andesites contain calcic cores, the composition and texture of which mimic those in Academy Nauk basalt. The earlier portions of andesite also contain rare xenocrysts of olivine, which occur as relicts in plagioclase-pyroxene aggregates. The compositions of olivine xenocrysts match those of olivines in Academy Nauk basalt. Compositional variations of glass and the presence of xenocrysts indicate that Karymsky magma reservoir was recharged by basalt at the onset of the 1996 eruptive cycle. The mixing of basalt with host andesite was both thorough and rapid, perhaps due to a modest contrast in temperature, viscosity, and density between the magmas.

Academy Nauk basalt contains granophyre xenoliths, the whole-rock compositions of which are identical to that of dacites erupted twice at 40,000 yr. BP and 7,900 yr. BP, and formed the neighboring Academy Nauk and Karymsky calderas. According to hydrothermal experiments and petrologic observations both dacites last equilibrated at 3-4 km depth. At the same depth granophyre phase assemblage is reproduced by isobaric crystallization of dacites, thus implying that the granophyres represent a crystallized silicic reservoir, which produced dacites 40,000 yr. BP and formed Academy Nauk caldera. In 1996 this crystallized body was sampled by ascending basalt, which erupted in the northern part of the caldera.

Table of Contents

List of Figures

List of Tables

List of Appendices

Acknowledgments

This thesis would never have been completed without guidance, support and encouragements from many people. First and foremost, I thank Prof. John Eichelberger, who introduced me to the exciting world of volcanoes, taught to see dynamics frozen in rocks, and continuously supplied enthusiasm and energy, both through encouragement and inspiring discussions.

Dr. Boris Ivanov, the Director of the Institute of Volcanic Geology and Geochemistry in Petropavlovsk-Kamchatsky (IVGG), introduced me to the most active, interesting and beautiful volcano of Kamchatka – Karymsky. He helped tremendously by providing his expertise and samples, and by supporting my field work through his grants funded by Russian Foundation for Basic Research.

I was very fortunate that at the beginning of my study, Prof. James Gardner arrived in Fairbanks and established his experimental laboratory. From him I learned the basics of the art of petrologic experiments, from welding capsules to interpreting the results. His thorough, scrupulous approach in every thing he does was really inspiring and motivating.

Prof. Ken Severin taught me to understand an electron microprobe, its wishes and complaints. Although many things were beyond my understanding, this helped me to become a "happy microprobe user", i.e. the person, who peacefully co-exists with the microprobe, obtains good quality data, and does not break the instrument very often. I appreciate all the time that Ken spent with me solving the technical problems, discussing the results of analyses and helping with sample preparation.

Prof. David Stone at University of Alaska Fairbanks and Prof. Leonid Parfenov at Yakutsk Institute of Geosciences (YIG) made the continuation of my education at UAF happen. They both provided me with invaluable advice and logistical support at the beginning of my study in Alaska. The indigenous "British" humor of David Stone made many of my dark and cold days in Alaska truly shining.

Working in the team of scientists at the Alaska Volcano Observatory (AVO) was a great advantage, which I used in all aspects of my study. Dr. Chris Nye was a member of my graduate committee and provided his expertise in whole-rock analyses and sample preparation. Dr. Tom Miller shared his broad and deep knowledge of both Kamchatkan volcanoes and Kamchatkan volcanologists, which was extremely helpful. Dr. Ken Dean, the Leader of the Remote Sensing Group at AVO, where I worked, introduced me to image analysis, and was patient and understanding, when greater amounts of my time was devoted to petrology, and not to remote sensing. Dr. Jonathan Dehn shared with me his ideas in physical volcanology, which were always very inspiring. Discussions with Dr. Jessica Faust-Larsen, Scott Dreher, Darren Chertkoff, Peter Stelling, Michell Coombs, Brandon Browne and many others were interesting, fruitful and stimulating.

Prof. Thomas Vogel and Dr. Lina Patino at Michigan State University provided me with high-quality trace element analyses of plagioclase phenocrysts. They both helped tremendously in acquiring and interpreting the data, as well as publishing the results of the plagioclase study.

I thank my Russian colleagues, who helped me in many aspects during the course of the study. Dr. Yaroslav Muravyev and Dr. Vladimir Budnikov of the Institute of

Volcanology (IV), Petropavlovsk-Kamchatsky provided me with ash samples from the beginning of the 1996 eruption of Karymsky. Dr. Alexander Maximov of IVGG helped enormously during my field trips to Karymsky and staying in Petropavlovsk-Kamchatsky. Conversations with Drs. Elena Gribb of IV, Alexander and Marina Belousov of IVGG, Vladimir Shkodzinsky of YIG were always interesting, stirring and motivating.

The overwhelming part of the financial support for this study was provided by Volcano Hazards Program of the U.S. Geological Survey through the Alaska Volcano Observatory. A travel grant from the Graduate School of UAF helped to cover my participation in the 2000 Fall meeting of the American Geophysical Meeting.

I thank my family – my father Edgar Izbekov, mother Lilia Izbekova, my wife Ludmila and my son Dima – for their unwavering support during the entire period of my study in Alaska.

Chapter 1. Introduction

The history of the Earth as recorded in rocks suggests that volcanic processes are among those natural phenomena that shape the surface of our planet. Chronicles of the human civilization demonstrate plentiful evidence of drastic and often dramatic effects of volcanic eruptions on the environment and, particularly, on our society. Although the last few decades have seen a greatly improved understanding of different aspects of volcanic processes, many uncertainties still remain. Every new eruption, however, brings new invaluable information, which helps to understand volcanic processes and to mitigate volcanic hazards.

The simultaneous eruption of Karymsky and Academy Nauk in 1996 is no exception. It presented a broad range of fundamental petrologic questions, from which one is the most intriguing: whether the eruption of andesites from the central vent of Karymsky was triggered by an influx of basalt, which erupted in the northern part of Academy Nauk caldera. The timing of the eruptions, the location of eruptive vents on the same active fault, and ground deformations in-between vents suggest that basalt ascended as a dike along the active longitudinally oriented fault and intercepted the crustal reservoir of Karymsky (Eichelberger and Izbekov, 2000).

This hypothesis can be tested using two independent petrologic approaches. First, if the basaltic replenishment indeed occurred, its fingerprints should be found in the form of xenocrysts of basaltic origin and in zoning of phenocrysts in Karymsky andesites. The availability of basaltic samples is a great advantage, because it allows a direct comparison of mineral phases in andesite and basalt. Second, if basaltic recharge occurred, it should

have affected the whole-rock composition of Karymsky magma, as well as the composition of its melt. The continuous eruption of Karymsky volcano provided an excellent opportunity for monitoring the composition of its reservoir by studying the pyroclastic rocks, which erupted and were sampled sequentially during 1996-1999.

The first chapter of this thesis presents the results of a petrologic study aimed directly at testing whether the Karymsky andesites contain fingerprints of the basaltic recharge, which supposedly occurred at the onset of the current eruptive cycle. The chapter describes the details of the eruption, the composition of erupted products, and the variations in tephra glass composition during the course of eruption. This chapter also provides estimates of temperatures and physical properties of Karymsky andesites and Academy Nauk basalts, which are crucial for testing the possibility of magma mixing.

The second chapter describes in greater detail the results of a comparative study of Karymsky and Academy Nauk plagioclase. Because the equilibrium composition of plagioclase in the andesite is significantly different from that in basalt, plagioclase xenocrysts of basaltic origin should be relatively easy to find in the andesite and serve as evidence for basaltic replenishment. Using plagioclase is especially appealing because it is the most abundant mineral phase in both Karymsky and Academy Nauk magmas, and because the growth rate of plagioclases is relatively well constrained experimentally.

The third chapter addresses another interesting question posed by eruption of Academy Nauk and Karymsky in 1996: do the xenoliths of granophyres, which were found in basalts, represent a crystallized silicic reservoir that produced a voluminous caldera-forming eruption ca. 40,000 yr BP? Hydrothermal experiments and petrologic

observations are used in this section for estimating pre-eruptive pressures and temperatures of caldera-forming dacites and answering this question.

All three chapters were originally written as stand-alone manuscripts, which have been or will be submitted for publication. The first paper is co-authored with Drs. John Eichelberger and Boris Ivanov. They also are my coauthors on the second paper, as well as Drs. Thomas Vogel and Lina Patino. The third paper is co-authored with Drs. James Gardner and John Eichelberger. In each case my coauthors helped tremendously by providing guidance, assisting with experiments, acquisition of analyses, and editing. As the first author I wrote each manuscript and contributed the overwhelming portion of work.

Chapter 2. 1996 Eruption of Karymsky volcano, Kamchatka: historical record of basaltic replenishment of an andesite reservoir*

ABSTRACT

The simultaneous eruption of andesite from Karymsky volcano and basalt from a vent 6 km away appear to provide a case of mafic recharge of an andesite reservoir where the time of recharge is exactly known and direct samples of the recharging magma are in hand. The explosive phreato-magmatic eruption of basalt terminated in less than 24 hours, whereas andesite erupted continuously during the following four years. Detailed petrologic study of volcanic ash, bombs and lavas of Karymsky andesite erupted during 1996-1999 provides evidence for basaltic replenishment at the beginning of the eruptive cycle, as well as a record of compositional variations within the Karymsky magma reservoir induced by basaltic recharge. Shortly after the beginning of eruption the composition of matrix glass of Karymsky tephra became more mafic and then, within two months, gradually returned to its original state and remained almost constant for the following three years. Further evidence for basaltic replenishment is the presence of xenocrysts of basaltic origin in andesites of Karymsky. A conspicuous portion of plagioclase phenocrysts in Karymsky andesites contains calcic cores, with composition and texture mimicking those of plagioclases in Academy Nauk basalts. In addition to plagioclase, the earlier portions of andesite contain rare xenocrysts of olivine, which occur as relicts in plagioclase-pyroxene aggregates. The composition of olivine

* Prepared for submission to the *Journal of Petrology* under the same title with authors Pavel E. Izbekov, John C. Eichelberger and Boris V. Ivanov

xenocrysts matches that of olivines in Academy Nauk basalts. The sequence of events appears to be: (1) injection of basaltic magma into the Karymsky chamber with immediate compensating expulsion of chamber magma from the Karymsky central vent, (2) direct mixing of magmatic melts and dispersal of associated phenocrysts, so that newly mixed magma appear at the vent within two months, (3) re-establishing of thermal equilibrium within the reservoir, with resulting crystallization in new liquid returning melt composition to "normal" and forming rims on inherited calcic plagioclase, and (4) resorption of dispersed olivine xenocrysts. Taken together, these findings indicate that Karymsky magma reservoir was recharged by basalt at the onset of the 1996 eruptive cycle. The rapidity and thoroughness of mixing of basalt with host andesite most likely reflects the modest contrast in temperature, viscosity, and density between the magmas.

INTRODUCTION

Basaltic replenishments transport heat and mass to long-lived crustal reservoirs of volcanoes and trigger their eruptions. Petrologic evidence for this process includes the presence of mafic enclaves and phenocryst zoning in many arc magmas (e.g. Eichelberger, 1975; Singer et al., 1995; Pallister et al., 1996; Davidson et al., 2001). Although the fingerprints of magma mixing – the major result of replenishment – are commonly found in volcanic rocks, the magmas produced by mixing may strongly vary by degree of homogenization both in space and time. In some cases, e.g. Soufrière Hills, Montserrat (Murphy et al., 2000), the presence of abundant mafic enclaves and non-equilibrium phenocryst assemblages in erupted rocks demonstrate that mixing of mafic

and silicic end-members had not advanced to complete homogenization prior to eruption. In others, e.g. Arenal, Costa Rica (Streck et al., 2002), the erupted rocks are homogeneous and the record of basaltic replenishment is preserved only in phenocrysts.

Several approaches have been used to explain this difference. Both physical and numerical models were offered to test the possibility of mixing and to describe its mechanisms (e.g., Sparks and Marshall, 1986; Snyder, 1996; Bergantz and Breidenthal, 2001). The best way to validate such models is to compare their predictions with records of actual basaltic replenishment events, where the dynamics of mixing can be inferred. Unfortunately, such records are limited to a few well-documented historical eruptions (Nakamura, 1995; Pallister et al., 1996; Streck et al., 2002).

The eruption of Karymsky volcano, Kamchatka, which started in 1996 with the simultaneous eruption of andesite and basalt from neighboring vents and continues at present, perhaps is an additional and especially illustrative case, from which the dynamics of mixing of andesite and basalt can be inferred. This paper presents new results of our petrologic study of lava, volcanic bombs, and tephra erupted by Karymsky volcano in 1996-1999. These results strengthen and extend findings reported earlier (Eichelberger and Izbekov, 2000; Izbekov et al., 2002). We argue that 1996 eruption of Karymsky was triggered by basaltic recharge using compositional variations of groundmass glass, presence of xenocrysts, and with support of eruption chronology and geological observations,. Homogeneity of Karymsky andesite erupted two months after the beginning of eruption suggests that mixing was fast and efficient, perhaps due to a modest contrast in temperatures and physical properties between basalt and andesite.

GEOLOGIC SETTING

Karymsky volcano and Academy Nauk caldera are located in the central part of the Eastern Volcanic Front of Kamchatka, which formed where the subducting Pacific plate reaches a depth of approximately 120 km (Gorbatov et al., 1997). With centers 9 km apart, both Karymsky and Academy Nauk belong to the greater Karymsky volcanic center – a group of volcanoes, calderas, and maars – constructed since the Pliocene (Masurenkov, 1980). Within this center, Karymsky and Academy Nauk belong to a chain of eruptive vents, whose location is thought to be controlled by a local North-South trending fault (Fig. 2.1). Magmas erupted during the Holocene along this fault varied in composition from basalt to rhyolite, with andesites and dacites being the most voluminous. Numerous hot springs and geysers are currently active along the fault in the vicinity of Karymsky and Academy Nauk.

Karymsky volcano

Karymsky is a stratovolcano that occupies most of a 5-km-diameter caldera. The caldera formed ca. 7,900 yr. BP as a result of a catastrophic eruption that produced 5-7 km^3 of dacite (Braitseva and Melekestsev, 1991). The cone of Karymsky was built by lavas, pyroclastic flows, and ash-fall deposits throughout the last 5,300 years, interrupted by a period of extended repose between ca. 2800 and 500 yr BP. In the 20^{th} century, Karymsky has been in a state of nearly continuous explosive and effusive activity during 1908-1915, 1921-1925, 1929-1935, 1943-1947, 1952-1967, 1970-1982 (Ivanov, 1970;

Tokarev, 1989). The most recent eruptive cycle of Karymsky started in January 1996 and continues at present.

The eruptive behavior of Karymsky is typically confined to a Strombolian type of activity with frequent, yet remarkably regular explosions that send ash and gas to the altitude up to 2-3 km above the vent. Continuous effusion of blocky lava flows often occurs at the same time and from the same vent as the explosions. Eruptive activity is usually more vigorous and regular at the beginning of an eruptive cycle, whereas closer to the end of the cycle eruptions become sporadic. The total volume of andesites erupted during a single cycle usually does not exceed 0.1 km^3 (Tokarev, 1989; Ivanov et al., 1991).

During the last 500 years Karymsky produced andesites of remarkably constant composition with a small range of 59-62 wt.% SiO_2. The andesites are homogeneous and almost never contain xenoliths. Phenocryst phases include plagioclase and lesser amounts of clinopyroxene, orthopyroxene, and magnetite. In addition, rare olivine xenocrysts ($Fo_{\sim 0.75}$) have been reported in banded lavas and volcanic bombs erupted at the beginning of the 1970-1982 eruptive cycle (Ivanov, 1996).

Seismic data collected by a temporary local network during March-December, 1985, indicated that hypocenters of volcano-tectonic earthquakes were clustered around a cylindrical zone that starts at 4 km below Karymsky and reaches a diameter of ca. 5 km at 6.5 km depth. The absence of earthquakes inside this zone suggests the presence of magma and thus the hypocenters may define the location of the roof of a Karymsky magma reservoir (Shirokov et al., 1988).

Academy Nauk caldera

Academy Nauk caldera is centered approximately 9 km south from Karymsky (Fig. 2.1). It was formed by a voluminous eruption of dacites and collapse of Academy Nauk volcano ca. 28,000-48,000 years ago. The age of the caldera is based on the fission-track study of obsidian xenoliths from the basal plinian fall layer (Masurenkov, 1980). At present the caldera is occupied by Karymsky Lake, which reaches ca. 60 meters deep (Ushakov and Fazlullin, 1998).

Since the caldera-forming event, activity within the caldera was confined to phreato-magmatic eruptions that produced small volumes of basalt at least twice since 5000 yr. BP (Braitseva, 1998; Belousov and Belousova, 2001). These eruptions formed distinctive maars in the northern and in the southern parts of the caldera.

1996 ERUPTION OF KARYMSKY AND ACADEMY NAUK

The first signs of unrest at Karymsky were observed in March 1995, after a 13-year period of dormancy, when the number of volcano-tectonic earthquakes at Karymsky and Academy Nauk began to increase. On January 1, 1996, the number of seismic events rose abruptly and in 4 hours culminated in a 6.6M earthquake. The epicenter of the mainshock was located 17 km south of Karymsky at ca. 10-km depth, on the lateral extension of the fault that connects Karymsky and Academy Nauk (Gordeev et al., 1998; Zobin and Levina, 1998).

Several hours after the mainshock, on January 2, the eruption of Karymsky began with a steady gas-and-ash emission from the summit vent forming a 3000-meter-high eruptive cloud trailing to the east from the volcano. Approximately 12 hours later, a separate eruption started from a new vent formed in the northern part of the Academy Nauk caldera (Belousov and Belousova, 2001). During the following eighteen hours the two vents erupted simultaneously: the summit vent of Karymsky produced a continuous ash plume, while a newly formed vent in the northern part of Academy Nauk caldera generated intermittent phreato-magmatic blasts, sending volcanic bombs, ash, and vapor to the altitude of 8000 m. Eighteen hours after its onset the eruption of Academy Nauk ceased, whereas Karymsky erupted continuously until 2000.

During the first six weeks, the eruptive style of Karymsky fluctuated significantly. Karymsky produced several pyroclastic flows associated with large explosions and the rate of explosions varied from 2-3 per day to 4-6 per hour. After February 1996, however, the eruption became more regular, characterized by 4-6 explosions per hour, sending ash plumes to the altitude of 400-900 m above the vent (Muravyev et al., 1998; Johnson et al., 1998). In addition to explosions, a lava flow was almost continually active on the western flank of the volcano. The activity remained constant until early 1999, when the eruption became sporadic, slowly declined, and ceased by mid 2000. In November 2001, however, it resumed and currently continues with the same remarkable regularity of explosions.

Omitting the details of the eruption, which can be found in Muravyev et al. (1998) and Belousov and Belousova (2001), we emphasize the main points relevant to this study.

First, the eruption was preceded by a strong 6.6M earthquake on the fault that hosts the vents, which was probably not coincidental. Whether the earthquake triggered eruption or, alternatively, the magma ascent facilitated the release of accumulated strain is still disputed (Zobin and Levina, 1998; Gordeev et al., 1998).

Second, significant ground deformation occurred between eruptive vents. Cracks as long as 700 m were formed parallel to the N-S fault (Leonov, 1998). The area of major ground cracks coincides with maximum E-W extension, reaching an amplitude of 2.33 m (Maguskin et al., 1998). Extension between eruptive vents likely occurred gradually rather than catastrophically, as no damage was done to a wood-frame building located nearby. The occurrence of gradual extension suggests that a basaltic dike propagated along the active fault. Such a dike could have intercepted a crustal magma system beneath Karymsky, and indeed, measurable extension occurred north of the Karymsky vent as well (Maguskin et al., 1998).

Third, the magmas simultaneously erupted from neighboring vents had different bulk compositions. Academy Nauk vent erupted basalt (51.8 wt.% SiO_2), while Karymsky summit vent erupted andesite (62.4 wt.% SiO_2). The latter was almost identical to those erupted during previous periods of activity (Ivanov, 1996). The 1996 magmas were compositionally distinct and lacked evidence of mechanical mixing, i.e., no mafic enclaves were found in andesites, nor were bands or xenoliths of andesite found in basalt, and no intermediate compositions were erupted.

Considered together, the peculiarities of the 1996 eruption of Karymsky and Academy Nauk are consistent with the hypothesis that a basalt dike was injected along

the pre-existing active fault, intersected a well-stirred, crustal reservoir beneath Karymsky, and triggered its eruption. The eruption of basalt was fortunate, because it provided samples of the hypothetical mixing end-member, thereby allowing us to test this hypothesis by direct comparison of phenocrysts in the basalt with those in erupted andesites.

SAMPLES AND ANALYTICAL METHODS

Volcanic ash, bombs, and lava flows of the 1996-1999 period of activity of Karymsky, as well as pyroclastics of Academy Nauk center, were sampled during 1997, 1998, and 1999 summer field work. Tephra samples of the January-July 1996 period of eruption were kindly supplied by Dr. Budnikov (IV RAS). Most volcanic ash samples were collected at Karymsky Volcano Station, ~3.6 km from the crater, and represent cumulative ash falls produced by discrete explosions of Karymsky during 0.5-4 hours. Dr. Muravyev (IV RAS) provided tephra samples of the 1996-1997 winter period, which were extracted from snow cores. Dr. Ivanov (IVGG RAS) provided samples of the previous period of activity of Karymsky (1970-1982). Availability of samples of Karymsky pyroclasts versus time of eruption is shown in figure 2.2.

Whole-rock compositions of volcanic bombs and lavas (Table 2.1) were completed at Washington State University using X-ray fluorescence spectrometry (major element oxides, Ni, Cr, V, Zr, Ga, Cu and Zn) and inductively coupled plasma mass spectrometry (Rare Earth Elements (REE), Ba, Th, Nb, Y, Hf, Ta, U, Pb, Rb, Cs, Sr and Sc). Analytical procedures and uncertainties are discussed in Nye et al. (1994). Modes of

minerals and glass were determined by point counting (1000 points) using a petrographic microscope and automated stage.

Ash particles were mounted into epoxy, polished, and carbon-coated to a thickness of 250 Å. Matrix glasses of tephras were analyzed for major elements at the University of Alaska Fairbanks using a Cameca SX-50 electron microprobe (EPMA), which is equipped with four wavelength-dispersive and one energy-dispersive spectrometer. The analytical conditions for analyses of glass were 15 kV accelerating voltage, 10 nA beam current, and 10 μm defocused electron beam. Na and Al were analyzed first in order to reduce the effect of volatilization. All analyses of tephra glass were completed in a single uninterrupted 72-hour session; the quality of data was monitored by repeated analyses of the internal standard Old Crow rhyolite tephra. At least five back scattered electron (BSE) images of different tephra particles within the same tephra sample were subsequently acquired in raster mode at 15 kV and 50-150 nA beam current. The microlite content in tephra was determined from BSE images using MicroImage software (Advanced Microbeam Co).

Samples of volcanic bombs and lavas were prepared as polished thin-sections, examined using a petrographic microscope, and carbon-coated. The analytical conditions for mineral analyses were similar to the glass analyses (15 kV, 10 nA), but a 1-3 μm focused electron beam was used. BSE images of plagioclase phenocrysts were acquired at 15 kV and 50-150 nA beam current.

Representative plagioclase phenocrysts from Academy Nauk basalt and Karymsky andesite were chosen for electron microprobe traverses from which more than

1600 major element analyses were obtained along core-to-rim traverses in 25 crystals. Sr and Ba contents in multiple spots along microprobe traverses of representative plagioclase phenocrysts were analyzed by using a Micromass Plasma laser-ablation inductively coupled plasma mass spectrometer (LA-ICP-MS) equipped with a Cetac LSX 200 laser-ablation system at Michigan State University. The 266 nm Nd:YAG laser was focused to a 25 μm spot size. The beam propagated into the sample with a rate of 3 μm/s. Concentrations of Sr and Ba were calculated by using peak intensities of ^{88}Sr, ^{138}Ba, and ^{44}Ca calibrated against a NIST 612 glass standard and EPMA determinations of Ca in analyzed spots as outlined in Norman et al. (1996).

PETROGRAPHY AND MINERALOGY OF ACADEMY NAUK BASALT

In less than 18 hours the eruption of Academy Nauk vent produced ca. 0.04 km^3 of volcanic bombs and ash, forming a tuff ring in the northern part of the Academy Nauk caldera (Muravyev et al., 1998). The predominant product of the eruption is porphyric basalt, the whole-rock composition of which is close to the composition of basalts erupted during similar events since 5000 yr. BP (Table 2.1). The basalt contains conspicuous but volumetrically minor silicic xenoliths: granophyres, granites, rhyolite pumices, and altered silicic tuffs (Grib, 1998; Izbekov et al., submitted). The xenoliths often show signs of disintegration and assimilation by basalt, such as melting and mechanical blending.

Basaltic bombs are highly vesicular (20-40 vol. % porosity) and phenocryst-rich, containing 40-45 vol. % phenocrysts of plagioclase, clinopyroxene, and olivine (Fig.

2.4a). Euhedral magnetite microphenocrysts occur as a minor phase. Orthopyroxene microphenocrysts occur in trace amounts as poikilitic inclusions in olivine. Though we attempted to collect samples of basalt with no visual signs of contamination by silicic material, rare 1-3-mm silicic enclaves, as well as xenocrysts of quartz, were occasionally observed petrographically. The whole-rock composition of the basalt shows little variation in both major and trace elements (Table 2.1, fig. 2.3).

Groundmass and melt inclusions

The groundmass of the Academy Nauk basalt is pilotaxitic and consists of 60 vol.% dark brown glass and 32 vol.% elongated plagioclase microlites. The amounts of clinopyroxene and magnetite microlites usually do not exceed 7 and 1 vol.%, respectively. Groundmass glass is andesitic and shows significant compositional variation (Table 2.2, fig. 2.5). Rare silicic enclaves in the basalt are often fused and jacketed by a light-brown glass with higher SiO_2 content. Therefore, the compositional variability of groundmass glass in the Academy Nauk basalt can most likely be attributed to contamination by silicic material.

Several 35-70-μm vesicle-free glass inclusions in clinopyroxenes were analyzed by electron microprobe to provide estimates of pre-eruptive volatile content in Academy Nauk basalts, following the techniques of Devine et al. (1995). When compared on an anhydrous basis, their compositions are very close to that of the matrix glass (Table 2.2). The deficit in totals of glass inclusion analyses averages 2.3 wt.%.

Plagioclase

Plagioclase phenocrysts comprise 30-35 vol.% of Academy Nauk basalt and show little variation in composition or texture. The majority of plagioclase is euhedral and has a coarse-sieved interior (Fig. 2.3c). This texture is due to the presence of abundant melt inclusions, which vary from circular to elongate and irregular. The high concentration of inclusions suggests that they form a system of interconnected channels permeating the crystals' interiors. Similar textures have been reproduced in decompression (Nelson and Montana, 1992) and heating (Johannes et al., 1994) experiments, where they resulted from dissolution rather than skeletal growth. Both melt inclusions and matrix glass are commonly vesicle- and microlite-rich, attributes that could be due to coupled syneruptive vesiculation and crystallization (Blundy and Cashman, 2001). The compositional and textural similarity of the melt inclusions in the plagioclase to the matrix glass and evidence of their syneruptive vesiculation indicates that the system of interconnected melt channels within plagioclase phenocrysts was open with respect to the surrounding medium during magma ascent.

Compositions of plagioclase cores, rims, microphenocrysts, and microlites of Academy Nauk basalt are nearly constant at 80 to 90 mol.% anorthite (An) (Fig. 2.3a). EPMA profiles across phenocrysts show either oscillatory or, rarely, normal zoning. Sr/Ca and Ba/Ca ratios are low and form a distinctive isolated cluster in compositional space (Fig. 2.3b).

Pyroxenes

Clinopyroxenes are ubiquitous in the Academy Nauk basalt and occur as phenocrysts, microphenocrysts, and microlites, whereas orthopyroxenes occur only in trace amounts as resorbed microphenocrysts (Table 2.1). Clinopyroxene phenocrysts are euhedral or slightly rounded, and contain abundant inclusions of glass and magnetite. Petrographic examination, back-scattered electron imagery, and EPMA transects show no apparent discontinuities or significant compositional variations within individual clinopyroxenes. Composition of clinopyroxenes is uniform ($En_{46}Fs_9Wo_{44}$) and does not vary among samples (Table 2.2).

Olivine

Olivine phenocrysts comprise 2-5 vol.% of the Academy Nauk basalt and occur as individual euhedral 0.5-5 mm grains, as well as in olivine-plagioclase-clinopyroxene aggregates. A small, but conspicuous, amount of individual phenocrysts is resorbed. Olivines often contain poikilitic inclusions of An_{80-90} plagioclase, magnetite, and, less frequently, melt inclusions. Olivine phenocrysts are usually unzoned ($Fo_{77\pm3}$), and show little compositional variation among grains and between samples.

Magnetite

Magnetite occures as euhedral equant microphenocrysts and microlites, normally not exceeding 0.5 mm in size. They also often occur as poikilitic inclusions in

clinopyroxene and olivine phenocrysts, and as an interstitial phase in crystal aggregates. Composition of magnetites does not vary significantly (Table 2.2).

PETROGRAPHY AND MINERALOGY OF KARYMSKY ANDESITE

Similar to previous eruptive events, the juvenile material erupted by Karymsky in 1996-1999 consists of porphyric andesite (modal content 25–32 vol.%) containing plagioclase, clinopyroxene, orthopyroxene, and magnetite (Table 2.1, fig. 2.4b). Lavas are normally vesicle-poor, whereas the porosity of volcanic bombs sometimes exceeds 50-60 vol.%. No enclaves occurred in andesites. Only a few small (1-3 mm) crystal-rich glomerocrysts of plagioclase, pyroxenes, and magnetite were found. The whole-rock composition of Karymsky andesites erupted during April 1996 - August 1999 is nearly constant at 61.9±0.4 wt.% SiO_2 and is almost identical to that of the previous cycle of eruptive activity (Table 2.1). The composition of lavas and volcanic bombs erupted during the first three months of 1996 is more variable, with silica content as low as 60.7 wt.% in early February 1996 (Muravyev et al., 1998).

Groundmass and melt inclusions

The groundmass of Karymsky andesite is pilotaxitic and consists of light-brown rhyolitic glass (50-70 vol.%), elongated plagioclase microlites (20-45 vol.%), and subordinate amounts of pyroxene and magnetite. The groundmass of volcanic bombs and volcanic ash typically contains 30-50 vol.% of microlites (Fig. 2.4f), whereas the

microlite content in the groundmass of lavas often exceeds 50-60 vol.%, which may be attributed to the slower cooling of the latter.

Microprobe analyses of groundmass glass of the Karymsky volcanic ash erupted from 1996 to 1999 show significant variations in major elements. The glasses of the earliest portions of andesite erupted on January 3, 1996, contain 73.9 wt.% of SiO_2 (Table 2.2). The glasses of the ash erupted one month later have the lowest SiO_2 (67.9 wt.%) and K_2O (2.3 wt.%) contents and the highest concentrations of Al_2O_3 (14.6 wt.%) and CaO (2.8 wt.%). Figure 2.5 shows that approximately two months after the onset of the eruptive activity, the silica content of glasses gradually increased and eventually stabilized at 72.0 wt.% SiO_2. At the same time, the concentration of K_2O rose to 3.0 wt.%, whereas the concentrations of Al_2O_3 and CaO gradually decreased to 12.2 wt.% and 1.6 wt.% respectively, and then remained nearly constant until the end of 1998.

Five to eight BSE images of each sample of volcanic ash were acquired in order to determine microlite content in the groundmass. The textural analysis showed that the microlite content of all samples is approximately the same, including those with the lowest SiO_2 in glass (Table 2.2), and does not vary significantly with time (Fig. 2.6a).

Glass inclusions within phenocrysts, predominantly clinopyroxenes, were analyzed by electron microprobe to provide estimates of pre-eruptive volatile content in Karymsky andesites. The deficit in totals of glass inclusion analyses averages at 1.4 wt.%.

Plagioclase

Plagioclase phenocrysts form 20–25 vol.% of Karymsky andesite. Unlike plagioclase in basalt, they show significant variations in composition and texture. The majority of the phenocrysts form two distinctive populations: (1) oscillatory-zoned sodic plagioclases (An_{48-62}) and (2) rimmed plagioclases, characterized by the presence of calcic cores ($An_{>90}$) and sodic rims (An_{48-62}). Oscillatory-zoned plagioclases comprise 70–80 vol.% of all phenocrysts and the majority of microphenocrysts (Fig. 2.2d). Their compositional profiles usually show fine oscillation superimposed on a weak normal zoning; small jumps in An content occur at major dissolution surfaces. Ba/Ca and Sr/Ca ratios of oscillatory-zoned plagioclases in andesite are significantly higher those in basalt, forming an isolated cluster without overlap in composition (Fig. 2.3b).

Rimmed plagioclases consist of euhedral calcic cores, often with coarse-sieved interiors, and oscillatory-zoned rims. The texture of calcic cores mimics that of plagioclase in basalt, but unlike the latter, voids are filled with sodic plagioclase and melt, rather than with melt only, forming a texture frequently referred as "patchy" zoning (Vance, 1965). Rimmed plagioclases were also present in andesite of previous eruptive cycle.

Both EPMA and LA-ICP-MS analyses show that the calcic cores of the andesitic plagioclase are compositionally similar to plagioclases in basalt, whereas compositions of rims outside and "patches" inside calcic cores are close to the composition of oscillatory-zoned plagioclases (Figs. 2.2c, 2.2d). Rimmed plagioclases typically have an abrupt boundary between core and rim, where composition changes from An_{80} to An_{52} within 30

μm distance. Their rims often lack major dissolution surfaces and associated jumps in An content, which are characteristic for coexisting large oscillatory-zoned plagioclases. Although we did not quantify variations in rim width with time of eruption, rims of plagioclases in andesites erupted 2–4 months after the beginning of eruption do appear to be smaller compared to ones erupted 2–3 years after that (Izbekov et al., 2002).

Pyroxenes

Clinopyroxene and orthopyroxene comprise 2-7 vol.% of Karymsky andesite and occurred throughout the course of eruption in all eruptive products as phenocrysts, microphenocrysts, and microlites. Phenocrysts of both pyroxene types are euhedral, and typically contain fewer glass inclusions as compared to pyroxenes in the Academy Nauk basalt.

In addition to the available polished thin sections (one for each sample of lava or volcanic bomb), more than 30 phenocrysts of clinopyroxene were separated from the bulk sample 98IPE27 (andesite lava erupted from April 6 to August 13, 1996) and prepared as polished sections. These phenocrysts were thoroughly investigated using BSE imagery and EPMA. We found no apparent compositional discontinuities or significant compositional variations within phenocrysts. The composition of clinopyroxenes is nearly constant at $En_{42}Fs_{15}Wo_{43}$ and overlaps considerably with that of clinopyroxenes in Academy Nauk basalt (Table 2.2). Orthopyroxene phenocrysts ($En_{66}Fs_{30}Wo_4$) are generally unzoned or, only infrequently, showing slight normal zoning.

Olivine

Olivine is extremely scarce in andesites of Karymsky. A few grains of olivine were found in the Karymsky andesites erupted at the beginning of the eruptive cycle in 1996. Olivine occurs as single anhedral grains in the cores of orthopyroxene phenocrysts, or orthopyroxene-plagioclase aggregates. Figure 2.4e shows an example of a 0.2-mm olivine grain attached to the calcic core of a plagioclase phenocryst at one side and jacketed by an orthopyroxene phenocryst at another. Both olivine and orthopyroxene are overgrown by the sodic rim of the plagioclase phenocryst. This particular example demonstrates clearly that (1) olivine is not an equilibrium phase in the andesite and was transformed to orthopyroxene, and (2) olivine and calcic plagioclase crystallized simultaneously in a magma other than their host andesite. Olivines are compositionally homogeneous ($Fo_{\sim 75}$) and overlap considerably with those in Academy Nauk basalts (Table 2.3).

Magnetite

Magnetite occurs in andesites of Karymsky as sub- to euhedral phenocrysts, microphenocrysts and microlites, as well as poikilitic inclusions in pyroxenes. Vermicular magnetite inclusions are found within orthopyroxene phenocrysts at the boundary with xenocrystic olivine cores. Magnetites are compositionally uniform and have significantly lower Cr_2O_3 and Al_2O_3 contents and higher TiO_2 compared to those in

Academy Nauk basalt (Table 2.3). No significant variations of Karymsky magnetite composition were observed throughout the 1996-1999 period of eruption.

DISCUSSION

Origin of variation of Karymsky melt composition

Three general explanations can be suggested to account for the variations in groundmass glass composition at the beginning of the eruption: (1) pre-eruptive compositional heterogeneity of Karymsky reservoir, (2) higher magma flux at the beginning of eruption, and (3) basaltic recharge.

If the Karymsky reservoir is compositionally heterogeneous, then why did the composition of volcanic glass stabilize and remain constant after the first two months of eruption? Indeed, previous periods of activity, with the exceptions noted, have shown that Karymsky is characterized by a very constant composition of magmas. Therefore, heterogeneity of the Karymsky reservoir developed prior to the eruption cannot account for variations of groundmass glass composition in the beginning of the current eruptive cycle.

The second possibility is that these variations could be related to higher magma flux at the beginning of the eruption, which produced magma that had undergone less syneruptive crystallization due to faster ascent and therefore erupted with less evolved glass. If so, this would be reflected by a variation of microlite content in glass, while the overall magma composition could be constant (Blundy and Cashman, 2001).

Experimental data on equilibrium crystallization in magma systems has led to the development of numerical models that can be used for simulating phase equilibria in crystallizing melts. One of them - COMAGMAT (Ariskin, 1999) - was used here to model compositional variations of melt during the crystallization of Karymsky andesite. According to the model, an increase of SiO_2 in crystallizing melt of 2 wt.%, when the major precipitating phase is An_{50} plagioclase, should correspond to an increase of volume fraction of microlites of 9 vol.% (Crystallization trend, fig. 2.6b). If variations of melt composition are related to different degrees of crystallization, then the microlite content in volcanic ash should follow the crystallization trend. The microlite content in the volcanic ash erupted in February1996, however, escapes from the trend, being nearly the same as the microlite content in the ash erupted during the following seventeen months, whereas the silica content in the February glasses is significantly lower as compared to the latter. This could not be explained solely by different degrees of syneruptive crystallization of andesitic batches, and thus eliminates this as a possible alternative.

With elimination of these alternatives and support from the eruption chronology, it appears that the third possible explanation is the most probable one: the significant variations of the composition of groundmass glass early in the eruption were caused by the input of heat or/and mafic melt as the result of basaltic replenishment. The addition of basalt, however, could lead to two different scenarios. First, if the temperature of the basalt was significantly hotter than that of the andesite, the andesite could be heated, and thus decrease its crystallinity and correspondingly make the composition of its melt more mafic. In this scenario the thermal equilibration would cause crystallization of basalt,

which would hinder its mixing with the host andesite (Eichelberger, 1978). Alternatively, if the temperatures and physical properties of basalt and andesite were not greatly dissimilar, the magmas could mix effectively and produce a hybrid with more mafic melt as compared to the host andesite.

We argue below that variations of groundmass glass composition were caused by basaltic recharge, which indeed led to the fast and efficient formation of a homogeneous hybrid andesite that erupted within two months after the beginning of eruption. The most convincing evidence is the presence of xenocrysts of basaltic origin in Karymsky andesites.

Origin of calcic plagioclase and olivine in Karymsky andesites

Calcic cores in rimmed plagioclases of Karymsky andesite texturally and compositionally mimic plagioclases in Academy Nauk basalt, which erupted at the beginning of the eruptive cycle in 1996. Detailed discussion of this observation is offered in Izbekov et al. (2002), whereas here, we only re-iterate the major points.

Two important questions regarding the origin of the calcic cores are (1) whether they originate from the same basalt erupted in Academy Nauk caldera, and (2) whether they were introduced to Karymsky andesite system by basaltic replenishment at the beginning of the 1996 eruption. The compositional similarity, in terms of both major and trace elements, suggests that the calcic cores indeed originate from the same basaltic source that produced Academy Nauk basalts (Figs. 2.7a, 2.7b). The textural similarity (Figs. 2.4c, 2.4d) also suggests that basaltic plagioclases and calcic cores in rimmed

plagioclases of Karymsky experienced similar dissolution events, perhaps during the ascent of basalt and associated decompression (Nelson and Montana, 1992). Additionally, thermodynamic modeling using COMAGMAT (Ariskin, 1999) indicates that plagioclase as calcic as $An_{\sim 96}$ cannot crystallize in magma of Karymsky andesite chemistry at any plausible pressure, temperature, or water content, and thus must have been introduced to the andesite from a more mafic source.

Similarity to Academy Nauk plagioclase does not necessarily imply, however, that the calcic plagioclase was introduced to Karymsky andesite at the beginning of the 1996 cycle of eruptive activity. The zoning and width of sodic rims of rimmed plagioclases can be used to distinguish calcic cores introduced in 1996 from those that may have been introduced during previous basaltic recharges. The rimmed plagioclases, whose sodic rims lack major dissolution boundaries and associated increases in An content, most likely experienced no disturbances and grew in equilibrium since the introduction of their calcic cores. Their calcic cores then must have been introduced by the most recent basaltic replenishment. Additionally, widths of the sodic rims, which we infer to have grown around these cores since 1996, are consistent with experimentally determined plagioclase growth rates (Izbekov et al., 2002).

Presence of $Fo_{\sim 3}$ olivine in earlier andesites is additional evidence for basaltic recharge. Ivanov (1996) provided petrochemical evidence that forsteritic olivine is not an equilibrium phase in Karymsky andesite. Our petrographic observations show that indeed olivine occurs in Karymsky andesite only as xenocrystic cores in orthopyroxene. Compositional similarity of olivine in Karymsky andesites to that in Academy Nauk

basalt, where it is a major equilibrium phase, implies that the latter is the most plausible source of the olivine xenocrysts in andesites. The overgrowth of both the olivine xenocryst and the calcic plagioclase core by the sodic plagioclase rim, which has no apparent dissolution boundaries (Fig. 2.4e), suggests that both olivine and calcic plagioclase were introduced to Karymsky andesite by the most recent basaltic replenishment, specifically at the beginning of 1996 eruption.

Mechanism of mixing at Karymsky magma system

The presence of xenocrysts and variations of Karymsky groundmass glass composition, eruption chronology, and the evidence of basaltic dike emplacement, indicate that at the beginning of the 1996 eruption, the Karymsky magma system was replenished by the same basalt that erupted simultaneously in the northern part of Academy Nauk caldera. An intriguing finding is that as soon as two months after the onset of the eruption Karymsky already produced homogeneous andesites. Why was the mixing at Karymsky so fast and efficient, whereas it never approached such a complete homogenization in many other cases, e.g. Unzen, Japan (Nakamura, 1995), Dutton, Alaska (Miller et al., 1999) and Soufrière Hills, Montserrat (Murphy et al., 2000)?

Sparks and Marshall (1986) suggest that the ability for magmas to mix depends on their physical properties after thermal equilibration, because thermal diffusion rates are orders of magnitude faster than chemical diffusion rates. The physical properties, particularly the viscosity and density of a magma, strongly depend on (1) the composition of melt including the concentration of water, (2) the volume fractions of solid phases and

bubbles suspended in the melt, (3) temperature, and (4) total pressure. It is difficult, however, is to estimate with adequate precision these four parameters.

According to the experimental study of Kadik et al. (1989), the simultaneous crystallization of olivine, clinopyroxene, and plagioclase in high-aluminum basalts of Kamchatka occurs at pressures lower than 700-750 MPa. The COMAGMAT model predicts that this assemblage is stable in Academy Nauk basalt at pressures lower than 600 MPa, assuming the water content in magma of 2.3 wt.%, as suggested by EPMA analyses of melt inclusions. The high volume fraction of phenocrysts in Academy Nauk basalt also supports the view that they were most likely stored in a crustal-level reservoir prior to the eruption. Therefore, we assume 600 MPa and the corresponding depth of 18 km as maximum limits for the crustal storage of Academy Nauk basalt.

All plagioclase phenocrysts in Academy Nauk basalt and calcic cores of rimmed plagioclases in Karymsky andesites typically have coarse-sieved interiors. The similarity of their texture to that reproduced in experiments of Nelson and Montana (1992) suggests that it was most likely formed by decompression during the ascent of Academy Nauk basalt from its crustal source. According to their experiments, a minimum of 200 MPa decompression during 60 hours is required to cause 10% resorption of plagioclase, whereas decompression on the order of 400 MPa for the same duration results in 30% of resorption. Although the experimental results should be applied with caution to Academy Nauk basalt because of the more silicic starting material (56.08 wt.% SiO_2) and very oxidizing conditions (Hematite-magnetite buffer in experiments), they suggest that 300 MPa might be a reasonable estimate for the decompression required to form a coarse-

sieved texture such as that of plagioclases in the Academy Nauk basalt. If this is correct, then Academy Nauk basalt experienced a pressure decrease from 600 to 300 MPa prior to entering the magma system of Karymsky, which corresponds to magma ascent from about 18 km to 9 km depth.

Only a very approximate estimate can be made for the depth, where mixing occurred. The minimum depth is constrained by the roof of the crustal reservoir of Karymsky, which is thought to be located approximately 4 km below the edifice of Karymsky volcano (Shirokov et al., 1988). The maximum depth is constrained by the depth where Academy Nauk basalt breached the bottom or the side of the Karymsky magma chamber (ca. 9 km). Therefore, the pressure in the volume where the mixing occurred lies in the interval from ca. 100 to 300 MPa.

The physical properties of the intruding basalt and the host andesite were estimated using COMAGMAT for modeling variations of volume fractions of solid phases in melts (Ariskin, 1999), and CONFLOW for calculating corresponding changes of viscosities and densities of magmas (Mastin and Ghiorso, 2000). We modeled isobaric crystallization of Academy Nauk basalt and Karymsky andesite at 200 MPa pressure, assuming concentrations of water of 2.3 wt.% in the basalt and 1.4 wt.% in the andesite inferred from EPMA analyses of melt inclusions in pyroxenes, and oxygen fugacity at Nickel-Nickel Oxide buffer, as suggested by whole-rock compositions of magmas (Grib, 1998).

Under the specified conditions the compositions of clinopyroxene, orthopyroxene, and plagioclase in Karymsky andesite are best reproduced by COMAGMAT at

temperatures from 1023 to 1057°C. The deviations of modeled compositions from natural ones do not exceed 5 mole % for all mineral phases. According to CONFLOW the viscosity of Karymsky andesite at this temperature range is $10^{3.3}$-$10^{3.6}$ Pa·s, and its bulk density is 2470 kg/m^3 (Fig. 2.8).

Assuming that the mineral assemblage of Academy Nauk basalt was last equilibrated at 600 MPa, we used olivine-melt and clinopyroxene-melt equilibria to estimate the basalt temperature before it ascended and entered Karymsky magma system. According to COMAGMAT, the compositions of olivine and clinopyroxene are best reproduced at temperatures from 1090 to 1120°C. This overlaps with the temperature interval where simultaneous crystallization of olivine-clinopyroxene-plagioclase assemblage is possible (1080-1115°C) at the given pressure and water content in Academy Nauk basalt. At these conditions the viscosity of the basalt ranges from $10^{1.6}$ to $10^{2.0}$ Pa·s, and its density is ca. 2550 kg/m^3.

The ascent of Academy Nauk basalt from deep crustal storage to the level where it encountered the Karymsky reservoir was probably close to isothermal, and therefore the temperature of the basalt upon entering andesitic magma system was approximately 1100°C. Assuming that the volume of the basaltic influx is subordinate to the volume of the host andesite and does not significantly affect the average temperature of the latter, thermal equilibration would have cooled the basalt to 1040°C, corresponding to an increase of its crystallinity to 35 vol.% and viscosity to $10^{3.3}$ Pa·s (Fig. 2.8). The combined effect of pressure decrease during the ascent and temperature decrease due to the thermal equilibration would cause the decrease of basalt density from 2550 to 2466

kg/m^3, virtually equal to the density of the host andesite. As a result, both Academy Nauk basalt and Karymsky andesite would have nearly the same physical properties after thermal equilibration, and thus have an ability to mix effectively.

Perhaps the factor that distinguishes the mixing scenario at Karymsky from dacitic-andesitic volcanoes, where mixing is less thorough, is the flux of mafic magma that maintains a heat and mass balance of the crustal magma reservoir under a particular volcano. In the case where replenishments are rare (once in hundreds of years), the temperature and viscosity contrasts between mafic input and sluggish, crystal-rich magma of the crustal reservoir are high. Mafic magma ponds at the bottom of the reservoir and crystallizes in a separate volume (Fig. 2.9a). Heating of adjacent parts of host magma initiates convection, which leads to mechanical disaggregation of quenched mafic magma and produces a hybrid. When the hybrid magma erupts, its composition shows distinctive signs of disequilibrium, such as presence of mafic enclaves, "dusty-zoned" plagioclases, and abundant xenocrysts (e.g. Koyaguchi and Kaneko, 2000).

In magma systems, such as that of Karymsky, where replenishments occur more frequently (once in a decade), cooling and crystallization of the reservoir magma during repose periods may not advance to the point when convection stops. The contrasts in temperature and viscosity between injected and stored magmas are less, and thus allow a different mechanism of mixing, one in which the mafic magma does not solidify due to thermal equilibration and becomes involved into convection immediately upon injection to the reservoir (Fig. 2.9b). The temperature of the hybrid storage magma may increase, but to a lesser extent compared to the previous case, because dispersal is thorough from

the outset – local concentration of hotter basaltic components never reach shallower levels. The erupted hybrid magma is usually texturally and compositionally homogeneous. The only petrologic signs of mixing are the presence of xenocrysts and subtle temporal variations of magma composition, which can only be observed in sequences of continually erupted volcanic rocks.

CONCLUSION

Petrologic observations provide additional evidence for basaltic replenishment of Karymsky magma system at the beginning of the current cycle of eruptive activity. Composition of glass of volcanic ash became more mafic almost immediately after the beginning of eruption and then, within two months, gradually returned to its original state and remained almost constant for the following three years. These variations cannot be explained by heterogeneity of Karymsky reservoir or by variations in magma flux at the beginning of eruption, and require an input of basaltic magma.

Further evidence for basaltic replenishment includes the presence of xenocrysts of basaltic origin in andesites of Karymsky. A conspicuous portion of plagioclase phenocrysts in Karymsky andesites contains calcic cores (An_{76-90}), which compositionally and texturally mimic plagioclases in Academy Nauk basalts. In addition to plagioclase, the earlier portions of andesite contained rare xenocrysts of olivine, which occurred as relicts in plagioclase-pyroxene aggregates. The composition of olivine xenocrysts matched that of olivines in Academy Nauk basalts.

Summarizing the results of our study discussed above, it appears that a basalt dike intruded along the preexisted fault, intercepted a shallow andesite magma system beneath Karymsky Caldera, and triggered the eruption of Karymsky volcano. Due to modest contrasts in temperature and viscosity between basalt and andesite, direct mixing of melts was possible, and mafic enclaves were not formed by the intruding magma. The introduced volume of basalt was quickly blended into the host andesitic magma, portions of which reached the surface soon after. In two months, however, the new "hybrid" andesite produced by mixing with basalt was either exhausted, or was blended with host andesite below detection, and then the regular andesite of Karymsky reservoir erupted.

ACKNOWLEDGEMENTS

This work was supported by the Volcano Hazards Program of the U.S. Geological Survey through the Alaska Volcano Observatory. Additional funding was provided by the Russian Foundation for Basic Research, grant 99-05-65495 to Boris Ivanov. Thomas A. Vogel and Lina C. Patino helped tremendously with LA-ICP-MS study of plagioclases. Discussions of the results with our colleagues at Alaska Volcano Observatory and the Institute of Volcanic Geology and Geochemistry, Petropavlovsk-Kamchatsky, significantly improved manuscript.

Table 2.1: Whole-rock composition of lavas and volcanic bombs

Sample	J-4491	97IPE3	98IPE22A	98IPE22B	98IPE22C	98IPE22D	BV170296
Location [a]	KAR	AN	AN	AN	AN	AN	KAR
Date of eruption	1976	01/02/96	01/02/96	01/02/96	01/02/96	01/02/96	2/17/96
Major elements							
SiO_2 [b]	62.89	51.98	51.87	51.58	51.62	51.72	61.46
Al_2O_3	16.33	18.73	19.02	19.18	19.17	19.31	16.41
TiO_2	0.88	0.74	0.73	0.74	0.74	0.74	0.91
FeO*	5.47	7.65	7.47	7.67	7.55	7.48	5.73
MnO	0.14	0.15	0.15	0.15	0.15	0.15	0.15
CaO	5.06	10.32	10.51	10.54	10.68	10.66	5.43
MgO	1.74	5.35	5.71	5.28	5.42	5.5	1.88
K_2O	1.67	0.59	0.58	0.59	0.57	0.56	1.56
Na_2O	4.78	2.84	2.86	2.9	2.84	2.88	4.63
P_2O_5	0.26	0.14	0.14	0.14	0.14	0.14	0.26
Total	99.22	98.49	99.03	98.76	98.88	99.13	98.41
Trace elements							
Ni	3	26	33	25	29	30	1
Cr	3	81	88	81	87	87	6
V	110	221	210	200	216	199	121
Zr	146	74	71	73	72	71	138
Ga	20	15	15	18	16	20	17
Cu	22	57	58	71	65	68	29
Zn	75	62	62	55	59	60	73
La	12.17	5.17	5.46	5.36	5.46	5.34	11.55
Ce	28.01	11.50	12.20	12.37	12.39	12.24	26.57

[a] Location abbreviated as KAR for Karymsky and Academy Nauk for Academy Nauk vents.

[b] Major oxides in wt.% with all Fe reported as FeO, concentrations of Ni-Zn (ppm) determined by XRF, concentrations of La-Sc (ppm) determined by ICP-MS; n.d. - not detected; n.a. – not analyzed.

[c] Modes of minerals and glass were determined by point counting (1000 points).

Table 2.1: Continued

Sample	J-4491	97IPE3	98IPE22A	98IPE22B	98IPE22C	98IPE22D	BV170296
Location [a]	KAR	AN	AN	AN	AN	AN	KAR
Date of eruption	1976	01/02/96	01/02/96	01/02/96	01/02/96	01/02/96	2/17/96
Pr [b]	3.75	1.66	1.74	1.74	1.74	1.73	3.73
Nd	17.65	8.26	8.12	8.33	8.21	8.34	17.40
Sm	4.95	2.42	2.52	2.49	2.56	2.50	4.91
Eu	1.51	0.91	0.95	0.92	0.94	0.93	1.49
Gd	5.24	2.69	2.79	2.70	2.70	2.72	5.17
Tb	0.88	0.45	0.46	0.46	0.46	0.46	0.86
Dy	5.57	2.89	2.92	2.91	2.93	2.84	5.54
Ho	1.17	0.60	0.60	0.59	0.61	0.59	1.16
Er	3.21	1.66	1.59	1.65	1.61	1.61	3.22
Tm	0.48	0.24	0.24	0.24	0.24	0.24	0.47
Yb	3.10	1.45	1.47	1.49	1.51	1.50	3.08
Lu	0.49	0.23	0.23	0.24	0.24	0.23	0.49
Ba	426	165	173	171	170	168	399
Th	1.79	0.52	0.61	0.59	0.60	0.57	1.76
Nb	3.45	1.30	1.40	1.37	1.44	1.33	3.30
Y	32.02	15.61	16.09	15.82	15.17	15.46	31.17
Hf	4.09	1.62	1.68	1.71	1.68	1.64	4.05
Ta	0.26	0.11	0.11	0.10	0.11	0.10	0.26
U	0.93	0.31	0.31	0.31	0.30	0.30	0.90
Pb	6.29	2.64	2.65	2.43	2.59	2.61	5.99
Rb	22.87	7.66	7.50	7.38	7.04	6.67	21.30
Cs	0.94	0.30	0.29	0.30	0.28	0.27	0.86
Sr	354	466	466	457	443	455	353
Sc	22.17	31.94	34.24	32.26	31.49	31.00	23.40
Modal analysis [c]							
Gl	72.9	61.2	58.8	54.5	56.7	69.8	74.7
Pl	21.4	28.1	30.6	29.9	35.1	23.0	21.5
CPx	3.3	7.8	7.2	9.2	2.8	4.1	1.8
OPx	0.8	0.8	0.6	0.0	0.0	0.3	0.4
Ol	n.d.	2.0	2.6	5.9	5.0	2.1	traces
Mt	1.5	0.2	0.1	0.6	0.3	0.7	1.7

Table 2.1: Continued

Sample	BV040496	98IPE27	98IPE28	98IPE29	97IPE5	98IPE25	98IPE24
Location [a]	KAR	KAR	KAR	KAR	KAR	KAR	KAR
Date of eruption	04/04/96	04/06/96 - 08/13/96	Sep.- Oct., 1996	Jan.- Feb., 1997	09/08/97	Dec. 97 - Feb. 98	Mar. - May, 1998
Major elements							
SiO_2 [b]	62.88	61.87	61.97	62.03	61.72	61.75	61.47
Al_2O_3	16.35	16.29	16.33	16.43	16.09	16.34	16.27
TiO_2	0.88	0.91	0.90	0.92	0.90	0.90	0.91
FeO*	5.26	5.76	5.91	5.61	5.92	5.90	5.92
MnO	0.14	0.15	0.15	0.15	0.15	0.14	0.15
CaO	4.94	5.31	5.33	5.37	5.31	5.34	5.37
MgO	1.64	1.91	1.85	1.94	1.92	1.91	1.92
K_2O	1.69	1.6	1.59	1.59	1.57	1.59	1.58
Na_2O	4.84	4.68	4.73	4.69	4.52	4.7	4.65
P_2O_5	0.26	0.26	0.26	0.26	0.26	0.26	0.26
Total	98.88	98.74	99.02	98.98	98.35	98.83	98.50
Trace elements							
Ni	3	4	3	4	0	2	0
Cr	6	10	12	7	7	12	9
V	115	135	131	143	130	128	123
Zr	148	143	141	140	139	143	142
Ga	18	19	16	19	19	19	20
Cu	18	30	28	29	37	38	38
Zn	74	71	73	69	76	76	78
La	11.84	11.95	11.12	11.28	11.26	11.54	11.58
Ce	27.39	26.68	25.95	26.21	25.28	25.66	26.77
Pr	3.72	3.62	3.57	3.64	3.52	3.59	3.61
Nd	17.33	17.17	16.95	16.95	16.41	17.17	16.75
Sm	4.93	5.02	4.70	4.88	4.84	4.94	4.77
Eu	1.47	1.54	1.46	1.48	1.47	1.54	1.48
Gd	5.07	5.23	5.04	5.10	5.03	5.38	5.06
Tb	0.87	0.87	0.85	0.87	0.85	0.87	0.85
Dy	5.51	5.58	5.45	5.48	5.37	5.52	5.45
Ho	1.18	1.12	1.14	1.17	1.15	1.12	1.14

Table 2.1: Continued

Sample	BV040496	98IPE27	98IPE28	98IPE29	97IPE5	98IPE25	98IPE24
Location [a]	KAR	KAR	KAR	KAR	KAR	KAR	KAR
Date of eruption	04/04/96	04/06/96 - 08/13/96	Sep.-Oct., 1996	Jan.-Feb., 1997	09/08/97	Dec. 97 - Feb. 98	Mar.-May, 1998
Er [b]	3.30	3.08	3.17	3.23	3.11	3.13	3.21
Tm	0.49	0.48	0.48	0.47	0.47	0.48	0.46
Yb	3.12	2.95	3.03	3.06	2.84	2.96	3.05
Lu	0.50	0.47	0.49	0.49	0.46	0.48	0.48
Ba	418	410	398	398	387	407	398
Th	1.80	1.62	1.77	1.80	1.31	1.62	1.63
Nb	3.44	3.23	3.28	3.26	3.15	3.24	3.14
Y	32.48	30.46	31.50	30.81	30.31	30.40	30.00
Hf	4.09	3.95	3.97	3.98	3.80	4.07	3.83
Ta	0.26	0.26	0.25	0.24	0.25	0.25	0.24
U	0.91	0.85	0.88	0.91	0.83	0.87	0.87
Pb	6.21	5.94	6.15	5.93	5.79	5.97	5.76
Rb	22.91	21.22	21.75	21.20	21.43	20.78	20.69
Cs	0.93	0.85	0.85	0.81	0.86	0.86	0.84
Sr	353	345	369	365	368	350	354
Sc	22.84	22.35	24.51	23.96	22.65	22.67	21.52
Modal analysis [c]							
Gl	71.6	73.1	73.6	69.4	70.2	69.3	67.8
Pl	24.8	22.6	21.0	23.2	22.0	22.7	27.3
CPx	1.6	2.1	2.6	4.9	6.2	4.3	3.9
OPx	1.3	0.9	1.5	0.9	0.8	1.3	0.4
Ol	n.d.	traces	n.d.	n.d.	n.d.	n.d.	n.d.
Mt	0.6	1.3	1.3	1.6	1.9	2.4	0.5

Table 2.1: Continued

Sample	98IPE26	98IPE33	99IPE 9	99IPE 8	99IPE 2a	99IPE 2b
Location [a]	KAR	KAR	KAR	KAR	AN	AN
Date of eruption	Jun.- July, 1998	07/21/98	08/09/99 - 08/23/99	08/24/99	4800 BP	4800 BP
Major elements						
SiO_2 [b]	61.77	61.99	61.8	61.8	56.22	52.91
Al_2O_3	16.3	16.41	16.81	16.51	16.39	16.45
TiO_2	0.91	0.91	0.90	0.91	0.80	0.86
FeO*	5.77	5.77	5.63	5.93	7.75	8.55
MnO	0.15	0.15	0.15	0.15	0.16	0.18
CaO	5.34	5.41	5.7	5.51	8.9	10.3
MgO	1.9	1.9	2.03	2.02	5.16	6.41
K_2O	1.6	1.58	1.52	1.55	1	0.72
Na_2O	4.67	4.7	4.61	4.57	3.27	2.76
P_2O_5	0.26	0.26	0.25	0.25	0.15	0.14
Total	98.66	99.09	99.40	99.20	99.80	99.28
Trace elements						
Ni	3	5	4	3	17	33
Cr	15	12	11	11	116	214
V	141	130	139	132	234	281
Zr	142	140	136	139	86	62
Ga	19	17	16	16	15	17
Cu	30	35	39	36	76	86
Zn	75	74	73	73	69	73
La	11.61	11.32	10.71	11.03	6.69	5.37
Ce	26.55	26.08	24.49	25.40	15.36	12.31
Pr	3.61	3.57	3.38	3.49	2.12	1.76
Nd	16.78	16.70	15.97	16.39	10.22	8.64
Sm	4.99	4.78	4.56	4.70	3.09	2.69
Eu	1.55	1.47	1.43	1.43	1.02	0.92
Gd	5.07	4.89	4.74	4.85	3.26	2.93
Tb	0.86	0.84	0.82	0.83	0.57	0.51
Dy	5.48	5.33	5.03	5.18	3.62	3.17
Ho	1.14	1.10	1.05	1.08	0.76	0.66

Table 2.1: Continued

Sample	98IPE26	98IPE33	99IPE 9	99IPE 8	99IPE 2a	99IPE 2b
Location [a]	KAR	KAR	KAR	KAR	AN	AN
Date of eruption	Jun.- July, 1998	07/21/98	08/09/99 - 08/23/99	08/24/99	4800 BP	4800 BP
Er [b]	3.11	3.10	3.01	2.97	2.11	1.85
Tm	0.46	0.45	0.44	0.44	0.31	0.26
Yb	2.97	2.98	2.75	2.89	1.99	1.67
Lu	0.47	0.46	0.45	0.45	0.32	0.27
Ba	394	392	385	391	244	186
Th	1.63	1.64	1.54	1.61	1.00	0.75
Nb	3.22	3.21	3.15	3.18	1.96	1.47
Y	30.29	29.62	30.23	31.50	22.14	18.84
Hf	3.90	3.83	3.76	3.76	2.34	1.69
Ta	0.25	0.24	0.23	0.24	0.14	0.10
U	0.87	0.85	0.79	0.84	0.52	0.41
Pb	5.84	5.74	5.52	5.65	3.69	3.51
Rb	20.96	21.50	20.33	21.23	14.06	9.18
Cs	0.82	0.83	0.84	0.86	0.52	0.44
Sr	354	366	376	374	381	414
Sc	21.49	24.19	23.08	22.92	40.44	45.52
Modal analysis [c]						
Gl	75.8	69.5	66.42	68.2	n.a.	n.a.
Pl	18.2	23.5	26.10	24.4	n.a.	n.a.
CPx	1.4	5.4	5.68	5.5	n.a.	n.a.
OPx	2.4	0.8	0.94	0.9	n.a.	n.a.
Ol	n.d.	n.d.	n.d.	n.d.	n.a.	n.a.
Mt	2.2	1.8	1.60	1.8	n.a.	n.a.

Table 2.2: Composition of matrix glass in volcanic ash and melt inclusions

Sample [a]	BV-280296-I	AN-MI	BV-280296-II	BV-110296	BV-180296
Day	01/02/96		01/02/96	02/11/96	02/18/96
n	31	22	17	6	12
SiO_2 [b]	56.01(2.62)	58.88(2.24)	73.87(1.38)	67.95(1.31)	68.31(0.78)
Al_2O_3	20.21(5.67)	15.97(2.93)	12.26(0.85)	14.14(0.28)	14.03(0.81)
TiO_2	0.79(0.54)	1.18(0.40)	0.81(0.12)	0.92(0.17)	0.85(0.07)
FeO*	5.55(3.25)	7.19(3.13)	3.10(0.56)	4.17(1.02)	3.83(0.30)
CaO	8.54(2.60)	6.85(1.47)	1.28(0.51)	2.79(0.35)	2.02(1.02)
MgO	1.70(1.03)	2.01(1.60)	0.28(0.10)	0.89(0.37)	0.87(0.24)
K_2O	0.81(0.49)	1.25(0.42)	3.38(0.62)	2.31(0.23)	2.62(0.78)
Na_2O	4.21(0.52)	4.25(0.67)	3.71(0.71)	5.33(0.13)	4.23(0.97)
Cl	0.07(0.05)	0.13(0.03)	0.12(0.04)	0.12(0.05)	0.05(0.05)
Total	98.52	97.71	99.16	99.09	97.27
Microlites	45.05(7.88)	n.a.	43.32(2.45)	42.15(5.54)	42.70(3.45)

[a] Sample BV-280296-I is the matrix glass of Academy Nauk volcanic ash. AN-MI and KAR-MI represent melt inclusions in phenocrysts of Academy Nauk basalts and Karymsky andesites, correspondingly. All other samples represent matrix glass of Karymsky volcanic ash erupted on specified days.

[b] The average of n analyses (in wt. %) is given together with the standard deviation (number in brackets) with all Fe reported as FeO; microlite content is reported in vol.%; n.a. – not analyzed.

Table 2.2: Continued

Sample	BV-220296	BV-280296	BV-010396	BV-240396	BV-080496
Day	02/22/96	02/28/96	03/01/96	03/24/96	04/08/96
n	12	9	18	12	9
SiO_2	68.55(1.60)	70.18(1.32)	72.98(1.10)	72.07(0.78)	71.07(1.08)
Al_2O_3	14.65(1.91)	14.15(0.97)	12.68(0.98)	12.23(0.63)	13.23(0.93)
TiO_2	0.78(0.21)	0.92(0.12)	0.77(0.14)	0.91(0.16)	1.00(0.15)
FeO*	3.62(1.06)	4.00(0.45)	3.24(0.43)	3.42(0.37)	4.15(0.36)
CaO	2.82(0.93)	1.97(0.53)	1.60(0.45)	1.43(0.29)	2.21(0.38)
MgO	0.69(0.41)	0.84(0.22)	0.37(0.11)	0.32(0.07)	0.55(0.09)
K_2O	2.74(0.60)	2.70(0.43)	3.03(0.52)	3.06(0.42)	2.70(0.16)
Na_2O	4.70(0.79)	3.56(1.43)	4.11(0.47)	4.13(0.72)	3.86(0.44)
Cl	0.04(0.04)	0.06(0.05)	0.09(0.04)	0.14(0.03)	0.10(0.03)
Total	98.99	98.82	99.22	98.08	99.33
Microlites	38.02(5.28)	35.30(5.35)	43.23(5.30)	41.12(8.18)	n.a

Sample	BV-180496	BV-250496	BV-010596	BV-100596	BV-270696
Day	04/18/96	04/25/96	05/01/96	05/10/96	06/27/96
n	11	15	11	13	11
SiO_2	70.53(0.82)	71.65(0.40)	71.61(0.86)	71.30(0.66)	72.43(0.79)
Al_2O_3	12.76(0.63)	12.57(0.22)	12.99(0.73)	12.73(0.48)	13.01(0.98)
TiO_2	0.98(0.18)	1.13(0.13)	0.95(0.13)	1.10(0.17)	0.94(0.18)
FeO*	4.45(0.39)	4.45(0.45)	4.12(0.31)	4.43(0.24)	3.83(0.63)
CaO	2.13(0.35)	1.99(0.15)	2.23(0.47)	2.04(0.24)	1.85(0.46)
MgO	0.77(0.47)	0.64(0.19)	0.63(0.18)	0.61(0.18)	0.40(0.13)
K_2O	2.73(0.19)	2.83(0.17)	2.77(0.22)	2.71(0.15)	2.93(0.41)
Na_2O	4.09(0.33)	3.88(0.43)	3.78(0.40)	3.87(0.33)	4.14(0.68)
Cl	0.12(0.04)	0.12(0.03)	0.13(0.03)	0.11(0.04)	0.10(0.03)
Total	99.04	99.77	99.66	99.39	100.05
Microlites	36.08(3.63)	37.25(8.73)	37.41(6.60)	n.a	35.83(6.78)

Table 2.2: Continued

Sample	BV-100796	K-3/9	K-3/8	K-3/7	K-3/6
Day	07/10/96	10/23/96	11/12/96	12/03/96	12/23/96
n	19	9	12	21	11
SiO_2	72.64(1.85)	71.03(0.71)	71.38(1.12)	71.78(0.59)	71.69(0.90)
Al_2O_3	12.73(1.11)	13.14(0.80)	12.99(0.51)	12.50(0.31)	12.72(0.67)
TiO_2	0.90(0.25)	0.99(0.17)	0.94(0.16)	0.98(0.12)	0.92(0.23)
FeO*	3.17(1.03)	4.24(0.67)	4.12(0.48)	4.32(0.29)	4.18(0.28)
CaO	1.67(0.67)	2.09(0.40)	2.15(0.50)	1.76(0.27)	1.97(0.49)
MgO	0.28(0.17)	0.51(0.28)	0.37(0.15)	0.40(0.11)	0.45(0.11)
K_2O	2.50(0.91)	2.97(0.34)	2.81(0.39)	3.05(0.31)	2.79(0.67)
Na_2O	4.77(0.92)	4.24(0.38)	4.32(0.58)	3.98(0.46)	4.17(0.82)
Cl	0.10(0.06)	0.13(0.04)	0.13(0.07)	0.14(0.03)	0.12(0.04)
Total	99.11	99.81	99.68	99.40	99.47
Microlites	38.60(3.76)	42.70(2.59)	n.a	n.a	n.a

Sample	K-3/5	K-3/4	K-3/3	K-3/2	K-3/1
Day	01/11/97	02/02/97	02/22/97	03/13/97	04/04/97
n	13	14	11	16	11
SiO_2	71.71(0.64)	72.07(0.65)	72.80(0.92)	72.65(0.61)	72.03(0.56)
Al_2O_3	12.63(0.33)	12.67(0.47)	12.31(0.21)	12.39(0.55)	12.57(0.45)
TiO_2	1.06(0.15)	1.00(0.15)	0.94(0.20)	0.90(0.12)	0.95(0.10)
FeO*	4.28(0.19)	4.00(0.39)	4.15(0.30)	3.84(0.38)	3.91(0.44)
CaO	1.77(0.18)	1.63(0.27)	1.66(0.37)	1.66(0.27)	1.70(0.23)
MgO	0.43(0.10)	0.35(0.13)	0.36(0.08)	0.35(0.07)	0.44(0.19)
K_2O	2.94(0.30)	2.89(0.26)	2.83(0.67)	2.70(0.43)	2.81(0.25)
Na_2O	4.35(0.26)	4.40(0.38)	4.38(0.68)	4.67(0.53)	4.46(0.31)
Cl	0.11(0.02)	0.13(0.04)	0.12(0.03)	0.11(0.02)	0.11(0.05)
Total	99.76	99.58	100.02	99.69	99.40
Microlites	43.00(0.89)	n.a	n.a	42.74(4.70)	n.a

Table 2.2: Continued

Sample	BV-030497	98IPE34	M-2113	KAR-MI
Day	04/03/97	07/18/98	07/25/98	
n	13	12	10	7
SiO_2	71.92(0.35)	72.20(0.50)	71.61(0.27)	67.61(3.92)
Al_2O_3	12.45(0.35)	12.30(0.23)	12.42(0.24)	13.94(0.94)
TiO_2	0.99(0.12)	0.89(0.10)	0.96(0.16)	0.89(0.20)
FeO*	4.08(0.33)	3.95(0.29)	4.19(0.26)	4.61(0.48)
CaO	1.56(0.23)	1.37(0.19)	1.82(0.21)	2.81(0.79)
MgO	0.36(0.12)	0.36(0.07)	0.48(0.06)	1.02(0.45)
K_2O	3.00(0.43)	3.15(0.15)	2.66(0.67)	2.77(0.15)
Na_2O	4.09(0.64)	4.25(0.18)	4.12(0.71)	4.81(0.48)
Cl	0.15(0.04)	0.11(0.03)	0.13(0.04)	0.17(0.05)
Total	99.05	99.02	98.85	98.63
Microlites	n.a	n.a	39.07(2.71)	n.a

Table 2.3: Composition of minerals in lavas and volcanic bombs

Location	AN	Karymsky	Karymsky	Karymsky	Karymsky
Type [a]	Plagioclase	Plagioclase (O)	Plagioclase (R)	Plagioclase (C)	Plagioclase (P)
n	35	225	148	186	45
SiO_2 [b]	47.76(1.49)	55.68(0.99)	55.18(1.69)	48.24(1.14)	54.58(0.88)
Al_2O_3	33.49(1.13)	28.28(0.65)	28.44(1.07)	33.05(0.71)	28.88(0.58)
FeO*	0.73(0.19)	0.63(0.08)	0.67(0.08)	0.74(0.10)	0.75(0.13)
CaO	16.95(1.07)	10.80(0.63)	11.18(1.17)	16.30(0.79)	11.63(0.65)
K_2O	0.04(0.02)	0.17(0.04)	0.16(0.04)	0.05(0.03)	0.17(0.10)
Na_2O	1.72(0.53)	5.26(0.40)	5.08(0.66)	2.14(0.45)	4.82(0.33)
Total	100.67	100.82	100.72	100.53	100.83

Location	AN	Karymsky	AN	Karymsky
Type	CPx	CPx	OPx	OPx
n	83	102	4	39
SiO_2	51.55(0.49)	51.84(0.60)	54.16(0.43)	53.63(0.88)
Al_2O_3	2.74(0.18)	2.21(0.67)	1.54(0.11)	0.84(0.13)
TiO_2	0.49(0.07)	0.57(0.11)	0.23(0.03)	0.29(0.09)
FeO*	7.68(0.52)	9.75(0.87)	15.51(0.44)	19.53(1.28)
CaO	20.98(0.40)	20.28(0.55)	1.75(0.12)	1.70(0.30)
MnO	0.21(0.07)	0.39(0.11)	0.37(0.07)	0.79(0.18)
MgO	15.78(0.30)	14.78(0.43)	26.02(0.22)	23.29(1.38)
Na_2O	0.27(0.05)	0.32(0.05)	n.d.	n.d.
Total	99.67	100.30	99.64	100.16

[a] Compositions of Karymsky plagioclase phenocrysts reported separately for oscillatory zoned plagioclases (O), rims (R) and cores (C) of rimmed plagioclases, and sodic patches in calcic cores (P). CPx- clinopyroxene, OPx - orthopyroxene.

[b] The average of n analyses (in wt. %) is given together with the standard deviation (number in brackets), with all Fe reported as FeO for all minerals except magnetites.

n.d. – not detected.

Table 2.3: Continued

Location	AN	Karymsky		AN	Karymsky
Type	Olivine	Olivine		Magnetite	Magnetite
n	67	96	n	9	48
SiO_2	38.34(0.45)	37.44(0.52)	FeO	34.24(0.68)	38.40(1.09)
Al_2O_3	n.d.	n.d.	Fe_2O_3	47.02(0.93)	43.88(1.91)
TiO_2	n.d.	n.d.	TiO_2	8.99(0.45)	12.02(0.91)
FeO*	22.34(1.88)	24.65(2.36)	Al_2O_3	4.25(0.20)	2.63(0.24)
CaO	0.17(0.03)	0.14(0.02)	MgO	3.41(0.29)	2.39(0.42)
MnO	0.37(0.10)	n.d.	MnO	0.36(0.05)	0.59(0.12)
MgO	38.79(1.47)	36.42(1.95)	Cr_2O_3	0.78(0.50)	0.05(0.03)
Total	100.08	99.22	Total	99.18	100.04

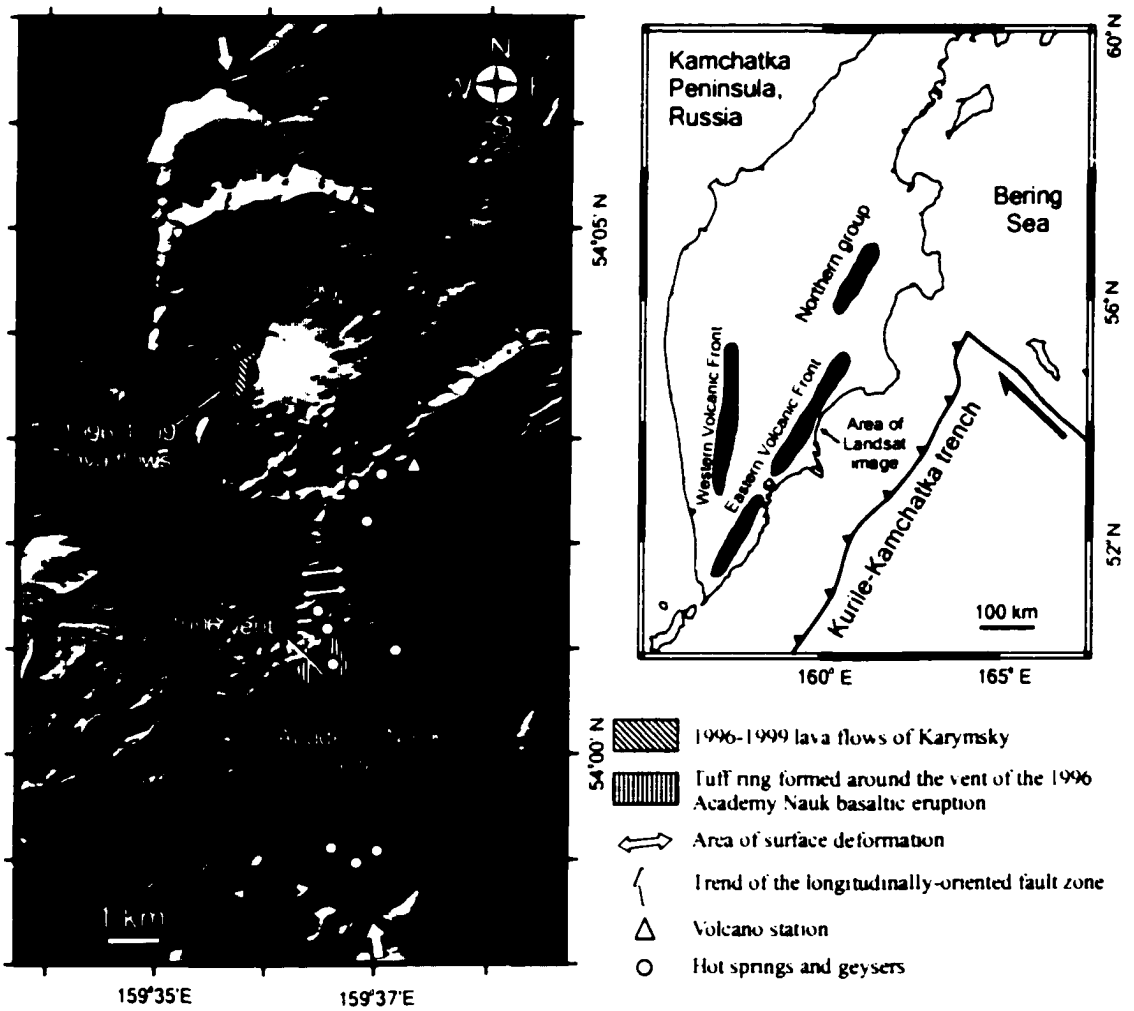

Figure 2.1 Landsat-4 image of Karymsky volcano and Academy Nauk caldera. Karymsky volcano occupies a caldera formed 7900 yr. BP. Academy Nauk caldera (~40,000 yr. BP) is centered 9 km south of it, on the same longitudinally-oriented fault zone, which trend is indicated by arrows. Dotted lines contour rims of Karymsky (north) and Academy Nauk (south) calderas.

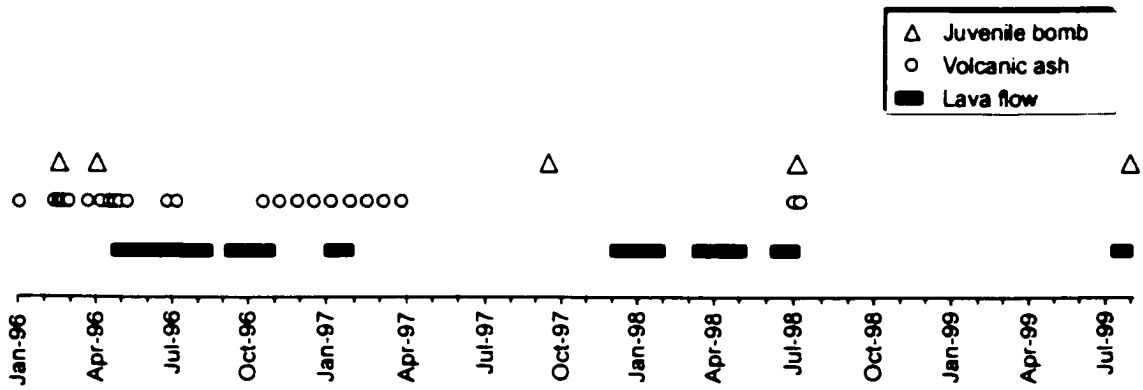

Figure 2.2 Samples of pyroclastics of Karymsky versus time of their eruption. Length of horizontal bars corresponds to an approximate time of the effusion of individual lava flows, which were sampled afterwards.

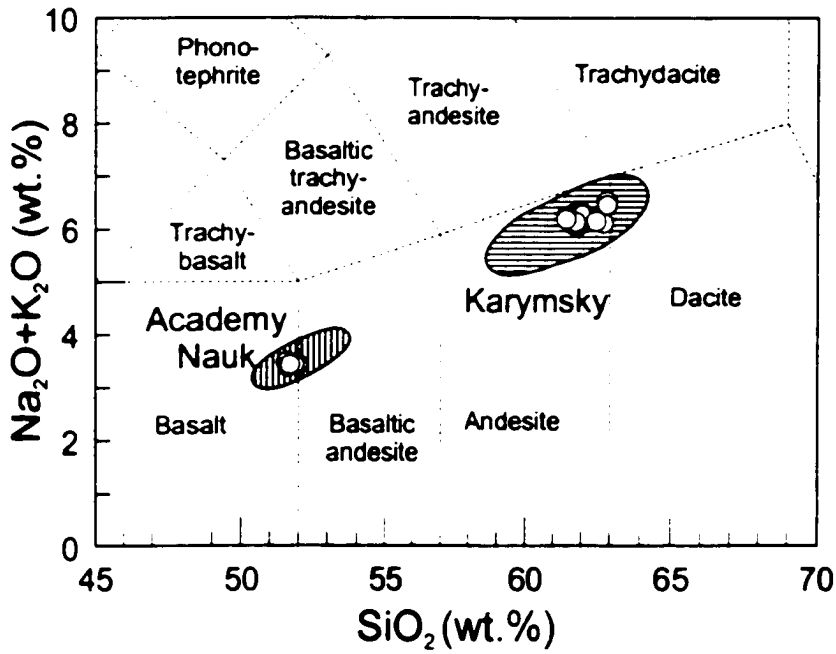

Figure 2.3 Total alkalies versus silica for Karymsky andesite and Academy Nauk basalt. Shaded areas correspond to mafic (vertical hatching) and intermediate (horizontal hatching) magmas erupted at Karymsky and Academy Nauk since 5,300 yr. BP (data from Braitseva et al. (1989) and Ivanov (1996)). Symbols represent compositions reported in this paper.

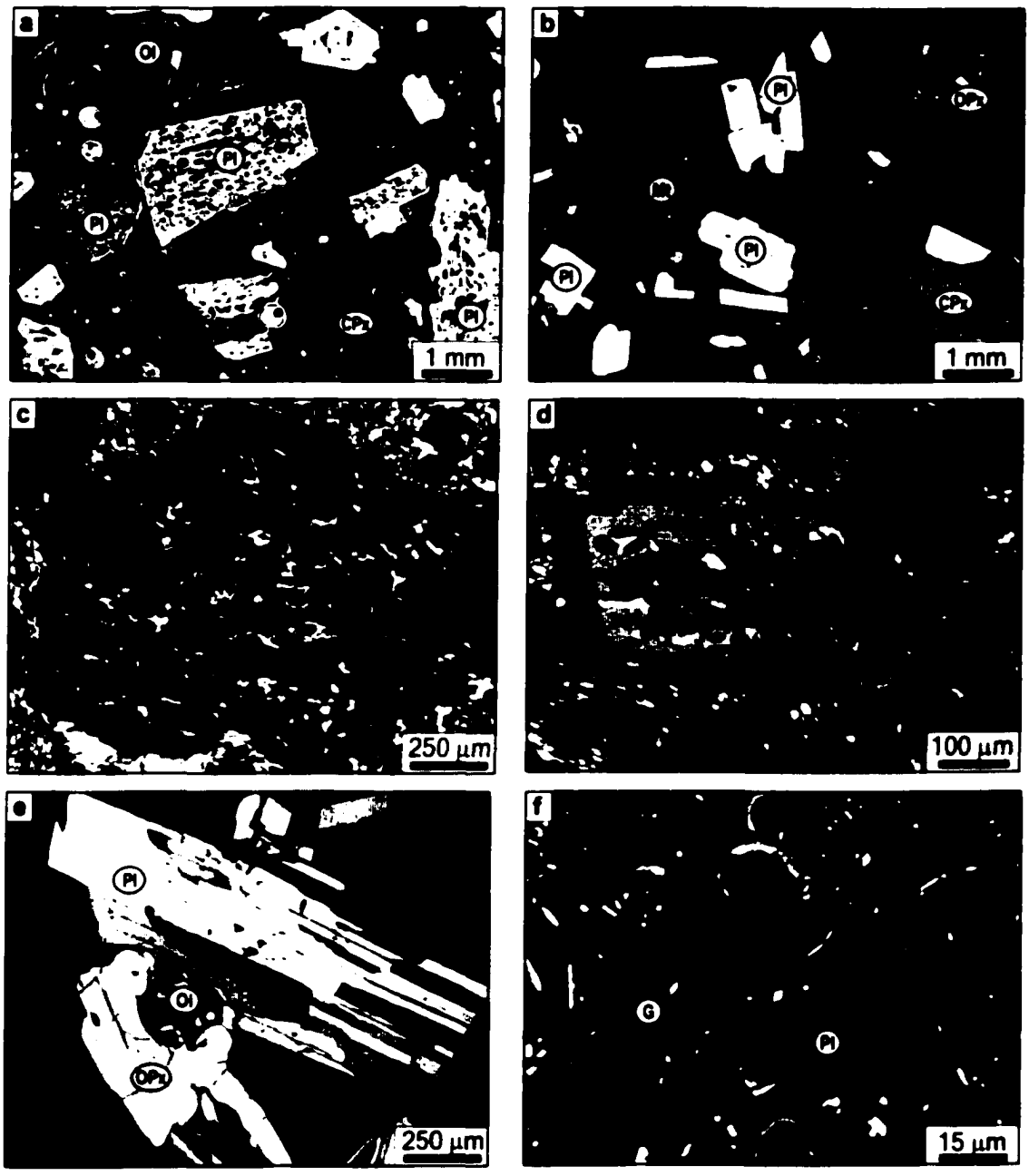

Figure 2.4 Photomicrographs of (a) Academy Nauk basalt and (b) Karymsky andesite showing phenocrysts of plagioclase (Pl), clinopyroxene (CPx), orthopyroxene (OPx), olivine (Ol) and magnetite (Mt) in transparent light. Back-scattered electron images (BSE) of (c) plagioclase phenocryst in Academy Nauk basalt and (d) rimmed plagioclase phenocryst in Karymsky andesite. Black areas are voids. (e) Photomicrograph of olivine xenocryst in the plagioclase-orthopyroxene aggregate. Note that olivine is attached to the calcic core of the plagioclase phenocryst (light is polarized). (f) BSE image of volcanic ash of Karymsky erupted on February 28, 1996 showing abundant plagioclase (dark) and pyroxene (bright) microlites in the matrix glass (G).

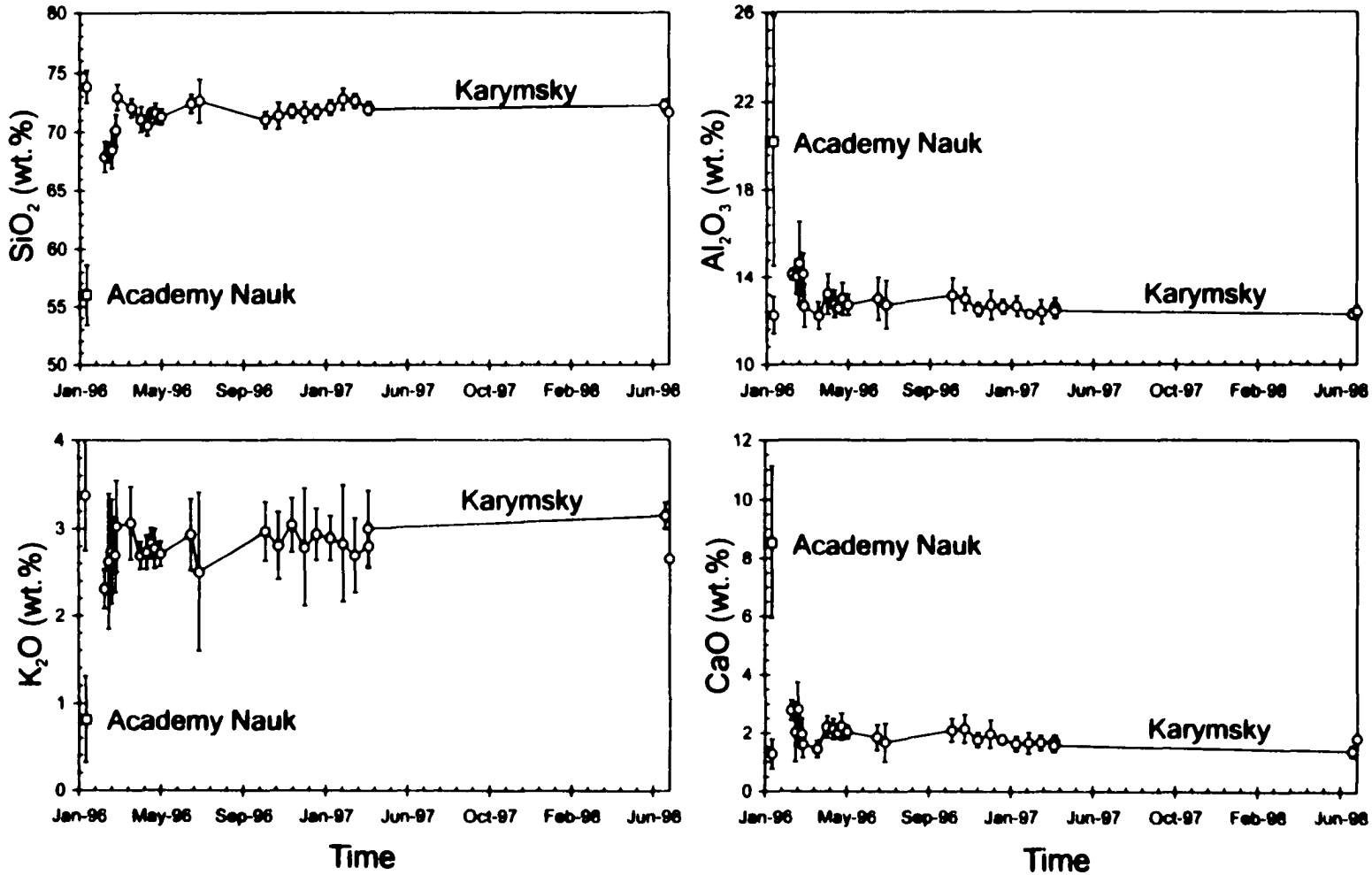

Figure 2. 5 Composition of volcanic ash glass plotted against the date of eruption. Melt of Karymsky andesite, which erupted in February 1996, was the most mafic. Error bars correspond to the standard deviation in electron microprobe analyses of matrix glass in the individual samples of volcanic ash.

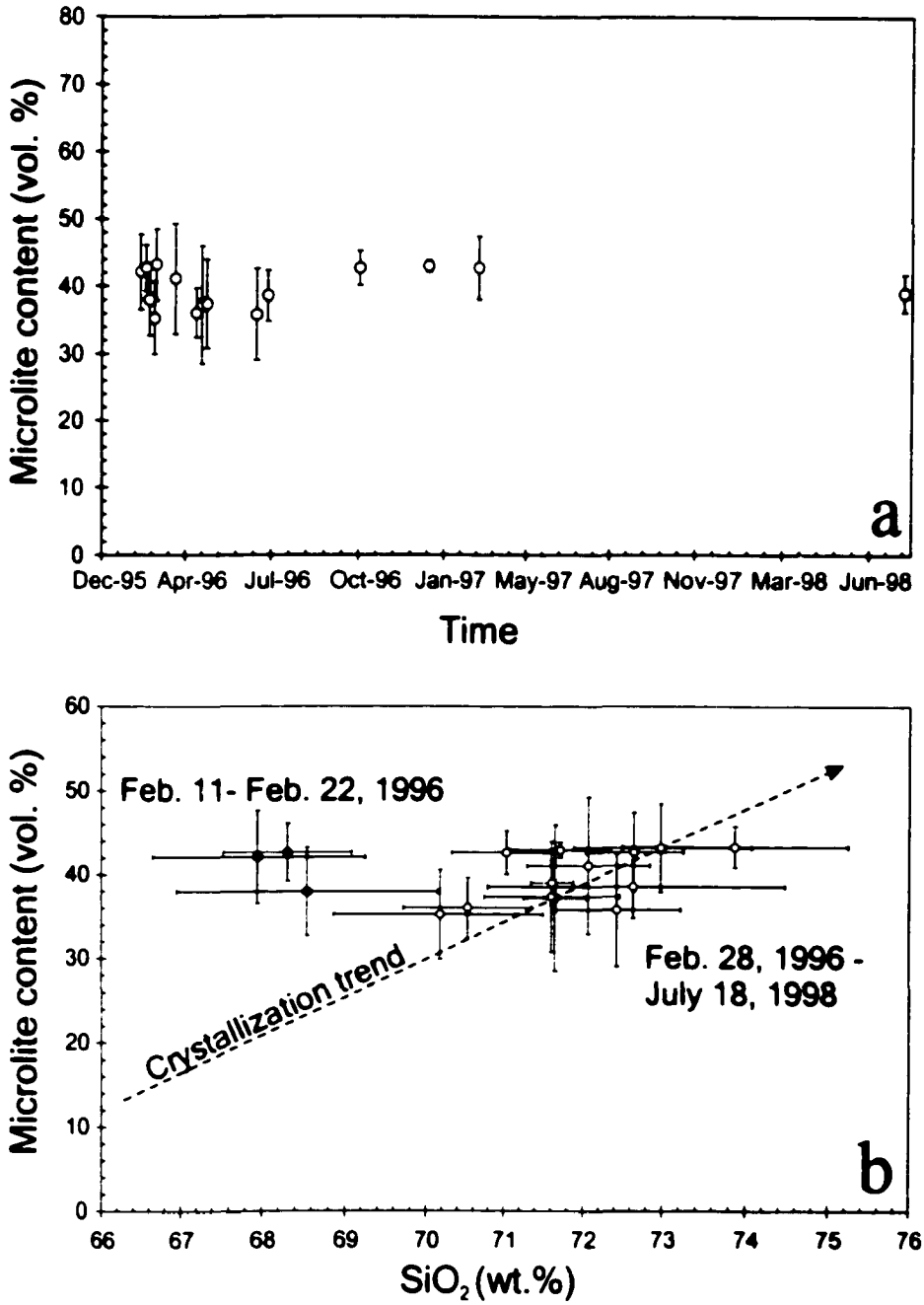

Figure 2. 6 (a) Variations of microlite content in Karymsky volcanic ash. (b) Microlite content versus SiO_2 in Karymsky volcanic ash. The difference in composition of the ash erupted during February 11-22, 1996 from the crystallization trend requires an addition of mafic component to the andesite at the beginning of eruption (see discussion in the text).

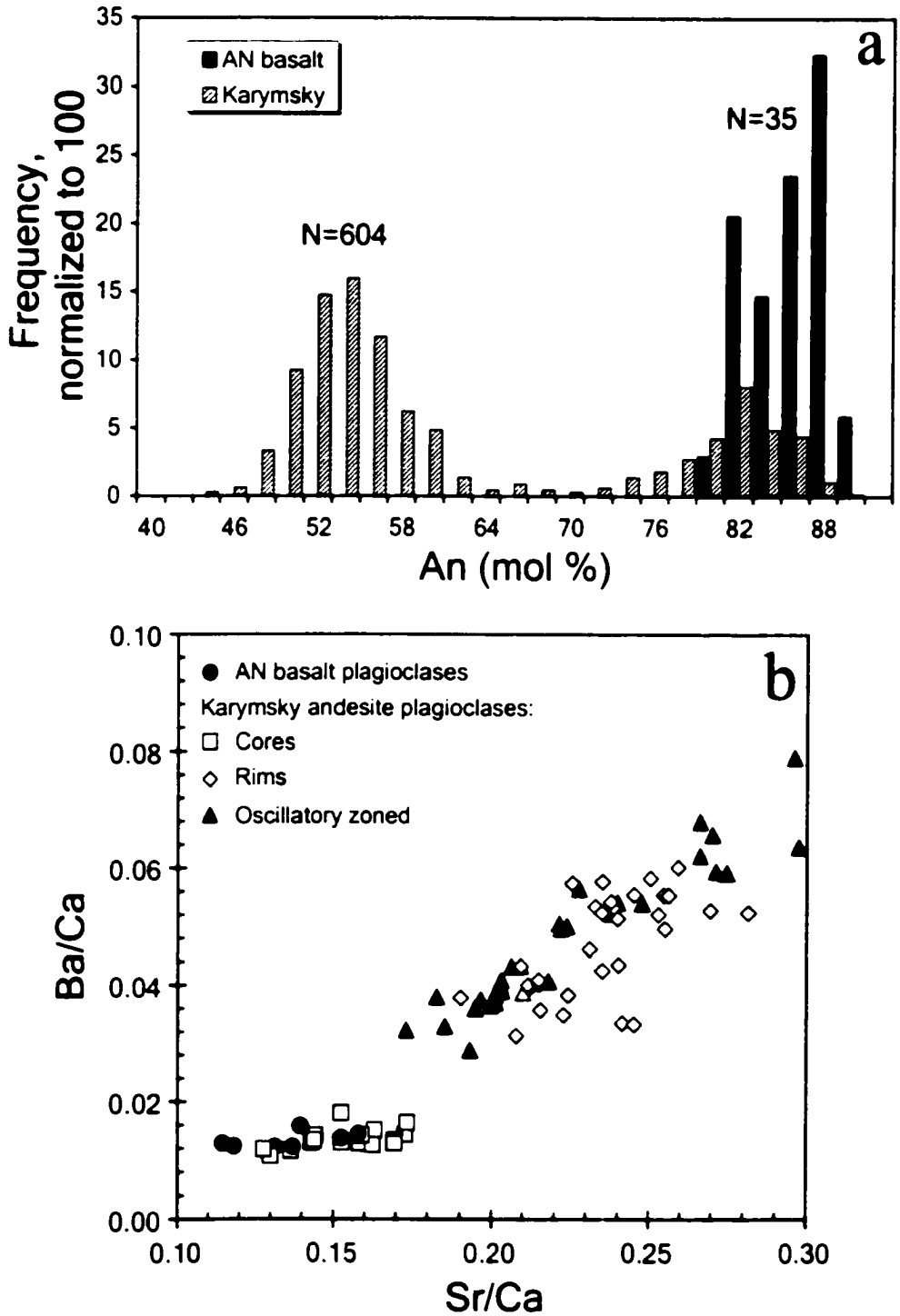

Figure 2.7 (a) Electron microprobe and (b) LA-ICP-MS data for plagioclase phenocrysts in Karymsky andesites and Academy Nauk basalts. Composition of Karymsky plagioclases is bi-modal due to the presence of calcic cores, which match Academy Nauk plagioclases in terms of major and trace elements.

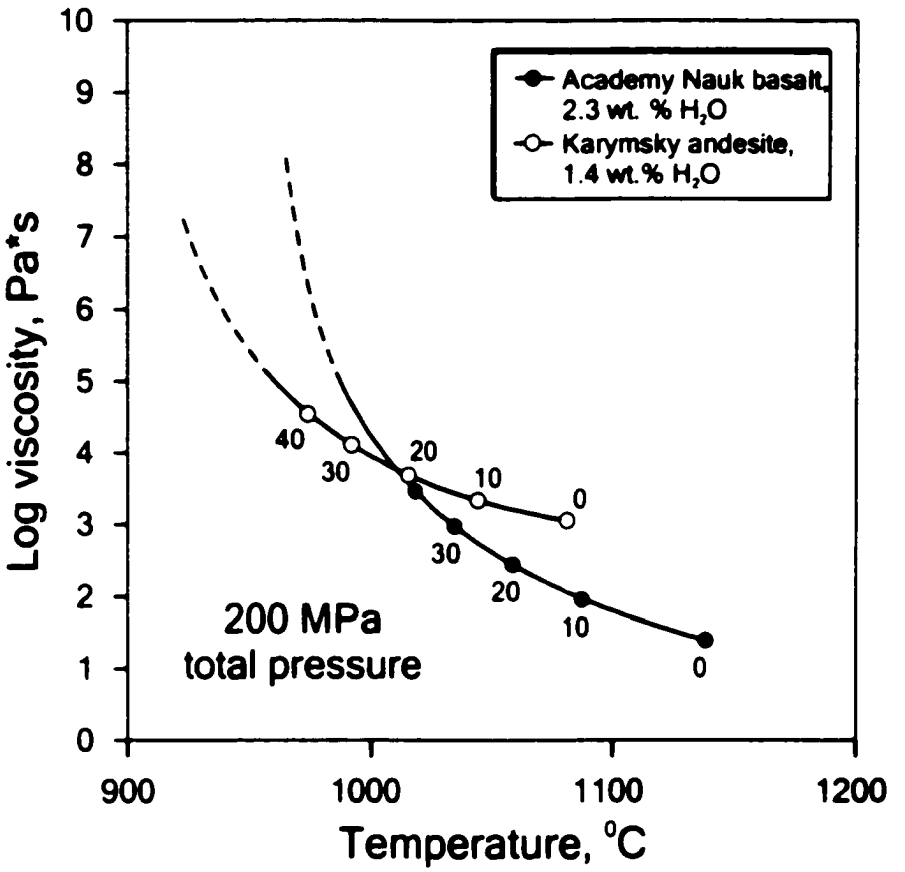

Figure 2.8 Variations of viscosity versus temperature in Academy Nauk basalt and Karymsky andesite, which crystallize isobarically at 200 MPa. Viscosity is calculated using CONFLOW algorithm (Mastin and Ghiorso, 2000). Numbers correspond to volume contents of solid phases, as predicted by COMAGMAT (Ariskin, 1999).

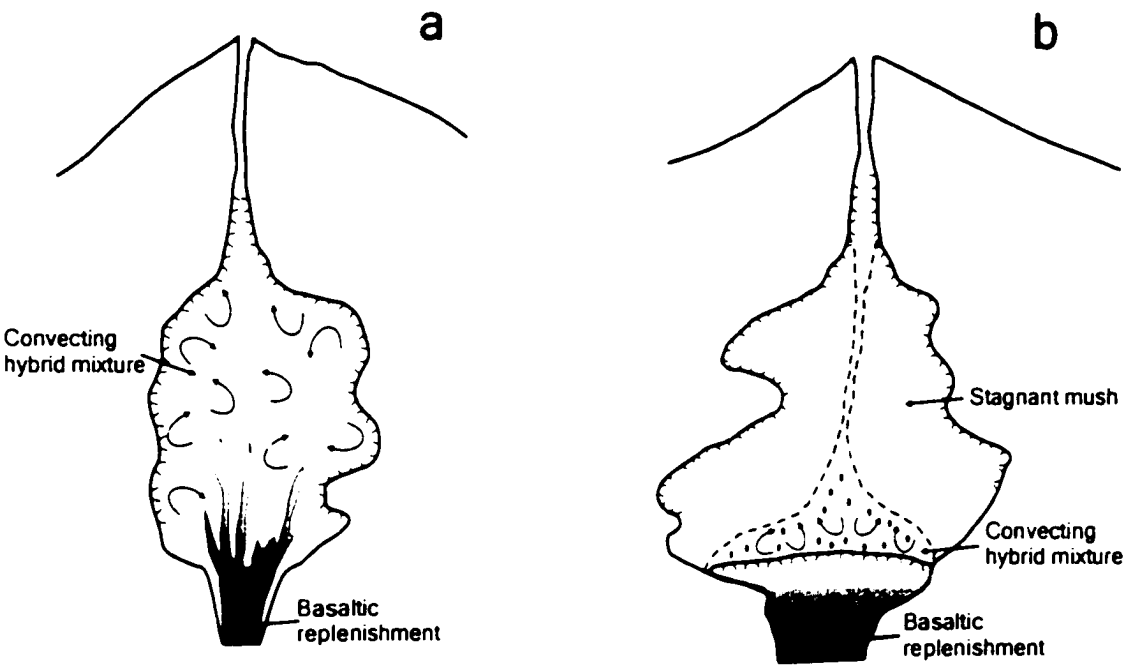

Figure 2.9 Schematic cartoon illustrating different mixing scenarios for crustal reservoirs with (a) short and (b) long intervals between basaltic replenishments. See text for discussion.

Chapter 3. Calcic cores of plagioclase phenocrysts in andesite from Karymsky volcano: Evidence for rapid introduction by basaltic replenishment*

ABSTRACT

Calcic cores in plagioclase of Karymsky andesite of the 1996–2000 cycle texturally and compositionally (both trace- and major-elements) mimic the plagioclase phenocrysts of basalt erupted 6 km away at the onset of the cycle. These observations support the view that simultaneous eruption of andesite and basalt at Karymsky in the beginning of the cycle represents an example of replenishment and eruption triggering of an andesitic reservoir. Homogeneity of andesitic output occurred within two months. This suggests to us that blending of injected basalt into reservoir magma was thorough and rapid.

INTRODUCTION

Mixing of compositionally distinct magmas is well documented by the presence of enclaves and zoning of phenocrysts in igneous rocks (Eichelberger, 1978; Davidson et al., 2001; Singer et al., 1995). Different approaches, including physical and numerical modeling, have been offered to test the possibility of mixing and to describe its mechanism (e.g. Sparks and Marshall, 1986; Bergantz and Breidenthal, 2001). The

---

* Published under the same title with authors Pavel E. Izbekov, John C. Eichelberger, Lina C. Patino, Thomas A. Vogel and Boris V. Ivanov in *Geology (Boulder)*, v.30 (9), p. 799-802.

question, which is crucial for validating such models, is how fast can the compositionally distinct magmas mix? Unfortunately, there are few volcanic eruptions, where a detailed historical record can be used to constrain the dynamics of mixing (e.g. Nakamura, 1995).

In this paper, we present results of a textural and compositional study of plagioclases from andesite and basalt that erupted simultaneously at Karymsky volcanic center beginning in January 1996. Textural observations coupled with electron-probe microanalysis (EPMA) and laser-ablation inductively coupled plasma–mass spectrometry (LA-ICP-MS) indicate that calcic cores in plagioclases of Karymsky andesites are identical to plagioclase phenocrysts of basalts. We argue from the surface expression of the system, eruption record, and petrology that the sequence represents interception of an andesitic magma pod by a rising basalt dike that produced a uniform mixture within 2 months.

GEOLOGIC FRAMEWORK

Karymsky volcano and Academy Nauk caldera belong to a chain of volcanoes, calderas, and maars, the location of which is controlled by a local north-trending fault (Fig. 3.1). Magmas erupted during Holocene time along the fault varied in composition from basalts to rhyolites, with andesites and dacites being the most voluminous. Basalt eruptions in the Karymsky–Academy Nauk area have been rare and subordinate in volume.

Karymsky is a ~5300-yr-old andesitic stratovolcano located in the center of a ~7900-yr-old caldera (Braitseva and Melekestsev, 1991). During the past 500 yr, the

volcano has been in a state of frequent but intermittent activity. In the twentieth century Karymsky had seven periods of continuous Strombolian eruptive activity, each lasting from 4 to 15 yr (Ivanov, 1970).

Academy Nauk caldera is centered 9 km south of Karymsky on the same fault system. Since its caldera-forming event (ca. 40,000 yr B.P.), the volcanic activity within the caldera was confined to phreatomagmatic eruptions of basalt, which have occurred at least twice since 5000 yr B.P. (Belousov and Belousova, 2001). These eruptions formed distinctive maars in the northern and southern parts of the caldera.

SIMULTANEOUS ERUPTION OF ANDESITE AND BASALT IN 1996

The most recent episode of volcanic activity at Karymsky started on January 2, 1996, after 13 yr of dormancy. It began with simultaneous eruption of andesite from the central vent of Karymsky volcano and basalt from a new vent, which formed in the northern part of Academy Nauk caldera (Fig. 3.1). The phreatomagmatic eruption of the Academy Nauk center was over in less than 18 h, whereas Vulcanian and then low-level Strombolian eruption of Karymsky continued for 4 yr. Omitting the details of the eruption, which can be found in Muravyev et al. (1998), we emphasize its main characteristics relevant to this study.

First, the magmas erupted from neighboring vents had strongly contrasting bulk compositions. Academy Nauk vent produced basalt (52.2 wt% SiO_2), while Karymsky summit vent erupted andesite (62.4 wt% SiO_2). The latter was almost identical to andesites produced during previous periods of activity. The magmas were

compositionally distinct and lacked evidence of mechanical mixing (mingling), i.e., no mafic enclaves were found in andesites, nor were bands or blobs of andesite found in basalt, and no intermediate compositions were erupted.

Second, significant ground deformation occurred between eruptive vents. Cracks as long as 700 m were formed parallel to the north-trending fault (Leonov, 1998). The area of major ground cracks coincides with a maximum in west-east extension, reaching an amplitude of 2.33 m (Maguskin et al., 1998). Extension between eruptive vents occurred gradually, which is consistent with propagation of basaltic dike along the active fault. As Karymsky itself lies well within the domain of measurable extension, such a dike could have intercepted a crustal magma system beneath Karymsky.

Third, within two months of the onset of eruption, the composition of melt of Karymsky andesite, as recorded by glass in tephra, shifted toward a more mafic composition and then gradually returned to its original state and remained constant for the rest of the eruption. The large amplitude of the chemical shift in melt composition cannot be explained by variations in magma flux that yielded variable rates of syneruptive crystallization; the large chemical shift requires addition of a mafic melt to the original melt of the andesite (Eichelberger and Izbekov, 2000). Because the eruptive batches of Karymsky andesite magma are plagioclase-rich and chemically monotonous, they likely represent small episodic withdrawals from the same larger, well-stirred, crustal reservoir. The eruption of basalt coincident with the start of the most recent cycle is suggestive of eruptive triggering, and the early shift in melt composition is at least consistent with some contact between stored andesite and injected basalt.

The foregoing characteristics of eruption indicate that in 1996, at the beginning of a 4 yr cycle of activity, a crustal reservoir of Karymsky was replenished by basalt. Whether the replenishment led to a complete blending of basalt into andesite in a period of time as short as two months could not be determined unless xenocrysts of basaltic origin could be found in andesite. Plagioclase was chosen for tracing basaltic xenocrysts in andesite because (1) plagioclase is the dominant phase of both basalt and andesite, (2) plagioclases of basaltic and andesitic provenance should be significantly different in composition and thus easily distinguishable, and (3) diffusion rates in plagioclase are slow, so that compositions from the time of growth are preserved despite changes in physical conditions of the magma or composition of the coexisting melt (e.g. Grove et al., 1984).

ANALYTICAL TECHNIQUES

The major element composition of plagioclase phenocrysts was analyzed by using the Cameca SX 50 electron microprobe at the University of Alaska, Fairbanks. Analytical conditions were 15 kV accelerating voltage, 10 nA beam current, and 1–3 μm focused electron beam. Backscattered-electron (BSE) images of plagioclase phenocrysts were acquired in raster mode at 15 kV and 80–150 nA beam current.

Because Sr and Ba are the most abundant trace elements in plagioclases and because their partitioning behavior is well defined by analytical and experimental work (e.g., Blundy and Wood, 1991; Bindeman and Bailey, 1999), they were chosen for fingerprinting plagioclases of different provenance. Sr and Ba contents in multiple spots

along microprobe traverses of representative plagioclase phenocrysts were analyzed by using a Micromass Plasma ICP-MS coupled with a Cetac LSX 200 laser-ablation system at Michigan State University. The 266 nm Nd:YAG laser was focused to a 25 μm sampling spot size and propagated into the sample with a rate of 3 μm/s. The concentrations of Sr and Ba were calculated by using peak intensities of ^{88}Sr, ^{138}Ba, and ^{44}Ca calibrated against a NIST 612 glass standard and EPMA determinations of Ca in analyzed spots as outlined in Norman et al. (1996).

TYPES OF PLAGIOCLASE

Plagioclase phenocrysts make up 30-35 vol.% of Academy Nauk basalt and show little variation in composition or texture. The majority of plagioclase phenocrysts in Academy Nauk basalt are euhedral and have a coarse-sieved interior (Fig. 3.2a). The coarse-sieved texture is due to the presence of abundant melt inclusions, which vary from circular to elongate and irregular. The high concentration of inclusions suggests that they form a system of interconnected channels permeating the crystals' interiors. This coarse-sieved texture resembles that reproduced in decompression (Nelson and Montana, 1992) and heating (Johannes et al., 1994) experiments, where the texture results from dissolution rather than skeletal growth. Both melt inclusions and matrix glass are commonly vesicle- and microlite-rich, attributes that could be due to coupled syneruptive vesiculation and crystallization (Blundy and Cashman, 2001). The similarity of the melt inclusions in the plagioclase to the matrix glass and evidence of their syneruptive

vesiculation indicates that the system of interconnected melt channels within plagioclase phenocrysts was open with respect to the surrounding medium during magma ascent.

Compositions of plagioclase cores, rims, subphenocrysts, and microlites of Academy Nauk basalt are nearly constant at 80 to 90 mol% anorthite (An) (Figs. 3.2, 3.3a). EPMA profiles across phenocrysts show either oscillatory or, rarely, normal zoning. Sr/Ba ratios of basaltic plagioclases are high and form a distinctive isolated cluster in composition space (Fig. 3.3b).

Plagioclase phenocrysts form 20–25 vol.% of Karymsky andesite. Unlike the plagioclase in basalt, they show significant variations in composition and texture. The majority of the plagioclases occur in two distinctive populations: (1) oscillatory-zoned sodic plagioclases (An_{48-62}) and (2) rimmed plagioclases, characterized by the presence of calcic cores (An_{76-90}) and sodic rims (An_{48-62}). Oscillatory-zoned plagioclases make up 70%–80% of all phenocrysts and the majority of subphenocrysts (Fig. 3.2b). Their EPMA profiles usually show fine oscillation superimposed on a weak normal zoning; small jumps in An content occur at major dissolution surfaces. Sr/Ba ratios of oscillatory-zoned plagioclases of the andesite are significantly lower than in plagioclases of the basalt, forming an isolated cluster without any overlap on a composition diagram (Fig. 3.3b).

Rimmed plagioclases occurred in Karymsky andesite throughout the 1996–2000 cycle of activity and were present in previously erupted andesite batches as well. They consist of euhedral calcic cores, often with coarse-sieved interiors, and oscillatory-zoned rims. The texture of calcic cores mimics that of plagioclase in basalt, but unlike the latter,

voids are filled with sodic plagioclase and melt, rather than with melt only, forming a texture frequently referred as "patchy" zoning (Vance, 1965).

Both EPMA and LA-ICP-MS analyses show that the andesitic plagioclases' calcic cores are compositionally similar to plagioclases in basalt (Figs. 3.3a, 3.3b), whereas compositions of rims outside and "patches" inside calcic cores are close to the composition of oscillatory-zoned plagioclases. A BSE image and an EPMA profile of a rimmed plagioclase in andesite (from a volcanic bomb erupted 2.7 yr after the beginning of eruption) show an abrupt boundary between core and rim, where composition changes from An_{80} to An_{52} within 30 μm distance (Fig. 3.2c). Its rim lacks major dissolution surfaces and associated jumps in An content, which are characteristic for large oscillatory-zoned plagioclases.

ORIGIN OF CALCIC PLAGIOCLASES IN KARYMSKY ANDESITE

The presence of calcic cores in plagioclases of Karymsky andesites and their striking similarity to plagioclases in simultaneously erupted basalt raises three questions. First, could the calcic cores crystallize in andesite, or were they introduced from a more mafic source as xenocrysts? Second, if the latter is correct, what is the possibility that their source magma was compositionally similar to Academy Nauk basalt? Third, have the calcic cores been introduced into the andesite by the same basalt as erupted in Academy Nauk caldera at the beginning of 1996–2000 cycle of eruptive activity?

Experimental data on equilibrium crystallization in magma systems led to the development of numerical models that can be used for simulating phase equilibria in

crystallizing andesites and basalts. One of them--COMAGMAT (Ariskin, 1999)—was used here for evaluating the possibility that calcic cores could represent an early stage of crystallization of Karymsky andesites at higher temperature, pressure, and, in general, lower crystallinity. The results of calculations show that in a magma with the bulk chemical composition of Karymsky andesite, the An content of plagioclase would not exceed 48–52 mol% at pressures of 0.1–200 MPa, temperatures of 800–1300 °C, and water contents of 0–4 wt%. The predicted composition of plagioclase is in close agreement with the composition of oscillatory-zoned plagioclases and rims of calcic-cored plagioclases (An_{48-62}). Plagioclase as calcic as $An_{\sim 90}$ could not crystallize in equilibrium in andesite magma at any plausible pressure, temperature, and water content and thus must have been introduced to the Karymsky andesite magma from a more mafic source.

Chemically homogeneous An_{80-90} plagioclase is the dominant mineral phase of Academy Nauk basalt, thus implying that this plagioclase crystallized in magma of Academy Nauk basalt chemistry, an inference supported by the COMAGMAT model. Hence, the compositional similarity of the calcic cores in Karymsky andesite to plagioclase from Academy Nauk basalt suggests that they crystallized at comparable *P-T* conditions in a basaltic magma of similar chemistry. In addition, the textural similarity of calcic plagioclase cores in andesite and plagioclase in basalt, i.e., their coarse-sieved interiors, suggests that the cores were subjected to the same process of dissolution prior to incorporation into andesite magma, perhaps linked to the decompression of ascending basalt (Coombs et al., 2000; Nelson and Montana, 1992). We conclude that the calcic

plagioclase cores in Karymsky andesite followed the same *P-T* path as plagioclase phenocrysts in Academy Nauk basalt, except that they become incorporated in Karymsky andesite prior to eruption.

Similarity to plagioclases in Academy Nauk basalt, however, does not necessarily imply that xenocrysts of calcic plagioclase were introduced to the andesite in 1996. Although characteristics of the 1996 eruption make it reasonable to suggest that this interpretation might be the case, calcic cores occur in plagioclases of earlier eruptions of Karymsky. If these eruptions were triggered by basaltic recharges that did not vent directly to the surface and the invading basalts had the same chemical and mineral compositions as Academy Nauk basalt, as seems plausible, then additional evidence is required for identification of those xenocrysts introduced by 1996 replenishment.

Chemical variations, texture, and width of rims of calcic-cored plagioclases might be used to distinguish calcic cores introduced by the most recent basaltic recharge from those previously introduced. Large oscillatory-zoned plagioclase crystals, which were present in the andesite from the beginning of the 1996–2000 eruption (Fig. 3.2b), exhibit multiple 6%–10% jumps in An content associated with major dissolution surfaces. If, as seems likely, the outermost one formed in 1996, the inner jumps are most likely linked to basaltic recharges that occurred prior to 1996. If already present in the Karymsky andesite, the rim of a calcic-cored plagioclase would have been subjected to similar disturbances, subsequent to the basaltic replenishment that introduced its calcic core to the andesite magma. The absence of major dissolution surfaces and associated increases

in An content in the rim (Fig. 3.2c) suggests to us that the calcic core of the phenocryst was introduced by the most recent basaltic replenishment.

Width of the rim may also be used as a criterion for distinguishing between the most recently introduced xenocrysts and the older ones by assuming plausible growth rates. Although we did not attempt to quantify variations in rim width with time of eruption, rims of plagioclases in andesites erupted 2–4 months after the beginning of eruption do appear to be smaller compared to ones erupted 2–3 yr after that. Of course, apparent width is also a function of a crystal's orientation in thin section, i.e., the observed width is equal or greater than the actual width, and therefore an inferred growth rate will be equal to, or greater than, the actual growth rate. If the calcic core of plagioclase shown in Figure 3.2c was introduced to the andesite magma in January 1996, then the 200-μm-wide sodic rim of this phenocryst was formed during the following 2.7 yr. This scenario requires the maximum plagioclase growth rate in the Karymsky reservoir to be on order of 2.5×10^{-9} mm/s, which is consistent with growth rates determined experimentally (e.g. Hammer and Rutherford, 2002). Thus, in the 1996–2000 Karymsky eruption, the calcic cores in plagioclase crystals with rims characterized by absence of major dissolution surfaces and associated jumps in An content may well have been introduced to the andesite system by the same basalt that erupted in Academy Nauk caldera in January 1996.

IMPORTANCE OF THE KARYMSKY CASE

Micrometer-scale major and trace element data provide a fingerprint for phenocrysts of different origins. Academy Nauk basalt carrying plagioclase with distinctively high An contents and Sr/Ba ratios was apparently injected into the andesite magma system beneath Karymsky in the beginning of the 1996–2000 eruptive cycle. Homogeneity of andesite erupted by late February 1996 suggests to us that thorough mixing of injected basalt and andesite occurred in a period of time as short as two months. Perhaps the rapid and effective blending was facilitated by an only modest contrast in viscosities and temperatures between the magmas and by a vigorous fluid dynamic regime in Karymsky reservoir. In this respect, Karymsky is a well-mixed end member case that reflects the short recurrence interval of recharges to the system. In contrast, Trident volcano in Alaska may represent an intermediate case, where both "clotting" and direct mixing occurs (Coombs et al., 2000), and Soufriere Hills in Montserrat – a poorly-mixed end member case, where clotting along is dominant (Murphy et al., 2000).

ACKNOWLEDGMENTS

This work was supported by the Volcano Hazards Program of the U.S. Geological Survey through the Alaska Volcano Observatory. Additional funding for field trips to Karymsky was provided by the Russian Foundation for Basic Research, grant 99-05-65495. Comments by George Bergantz, Jon Davidson, Ben A. van der Pluijm, as well editing by Anika Burkard significantly improved manuscript.

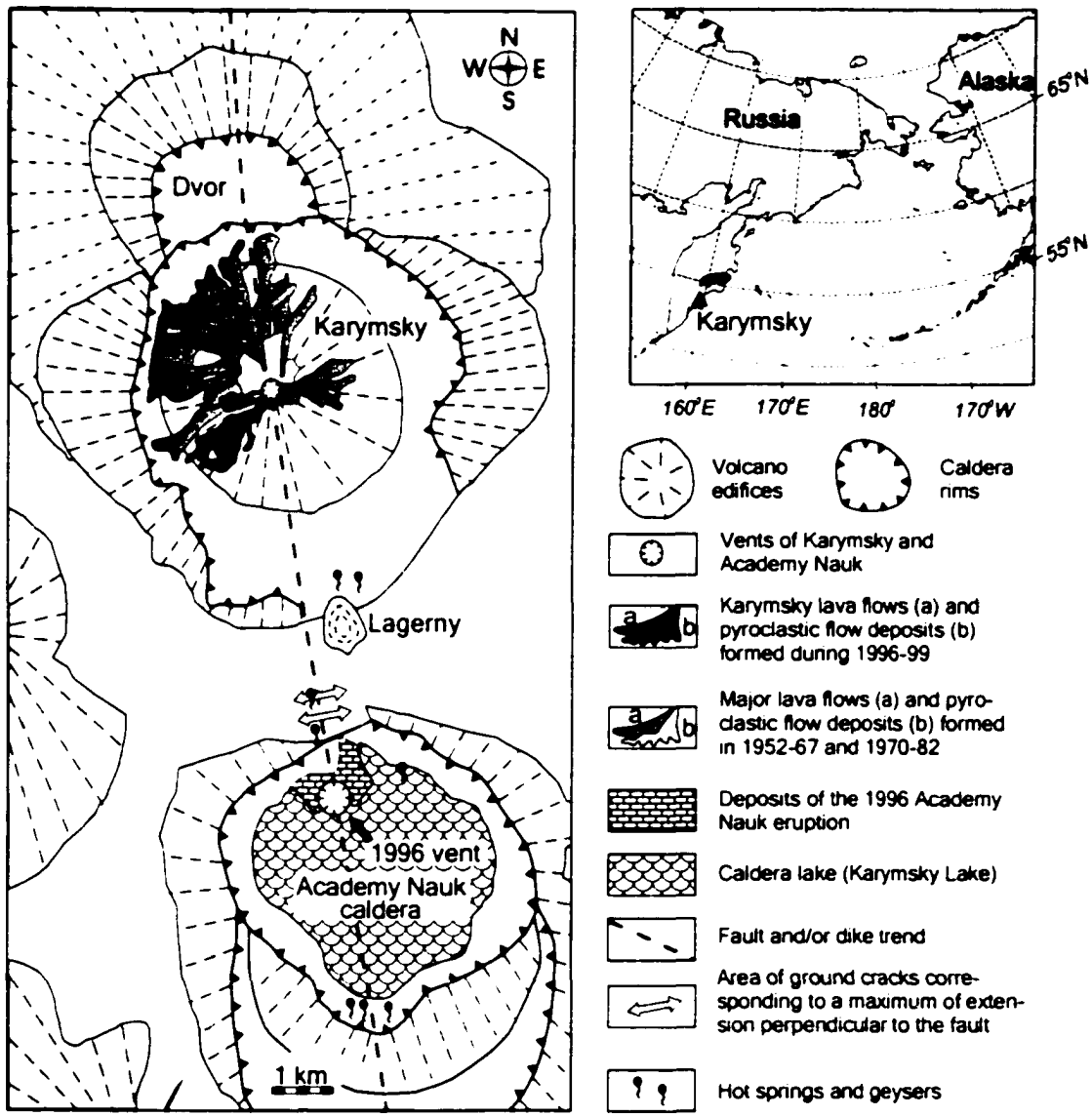

Figure 3.1 Generalized map of Karymsky and Academy Nauk. The 1996-2000 eruptive cycle started with simultaneous eruption of andesite from Karymsky summit vent and basalt from a new vent formed in northern part of Academy Nauk caldera.

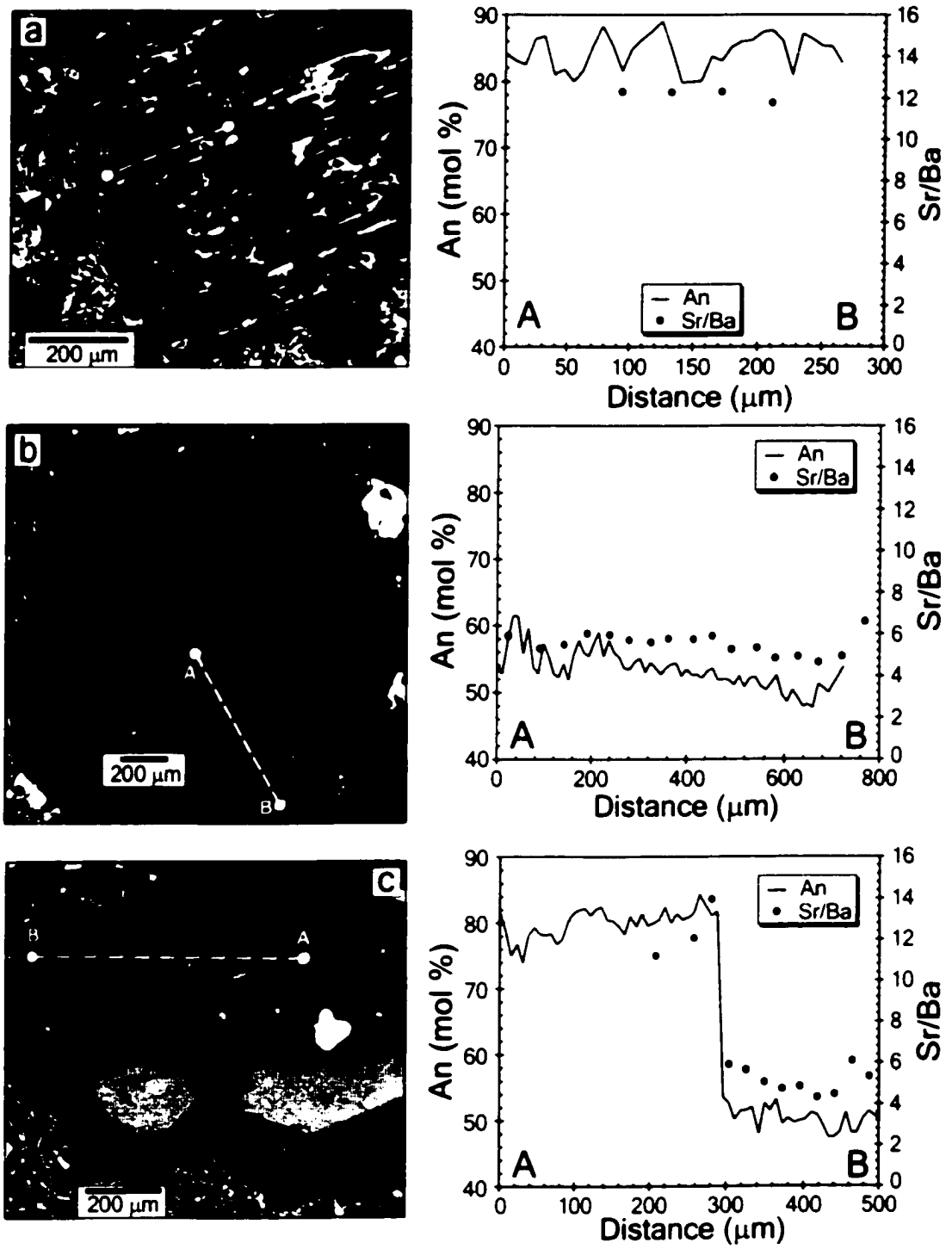

Figure 3.2 BSE images and compositional diagrams of representative plagioclases. (a) Coarse-sieved plagioclase phenocryst from Academy Nauk basalt erupted on January 2, 1996. (b) Oscillatory-zoned plagioclase from Karymsky andesite erupted on February 17, 1996. (c) Rimmed (calcic-cored) plagioclase from Karymsky andesite erupted in July 1998.

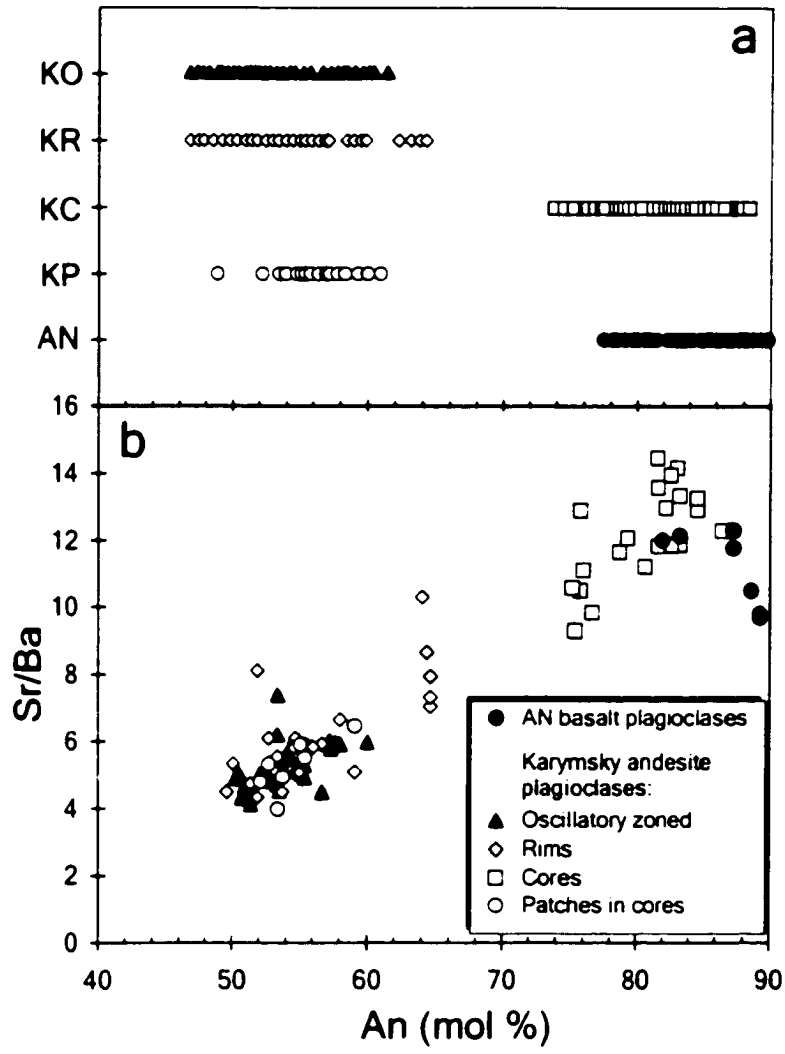

Figure 3.3 Compositions of plagioclases in Karymsky andesite (KO - oscillatory-zoned plagioclase, KR - rims of rimmed plagioclase, KC - cores of rimmed plagioclase, KP - patches in calcic cores) and in Academy Nauk basalt (AN).

Chapter 4. Comagmatic granophyre and dacite from Karymsky volcanic center, Kamchatka: experimental constraints for magma storage conditions*

ABSTRACT

Despite an approximately 30,000 year difference in age, two caldera forming eruptions at Karymsky volcanic center, Kamchatka, – Karymsky (7,900 yr. BP) and Academy Nauk (ca. 40,000 yr. BP) – produced two-pyroxene dacites with the same composition and mineralogy. Granophyric xenoliths of the identical whole-rock chemistry were found in basalts erupted within Academy Nauk caldera in 1996. Unlike the dacites, however, the granophyres are holo-crystalline and contain biotite and amphibole. Large amphibole phenocrysts contain rare inclusions of clinopyroxenes, which compositionally overlap with clinopyroxenes in the dacites. The Al content of the amphiboles suggests they crystallized at a pressure of about 100 MPa. Results of hydrothermal experiments and petrologic observations indicate that Academy Nauk and Karymsky dacites were last equilibrated at 883±19°C, 100±15 MPa and 871±19°C, 85±18 MPa, respectively, both at water-saturated conditions. The mineral assemblage of the granophyre is reproduced by isobaric crystallization of the dacite at 100 MPa, implying that the granophyres were sampled from the crystallized silicic reservoir that produced the caldera-forming eruption of Academy Nauk. Similar chemical compositions

---

* Submitted under the same title with authors Pavel Izbekov, James E. Gardner and John C. Eichelberger to the Journal of Volcanic and Geothermal Research.

of Karymsky and Academy Nauk dacites indicate that both were derived from the same crustal-level source. The eruptive history of the calderas can best be explained by two 10-12 km^3 dacitic batches that detached from a parental body situated in the lower crust, which then ascended to 3-4 km depth, re-equilibrated, and erupted.

INTRODUCTION

Nested or closely located calderas are common features of volcanic arcs, e.g., Taupo, New Zealand (Sutton et al., 1995), Aso, Japan (Lipman, 1967) and Ksudach, Russia (Volynets et al., 1999). They form as the result of repeated voluminous eruptions of silicic magmas at a single volcanic center. Different models have been proposed to explain the recurrence of silicic volcanism, ranging from those in which the magmas are fed from a single long-lived reservoir to those in which they are generated by fast, repetitive partial melting (Huppert and Sparks, 1988; Sparks et al., 1990). Volumes, depths, residence times, and histories of replenishments of individual magma systems linked to caldera-forming eruptions vary significantly from one volcanic center to another, and thus each case must be considered on an individual basis.

This paper presents results of a petrologic and phase-equilibria experimental study, which provides a basis for understanding the magma system at Karymsky and Academy Nauk, neighboring eruptive centers of the eastern volcanic front of Kamchatka. An important finding is that the dacites of the last two caldera-forming eruptions are exactly the same in composition, despite being separated in time by ~30,000 years. In addition, granophyric inclusions in basalts erupted in 1996 match the dacites in

composition. These findings raise two questions concerning the system. First, were the granophyric xenoliths sampled from the crystallized silicic reservoir that produced either of the calderas? And second, what magmatic process could repeatedly produce dacitic magma of exactly the same composition within ca. 30,000 years?

GEOLOGICAL BACKGROUND

Karymsky volcanic center is located in the middle of the eastern volcanic front of Kamchatka, approximately 120 km above the westward-dipping subducting slab of Pacific plate (Fig. 4.1). The center consists of several volcanoes and calderas, three of which – Karymsky, Maly Semiachek, and Academy Nauk – erupted in the 20th century. Volcanic activity at Karymsky volcanic center started about 2 Ma ago. Since that time the volume of erupted magmas has decreased significantly, whereas their composition progressed from strongly bi-modal to uni-modal, although the overall range of compositions remained the same - from basalts to rhyolites (Masurenkov, 1980).

Academy Nauk and Karymsky are two adjacent 5-km-diameter calderas, situated on a local longitudinally oriented fault zone (Fig. 4.1). Academy Nauk caldera is the second caldera formed in a succession of two alternating cone-building and caldera-forming events. The age of the caldera is believed to be ca. 40,000 yr. BP, based on the fission-track study of obsidian xenoliths from the basal plinian fall layer (Masurenkov, 1980). Following the last caldera-forming event, eruptive activity within the caldera has been restricted to phreatomagmatic basaltic eruptions, the most recent of which occurred in 1996 (Belousov and Belousova, 2001; Braitseva, 1998; Izbekov et al., 2002).

Basalts, which erupted in the northern part of Academy Nauk caldera in 1996, contained xenoliths of silicic rocks – granites, pumices, and altered tuffs - which were plucked from the walls of the conduit by the ascending magma. Grib (1998) suggested that some of the xenoliths, i.e. dacite-rhyolite pumices, could represent the silicic magma reservoir, which produced the caldera-forming eruption 40,000 yr. BP.

Karymsky caldera was explosively formed 7,900 yr. BP as the result of eruption of 5-7 km^3 of dacite with collapse of Pra-Karymsky volcano (Braitseva and Melekestsev, 1991). After a 2500-years-period of quiescence, activity within the caldera resumed with the eruption of basalts, and a stratocone of the modern Karymsky began to grow. The composition of erupted magma quickly changed to andesitic, and has remained almost constant for the last 500 years. Karymsky volcano, which now occupies most of the caldera, had 7 periods of intermittent eruptive activity in the 20^{th} century (Ivanov, 1970). The last period started in January 1996, simultaneously with basaltic eruption within Academy Nauk caldera, and continues at present.

SAMPLES AND TECHNIQUES

The sample of the Academy Nauk caldera-forming eruption (99IPE6) consists of pumice clasts collected from the basal Plinian fall deposit (Site no. 274 of Masurenkov, 1980). The sample of 7900 yr. BP Karymsky caldera-forming eruption (99IPE4) was collected from a 3-meter-thick layer of tightly packed pumice blocks, located in the middle of pyroclastic flow deposit (KPM unit of Braitseva and Melekestsev, 1991). Five samples of granophyric xenoliths, including 97IPE7, were collected from the top of the

lapilli-ash tuff ring formed by the 1996 basaltic eruption, located in the northern part of Academy Nauk caldera. In this study we used only the interiors of large, 0.3-0.4-meter, granophyric blocks, which show no signs of reaction with the host basalt.

Experimental techniques

Natural dacite pumices were crushed to a fine powder in order to be used as starting materials for hydrothermal experiments. An experimental run consisted of either natural powder or pre-run material plus water, contained in $Ag_{70}Pd_{30}$ tubes. The tubes (2 or 5 mm in diameter) were welded with an oxy-acetylene torch at one end. Between 30 and 450 mg of sample, plus a weighted amount of deionized water, were added. The amount of water added was sufficient to ensure that excess water vapor was present in each run. Finally, the open end of the tube was welded shut. Capsules were weighed before and after welding to ensure that no water was lost.

All experiments were run in externally heated, René-style pressure vessels with nickel filler rods, and water as the pressurizing media. Reaction between the Ni-alloy vessel, filler rod and the pressurizing water buffered oxygen fugacity of the run at an f_{O_2} of 0.5-1.0 log units above Ni-NiO buffer curve (Geschwind and Rutherford, 1992; Gardner et al., 1995). Pressure was monitored using a pressure transducer precise to ±0.1 MPa. Temperature was measured using chromel-alumel thermocouples precise to ±3°C.

Two sets of experiments were conducted. The first set constrained the pre-eruptive storage conditions of Academy Nauk and Karymsky dacites (Table 4.7). Pressures and temperatures for such experiments were chosen based on those estimated

using compositions of hornblende and Fe-Ti-oxides in our natural samples. Depending on the choice of starting material, experiments were either for "crystallization", which used a relatively "crystal-poor" aliquot of a previous run, or for "melting", which used a relatively "crystal-rich" aliquot. Many experiments were reversal, where two charges in separate capsules, one of which was a "crystallization" experiment and another a "melting", were run side-by-side at the same conditions and in the same pressure vessel, thus approaching crystal-melt-vapor equilibrium from two directions. The majority of experiments were run for 96 hours. Several low-temperature experiments were allowed to equilibrate for 360 hours.

A second set of experiments simulated isobaric crystallization of the dacites at 100 and 200 MPa (Table 4.7). In these experiments, a 450-mg charge of dacite was first equilibrated at near-liquidus, water-saturated temperatures. After quenching, the sample was extracted and part of it was prepared as a polished thin-section. The remaining material plus additional water was run again at the same pressure but at a lower temperature. Repeated several times, the experiments modeled sequential, step-wise crystallization of the dacite. This design allowed the runs to achieve equilibrium, as well as grow larger microlites while approaching the solidus. Most experiments in the second set were run for 96 hours.

Analytical methods

Whole-rock compositions (Table 4.1) were determined at Washington State University, using X-ray fluorescence spectrometry (major element oxides, Ni, Cr, V, Zr,

Ga, Cu and Zn) and Inductively coupled plasma mass spectrometry (REE, Ba, Th, Nb, Y, Hf, Ta, U, Pb, Rb, Cs, Sr and Sc). Analytical procedures and uncertainties are discussed in Nye et al. (1994). Modes of minerals and glass in the dacite pumices were calculated by mass balance using their whole-rock, mineral, and matrix glass compositions. The modes in granophyres were determined by point counting (1000 points) using a petrographic microscope.

Compositions of natural and synthesized minerals and glasses were obtained using the Cameca SX-50 electron microprobe at the University of Alaska Fairbanks (Tables 4.2-4.6, 4.8, 4.9). Quantitative analysis of glasses was performed using 15 kV accelerating voltage, 10 nA beam current, and a defocused beam (~10 μm diameter). In order to minimize Na migration, the count rate of Na was scanned through time and corrected using a built-in procedure (Devine et al., 1995). The composition of minerals was determined using similar analytical conditions, but with a focused beam.

The concentration of water in melt inclusions contained in natural pyroxene phenocrysts was estimated from either electron probe analyses using the "volatiles by difference" method (Devine et al., 1995), or Fourier transform infrared spectroscopy (FTIR) analysis completed at Menlo Park, following the analytical procedures described in Lowenstern et al. (1997). Precision and accuracy of electron probe analyses of melt inclusions were monitored by repetitive measurements of KN-18 glass standard during analytical sessions (Devine et al., 1995).

PETROLOGY

40,000 yr. BP Academy Nauk dacite

Dacite of the Academy Nauk caldera-forming eruption is highly vesicular and consists of 79 vol.% microlite-free matrix glass, 16 vol.% plagioclase phenocrysts, 3 vol.% orthopyroxene, 1 vol.% clinopyroxene, and 1 vol.% magnetite ± ilmenite and apatite (Fig. 4.3a). Matrix glass is rhyolitic (74.31±0.49 of SiO_2) and does not vary among pumice clasts by more than analytical uncertainty (Table 4.2).

Plagioclase phenocrysts are euhedral, and contain a fine, 3-10-μm-scale oscillatory zoning superimposed on an overall normal zoning. Despite variations in their interior compositions (An_{48-63}), all plagioclases have rims of the same composition (An_{47-51}; average of 5 grains). Phenocrysts of ortho- and clinopyroxenes are euhedral, unzoned, and contain abundant inclusions of glass and magnetite. Magnetite phenocrysts are ubiquitous, whereas ilmenites are rare. To analyze ilmenites, several pumices were crushed and a hand magnet was used to make a magnetic concentrate. One magnetite-ilmenite pair and several euhedral grains of ilmenite in contact with matrix glass were found. The compositions of magnetite and ilmenite in the pair are homogeneous, uniform, and in equilibrium according to their Mg and Mn contents (Bacon and Hirschmann, 1988). The individual ilmenite grains compositionally overlap that of the ilmenite contacting the magnetite.

Nine 20-40-μm vesicle-free glass inclusions in pyroxenes were analyzed by electron microprobe. When compared on an anhydrous basis, their compositions match

that of the matrix glass. The deficit in totals of glass inclusion analyses ranges from 3.8 to 4.9 wt.%, and averages at 4.3±0.4 wt.%.

7,900 yr. BP Karymsky dacite

The whole-rock composition of the dacite pumice of Karymsky caldera-forming eruption is the same as that of Academy Nauk dacite (Table 4.1; fig. 4.2). Karymsky dacite consists of 74 vol.% highly vesicular, microlite-free rhyolitic glass, 20 vol.% plagioclase phenocrysts, 2 vol.% clinopyroxene, 2 vol.% orthopyroxene, and 2 vol.% magnetite ± ilmenite and apatite (Fig. 4.3b). The matrix glass is more silicic in composition (75.62±0.39 wt.%), relative to that in Academy Nauk dacite (Table 4.2).

Plagioclase phenocrysts are euhedral, and show a fine oscillatory zoning superimposed on a normal zoning, similar to those in Academy Nauk dacite. The composition of Karymsky plagioclase is more sodic relative to that of Academy Nauk plagioclase, with cores of An_{43} to An_{50} and rims of $An_{44\pm1}$. Euhedral phenocrysts of ortho- and clinopyroxenes are homogeneous, and compositionally overlap with those in Academy Nauk dacite (Table 4.4). Magnetite is abundant, whereas only three ilmenite grains surrounded by glass were found in a magnetic concentrate. Compositions of magnetite and ilmenite are uniform and in equilibrium according to their Mg and Mn contents (Bacon and Hirschmann, 1988).

Pyroxene phenocrysts contain abundant glass inclusions, whose compositions overlap with that of matrix glass, on an anhydrous basis. The deficit in totals of the glass-inclusion analyses averages 3.6±1.3 wt.%. Three glass inclusions were also analyzed by

FTIR (2.52±0.06, 3.67±0.09, 5.07±0.14 wt.% of H_2O). CO_2 contents of the glass inclusions are below detection limit for FTIR (25 ppm).

Granophyric xenoliths

The whole-rock compositions of the granophyres are the same as those of the Karymsky and Academy Nauk dacites (Table 4.1; fig. 4.2). Granophyres are porphyritic (70 vol.% groundmass), holo-crystalline, and the phenocryst portion consists of 41 vol.% plagioclase, 20 vol.% orthoclase, 28 vol.% quartz, 4 vol.% hornblende, 6 vol.% biotite, and 1 vol.% magnetite ± clinopyroxene, apatite, and zircon. The most remarkable feature of the granophyres is the micrographic texture of their groundmasses, which is formed by regular, interlocking aggregates of quartz and feldspar (Fig. 4.3c).

Plagioclase phenocrysts are euhedral, normally zoned, and are often in optical continuity with fringes of groundmass plagioclase radiating from their rims. Interiors of large phenocrysts range in composition from An_{27} to An_{43}. Compositions of phenocryst rims and groundmass plagioclase overlap and average $An_{29\pm5}$. Orthoclase occurs commonly as an intergrowth with quartz in the groundmass, and ranges in composition from $An_1Ab_{41}Or_{58}$ to $An_1Ab_4Or_{52}$.

Hornblende occurs both as euhedral, compositionally homogeneous phenocrysts and as microlites in the groundmass. A few large phenocrysts of hornblende contain inclusions of clinopyroxene (Fig. 4.3d), the compositions of which are close to those of clinopyroxene in Academy Nauk and Karymsky dacites (Table 4.4). Hornblende is closely associated with biotite, which has an average composition of

$Annite_{31}Phlogopite_{6}$-$Siderophyllite_{2}$. Magnetite abounds and often contains exsolution lamella of ilmenite.

EXPERIMENTAL RESULTS

Because whole-rock compositions of Karymsky and Academy Nauk dacites are identical, phase equilibrium experiments were performed on Karymsky dacite as a proxy for both (99IPE4; table 4.1). Mineral-melt equilibrium was studied over a range of water-saturated pressures from 50 to 300 MPa and temperatures from 700 to 900° C (Fig. 4.4). Microlites crystallized in all experiments, being most abundant at low temperatures. Presence of euhedral microlites (Fig. 4.3e) and overlapping compositions of melt in reversal experiments indicated that compositional equilibrium was reached in all experiments, including those run for 96 hours. Plagioclase microlites are usually larger than ten microns, which allowed for quantitative microprobe analysis. Other crystal phases are usually 1-4 μm in size, limiting their analysis to qualitative identification.

Pyroxenes are the first phases to crystallize at near-liquidus conditions within the investigated pressure range (Fig. 4.4). Lower temperature causes precipitation of magnetite and ilmenite, and then plagioclase. Further crystallization follows two significantly different scenarios. At pressures below 100 MPa orthopyroxene, clinopyroxene, plagioclase, magnetite, and ilmenite crystallize simultaneously. Isobaric cooling at pressures above 100 MPa causes crystallization of hornblende and dissolution of orthopyroxene. Continued temperature decrease causes dissolution of clinopyroxene, and then crystallization of biotite and quartz. Orthopyroxene never grew in equilibrium

with hydrous minerals (Fig. 4.3f), similar to experimental results for the Toba Tuff (Gardner et al., 2002).

Residual melts in our experiments vary systematically in composition with pressure and temperature (Table 4.8). Concentrations of SiO_2 and K_2O increase, and concentrations of FeO, MgO, Al_2O_3 and CaO decrease, as temperature decreases isobarically (Fig. 4.5). Concentrations of SiO_2 and K_2O decrease, and concentrations of Al_2O_3 and CaO increase, as pressure increases isothermally. Concentrations of FeO and MgO in melt depend strongly on temperature, whereas their variations with pressure are not systematic.

Composition of plagioclase microlites in our experiments varies systematically with pressure and temperature (Table 4.9). Plagioclase becomes progressively more sodic with decreasing temperature and pressure (Fig. 4.6).

DISCUSSION

A very intriguing finding of this study is that the caldera-forming dacites of Karymsky and Academy Nauk have remarkably similar whole-rock compositions, despite their separation in time by ca. 30,000 years. Mineral assemblages of the dacites are also the same, although the compositions of phenocrysts and matrix glasses are conspicuously different. The granophyres have the same whole-rock composition as the dacites, but unlike the dacites they are holo-crystalline and contain a drastically different mineral assemblage.

In the following sections, the origin of the xenoliths is discussed first and then used in conjunction with glass inclusion data to argue that the dacitic magmas were water-saturated immediately prior to their erupting. Experimental and mineral data are then used to constrain the pre-eruptive pressures and temperatures for both dacitic magmas. Lastly, possible scenarios are discussed for the origin of compositionally similar dacites of Karymsky and Academy Nauk caldera-forming eruptions.

Origin of granophyric xenoliths

Granophyric xenoliths were transported to the surface in 1996 by basaltic magma, which ascended as a dike along a longitudinally oriented fault (Fedotov, 1998; Eichelberger and Izbekov, 2000). Assuming that the dike ascended vertically, then the granophyres were incorporated directly below the 1996 vent. Because the vent is located within the Academy Nauk caldera, the source of xenoliths would thus be from a plutonic body situated beneath the caldera. This does not imply necessarily that the pluton is the crystallized remains of the magma chamber that fed the caldera-forming eruption of Academy Nauk. Indeed, for the last 2 Ma many silicic magmas have erupted at Karymsky volcanic center, and their plutonic remnants may be situated below Academy Nauk caldera as well (Ivanov, 1970). In addition, granitic plutons compose the Cretaceous metamorphic basement, the upper surface of which is approximately 3-4 km below Academy Nauk caldera (Balesta, 1991; Sugrobov and Yanovsky, 1991).

We believe, however, that the compositional and textural characteristics of the granophyres clearly indicate that they are genetically linked to the Academy Nauk dacite,

rather than to another source. First, the whole-rock compositions of the granophyres match that of Academy Nauk dacite (Table 4.1), whereas no other silicic magma erupted in the area shows such similarity (Masurenkov, 1980). Second, the compositions of plagioclase cores and rare inclusions of clinopyroxenes in the granophyres overlap with those in the Academy Nauk dacite (Tables 4.3, 4.4). Finally, the micrographic texture of the groundmass of granophyre is consistent with rapid crystallization caused by significant undercooling, which is likely to occur at a relatively shallow depth (e.g., Lipman et al., 1997; Lowenstern et al., 1997), and therefore could be related to the caldera-forming eruption of Academy Nauk.

Despite their similar bulk compositions, the mineral assemblage of the granophyres differs from that of the Academy Nauk dacite by the presence of hornblende and biotite, whereas clinopyroxene occurs only as rare inclusions in amphibole phenocrysts. Presence of hornblende + quartz in the granophyre allows its crystallization pressure to be inferred using the Al-in-hornblende geobarometer of Johnson and Rutherford (1989), which was calibrated experimentally using similar whole-rock compositions. The concentration of Al_2O_3 in hornblende averages 6.14±0.17 wt.% (Table 4.5), which suggests a crystallization pressure of 100±50 MPa. This pressure is slightly below the calibrated range of the geobarometer, but because Al_2O_3 content in hornblende varies linearly with pressure (Johnson and Rutherford, 1989, fig. 9), we believe that 100 MPa approximates that of the crystallization pressure of the granophyre. The inclusions of clinopyroxenes could then be relicts of the reaction of clinopyroxene + melt going to amphibole + biotite, and the overall change from orthopyroxene + clinopyroxene to

amphibole + biotite is consistent with isobaric crystallization of the dacite at pressures greater than ~100 MPa (Fig. 4.4).

Whether granophyre crystallized prior to or after the caldera-forming eruption is uncertain. In either case, the depth of its crystallization may be approximately the same as the pre-eruptive depth of Academy Nauk dacite. Therefore, we assume that 100 MPa is a close estimate for the pre-eruptive pressure at which Academy Nauk dacite was last equilibrated. The solubility of water in rhyolite melt increases with pressure, and equals ~4 wt.% at 100 MPa (e.g., Gardner et al., 1999). Glass inclusions in pyroxenes of the Academy Nauk dacite contain 4.3±0.4 wt.% of volatiles, which matches that expected for water solubility at 100 MPa. This correspondence suggests that Academy Nauk dacite was saturated with water immediately prior to its eruption.

Pre-eruptive conditions for Academy Nauk and Karymsky dacites

Equilibrium compositions of minerals and melts in water-saturated magma are controlled by temperature, pressure, and oxygen fugacity. Pre-eruptive temperatures and oxygen fugacities of Karymsky and Academy Nauk dacites can be estimated using the magnetite-ilmenite geothermometer. Using the mineral formula calculation scheme of Stormer (1983) and the algorithm of Andersen and Lindsley (1988), we estimate that the temperature of Academy Nauk dacite was 883±19°C at an log f_{O_2} of -10.92±0.12, whereas the temperature of Karymsky dacite was 871±19°C at a log f_{O_2} of -11.26±0.13. The oxygen fugacity of both dacites is approximately one order of magnitude greater than

the Ni-NiO buffer curve (NNO+1), which allows us to apply our experimental results to Academy Nauk and Karymsky magma systems.

The temperatures inferred above, and the experimentally determined phase relations indicate that the mineral assemblage of the dacites crystallized at pressures below 125 MPa (Fig. 4.4). Pre-eruptive pressures and temperatures of Karymsky and Academy Nauk dacites can be further constrained by comparing the compositions of matrix glass in natural samples with those of the experimental runs (e.g., Rutherford et al., 1985; Gardner et al., 1995). In order to determine the most likely pressure-temperature conditions we have defined compositional isopleths as a function of pressure and temperature (Fig. 4.5). Each isopleth represents a line in pressure-temperature space where the experimental results match the natural compositions of the matrix glasses of the two dacites. Similar compositional isopleths were determined for plagioclase (Fig. 4.6). The intersection of such isopleths ($\pm\sigma$) for all elements defines a P-T-field, in which the compositions of experimental glasses coincide with that of natural samples. Using the glass and plagioclase isopleths in conjunction with the temperatures determined from the natural magnetites and ilmenites constrains the most likely pressure for last equilibrium for the Academy Nauk dacite to 100±15 MPa. Likewise, the pressure for last equilibrium of the Karymsky dacite was 85±18 MPa (Fig. 4.7). We note that the determined pressures match those expected from the average water contents in the glass inclusions.

The determined pre-eruptive pressures for Karymsky and Academy Nauk dacites overlap, and correspond to a depth of approximately 3-4 km, assuming a density of 2.6 g/cm^3 for the upper crustal volcanic rocks. Interestingly, those depths coincide with a

regional boundary between Cretaceous metamorphic basement and an overlying volcano-sedimentary layer (Balesta, 1991; Sugrobov and Yanovsky, 1991). It is thus possible that the crustal boundary acted as a density window that controlled the emplacement of the dacitic magma bodies below the Karymsky volcanic center.

Magma system of Karymsky and Academy Nauk

The similarity of whole-rock compositions, mineral assemblages, and pre-eruptive conditions poses an intriguing question. What magma system could produce compositionally identical magmas, whose eruptions formed similarly sized calderas, yet differ in age by ~30,000 years? The following constraints provide a framework for understanding the magma system at Karymsky and Academy Nauk. (1) Karymsky and Academy Nauk calderas have similar sizes, being centered ~9 km apart. (2) The whole-rock compositions of dacites are the same. (3) Karymsky dacite erupted ~30,000 years after the Academy Nauk dacite. (4) Pre-eruptive temperatures of Karymsky and Academy Nauk dacites were 871±19° C and 883±19° C. (5) Karymsky and Academy Nauk dacites were last equilibrated approximately at the same depth of ca. 3-4 kilometers. (6) Volcanic activity at Karymsky resumed only 2500 years after the caldera-forming eruption, which suggests that the remnants of the Karymsky dacitic reservoir were already solidified.

One way to resolve all of the constraints is that caldera-forming events at Karymsky and Academy Nauk resulted from two separate episodes of partial melting of the lower crust, subsequent ascent, and eruption of separate dacitic batches at 40,000 yr. BP and 7900 yr. BP (Fig. 4.8a). Repeated production of compositionally similar magmas

is possible if the composition of a crustal substrate was not modified by previous withdrawals, and /or if the composition of produced melt was strictly constrained by a limited number of factors. These factors may include, for example, the critical porosity of a partially molten substrate at which melt is able to segregate to larger volumes and then to ascend. The close location of the calderas, however, suggests that both Karymsky and Academy Nauk dacites originated from the same crustal domain or, if separate, from two closely located crustal domains. Even if it were possible to generate large volumes of dacitic magma in a period as short as 30,000 years, it would be still very unlikely that the composition of the parental substrate would not be modified by previous melting episodes and the trace element composition of the produced melts would remain exactly the same.

Alternatively both dacites could have been generated at the same time and, at least temporally, shared the same magma reservoir. Because Karymsky and Academy Nauk dacites were last equilibrated at the same pressure (3-4 km depth), they could have erupted from the same longitudinally elongated magma body (Fig. 4.8b), which intruded to that level approximately 40,000 years ago (Ivanov, 1970). Thermal balance considerations in conjunction with outlined earlier constraints can help to evaluate this scenario. Numerical modeling of the thermal regime using the HEAT algorithm (Wohletz et al., 1999) requires the minimum volume of the reservoir to have been ~200 km^3 in order for it to cool from 885^0C to 870^0C in ca. 30,000 years. The total volume of dacite erupted 7900 BP at Karymsky is 5-7 km^3 (Braitseva and Melekestsev, 1991), and so there should be more than 190 km^3 of magma remained in the reservoir. The eruption of basalts

2500 years after the formation of Karymsky caldera suggests that the portion of reservoir that remained beneath caldera had already solidified. It seems unlikely that 190 km^3 of magma could solidify so rapidly, given that it was cooling so slowly before the eruption. Indeed, our modeling suggests a magma body greater than 5 km^3 would still be molten after 2500 years, even assuming efficient heat loss through a highly conductive convective layer of cauldron material. In addition, it seems unlikely that a single elongated reservoir would form two separate circular-shaped calderas, instead of one.

We believe the identical compositions of Karymsky and Academy Nauk dacite require that both were derived from the same magma source, which did not evolve compositionally and did not cool significantly in 30,000 years. In contrast, a relatively fast solidification of the remnants of the Karymsky dacite reservoir requires that its pre-eruptive volume would not exceed 10-12 km^3, which is the total of magma erupted (5-7 km^3) and the maximum volume of magma remained (5 km^3). One hypothesis, which may account for these two observations, is that two separate 10-12 km^3 batches of dacite were derived from a single large source situated in the lower crust (Fig. 4.8c). At 40,000 yr. BP, the first portion of dacite detached from the parental body, ascended along the active fault zone until it reached the structural boundary at 3 km, re-equilibrated to that shallow depth, and then erupted. At 7900 yr. BP, a second portion of dacite, perhaps the entire remaining part of the parental body, ascended along the same fault zone until reaching the 3-km boundary, re-equilibrated, and erupted. The time required for the dacites to re-equilibrate is not known, but it must be long enough to erase any vestige of a high-

pressure mineral assemblage. For example, hornblende would be stable in the magmas at water pressures greater than 200 MPa.

This lower crustal source could itself be of dacite magma, similar to what erupted, but with a different phase assemblage reflecting its deeper storage. Alternatively, it could be a more mafic mush zone with interstitial dacitic melt and a lifetime and volume much greater than individual caldera cycle. A small portion of this melt occasionally escapes, changing to overall source region very little and cleanly leaving behind high-pressure crystalline phases in the interlocking mush network. Such a zone need not have disappeared to permit the basalt eruption of 1996. At the high strain rates accompanying the basaltic intrusion, this zone would behave as a brittle solid with dikes passing directly through it.

CONCLUSIONS

Granophyre xenoliths were sampled by ascending basalt from crystallized silicic reservoir, which produced caldera-forming eruption of Academy Nauk 40,000 yr. BP. According to Al-in-hornblende geobarometer, granophyre crystallized at depth corresponding to 100 MPa.

Composition of Fe-Ti-oxides, H_2O contents of glass inclusions, and results of phase equilibria experiments suggest that Academy Nauk and Karymsky dacites were last equilibrated at water-saturated conditions and an oxygen fugacity of Ni-NiO+1. Immediately prior to eruption, Academy Nauk dacite was stored at 883±19° C and

situated at depth corresponding to a pressure of 100±15 MPa. Pre-eruptive conditions for 7,900 yr. BP Karymsky dacite were 871±19° C and 85±18 MPa.

Similar whole-rock compositions of Academy Nauk and Karymsky dacites suggest that they were derived from the same dacite-bearing crustal source, which did not evolve compositionally between the two caldera-forming eruptions. Most likely, a small (~10 km^3) batch of the dacite detached from the parental reservoir, ascended to a stratigraphic boundary at 3 km depth, and erupted at 40,000 yr. BP. This process was repeated at 7,900 yr. BP.

ACKNOWLEDGEMENTS

This work was supported by the Volcano Hazards Program of the U.S. Geological Survey through the Alaska Volcano Observatory. Help of Jessica Larsen and Jacob Lowenstern in acquiring the FTIR data is greatly appreciated.

Table 4.1: Whole-rock composition of 40,000 BP Academy Nauk dacite, 7,900 BP Karymsky dacite and granophyre xenolith

Sample [a]	99IPE 6	97IPE7	99IPE 4
SiO_2[b]	69.54	70.43	69.58
Al_2O_3	15.37	14.83	15.06
TiO_2	0.493	0.47	0.526
FeO*	3.23	3.31	3.33
MnO	0.093	0.064	0.088
CaO	3.27	2.79	3.28
MgO	1.04	0.93	1.09
K_2O	2.45	2.61	2.37
Na_2O	4.4	4.46	4.56
P_2O_5	0.105	0.093	0.113
Total	100	100	100
Ni	6	7	3
Cr	5	3	5
V	63	47	65
Zr	190	206	184
Ga	14	17	15
Cu	12	12	9
Zn	47	32	44
La	12.48	12.64	12.33
Ce	27.62	27.27	26.85
Pr	3.51	3.41	3.47
Nd	15.64	14.93	15.24

Sample	99IPE 6	97IPE7	99IPE 4
Sm	4.15	4.02	4.10
Eu	1.01	1.00	0.99
Gd	4.07	3.96	4.10
Tb	0.73	0.67	0.73
Dy	4.60	4.38	4.59
Ho	0.97	0.92	0.94
Er	2.86	2.74	2.79
Tm	0.44	0.43	0.43
Yb	2.91	2.80	2.76
Lu	0.46	0.46	0.45
Ba	532	557	520
Th	2.62	2.55	2.55
Nb	3.57	3.28	3.72
Y	29.78	26.70	28.61
Hf	5.28	5.43	5.10
Ta	0.29	0.30	0.30
U	1.33	1.40	1.30
Pb	8.18	5.38	7.92
Rb	35.6	35.9	34.4
Cs	1.56	1.23	1.37
Sr	248	205	241
Sc	12.00	10.10	13.10

[a] Samples are Academy Nauk dacite (99IPE6), Karymsky dacite (99IPE4) and granophyre xenolith (97IPE7)

[b] Major oxides in wt.% with all Fe reported as FeO, concentrations of Ni-Zn (ppm) determined by XRF, concentrations of La-Sc (ppm) determined by ICP-MS.

Table 4.2: Composition of glass in natural samples

Sample [a]	99IPE4 M	99IPE4 I	99IPE6 M	99IPE6 I
n	7	15	7	9
SiO_2 [b]	75.62 (0.39)	75.64 (0.49)	74.31 (0.49)	75.37 (1.15)
Al_2O_3	12.77 (.27)	13.05 (.23)	13.52 (.32)	12.78 (.71)
TiO_2	0.21 (.05)	0.35 (.08)	0.20 (.05)	0.16 (.10)
FeO^t	1.77 (.17)	1.55 (.16)	1.82 (.10)	2.16 (.27)
CaO	1.44 (.07)	1.42 (.06)	1.68 (.13)	1.42 (.47)
MgO	0.32 (.03)	0.29 (.03)	0.35 (.03)	0.30 (.12)
K_2O	3.15 (.09)	3.17 (.18)	3.04 (.08)	3.49 (.42)
Na_2O	4.55 (.25)	4.35 (.23)	4.91 (.17)	4.13 (.15)
Cl	0.16 (.02)	0.19 (.03)	0.18 (.02)	0.19 (.02)
Total	98.50	96.42	98.36	95.71

[a] Samples are Karymsky dacite (99IPE4) and Academy Nauk dacite (99IPE6). M - matrix glass, I - glass inclusions in pyroxenes.

[b] The average of n analyses (in wt. %) is given together with the standard deviation (number in brackets). Analyses are normalized to 100 wt.%, however the non-normalized total is reported.

Table 4.3: Composition of plagioclases in natural samples

Sample[a]	99IPE4, R	99IPE4, C	99IPE6, R	99IPE6, C	97IPE7 R	97IPE7 C
n	7	6	5	8	9	5
SiO_2[b]	56.33(.38)	56.15(.17)	56.08(.70)	51.95(.66)	60.61(1.19)	58.03(.72)
Al_2O_3	26.68(.17)	27.29(.76)	27.22(.62)	29.83(.39)	25.29(.83)	26.93(.71)
FeO[c]	0.45(.06)	0.42(.05)	0.47(.10)	0.47(.04)	0.27(.10)	0.42(.06)
CaO	8.85(.15)	9.12(.29)	9.41(.30)	12.36(.45)	5.73(.90)	7.61(.68)
K_2O	0.27(.02)	0.23(.04)	0.24(.06)	0.13(.02)	0.40(.08)	0.30(.03)
Na_2O	6.33(.13)	5.92(.43)	5.88(.22)	4.44(.15)	7.53(.54)	6.49(.39)
Total	98.91	99.14	99.30	99.18	99.83	99.77

[a] Samples are Karymsky dacite (99IPE4), Academy Nauk dacite (99IPE6) and granophyre (97IPE7). R - rim, C - core.

[b] The average of n analyses (in wt. %) is given together with the standard deviation (number in brackets).

Table 4.4: Composition of pyroxenes in natural samples

Sample [a]	99IPE4, CPx	99IPE6, CPx	97IPE7, CPx	99IPE4, OPx	99IPE6, OPx
n	50	6	7	50	6
SiO_2[b]	53.06(.41)	51.96(.75)	52.45(.32)	53.79(.63)	52.16(.25)
Al_2O_3	1.04(.14)	1.61(.37)	0.87(.03)	0.51(.14)	0.66(.05)
TiO_2	0.27(.05)	0.36(.11)	0.23(.04)	0.16(.04)	0.16(.02)
FeO^t	8.91(.36)	9.05(.40)	9.6(.21)	20.13(.53)	20.04(.46)
CaO	21.49(.32)	21.21(.20)	21.95(.15)	1.18(.06)	1.19(.13)
MnO	0.47(.08)	0.51(.03)	0.47(.08)	0.95(.12)	1.08(.13)
MgO	14.46(.23)	14.85(.32)	14.57(.33)	22.56(.28)	23.36(.36)
Na_2O	0.34(.04)	0.33(.03)	0.31(.04)	0.02(.02)	0.02(.02)
Total	100	99.89	100.5	99.3	98.67

[a] Samples are Karymsky dacite (99IPE4), Academy Nauk dacite (99IPE6) and granophyre (97IPE7). CPx – clinopyroxene, OPx - orthopyroxene.

[b] The average of n analyses (in wt. %) is given together with the standard deviation (number in brackets).

Table 4.5: Composition of hornblende and biotite in granophyres

Sample [a]	97IPE7, Bt	97IPE7, Hb
n	12	8
SiO_2[b]	39.66(.54)	48.42(.29)
Al_2O_3	12.87(.35)	6.14(.17)
TiO_2	4.00(.44)	1.48(.21)
FeO^t	13.07(.67)	14.92(.31)
CaO	0.15(.06)	10.89(.24)
MnO	0.27(.09)	0.47(.09)
MgO	15.88(.61)	13.73(.17)
K_2O	8.33(.26)	0.44(.05)
Na_2O	0.30(.02)	1.72(.10)
Cl	0.30(.06)	n.d.
F	0.94(.28)	n.d.
Total	95.79	98.21

[a] Bt - biotite, Hb - hornblende.

[b] The average of n analyses (in wt. %) is given together with the standard deviation (number in brackets); n.d - not detected.

Table 4.6: Composition of magnetite-ilmenite pairs

Sample [a]	99IPE4, Mt	99IPE4, Ilm	99IPE6, Mt	99IPE6, Ilm
TiO_2 [b]	9.25	42.16	9.17	40.36
Al_2O_3	2.00	0.25	1.95	0.26
Cr_2O_3	0.08	0.02	0.07	0.02
Fe_2O_3	49.56	21.72	49.76	25.12
FeO	36.71	32.28	36.3	30.86
MnO	0.65	0.74	0.68	0.61
MgO	1.69	2.74	1.85	2.7
Total	99.94	99.91	99.78	99.93

[a] Samples are Karymsky dacite (99IPE4) and Academy Nauk dacite (99IPE6). Mt - magnetite, Ilm - ilmenite.

[b] The average of n analyses (in wt. %) is given together with the standard deviation (number in brackets).

Table 4.7: Conditions of experimental runs

Run	Starting material	P (MPa)	T (C)	Duration (hours)	Products [a]
PI-1	99IPE4	100	850	96	Pl, OPx, CPx, Op, G, V
PI-2	99IPE4	100	900	96	OPx, CPx,, G, V
PI-3	PI-1	100	875	96	Pl, OPx, CPx, Op, G, V
PI-4	PI-2	100	875	96	Pl, OPx, CPx, Op, G, V
PI-5	PI-1	50	875	120	Pl, OPx, CPx, Op, G, V
PI-6	PI-2	50	875	120	Pl, OPx, CPx, Op, G, V
PI-7	PI-1	150	875	96	OPx, CPx, Op, G, V
PI-8	PI-2	150	875	96	OPx, CPx, Op, G, V
PI-9	99IPE4	100	900	120	OPx, CPx,, G, V
PI-10	PI-1	75	875	120	Pl, OPx, CPx, Op, G, V
PI-11	PI-9	75	875	120	Pl, OPx, CPx, Op, G, V
PI-12	99IPE4	100	825	96	Pl, OPx, CPx, Op, G, V
PI-13	99IPE4	200	825	120	Pl, Hb, CPx, G, V
PI-14	PI-12	50	900	96	Pl, OPx, CPx, Op, G, V
PI-15	PI-2	50	900	96	Pl, OPx, CPx, Op, G, V
PI-16	PI-12	100	800	120	Pl, OPx, CPx, Op, G, V
PI-17	PI-13	200	800	96	Pl, Hb, CPx, G, V
PI-19	PI-16	100	775	96	Pl, OPx, CPx, Op, G, V
PI-20	PI-17	200	775	96	Pl, Hb, CPx, G, V
PI-21	PI-17	200	750	96	Pl, Hb, G, V
PI-22	PI-19	100	750	96	Pl, OPx, CPx, Op, G, V
PI-23	PI-22	100	725	144	Pl, OPx, CPx, Op, G, V

[a] Pl - plagioclase, OPx - orthopyroxene, CPx - clinopyroxene, Hb - hornblende, Bt - biotite, Q - quartz, Op - opaque mineral, G - glass, V - vapor

Table 4.7: Continued

Run	Starting material	P (MPa)	T (C)	Duration (hours)	Products [a]
PI-24	PI-21	200	725	144	Pl, Hb, Bt, Q, G, V
PI-26	PI-24	200	700	96	Pl, Hb, Bt, Q, G, V
PI-27	PI-26	200	725	360	Pl, Hb, Bt, Q, G, V
PI-28	PI-12	100	725	360	Pl, OPx, CPx, Op, G, V
PI-29	99IPE4	300	725	312	Pl, Hb, Bt, Q, G, V
PI-30	99IPE4	300	700	288	Pl, Hb, Bt, Q, G, V
PI-31	PI-9	75	900	204	Pl, OPx, CPx, Op, G, V
PI-32	PI-28	75	900	204	Pl, OPx, CPx, Op, G, V
PI-33	PI-9	75	850	204	Pl, OPx, CPx, Op, G, V
PI-34	PI-28	75	850	204	Pl, OPx, CPx, Op, G, V
PI-35	PI-23	150	725	336	Pl, Hb, Bt, Q, G, V
PI-36	PI-24	150	725	336	Pl, Hb, Bt, Q, G, V
PI-37	PI-20	150	825	96	Pl, OPx, CPx, Op, G, V
PI-38	PI-9	150	825	96	Pl, OPx, CPx, Op, G, V
PI-39	PI-3	125	875	96	OPx, CPx, Op, G, V
PI-40	PI-8	125	875	96	OPx, CPx, Op, G, V

Table 4.8: Composition of residual melt in experimental runs

Run	PI-1	PI-2	PI-3	PI-4	PI-5
n	8	5	15	15	15
SiO_2 [a]	75.27(.24)	74.48(.32)	74.94(.31)	74.59(.44)	76.21(.90)
Al_2O_3	13.21(.20)	13.49(.21)	13.26(.22)	13.22(.16)	12.54(.60)
TiO_2	0.24(.08)	0.22(.07)	0.25(.07)	0.27(.07)	0.23(.17)
FeO[t]	1.67(.11)	2.00(.11)	1.79(.09)	2.03(.11)	1.71(.21)
CaO	1.40(.05)	1.72(.11)	1.62(.09)	1.77(.12)	1.19(.30)
MgO	0.27(.03)	0.34(.03)	0.34(.06)	0.36(.04)	0.18(.03)
K_2O	3.24(.10)	2.94(.11)	3.12(.13)	3.02(.08)	3.35(.19)
Na_2O	4.48(.26)	4.47(.16)	4.40(.20)	4.35(.32)	4.32(.31)
Cl	0.03(.02)	0.12(.01)	0.08(.03)	0.16(.02)	0.07(.02)
Total	95.91	96.07	96.60	96.87	98.22

Run	PI-6	PI-7	PI-8	PI-10	PI-11
n	16	13	11	23	13
SiO_2 [a]	75.58(.72)	74.44(.36)	74.74(.41)	75.29(.35)	74.86(.26)
Al_2O_3	12.68(.44)	13.40(.21)	13.44(.29)	13.26(.14)	13.25(.12)
TiO_2	0.26(.10)	0.25(.09)	0.24(.07)	0.29(.14)	0.35(.14)
FeO[t]	1.95(.19)	2.01(.12)	1.83(.11)	1.66(.17)	1.97(.14)
CaO	1.41(.26)	1.84(.08)	1.80(.17)	1.42(.06)	1.58(.09)
MgO	0.34(.13)	0.43(.04)	0.37(.04)	0.27(.03)	0.29(.04)
K_2O	3.15(.12)	2.92(.11)	3.03(.11)	3.27(.11)	3.06(.12)
Na_2O	4.25(.21)	4.37(.24)	4.31(.23)	4.29(.16)	4.29(.20)
Cl	0.15(.02)	0.12(.02)	0.05(.02)	0.06(.02)	0.13(.03)
Total	98.38	95.85	96.39	96.23	96.14

[a] The average of n analyses (in wt. %) is given together with the standard deviation (number in brackets). Analyses are normalized to 100 wt.%, however the non-normalized total is reported.

Table 4.8: Continued

Run	PI-12	PI-13	PI-14	PI-15	PI-16
n	20	18	11	8	8
SiO_2[a]	75.35(.51)	74.96(.64)	76.09(.33)	75.11(.42)	77.08(.63)
Al_2O_3	13.09(.17)	13.64(.35)	12.26(.31)	12.93(.33)	12.38(.26)
TiO_2	0.42(.23)	0.26(.14)	0.23(.05)	0.58(.11)	0.36(.30)
FeO[t]	1.70(.19)	1.61(.14)	1.95(.12)	1.81(.10)	1.16(.14)
CaO	1.42(.16)	1.74(.12)	1.28(.07)	1.35(.08)	1.05(.10)
MgO	0.28(.11)	0.29(.05)	0.24(.03)	0.21(.03)	0.10(.02)
K_2O	3.21(.10)	3.06(.10)	3.29(.11)	3.42(.12)	3.55(.12)
Na_2O	4.19(.20)	4.12(.19)	4.31(.20)	4.32(.25)	4.07(.24)
Cl	0.15(.02)	0.13(.02)	0.14(.03)	0.06(.03)	0.13(.03)
Total	94.17	92.55	97.70	98.10	94.81

Run	PI-17	PI-20	PI-21	PI-22	PI-23
n	7	7	6	7	7
SiO_2[a]	75.78(.54)	75.59(.53)	76.48(.58)	78.81(.34)	78.05(.32)
Al_2O_3	13.28(.26)	13.41(.19)	12.95(.23)	11.27(.16)	11.48(.30)
TiO_2	0.30(.10)	0.08(.07)	0.12(.07)	0.12(.09)	0.25(.07)
FeO[t]	1.47(.11)	1.22(.15)	1.06(.12)	0.94(.09)	0.93(.11)
CaO	1.59(.08)	1.63(.06)	1.58(.05)	0.72(.08)	0.47(.06)
MgO	0.16(.02)	0.12(.02)	0.09(.01)	0.09(.01)	0.05(.02)
K_2O	3.07(.11)	3.21(.15)	3.03(.11)	3.81(.06)	4.67(.15)
Na_2O	4.10(.34)	4.56(.30)	4.50(.37)	4.07(.26)	3.92(.29)
Cl	0.09(.02)	0.04(.02)	0.07(.04)	0.06(.02)	0.07(.03)
Total	92.00	91.74	91.91	95.52	96.14

Table 4.8: Continued

Run	PI-24	PI-26	PI-27	PI-28
n	7	5	7	8
SiO_2[a]	77.19(.58)	77.17(.68)	77.09(.29)	78.98(.50)
Al_2O_3	12.63(.46)	12.78(.52)	13.28(.35)	11.41(.43)
TiO_2	0.10(.06)	0.10(.05)	0.08(.05)	0.10(.06)
FeO^t	1.06(.09)	0.77(.12)	0.96(.09)	0.92(.28)
CaO	0.96(.05)	0.91(.18)	0.96(.08)	0.51(.07)
MgO	0.06(.01)	0.04(.01)	0.06(.01)	0.07(.05)
K_2O	3.59(.12)	3.82(.23)	3.48(.07)	4.30(.15)
Na_2O	4.22(.34)	4.28(.30)	3.94(.22)	3.50(.19)
Cl	0.07(.03)	0.04(.03)	0.05(.03)	0.12(.03)
Total	93.76	95.12	94.46	95.24

Run	PI-29	PI-30	PI-31	PI-32
n	6	8	7	7
SiO_2[a]	77.62(.38)	77.02(.88)	74.62(.24)	74.66(.37)
Al_2O_3	12.96(.49)	12.54(.60)	13.48(.19)	12.96(.27)
TiO_2	0.05(.08)	0.05(.06)	0.23(.07)	0.21(.06)
FeO^t	0.73(.17)	0.90(.32)	2.21(.16)	2.16(.13)
CaO	1.14(.15)	1.05(.29)	1.70(.10)	1.84(.05)
MgO	0.08(.05)	0.09(.05)	0.21(.02)	0.24(.02)
K_2O	3.28(.11)	4.34(.41)	3.01(.13)	3.27(.08)
Na_2O	4.00(.15)	3.88(.34)	4.20(.38)	4.30(.40)
Cl	0.05(.04)	0.03(.02)	0.09(.02)	0.12(.02)
Total	91.02	91.58	97.19	96.19

Table 4.8: Continued

Run	PI-33	PI-34	PI-35	PI-36
n	6	5	6	10
SiO_2[a]	75.92(.44)	76.11(.60)	76.84(.29)	78.48(.49)
Al_2O_3	12.57(.13)	12.80(.49)	12.93(.35)	12.07(.14)
TiO_2	0.20(.05)	0.17(.05)	0.23(.19)	0.17(.16)
FeO[t]	1.74(.13)	1.68(.13)	0.93(.19)	0.74(.19)
CaO	1.28(.06)	1.26(.13)	0.87(.11)	0.74(.06)
MgO	0.14(.02)	0.14(.02)	0.09(.05)	0.06(.03)
K_2O	3.40(.13)	3.29(.17)	4.13(.18)	3.78(.15)
Na_2O	4.41(.34)	4.22(.22)	3.74(.13)	3.86(.25)
Cl	0.16(.03)	0.15(.02)	0.12(.03)	0.01(.01)
Total	97.06	97.82	93.93	93.65

Table 4.9: Composition of plagioclase microlites in experimental runs

Run	PI-1	PI-3	PI-4	PI-5	PI-6
n	4	3	2	2	3
SiO_2[a]	57.62(0.76)	57.69(0.54)	56.81(1.01)	59.71(0.54)	59.69(0.38)
Al_2O_3	26.65(0.44)	26.35(0.41)	27.64(0.70)	25.01(0.50)	25.12(0.51)
FeO^t	0.51(.07)	0.52(.09)	0.56(.16)	0.52(.11)	0.46(.14)
CaO	8.72(0.31)	8.58(0.17)	9.51(0.85)	6.75(0.04)	6.83(0.25)
K_2O	0.31(.08)	0.31(.00)	0.27(.03)	0.43(.00)	0.46(.08)
Na_2O	6.22(.13)	6.27(.02)	5.81(.33)	7.21(.07)	6.91(.14)
Total	99.40	99.73	100.59	99.63	99.46

Run	PI-7	PI-10	PI-11	PI-12	PI-14
n	3	7	4	4	5
SiO_2[a]	56.53(0.32)	57.24(0.67)	56.77(0.80)	58.35(0.45)	58.10(0.67)
Al_2O_3	26.81(0.13)	26.35(0.47)	26.99(0.47)	26.31(0.51)	26.41(0.41)
FeO^t	0.50(.02)	0.49(.11)	0.48(.06)	0.50(.12)	0.51(.03)
CaO	8.81(0.03)	8.45(0.44)	8.91(0.45)	8.22(0.33)	8.27(0.21)
K_2O	0.27(.04)	0.32(.05)	0.29(.04)	0.34(.09)	0.34(.07)
Na_2O	6.07(.08)	6.33(.37)	6.01(.18)	6.58(.18)	6.39(.14)
Total	98.99	99.19	99.45	100.30	100.03

[a] The average of n analyses (in wt. %) is given together with the standard deviation (number in brackets).

Table 4.9: Continued

Run	PI-15	PI-16	PI-17	PI-20	PI-21
n	5	7	4	4	4
SiO_2[a]	57.39(0.13)	58.50(1.06)	56.35(0.48)	56.99(1.24)	60.55(0.40)
Al_2O_3	26.50(0.35)	25.14(0.80)	26.78(0.24)	26.47(0.37)	24.00(0.45)
FeO^t	0.52(.08)	0.48(.17)	0.45(.02)	0.51(.06)	0.24(.11)
CaO	8.46(0.27)	7.04(0.75)	9.13(0.43)	8.57(0.31)	5.83(0.33)
K_2O	0.34(.04)	0.34(.07)	0.27(.03)	0.29(.06)	0.46(.05)
Na_2O	6.31(.06)	7.12(.39)	6.05(.16)	6.20(.19)	7.43(.21)
Total	99.51	98.62	99.04	99.02	98.51

Run	PI-22	PI-24	PI-29	PI-30	PI-31
n	7	4	3	1	4
SiO_2[a]	61.14(0.55)	61.25(0.85)	60.12(1.59)	58.95	57.27(0.49)
Al_2O_3	24.10(0.50)	23.56(0.62)	24.15(1.21)	25.97	26.73(0.53)
FeO^t	0.27(.07)	0.29(.10)	0.50(.20)	0.44	0.49(.05)
CaO	5.76(0.09)	5.31(0.33)	6.35(1.26)	7.73	8.83(0.41)
K_2O	0.43(.01)	0.53(.08)	0.44(.07)	0.38	0.29(.03)
Na_2O	7.87(.09)	7.79(.37)	7.26(.41)	7.01	6.34(.29)
Total	99.11	98.73	98.82	100.47	99.95

Run	PI-33	PI-34
n	5	6
SiO_2[a]	59.04(0.37)	57.31(0.35)
Al_2O_3	25.55(0.56)	26.61(0.21)
FeO^t	0.38(.03)	0.40(.07)
CaO	7.71(0.30)	8.78(0.27)
K_2O	0.40(.07)	0.30(.03)
Na_2O	7.21(.17)	6.71(.07)
Total	100.29	100.11

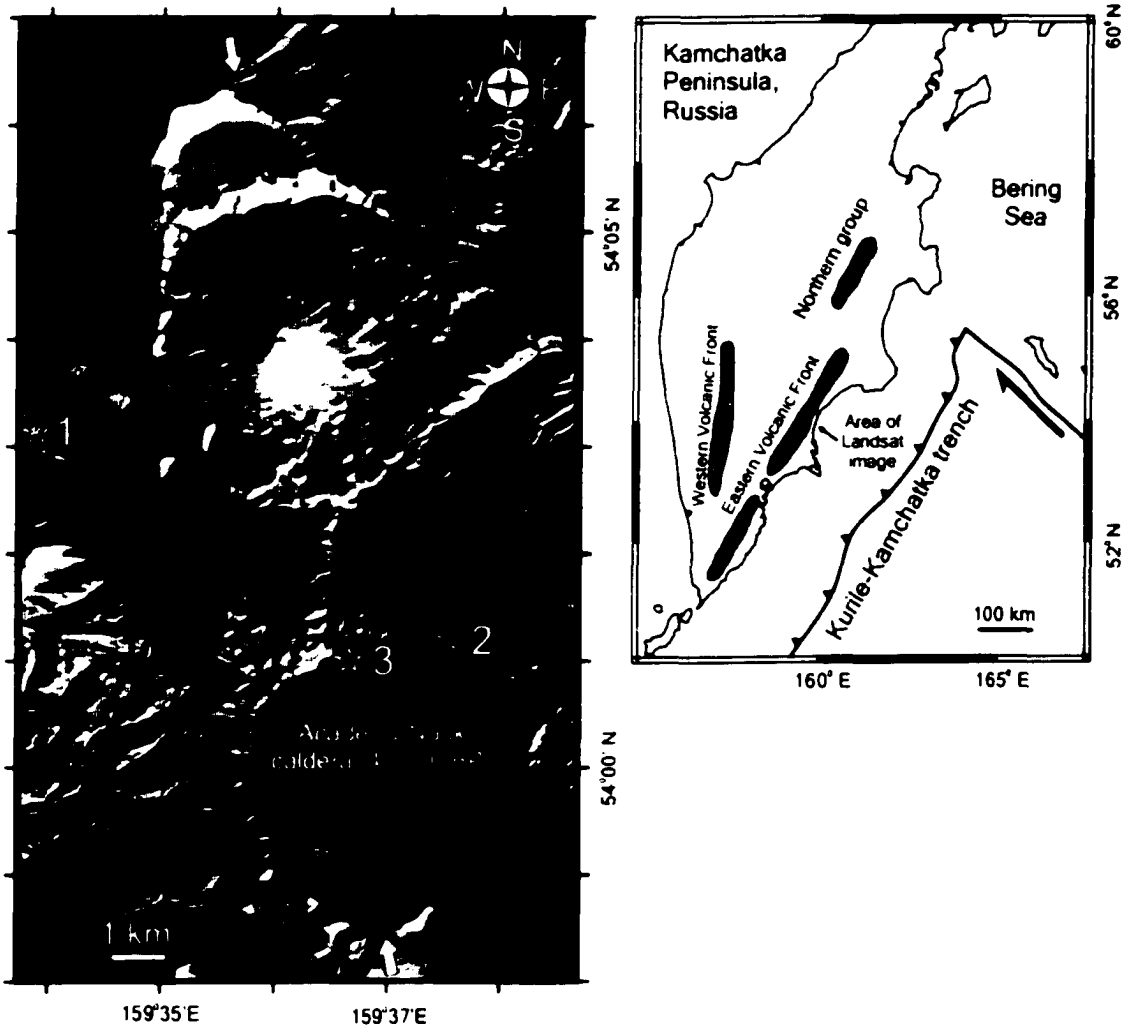

Figure 4.1 Landsat-4 image of Karymsky volcano and AN caldera centered 9 km apart. Arrows indicate a longitudinally oriented fault zone between the volcanoes. Stars show the sites of sample collection: 1 - Karymsky dacites (99IPE4), 2 - AN dacites (99IPE6) and 3 - granophyre xenoliths from basalts erupted in 1996 (97IPE7). Caldera rims are delineated with dotted lines. The position of the volcanoes within the volcanic arc of Kamchatka is shown on the insert.

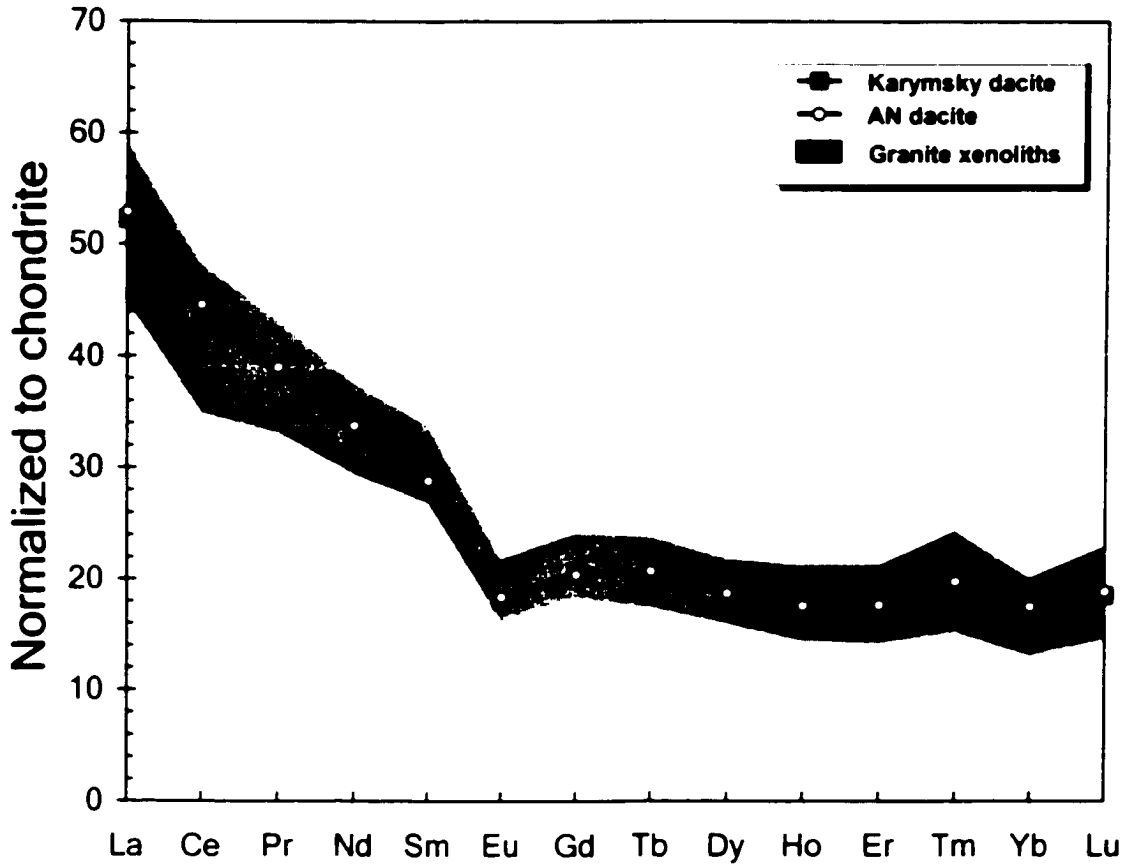

Figure 4.2 Rare-Earth element concentrations in AN dacite, Karymsky dacite, and granophyre xenoliths (spread in values for 5 xenoliths) normalized to the concentrations in Orgueil chondrite (Anders and Grevesse, 1989)

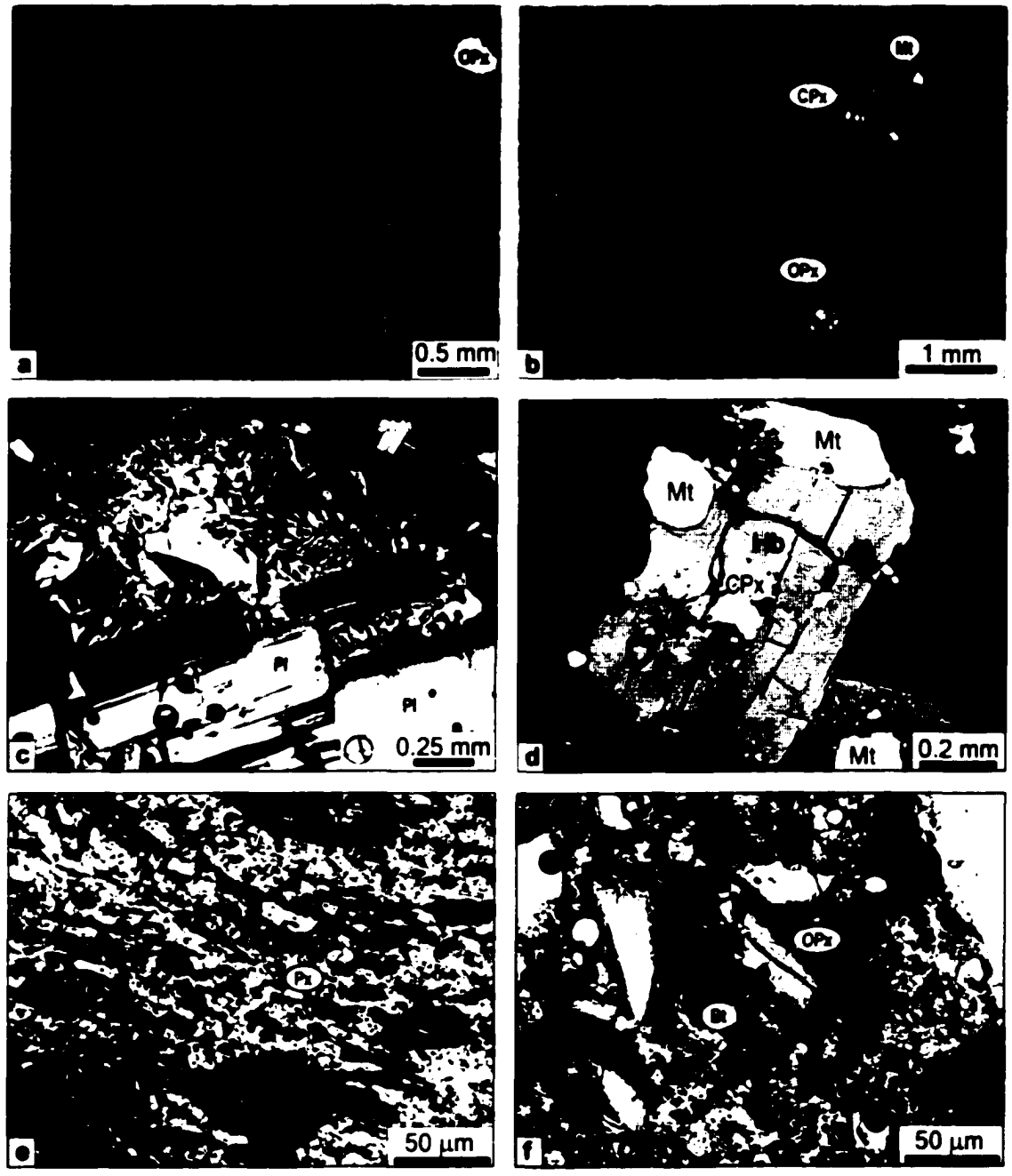

Figure 4.3 Back-scattered electron images of (**a**) AN and (**b**) Karymsky dacite pumices showing phenocrysts of plagioclase (Pl), clinopyroxene (CPx), orthopyroxene (OPx), and magnetite (Mt). (**c**) Photomicrograph of granophyre showing "micrographic" texture of groundmass formed by quartz-feldspar intergrowth (light is polarized). (**d**) BSE image of granophyre showing a clinopyroxene inclusion inside a hornblende (Hb) phenocryst. (**e**) Photomicrograph of experimental run PI-37 showing euhedral microlites of pyroxenes. (**f**) Photomicrograph of experimental run PI-30 showing biotite (Bt) reaction rim surrounding orthopyroxene.

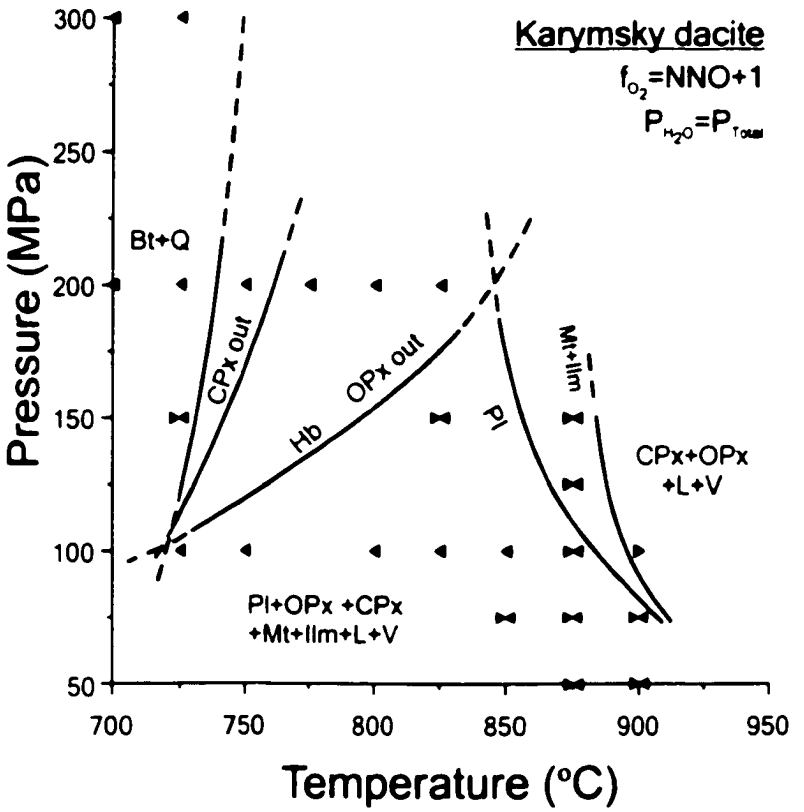

Figure 4.4 Phase diagram for the Karymsky dacitic bulk composition, showing determined fields of stability of hornblende (Hb), biotite (Bt), clinopyroxene (CPx), orthopyroxene (OPx), magnetite (Mt), ilmenite (Ilm), and quartz (Q). Left-pointing arrows represent crystallization experiments; right-pointing arrows represent melting experiments.

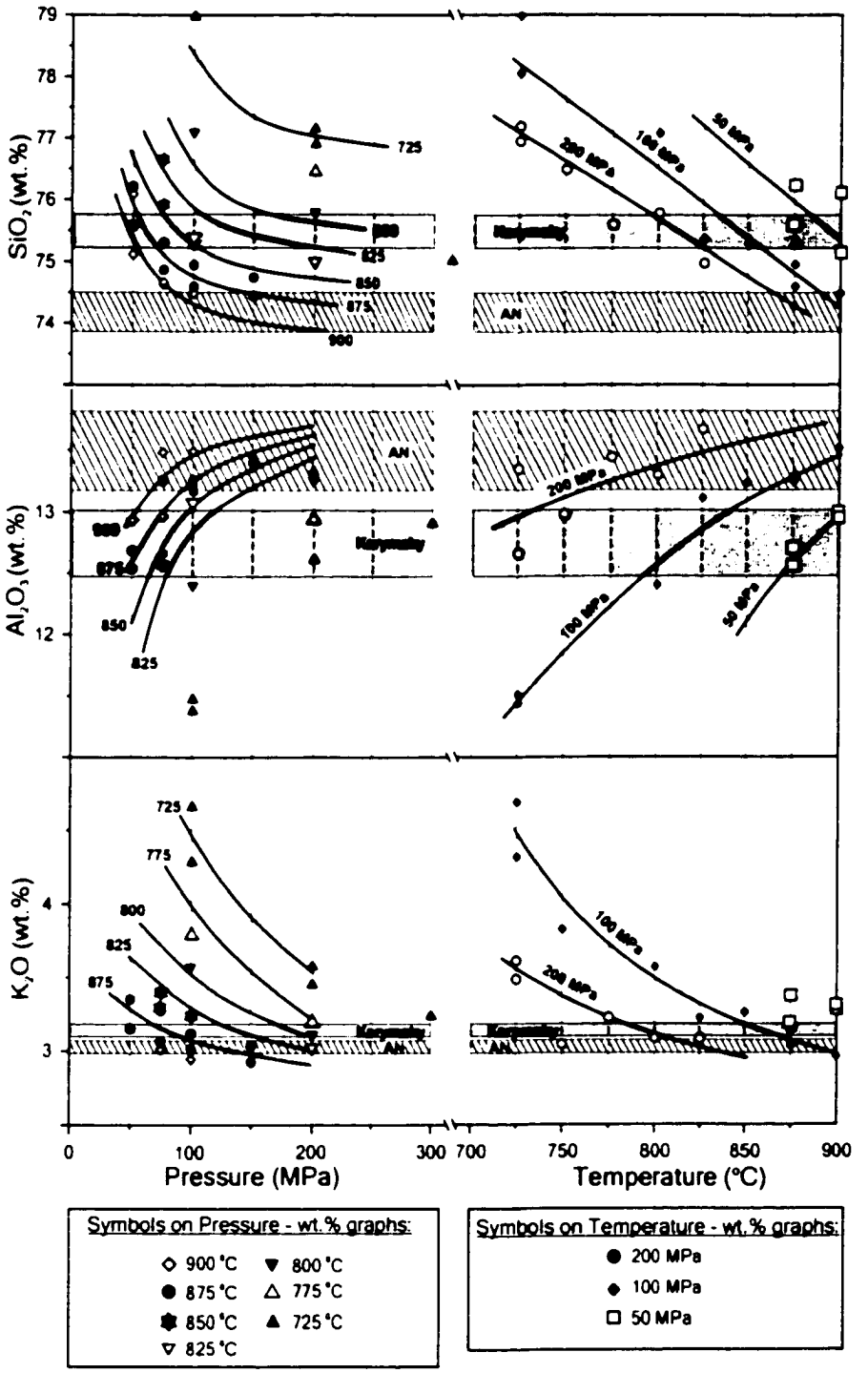

Figure 4.5 Variations of experimental melt composition as a function of temperature and pressure. Shaded areas correspond to the average compositions (±1σ) of matrix glasses in Karymsky and Academy Nauk dacites.

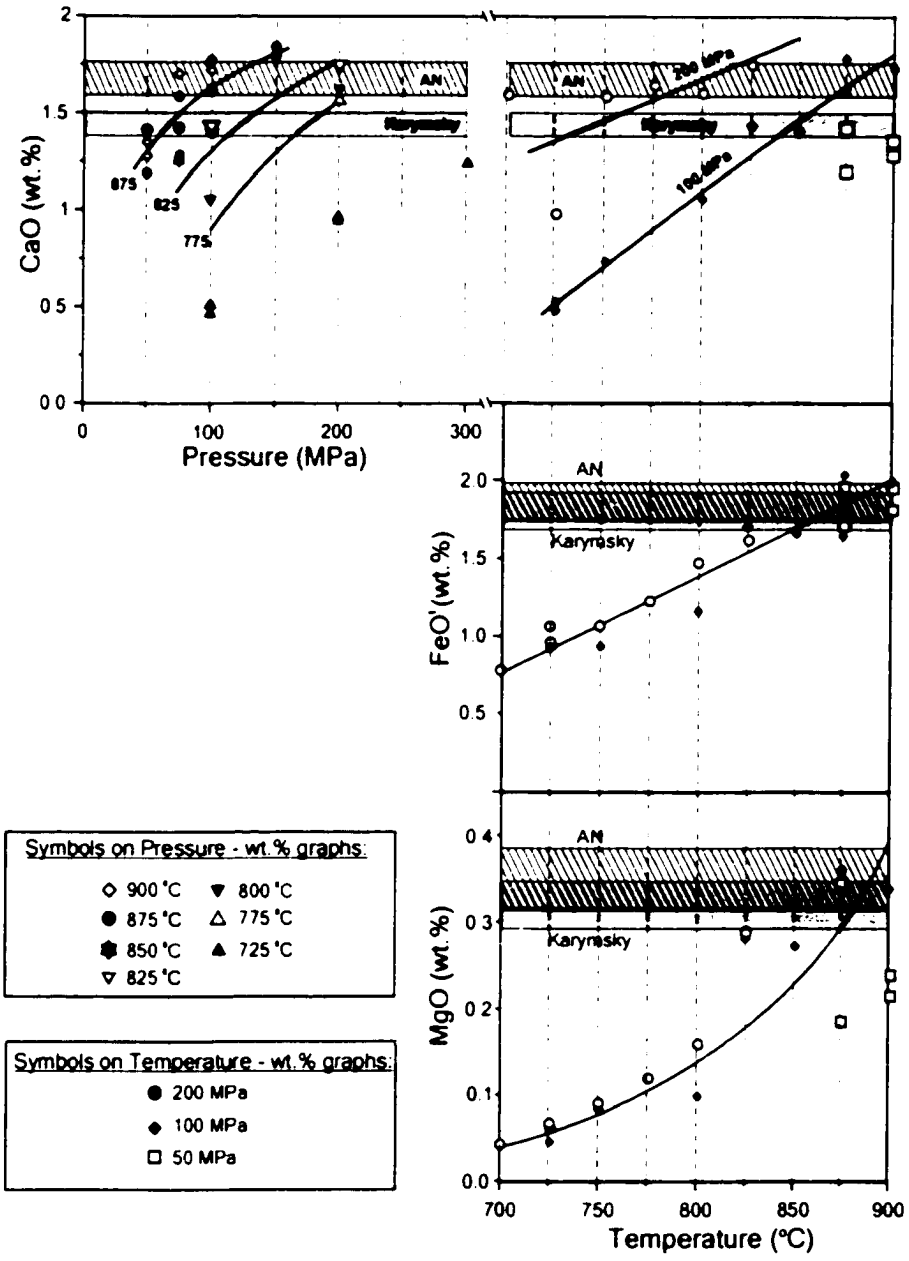

Figure 4.5 continued from the previous page.

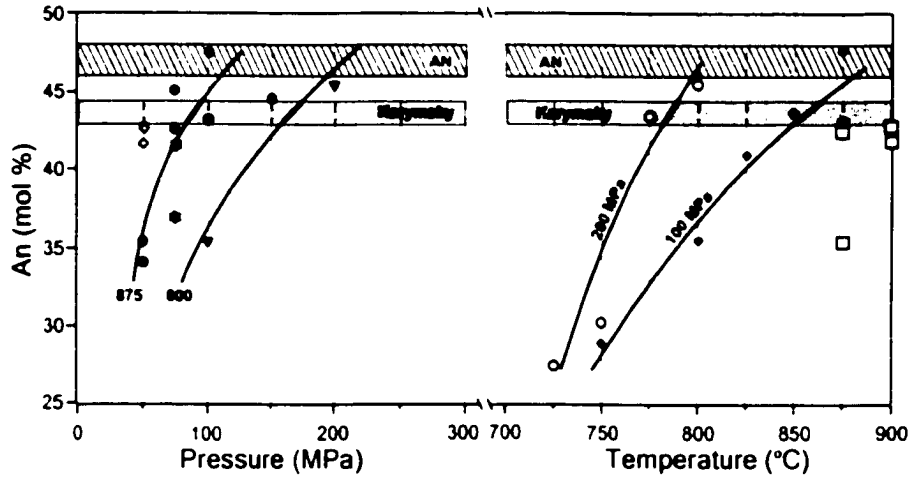

Figure 4.6 Variations of experimental plagioclase composition. Shaded areas correspond to average composition (±1σ) of natural plagioclase rims in Karymsky and AN dacites. Symbols are the same as in figure 4.5.

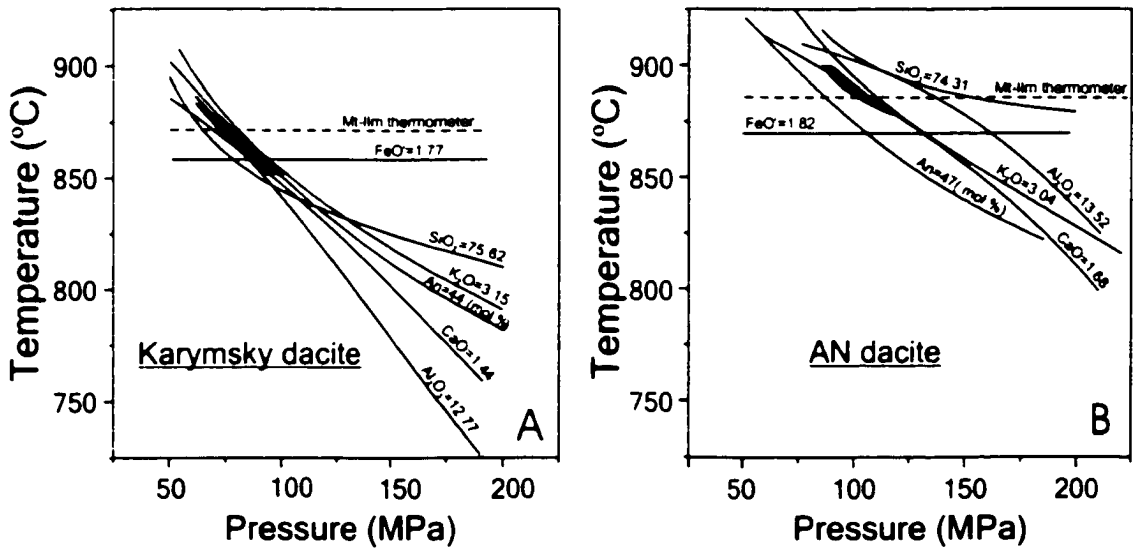

Figure 4.7 Isopleths of major oxides in experimental glass and plagioclase compositions (solid lines) that correspond to compositions of matrix glass and plagioclase in Karymsky (**A**) and AN (**B**) dacites. Dashed lines show temperatures estimated from natural magnetite-ilmenite pairs in the dacites. Shaded areas correspond to P-T conditions, where compositions of experimentally produced glass and plagioclase best match those in natural samples.

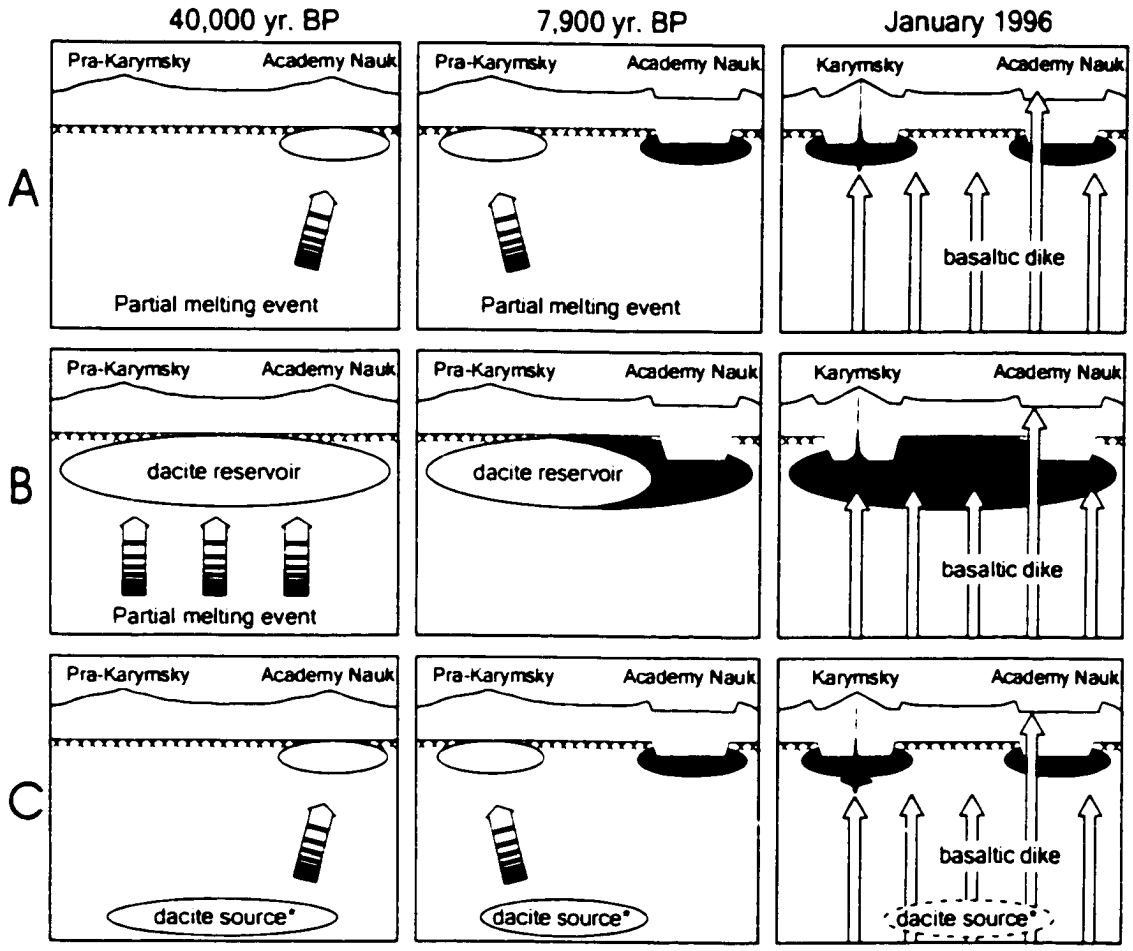

Figure 4.8 Possible scenarios for the sequence of caldera-forming events at Karymsky and Academy Nauk (see text for discussion). (**A**) Separate partial melting events produce small batches of dacite (10-12 km^3), which ascend and cause the caldera-forming eruptions at 40,000 yr. BP and 7,900 yr. BP. (**B**) Large dacitic body (~200 km^3) ascends and feeds the caldera-forming eruptions at 40,000 yr. BP and 7,900 yr. BP. (**C**) Two separate 10-12 km^3 batches of dacite are derived from a single magma reservoir situated in the lower crust. In all scenarios a basaltic dike in January 1996 samples the crystallized dacitic reservoir, which produced AN caldera-forming eruption. Grey area represents crystallized dacite. Black area represents the andesitic reservoir of Karymsky stratovolcano. The shaded horizontal line represents a regional boundary between Cretaceous metamorphic basement and an overlaying volcano-sedimentary layer at a 3-4 km depth (Balesta, 1991; Sugrobov and Yanovsky, 1991).

(*) Either a dacite reservoir produced by previous partial melting, or, alternatively, a large, long-lived mafic zone with extractable interstitial dacitic melt.

Chapter 5. Conclusions

Geological records show that volcanic eruptions have dramatically affected the shape of our planet, its environment, and population. The majority of volcanoes erupt infrequently, however, with repose periods orders of magnitude longer then the life expectance of any individual researcher. As the result, our understanding of volcanic processes is based largely on studies of past eruptions recorded in ancient volcanic deposits, where critical information on the dynamics of volcanic processes is either lost or hard to derive. From this perspective, due to the frequent and continuous cycles of eruptive activity, Karymsky volcano represents a unique natural laboratory, where the dynamics of volcanic processes can be observed, recorded, and used to test petrological models.

This thesis presents petrologic observations of the current eruptive cycle of Karymsky, which started in January, 1996, with simultaneous eruptions of andesite and basalt from neighboring vents. The eruption chronology, the location of eruptive vents, and the significant ground deformation between the vents suggest that the eruption of Karymsky was most likely initiated by the injection of basalt, which ascended as a dike along the active, longitudinally oriented fault. Petrologic observations provide additional evidence for basaltic replenishment and put some important constraints on the time-scale of mixing basalts into the stored andesite in Karymsky magma system.

Electron microprobe studies show that soon after the beginning of eruption the composition of tephra glass became more mafic, and then, within two months, gradually returned to its original state and remained almost constant for the following three years.

These variations cannot be explained solely by heterogeneity within the Karymsky reservoir and/or fluctuation of magma flux at the beginning of eruption, but instead require an input of basaltic magma.

Further evidence for basaltic replenishment is the presence of xenocrysts of basaltic origin in the andesites of Karymsky. A conspicuous portion of plagioclase phenocrysts in Karymsky andesites contains calcic cores, which compositionally and texturally mimic those in Academy Nauk basalt. In addition, the earlier portions of andesite contain rare xenocrysts of olivine, which occur as relicts in plagioclase-pyroxene aggregates. The composition of olivine xenocrysts in Karymsky andesite matches that of olivines in Academy Nauk basalt. Both compositional fingerprinting and textural analysis suggest that calcic plagioclase and olivine were introduced to Karymsky andesite by basalt at the onset of the 1996 eruptive cycle.

By late February, 1996, Karymsky volcano has been erupting homogeneous andesites, which contained neither xenoliths nor textural banding. The homogeneity of andesite suggests that thorough mixing of basalt and andesite occurred in a period of time as short as two months. This finding is surprising and counter-intuitive. Most likely the rapid and effective blending was facilitated by small contrasts in viscosity and temperature between the magmas and by a vigorous fluid dynamic regime in Karymsky reservoir. In this respect, Karymsky is a well-mixed end-member case that reflects the short recurrence interval of recharges to the system. In contrast, Trident volcano in Alaska may represent an intermediate case, where both "clotting" and direct mixing

occurred (Coombs et al., 2000), and Soufriere Hills in Montserrat – a poorly-mixed case, where clotting is dominant (Murphy et al., 2000).

The study of granophyres, which occurred as xenoliths in Academy Nauk basalts, and dacites of the two most recent caldera-forming eruptions provide new information on the eruptive history of Karymsky volcanic center, as well as the structure of the upper crust immediately below Karymsky and Academy Nauk. Whole-rock compositions, electron microprobe analyses, and phase-equilibria experiments suggest that the granophyre xenoliths represent a crystallized dacitic reservoir, which produced the 40,000 BP caldera-forming eruption of Academy Nauk. The plutonic remnants of the dacite must be located at depth corresponding to a pressure of 100±15 MPa. Another plutonic body, the eruption of which formed the 7,900 BP Karymsky caldera, is likely located at a similar depth, approximately 3 km below the basement of Karymsky volcano. Interestingly, seismic and deformation studies suggest that the roof of the active reservoir of Karymsky volcano is also located at 3-4 km depth. This depth coincides with the regional stratigraphic boundary between a lower metamorphic basement and upper volcano-sedimentary layer, which apparently acts as a trap for ascending magmas.

In conclusion, the findings presented in this thesis provide constraints for understanding of magma mixing in general, and the magmatic system at Karymsky and Academy Nauk in particular. Most importantly, it illustrates that igneous processes, which are often thought to last for hundreds and thousands of years, can indeed be remarkably fast.

Appendix 1: List of samples

Sample	Time of eruption	Type
Lavas, volcanic bombs and xenoliths		
97IPE1	1996-1997	Volcanic bomb of Karymsky volcano
97IPE2	1/2/1996	Xenolith of silicic pumice from 1996 AN basalts
97IPE3	1/2/1996	Volcanic bomb of 1996 Academy Nauk eruption
97IPE4	4/6/96 -08/13/96	Andesitic lava flow of Karymsky
97IPE5	9/8/1997	Volcanic bomb of Karymsky volcano
97IPE6	1973	Pyroclastic flow of Karymsky volcano
97IPE7	1/2/1996	Granophyre xenolith from 1996 AN basalts
97IPE8	1/2/1996	Xenolith of altered silicic tuff from 1996 Academy Nauk basalts
98IPE20	1/2/1996	Basaltic lava of monogenetic Lagerny cone
98IPE22a	1/2/1996	Volcanic bomb of 1996 Academy Nauk eruption
98IPE22b	1/2/1996	Volcanic bomb of 1996 Academy Nauk eruption
98IPE22c	1/2/1996	Volcanic bomb of 1996 Academy Nauk eruption
98IPE22d	1/2/1996	Volcanic bomb of 1996 Academy Nauk eruption
98IPE24	Mar. - May, 1998	Lava flow of Karymsky volcano
98IPE25	Dec. 97 - Feb. 98	Lava flow of Karymsky volcano
98IPE26	Jun.- Jul., 1998	Lava flow of Karymsky volcano
98IPE27	4/6/96 - 8/13/96	Lava flow of Karymsky volcano
98IPE28	Sep.-Oct., 1996	Lava flow of Karymsky volcano
98IPE29	Jan.-Feb., 1997	Lava flow of Karymsky volcano
98IPE33	7/21/1998	Volcanic bomb of Karymsky volcano
99IPE 11	5,300-2,800 yr. BP	Lava flow of Karymsky volcano
99IPE 12	Pleistocene	Andesite of Pra-Karymsky volcano exposed at the wall of Karymsky caldera
99IPE 1ab	1/2/1996	Mafic enclave in the granophyre xenolith (sample 99IPE1ag)
99IPE 1ag	1/2/1996	Granophyre xenolith from 1996 AN basalts
99IPE 1c	1/2/1996	Xenolith of silicic pumice from 1996 AN basalts
99IPE 2a	4,800 yr. BP	Basaltic scoria of 4800 yr. BP eruption in Academy Nauk caldera

Appendix 1 continued

Sample	Time of eruption	Type
99IPE 2b	4,800 yr. BP	Basaltic scoria of 4800 yr. BP eruption in Academy Nauk caldera
99IPE 3	Pleistocene	Andesite of Odnoboky volcano exposed near the wall of Academy Nauk caldera
99IPE 4	7,900 yr. BP	Pumice of Karymsky caldera-forming eruption
99IPE 6	40,000 yr. BP	Pumice of Academy Nauk caldera-forming event (~40,000 BP)
99IPE 8	8/24/1999	Andesite volcanic bomb of Karymsky
99IPE 9	8/9/99 - 8/23/99	Lava flow of Karymsky volcano
BV-040496	4/4/1996	Volcanic bomb of Karymsky volcano
BV-170296	2/17/1996	Lava flow of Karymsky volcano
J-4250	7,900 yr. BP	Pumice of Karymsky caldera-forming eruption
J-4491	1976	Lava flow of Karymsky volcano
J-4734	1/2/1996	Volcanic bomb of 1996 Academy Nauk eruption
J-4740	1/2/1996	Xenolith of altered silicic tuff from 1996 Academy Nauk basalts
J-4741	1/2/1996	Xenolith of altered silicic tuff from 1996 Academy Nauk basalts
J-4752	4/6/96 - 8/13/96	Lava flow of Karymsky volcano
J-4756	1/2/1996	Granophyre xenolith from 1996 AN basalts
J-4757	40,000 yr. BP	Obsidian clast from Academy Nauk caldera
J-4758	1/2/1996	Granophyre xenolith from 1996 AN basalts
J-4761	1/2/1996	Granophyre xenolith from 1996 AN basalts
Volcanic ash		
BV-280296-I	1/2/1996	Volcanic ash of Academy Nauk vent
BV-280296-II	1/2/1996	Volcanic ash of Karymsky volcano
BV-280296-III	1/2/1996	Volcanic ash of Academy Nauk vent
BV-110296	2/11/1996	Volcanic ash of Karymsky volcano
BV-180296	2/18/1996	Volcanic ash of Karymsky volcano
BV-220296	2/22/1996	Volcanic ash of Karymsky volcano

Appendix 1 continued

Sample	Time of eruption	Type
BV-280296	2/28/1996	Volcanic ash of Karymsky volcano
BV-010396	3/1/1996	Volcanic ash of Karymsky volcano
BV-240396	3/24/1996	Volcanic ash of Karymsky volcano
BV-080496	4/8/1996	Volcanic ash of Karymsky volcano
BV-180496	4/18/1996	Volcanic ash of Karymsky volcano
BV-250496	4/25/1996	Volcanic ash of Karymsky volcano
BV-010596	5/1/1996	Volcanic ash of Karymsky volcano
BV-100596	5/10/1996	Volcanic ash of Karymsky volcano
BV-270696	6/27/1996	Volcanic ash of Karymsky volcano
BV-100796	7/10/1996	Volcanic ash of Karymsky volcano
K-3/9	10/23/1996	Volcanic ash of Karymsky volcano
K-3/8	11/12/1996	Volcanic ash of Karymsky volcano
K-3/7	12/3/1996	Volcanic ash of Karymsky volcano
K-3/6	12/23/1996	Volcanic ash of Karymsky volcano
K-3/5	1/11/1997	Volcanic ash of Karymsky volcano
K-3/4	2/2/1997	Volcanic ash of Karymsky volcano
K-3/3	2/22/1997	Volcanic ash of Karymsky volcano
K-3/2	3/13/1997	Volcanic ash of Karymsky volcano
K-3/1	4/4/1997	Volcanic ash of Karymsky volcano
BV-030497	4/3/1997	Volcanic ash of Karymsky volcano
98IPE34	7/18/1998	Volcanic ash of Karymsky volcano
M-2113	7/25/1998	Volcanic ash of Karymsky volcano

Appendix 2: Whole-rock data for Karymsky and Academy Nauk pyroclastic rocks

Whole-rock compositions of volcanic bombs and lavas were completed at Washington State University using X-ray fluorescence analysis (major element oxides, Ni, Cr, V, Zr, Ga, Cu, and Zn) and Inductively coupled plasma mass spectrometry (Rare Earth Elements, Ba, Th, Nb, Y, Hf, Ta, U, Pb, Rb, Cs, Sr, and Sc). Major oxides are in wt.%, with all Fe reported as FeO, whereas trace elements are in ppm. The analytical uncertainties for major elements (in relative %) are 0.2% for SiO_2, 0.5% for Al_2O_3 and CaO, 1% for MnO, P_2O_5, Na_2O, TiO_2, and K_2O, and 1.5% for MgO and FeO. XRF precision (in relative %) is 50% for Ni and Cr, 10% for Cu, V, and Ga, 1.5% for Zr, and 4% for Zn. ICP-MS precision is 1% for Ba, Th, and Cs, 2% for all REE except Pr (3%), Y, U, Pb, and Hf, 2% for Rb, 5% for Nb, and 10% for Ta. Analytical procedures are discussed in Nye et al. (1994).

Appendix 2 continued

Sample	97IPE1	97IPE2	97IPE3	97IPE4	97IPE5	97IPE6	97IPE7	97IPE8	98IPE20
SiO_2	62.65	75.45	51.98	61.89	61.72	62.67	70.13	70.00	56.31
Al_2O_3	15.09	12.96	18.73	16.40	16.09	16.33	14.77	14.21	16.33
TiO_2	0.752	0.149	0.739	0.892	0.901	0.860	0.468	0.472	0.808
FeO*	5.58	1.23	7.65	5.96	5.92	5.51	3.30	2.36	7.30
MnO	0.142	0.052	0.146	0.143	0.145	0.139	0.064	0.087	0.157
CaO	4.43	1.20	10.32	5.43	5.31	5.11	2.78	3.63	8.56
MgO	1.84	0.15	5.35	2.02	1.92	1.70	0.93	0.85	4.74
K_2O	1.64	3.59	0.59	1.54	1.57	1.64	2.60	2.02	1.05
Na_2O	3.94	4.07	2.84	4.54	4.52	4.62	4.44	3.01	3.42
P_2O_5	0.154	0.034	0.141	0.254	0.256	0.259	0.093	0.113	0.164
Total	96.22	98.89	98.49	99.07	98.35	98.84	99.58	96.75	98.84
Ni	4	7	26	2	0	1	7	8	14
Cr	8	0	81	9	7	4	3	6	112
V	95	10	221	122	130	109	47	44	212
Zr	127	130	74	139	139	143	206	208	94
Ga	16	11	15	15	19	19	17	21	18
Cu	27	19	57	50	37	34	12	12	62
Zn	79	25	62	72	76	70	32	50	63
La	14.58	16 18	5.17	10.81	11.26	11.93	12.64	14.45	7.99
Ce	24.21	33.22	11.50	24.51	25.28	26.21	27.27	33.39	17.89
Pr	4.59	4.04	1.66	3.39	3.52	3.64	3.41	4.41	2.42
Nd	23.01	16.62	8.26	16.08	16.41	16.93	14.93	19.86	11.44
Sm	6.21	4.02	2.42	4.69	4.84	4.93	4.02	5.26	3.41
Eu	1.86	0.68	0.91	1.44	1.47	1.53	1.00	1.38	1.14
Gd	7.17	3.65	2.69	4.87	5.03	5.25	3.96	5.20	3.67
Tb	1.14	0.64	0.45	0.83	0.85	0.87	0.67	0.92	0.63
Dy	7.12	4.23	2.89	5.36	5.37	5.60	4.38	5.55	4.06
Ho	1.54	0.91	0.60	1.10	1.15	1.17	0.92	1.16	0.84
Er	4.23	2.66	1.66	3.02	3.11	3.21	2.74	3.20	2.33

Appendix 2 continued

Sample	97IPE1	97IPE2	97IPE3	97IPE4	97IPE5	97IPE6	97IPE7	97IPE8	98IPE20
Tm	0.60	0.43	0 24	0.44	0.47	0.48	0.43	0.49	0.35
Yb	3.61	2.80	1.45	2.86	2.84	3.14	2.80	3.27	2.19
Lu	0.58	0.46	0.23	0.46	0.46	0.49	0.46	0.52	0.35
Ba	321	648	165	371	387	403	557	427	278
Th	1.15	3.01	0.52	1.35	1.31	1.51	2.55	2.21	1.12
Nb	2.36	3.95	1.30	3.12	3.15	3.22	3.28	3.48	2.09
Y	45.49	26.37	15.61	30.09	30.31	30.92	26.70	32.10	22.86
Hf	3.58	4.28	1.62	3.83	3.80	3.96	5.43	5.63	2.68
Ta	0.18	0.38	0.11	0.24	0.25	0.26	0.30	0.26	0.17
U	0.67	1.76	0.31	0.82	0.83	0.92	1.40	1.26	0.59
Pb	6.06	8.57	2.64	5.39	5.79	6.30	5.38	8.71	4.15
Rb	19.0	56.1	7.7	20.9	21.4	22.5	35.9	35.1	14.7
Cs	1.01	0.31	0.30	0.83	0.86	0.93	1.23	4.70	0.58
Sr	319	128	466	355	368	347	205	239	371
Sc	23.0	3.2	31.9	22.4	22.6	20.8	10.1	9.5	37.0

Appendix 2 continued

Sample	98IPE22a	98IPE22b	98IPE22c	98IPE22d	98IPE24	98IPE25	98IPE26
SiO_2	51.87	51.58	51.62	51.72	61.47	61.75	61.77
Al_2O_3	19.02	19.18	19.17	19.31	16.27	16.34	16.30
TiO_2	0.728	0.736	0.738	0.736	0.912	0.902	0.906
FeO*	7.47	7.67	7.55	7.48	5.92	5.90	5.77
MnO	0.147	0.145	0.147	0.146	0.145	0.144	0.145
CaO	10.51	10.54	10.68	10.66	5.37	5.34	5.34
MgO	5.71	5.28	5.42	5.50	1.92	1.91	1.90
K_2O	0.58	0.59	0.57	0.56	1.58	1.59	1.60
Na_2O	2.86	2.90	2.84	2.88	4.65	4.70	4.67
P_2O_5	0.141	0.140	0.139	0.140	0.261	0.257	0.261
Total	99.03	98.76	98.88	99.13	98.50	98.83	98.66
Ni	33	25	29	30	0	2	3
Cr	88	81	87	87	9	12	15
V	210	200	216	199	123	128	141
Zr	71	73	72	71	142	143	142
Ga	15	18	16	20	20	19	19
Cu	58	71	65	68	38	38	30
Zn	62	55	59	60	78	76	75
La	5.46	5.36	5.46	5.34	11.58	11.54	11.61
Ce	12.20	12.37	12.39	12.24	26.77	25.66	26.55
Pr	1.74	1.74	1.74	1.73	3.61	3.59	3.61
Nd	8.12	8.33	8.21	8.34	16.75	17.17	16.78
Sm	2.52	2.49	2.56	2.50	4.77	4.94	4.99
Eu	0.95	0.92	0.94	0.93	1.48	1.54	1.55
Gd	2.79	2.70	2.70	2.72	5.06	5.38	5.07
Tb	0.46	0.46	0.46	0.46	0.85	0.87	0.86
Dy	2.92	2.91	2.93	2.84	5.45	5.52	5.48
Ho	0.60	0.59	0.61	0.59	1.14	1.12	1.14
Er	1.59	1.65	1.61	1.61	3.21	3.13	3.11

Appendix 2 continued

Sample	98IPE22a	98IPE22b	98IPE22c	98IPE22d	98IPE24	98IPE25	98IPE26
Tm	0.24	0.24	0.24	0.24	0.46	0.48	0.46
Yb	1.47	1.49	1.51	1.50	3.05	2.96	2.97
Lu	0.23	0.24	0.24	0.23	0.48	0.48	0.47
Ba	173	171	170	168	398	407	394
Th	0.61	0.59	0.60	0.57	1.63	1.62	1.63
Nb	1.40	1.37	1.44	1.33	3.14	3.24	3.22
Y	16.09	15.82	15.17	15.46	30.00	30.40	30.29
Hf	1.68	1.71	1.68	1.64	3.83	4.07	3.90
Ta	0.11	0.10	0.11	0.10	0.24	0.25	0.25
U	0.31	0.31	0.30	0.30	0.87	0.87	0.87
Pb	2.65	2.43	2.59	2.61	5.76	5.97	5.84
Rb	7.5	7.4	7.0	6.7	20.7	20.8	21.0
Cs	0.29	0.30	0.28	0.27	0.84	0.86	0.82
Sr	466	457	443	455	354	350	354
Sc	34.2	32.3	31.5	31.0	21.5	22.7	21.5

Appendix 2 continued

Sample	98IPE27	98IPE28	98IPE29	98IPE33	99IPE 11	99IPE 12	99IPE 1ab
SiO_2	61.87	61.97	62.03	61.99	62.76	60.21	55.95
Al_2O_3	16.29	16.33	16.43	16.41	16.52	16.44	16.88
TiO_2	0.912	0.901	0.916	0.914	0.786	1.110	0.686
FeO*	5.76	5.91	5.61	5.77	5.45	7.21	8.02
MnO	0.147	0.145	0.145	0.147	0.132	0.180	0.203
CaO	5.31	5.33	5.37	5.41	5.28	6.02	8.34
MgO	1.91	1.85	1.94	1.90	2.09	2.50	4.78
K_2O	1.60	1.59	1.59	1.58	1.64	1.30	0.40
Na_2O	4.68	4.73	4.69	4.70	4.47	4.44	3.61
P_2O_5	0.263	0.261	0.262	0.261	0.189	0.267	0.050
Total	98.74	99.02	98.98	99.09	99.32	99.67	98.91
Ni	4	3	4	5	4	0	8
Cr	10	12	7	12	12	11	41
V	135	131	143	130	138	178	254
Zr	143	141	140	140	142	120	54
Ga	19	16	19	17	20	20	16
Cu	30	28	29	35	14	53	22
Zn	71	73	69	74	62	87	87
La	11.95	11.12	11.28	11.32	10.82	10.10	5.91
Ce	26.68	25.95	26.21	26.08	24.00	23.55	15.04
Pr	3.62	3.57	3.64	3.57	3.24	3.29	2.51
Nd	17.17	16.95	16.95	16.70	14.84	16.07	12.32
Sm	5.02	4.70	4.88	4.78	4.18	4.74	4.05
Eu	1.54	1.46	1.48	1.47	1.26	1.53	0.91
Gd	5.23	5.04	5.10	4.89	4.39	4.91	4.51
Tb	0.87	0.85	0.87	0.84	0.74	0.85	0.82
Dy	5.58	5.45	5.48	5.33	4.77	5.39	5.47
Ho	1.12	1.14	1.17	1.10	0.98	1.12	1.15
Er	3.08	3.17	3.23	3.10	2.78	3.14	3.31

Appendix 2 continued

Sample	98IPE27	98IPE28	98IPE29	98IPE33	99IPE 11	99IPE 12	99IPE 1ab
Tm	0.48	0.48	0.47	0.45	0.42	0.46	0.51
Yb	2.95	3.03	3.06	2.98	2.70	2.91	3.25
Lu	0.47	0.49	0.49	0.46	0.43	0.46	0.50
Ba	410	398	398	392	416	352	179
Th	1.62	1.77	1.80	1.64	1.74	1.24	1.27
Nb	3.23	3.28	3.26	3.21	3.11	3.01	1.93
Y	30.46	31.50	30.81	29.62	27.81	30.95	32.55
Hf	3.95	3.97	3.98	3.83	4.04	3.39	1.78
Ta	0.26	0.25	0.24	0.24	0.25	0.22	0.14
U	0.85	0.88	0.91	0.85	0.91	0.64	0.86
Pb	5.94	6.15	5.93	5.74	6.00	4.34	8.61
Rb	21.2	21.7	21.2	21.5	24.4	16.1	3.8
Cs	0.85	0.85	0.81	0.83	0.98	0.41	0.55
Sr	345	369	365	366	343	395	285
Sc	22.4	24.5	24.0	24.2	21.3	29.0	42.8

Appendix 2 continued

Sample	99IPE 1ag	99IPE 1c	99IPE 2a	99IPE 2b	99IPE 3	99IPE 4	99IPE 6
SiO_2	69.42	65.75	56.22	52.91	67.57	68.33	67.95
Al_2O_3	15.67	16.17	16.39	16.45	15.82	14.79	15.02
TiO_2	0.474	0.594	0.797	0.863	0.607	0.517	0.482
FeO*	2.67	4.25	7.75	8.55	3.72	3.27	3.16
MnO	0.054	0.063	0.159	0.176	0.119	0.086	0.091
CaO	3.48	4.11	8.90	10.30	3.34	3.22	3.20
MgO	0.99	1.60	5.16	6.41	1.07	1.07	1.02
K_2O	2.30	1.87	1.00	0.72	2.07	2.33	2.39
Na_2O	4.40	4.18	3.27	2.76	5.13	4.48	4.30
P_2O_5	0.079	0.152	0.153	0.144	0.169	0.111	0.103
Total	99.54	98.74	99.80	99.28	99.61	98.21	97.71
Ni	2	2	17	33	3	3	6
Cr	5	9	116	214	0	5	5
V	54	103	234	281	57	65	63
Zr	198	157	86	62	173	184	190
Ga	17	18	15	17	16	15	14
Cu	28	15	76	86	14	9	12
Zn	31	43	69	73	61	44	47
La	10.60	11.29	6.69	5.37	10.71	12.33	12.48
Ce	21.64	24.68	15.36	12.31	25.25	26.85	27.62
Pr	2.98	3.25	2.12	1.76	3.43	3.47	3.51
Nd	13.61	14.62	10.22	8.64	15.98	15.24	15.64
Sm	3.87	3.93	3.09	2.69	4.63	4.10	4.15
Eu	1.15	1.12	1.02	0.92	1.36	0.99	1.01
Gd	4.05	4.13	3.26	2.93	4.79	4.10	4.07
Tb	0.73	0.71	0.57	0.51	0.85	0.73	0.73
Dy	4.83	4.53	3.62	3.17	5.43	4.59	4.60
Ho	1.03	0.97	0.76	0.66	1.13	0.94	0.97
Er	2.96	2.79	2.11	1.85	3.30	2.79	2.86

Appendix 2 continued

Sample	99IPE 1ag	99IPE 1c	99IPE 2a	99IPE 2b	99IPE 3	99IPE 4	99IPE 6
Tm	0.44	0.42	0.31	0.26	0.49	0.43	0.44
Yb	2.82	2.80	1.99	1.67	3.28	2.76	2.91
Lu	0.46	0.45	0.32	0.27	0.53	0.45	0.46
Ba	526	505	244	186	501	520	532
Th	2.75	2.09	1.00	0.75	2.06	2.55	2.62
Nb	3.62	3.19	1.96	1.47	3.74	3.72	3.57
Y	29.53	28.08	22.14	18.84	33.23	28.61	29.78
Hf	5.73	4.49	2.34	1.69	4.86	5.10	5.28
Ta	0.30	0.25	0.14	0.10	0.28	0.30	0.29
U	1.20	1.05	0.52	0.41	1.02	1.30	1.33
Pb	6.04	5.78	3.69	3.51	8.80	7.92	8.18
Rb	31.1	36.5	14.1	9.2	25.9	34.4	35.6
Cs	0.86	2.51	0.52	0.44	0.74	1.37	1.56
Sr	279	298	381	414	277	241	248
Sc	16.1	17.9	40.4	45.5	16.6	13.1	12.0

Appendix 2 continued

Sample	99IPE 8	99IPE 9	BV040496	BV170296	J-4250	J-4491	J-4734
SiO_2	61.80	61.80	62.88	61.46	68.16	62.89	52.93
Al_2O_3	16.51	16.81	16.35	16.41	14.68	16.33	18.55
TiO_2	0.913	0.899	0.877	0.905	0.504	0.876	0.714
FeO*	5.93	5.63	5.26	5.73	3.21	5.47	7.51
MnO	0.146	0.146	0.140	0.145	0.081	0.143	0.144
CaO	5.51	5.70	4.94	5.43	3.12	5.06	9.88
MgO	2.02	2.03	1.64	1.88	0.95	1.74	5.41
K_2O	1.55	1.52	1.69	1.56	2.30	1.67	0.69
Na_2O	4.57	4.61	4.84	4.63	4.41	4.78	2.93
P_2O_5	0.252	0.249	0.264	0.258	0.126	0.258	0.135
Total	99.20	99.40	98.88	98.41	97.54	99.22	98.89
Ni	3	4	3	1	7	3	28
Cr	11	11	6	6	7	3	71
V	132	139	115	121	65	110	190
Zr	139	136	148	138	184	146	80
Ga	16	16	18	17	17	20	18
Cu	36	39	18	29	13	22	62
Zn	73	73	74	73	71	75	63
La	11.03	10.71	11.84	11.55	12.91	12.17	5 61
Ce	25.40	24.49	27.39	26.57	27.55	28.01	12.93
Pr	3.49	3.38	3.72	3.73	3.54	3.75	1.81
Nd	16.39	15.97	17.33	17.40	15.42	17.65	8.96
Sm	4.70	4.56	4.93	4.91	4.15	4.95	2.55
Eu	1.43	1.43	1.47	1.49	0.97	1.51	0.93
Gd	4.85	4.74	5.07	5.17	4.23	5.24	2.92
Tb	0.83	0.82	0.87	0.86	0.73	0.88	0.48
Dy	5.18	5.03	5.51	5.54	4.60	5.57	3.07
Ho	1.08	1.05	1.18	1.16	1.00	1.17	0.64
Er	2.97	3.01	3.30	3.22	2.86	3.21	1.72

Appendix 2 continued

Sample	99IPE 8	99IPE 9	BV040496	BV170296	J-4250	J-4491	J-4734
Tm	0.44	0.44	0.49	0.47	0.44	0.48	0.26
Yb	2.89	2.75	3.12	3.08	2.78	3.10	1.53
Lu	0.45	0.45	0.50	0.49	0.45	0.49	0.25
Ba	391	385	418	399	490	426	178
Th	1.61	1.54	1.80	1.76	2.21	1.79	0.56
Nb	3.18	3.15	3.44	3.30	3.66	3.45	1.43
Y	31.50	30.23	32.48	31.17	27.14	32.02	16.06
Hf	3.76	3.76	4.09	4.05	5.13	4.09	1.86
Ta	0.24	0.23	0.26	0.26	0.31	0.26	0.11
U	0.84	0.79	0.91	0.90	1.34	0.93	0.34
Pb	5.65	5.52	6.21	5.99	8.79	6.29	2.85
Rb	21.2	20.3	22.9	21.3	32.9	22.9	9.1
Cs	0.86	0.84	0.93	0.86	1.48	0.94	0.39
Sr	374	376	353	353	242	354	437
Sc	22.9	23.1	22.8	23.4	12.4	22.2	30.2

Appendix 2 continued

Sample	J-4740	J-4741	J-4752	J-4756	J-4757	J-4758	J-4761
SiO_2	65.26	66.66	62.51	68.68	75.69	64.88	70.10
Al_2O_3	15.40	15.36	16.05	15.24	13.21	15.60	14.36
TiO_2	0.500	0.504	0.901	0.516	0.162	0.541	0.483
FeO*	2.56	2.63	5.96	3.57	1.32	4.38	3.37
MnO	0.106	0.099	0.144	0.071	0.061	0.090	0.068
CaO	4.10	4.34	5.13	3.22	1.14	4.50	2.93
MgO	0.75	0.74	1.90	0.93	0.17	1.83	0.97
K_2O	2.06	1.76	1.61	2.32	3.36	2.32	2.57
Na_2O	3.15	3.13	4.54	4.70	4.54	3.77	4.40
P_2O_5	0.117	0.117	0.262	0.123	0.037	0.130	0.100
Total	94.00	95.34	99.01	99.37	99.69	98.04	99.35
Ni	8	6	2	6	6	10	4
Cr	4	1	9	6	0	17	5
V	49	33	123	43	1	96	59
Zr	240	242	144	208	129	164	211
Ga	16	18	16	16	13	17	16
Cu	4	1	26	14	4	16	8
Zn	58	55	77	40	30	48	33
La	15.58	15.59	11.30	13.92	15.87	13.07	13.46
Ce	34.59	34.83	25.59	29.88	33.61	28.19	29.69
Pr	4.52	4.73	3.50	3.87	4.02	3.57	3.90
Nd	20.93	21.50	16.43	17.34	16.83	15.68	17.40
Sm	5.69	5.78	4.74	4.86	3.95	4.02	4.70
Eu	1.36	1.49	1.42	1.20	0.67	0.89	1.08
Gd	5.43	5.66	4.87	4.81	3.87	3.65	4.59
Tb	0.93	0.97	0.82	0.84	0.65	0.62	0.82
Dy	5.84	6.00	5.19	5.37	4.28	3.93	5.33
Ho	1.26	1.27	1.09	1.17	0.90	0.80	1.15
Er	3.55	3.59	3.06	3.44	2.71	2.31	3.26

Appendix 2 continued

Sample	J-4740	J-4741	J-4752	J-4756	J-4757	J-4758	J-4761
Tm	0.53	0.54	0.46	0.54	0.44	0.34	0.52
Yb	3.43	3.35	2.87	3.34	2.83	2.18	3.23
Lu	0.56	0.54	0.46	0.56	0.47	0.36	0.53
Ba	365	349	377	478	653	392	550
Th	2.23	2.17	1.26	2.44	2.97	2.27	2.66
Nb	3.55	3.75	3.05	3.76	3.98	2.81	4.21
Y	33.82	34.58	29.68	32.16	26.79	22.14	31.84
Hf	6.01	6.16	3.70	5.95	4.31	4.78	6.33
Ta	0.30	0.30	0.24	0.33	0.38	0.25	0.35
U	1.33	1.29	0.80	1.30	1.81	1.23	1.38
Pb	9.14	8.91	5.46	10.08	9.42	4.56	5.70
Rb	45.0	35.5	20.8	28.1	50.0	34.4	38.7
Cs	23.74	31.52	0.92	1.02	1.76	0.44	1.07
Sr	460	697	358	245	108	300	244
Sc	9.6	10.4	21.0	12.8	3.7	13.2	12.1

Appendix 3: Electron microprobe analyses of glass in natural samples

All samples were polished and carbon-coated to a thickness of ca. 250 Å. Matrix glasses and glass inclusions were analyzed for major elements at the University of Alaska Fairbanks using a Cameca SX-50 electron microprobe, which is equipped with four wavelength-dispersive and one energy-dispersive spectrometers. A 15 keV, 10 nA, 10-μm-diameter beam was used for all analyses. Na and Al were analyzed first in order to reduce the effect of volatilization. Major oxides are in wt.% with all Fe reported as FeO. Details about counting times, standards, and analytical errors are summarized below.

Element	Counting Time		Standard	Typical Analytical Error (wt.%, 1 sigma)*
	Peak (sec.)	Background (sec.)		
Na	10	5	Rhyolitic Glass (USNM 72854)	0.068
Mg	10	5	Basaltic Glass (USNM 113498/1)	0.086
Al	10	5	Orthoclase (CM Taylor)	0.092
Si	30	15	Wollastonite (CM Taylor)	0.137
Cl	10	5	Scapolite (USNM R6600-1)	0.014
K	10	5	Orthoclase (CM Taylor)	0.023
Ca	10	5	Wollastonite (CM Taylor)	0.072
Ti	15	7.5	Basaltic Glass (USNM 113498/1)	0.037
Fe	15	7.5	Basaltic Glass (USNM 113498/1)	0.109

* Typical analytical errors for a representative sample calculated after Scott et al. (1995).

Appendix 3 continued

Na_2O	MgO	Al_2O_3	SiO_2	Cl	K_2O	CaO	TiO_2	FeO*	Total
BV-280296-I volcanic ash of Academy Nauk									
3.66	3.11	14.58	56.74	0.10	1.13	6.56	1.05	8.05	94.98
4.35	2.20	16.81	57.38	0.11	0.98	7.37	1.06	7.13	97.40
3.71	2.79	14.00	57.50	0.18	1.38	6.12	1.46	9.81	96.96
3.91	3.23	13.89	57.64	0.12	1.31	5.97	1.27	9.61	96.93
4.42	1.84	18.66	57.68	0.11	0.95	7.35	0.84	6.38	98.24
3.66	2.96	13.90	57.90	0.12	1.31	6.44	1.27	9.44	96.99
3.81	2.62	14.15	58.08	0.12	1.25	6.05	1.67	9.42	97.16
4.09	2.39	15.13	58.18	0.09	1.11	6.49	1.58	8.56	97.59
4.56	1.62	17.63	58.69	0.06	1.17	6.78	1.05	6.04	97.60
4.11	2.63	14.76	58.86	0.12	1.54	5.63	1.09	8.94	97.68
4.17	2.17	14.91	60.00	0.09	1.55	5.52	1.38	8.08	97.88
BV-280296-II volcanic ash of Karymsky									
2.59	0.40	15.07	71.27	0.07	2.00	2.87	0.89	3.17	98.33
3.51	0.33	12.26	72.43	0.15	4.47	1.50	0.99	3.26	98.90
3.47	0.50	11.95	72.53	0.14	3.44	1.21	0.79	4.47	98.49
5.02	0.24	13.06	72.63	0.10	2.32	1.69	0.72	2.44	98.21
3.49	0.39	12.05	72.70	0.09	4.41	1.31	0.80	3.74	98.98
4.34	0.32	12.39	73.00	0.09	3.26	1.23	1.02	3.37	99.01
3.52	0.27	12.76	73.32	0.14	2.91	1.49	0.92	3.25	98.59
1.77	0.42	12.59	73.33	0.07	3.89	1.63	0.88	3.69	98.27
4.20	0.25	12.02	73.85	0.10	3.32	1.09	0.83	3.11	98.78
4.12	0.26	11.84	74.40	0.09	3.13	1.34	0.78	3.31	99.28
4.02	0.27	11.94	74.46	0.21	3.02	1.27	0.86	3.02	99.06
3.72	0.29	11.93	74.51	0.16	3.35	1.02	0.72	3.10	98.80
3.72	0.19	12.18	74.79	0.13	3.52	0.77	0.90	2.68	98.88
3.70	0.16	11.99	75.00	0.14	3.50	0.86	0.58	2.86	98.79
3.93	0.18	11.29	75.40	0.15	3.61	0.93	0.69	2.64	98.81

Appendix 3 continued

Na_2O	MgO	Al_2O_3	SiO_2	Cl	K_2O	CaO	TiO_2	FeO*	Total
3.94	0.22	11.27	76.02	0.11	3.76	0.71	0.65	2.50	99.17
4.03	0.11	11.83	76.17	0.17	3.55	0.76	0.75	2.15	99.50
BV-280296-III volcanic ash of Academy Nauk									
3.04	6.56	14.06	53.78	0.07	0.60	9.99	1.09	9.91	99.10
3.98	2.86	14.99	56.83	0.05	1.13	6.06	1.27	8.86	96.02
4.32	2.23	17.30	56.84	0.08	0.95	7.64	0.88	7.41	97.63
3.82	3.54	13.90	56.94	0.11	1.20	6.48	1.00	9.38	96.37
4.35	2.13	17.62	57.01	0.12	0.91	7.34	0.76	6.86	97.09
3.89	3.33	14.36	57.18	0.15	1.10	6.69	1.31	8.79	96.79
4.12	2.56	15.48	57.38	0.13	1.19	6.72	0.97	8.58	97.12
3.87	2.89	13.95	57.85	0.15	1.27	6.33	1.22	9.68	97.22
3.85	2.80	14.12	58.09	0.13	1.34	6.04	1.22	8.92	96.52
4.08	2.04	15.96	58.13	0.13	1.12	6.47	1.25	8.66	97.83
2.64	7.26	10.82	58.47	0.08	1.28	5.24	1.02	10.94	97.74
4.40	1.36	17.64	60.15	0.11	1.43	6.23	0.95	6.10	98.36
BV-110296 volcanic ash of Karymsky									
5.54	0.19	14.46	70.50	0.08	2.35	2.16	0.79	2.32	98.39
5.40	0.89	14.51	67.03	0.14	2.39	2.75	0.85	3.70	97.64
5.25	1.28	13.87	67.30	0.16	2.41	2.80	1.03	4.82	98.93
5.17	1.05	13.97	68.10	0.13	2.37	2.83	1.20	4.56	99.36
5.31	1.04	14.12	67.18	0.16	2.50	3.02	0.76	4.49	98.57
5.30	0.89	13.95	67.58	0.04	1.86	3.21	0.89	5.13	98.84
BV-180296 volcanic ash of Karymsky									
4.85	1.21	14.23	67.01	0.00	2.48	3.44	0.92	3.99	98.13
3.59	0.99	14.08	67.54	0.11	2.20	1.67	0.87	3.81	94.86
3.50	1.04	13.93	67.69	0.04	2.28	2.04	0.85	3.79	95.16
5.06	0.39	15.10	67.89	0.09	2.05	3.77	0.87	3.21	98.42
5.17	0.73	13.98	67.92	0.00	2.21	2.68	0.87	3.62	97.18

Appendix 3 continued

Na_2O	MgO	Al_2O_3	SiO_2	Cl	K_2O	CaO	TiO_2	FeO*	Total
2.85	0.94	14.27	67.93	0.01	4.17	0.37	0.75	3.67	94.94
4.74	0.57	12.59	68.41	0.13	2.32	2.33	0.91	3.92	95.92
4.36	0.64	12.32	68.69	0.14	2.66	1.74	0.80	4.16	95.49
2.60	0.91	14.36	68.72	0.01	4.23	0.41	0.80	3.72	95.76
5.86	0.89	14.11	68.93	0.00	1.75	2.35	1.01	4.44	99.34
4.09	1.09	14.61	69.45	0.04	2.51	1.53	0.76	3.75	97.83
4.07	1.00	14.74	69.53	0.05	2.60	1.96	0.81	3.91	98.67
BV-220296 volcanic ash of Karymsky									
5.51	0.32	18.06	65.60	0.04	2.23	4.61	0.52	2.53	99.43
4.56	1.11	14.19	67.22	0.03	2.43	3.08	0.70	4.00	97.33
4.96	1.00	14.39	67.52	0.04	2.53	2.95	0.71	4.12	98.21
5.68	0.12	17.51	67.76	0.01	2.16	3.91	0.49	2.00	99.64
4.08	1.15	13.57	68.26	0.03	2.29	2.25	0.70	4.58	96.90
4.45	0.79	13.68	68.31	0.04	3.83	1.62	0.80	4.14	97.65
5.28	0.44	15.89	68.38	0.09	2.25	3.53	0.66	3.11	99.63
5.98	0.12	16.44	68.65	0.01	2.14	3.48	0.63	2.31	99.77
3.27	1.01	14.21	68.67	0.00	3.48	2.09	0.89	2.54	96.16
4.04	1.28	11.93	69.71	0.03	3.32	2.51	0.99	5.21	99.01
4.29	0.50	12.79	71.24	0.15	2.93	1.80	1.12	4.35	99.15
4.30	0.49	13.14	71.26	0.07	3.26	2.08	1.10	4.50	100.22
BV-280296 volcanic ash of Karymsky									
1.76	0.63	14.88	71.14	0.02	3.46	1.21	0.80	3.91	97.79
4.81	0.63	15.33	69.13	0.06	2.09	2.23	0.97	3.28	98.53
4.46	0.71	13.07	70.38	0.09	2.80	2.28	0.87	4.14	98.80
4.18	0.72	14.87	69.75	0.13	2.29	1.76	1.05	4.10	98.85
3.96	0.72	12.35	72.43	0.12	2.81	1.66	0.81	4.13	98.99
4.23	0.82	13.59	69.50	0.10	2.82	1.72	1.15	4.12	98.03
5.24	0.93	14.07	67.84	0.00	2.23	3.07	0.88	4.20	98.45

Appendix 3 continued

Na_2O	MgO	Al_2O_3	SiO_2	Cl	K_2O	CaO	TiO_2	FeO*	Total
2.00	1.09	14.64	71.02	0.01	2.91	2.09	0.93	3.39	98.07
1.41	1.27	14.55	70.41	0.00	2.91	1.71	0.84	4.78	97.89
BV-010396 volcanic ash of Karymsky									
5.04	0.36	15.16	70.18	0.10	2.26	2.75	0.55	2.86	99.24
4.61	0.35	14.81	71.38	0.10	2.52	2.53	0.54	2.73	99.55
4.52	0.39	13.53	71.98	0.09	2.73	2.03	0.91	3.37	99.56
4.14	0.17	12.88	72.19	0.13	4.60	1.16	0.73	2.24	98.23
4.28	0.34	13.49	72.55	0.11	2.73	1.91	0.80	3.14	99.35
3.83	0.50	12.43	72.59	0.14	2.69	1.63	0.94	3.17	97.92
4.27	0.33	12.34	72.74	0.14	2.87	1.33	0.73	3.43	98.17
3.60	0.66	12.32	72.76	0.10	2.79	1.54	0.59	3.55	97.89
3.76	0.42	12.33	72.79	0.11	3.07	1.46	0.79	4.00	98.73
3.61	0.46	12.52	72.92	0.10	2.82	1.64	0.89	3.37	98.32
4.05	0.32	12.11	73.64	0.09	2.94	1.42	0.70	3.35	98.62
3.98	0.34	12.01	73.66	0.11	3.35	1.31	0.79	3.38	98.91
4.16	0.45	12.58	73.70	0.11	2.92	1.66	0.82	3.49	99.87
3.20	0.45	12.13	73.81	0.09	2.86	1.42	0.65	3.51	98.11
4.57	0.24	11.84	73.99	0.00	3.60	1.42	0.76	2.90	99.31
3.89	0.40	11.72	74.20	0.09	3.06	1.30	0.83	3.72	99.19
3.73	0.33	11.86	74.22	0.09	3.11	1.32	0.74	3.47	98.87
4.74	0.22	12.11	74.32	0.02	3.62	0.97	1.08	2.57	99.64
BV-240396 volcanic ash of Karymsky									
3.97	0.39	12.00	70.60	0.20	2.87	1.59	0.91	3.35	95.88
2.78	0.26	12.87	71.34	0.10	2.89	1.61	0.87	2.95	95.66
5.16	0.40	13.88	71.43	0.17	2.44	2.13	1.14	3.00	99.75
4.08	0.42	12.09	71.50	0.13	2.95	1.36	0.65	3.69	96.87
4.14	0.45	11.71	71.70	0.11	3.06	1.30	1.01	3.75	97.23
4.45	0.27	11.98	72.10	0.13	3.48	1.25	0.94	3.69	98.29

Appendix 3 continued

Na_2O	MgO	Al_2O_3	SiO_2	Cl	K_2O	CaO	TiO_2	FeO*	Total
4.44	0.27	11.93	72.23	0.10	3.22	1.37	1.05	3.97	98.60
4.04	0.25	12.49	72.35	0.15	3.37	1.42	0.67	2.94	97.69
2.86	0.24	12.07	72.63	0.15	3.33	1.57	0.87	2.96	96.66
4.45	0.27	12.35	72.64	0.18	3.05	1.28	1.12	3.48	98.84
5.05	0.33	11.69	73.10	0.10	2.32	1.44	0.79	3.52	98.34
4.14	0.30	11.64	73.19	0.13	3.79	0.88	0.84	3.72	98.64
BV-080496 volcanic ash of Karymsky									
4.63	0.52	14.36	69.60	0.06	2.68	2.57	0.80	3.82	99.03
4.41	0.42	14.52	69.69	0.10	2.51	2.64	0.77	3.43	98.49
4.11	0.73	12.88	70.26	0.08	2.51	2.16	1.12	4.36	98.21
3.98	0.55	14.34	70.34	0.11	2.55	2.84	1.03	4.06	99.79
3.44	0.51	12.77	71.67	0.13	2.92	1.89	1.10	4.49	98.92
3.61	0.53	13.03	71.81	0.05	2.78	2.16	0.86	4.16	98.98
3.51	0.65	12.04	72.06	0.09	2.68	1.90	1.18	4.44	98.54
3.48	0.48	12.64	72.10	0.10	2.91	1.83	1.09	4.55	99.19
3.59	0.52	12.46	72.14	0.14	2.75	1.91	1.08	4.02	98.61
BV-180496 volcanic ash of Karymsky									
4.18	1.80	12.11	69.08	0.11	2.69	2.26	0.97	5.25	98.45
4.20	0.49	14.48	69.42	0.19	2.33	3.00	0.76	3.86	98.73
3.50	1.54	12.27	69.45	0.06	2.61	2.32	1.13	4.85	97.74
4.64	0.61	12.36	70.44	0.14	2.93	2.05	0.87	4.23	98.28
3.94	0.55	12.56	70.75	0.14	2.75	2.01	0.83	4.46	97.99
3.75	0.89	12.76	70.94	0.11	2.67	2.00	1.12	4.80	99.04
4.29	0.46	12.64	70.97	0.14	3.04	1.61	1.36	4.42	98.92
4.54	0.50	13.00	71.11	0.11	2.58	1.98	0.79	4.31	98.91
4.00	0.59	12.56	71.12	0.07	2.89	1.84	0.90	4.08	98.03
3.91	0.50	12.88	71.28	0.08	2.77	2.12	1.09	4.34	98.96
3.99	0.55	12.77	71.28	0.13	2.78	2.23	0.94	4.31	98.99

Appendix 3 continued

Na_2O	MgO	Al_2O_3	SiO_2	Cl	K_2O	CaO	TiO_2	FeO*	Total
BV-250496 volcanic ash of Karymsky									
3.97	1.08	12.40	70.88	0.07	2.94	2.15	1.18	4.96	99.63
4.43	0.84	12.66	70.99	0.09	2.78	1.97	1.04	4.68	99.48
3.78	0.63	12.88	71.41	0.15	2.79	2.08	1.32	4.70	99.74
3.99	0.51	12.50	71.50	0.12	3.11	1.88	1.04	4.50	99.15
3.56	0.53	12.70	71.56	0.14	2.68	1.98	0.99	4.69	98.81
3.32	0.95	12.04	71.59	0.16	2.90	2.18	1.22	5.21	99.57
3.67	0.55	12.69	71.67	0.10	2.70	1.88	1.02	4.29	98.56
3.79	0.56	12.82	71.70	0.16	2.71	2.26	1.18	4.24	99.41
4.23	0.46	12.39	71.70	0.11	3.17	1.70	1.35	4.24	99.36
4.07	0.49	12.49	71.73	0.15	2.93	1.96	1.22	4.14	99.17
3.48	0.65	12.73	71.92	0.11	2.72	1.82	1.21	4.29	98.93
4.03	0.54	12.36	71.99	0.16	2.93	2.11	1.08	4.66	99.85
3.23	0.57	12.70	72.07	0.12	2.80	1.88	0.91	4.42	98.70
4.77	0.57	12.67	72.42	0.05	2.53	1.99	1.15	3.28	99.43
BV-010596 volcanic ash of Karymsky									
4.46	0.52	14.13	70.30	0.10	2.36	2.54	0.92	3.52	98.84
3.84	0.52	13.59	70.52	0.08	2.62	2.87	0.91	3.88	98.83
4.08	0.52	13.99	70.74	0.10	2.57	2.51	0.76	4.00	99.26
4.28	0.58	13.72	70.95	0.13	2.64	2.61	0.85	4.11	99.87
3.94	1.11	11.91	71.58	0.15	3.07	1.23	1.05	4.30	98.35
3.37	0.74	12.39	71.83	0.14	2.72	2.46	1.11	4.47	99.21
3.78	0.51	12.70	72.02	0.14	3.02	2.44	0.84	3.79	99.25
3.80	0.72	12.81	72.10	0.16	3.05	1.98	1.16	4.52	100.29
3.32	0.62	12.52	72.23	0.13	2.73	2.07	0.80	4.04	98.45
3.41	0.52	12.66	72.48	0.14	2.92	1.83	1.05	4.32	99.33
3.30	0.59	12.51	72.92	0.14	2.81	1.92	0.97	4.38	99.54

Appendix 3 continued

Na_2O	MgO	Al_2O_3	SiO_2	Cl	K_2O	CaO	TiO_2	FeO*	Total
BV-100596 volcanic ash of Karymsky									
4.00	0.82	13.47	70.27	0.14	2.45	2.39	1.11	4.47	99.11
4.26	0.51	13.80	70.30	0.13	2.53	2.54	0.78	4.17	99.02
3.92	0.59	12.52	70.60	0.11	2.69	1.93	1.26	4.37	97.98
4.03	0.47	13.25	70.69	0.13	2.56	2.20	0.88	3.91	98.10
3.41	1.13	12.52	70.93	0.16	2.66	2.23	0.80	4.75	98.58
3.62	0.61	12.36	71.27	0.16	2.65	2.03	1.15	4.74	98.59
4.09	0.63	12.68	71.68	0.13	2.72	1.99	1.27	4.34	99.54
4.23	0.50	12.16	71.70	0.13	2.97	1.90	1.06	4.52	99.17
3.29	0.52	12.32	71.79	0.14	2.81	1.88	1.18	4.72	98.65
3.47	0.60	12.51	71.83	0.06	2.79	1.75	1.12	4.36	98.49
4.21	0.52	12.66	71.89	0.09	2.85	2.00	1.27	4.63	100.13
3.77	0.46	12.53	71.96	0.04	2.77	1.80	1.27	4.35	98.95
4.02	0.52	12.73	71.99	0.05	2.83	1.85	1.11	4.28	99.38
BV-270696 volcanic ash of Karymsky									
4.60	0.40	13.67	71.71	0.09	2.97	2.16	0.98	3.73	100.32
3.95	0.49	12.48	71.91	0.09	3.48	1.94	1.07	4.03	99.44
3.96	0.31	12.37	72.52	0.13	3.39	1.19	1.14	3.77	98.77
3.33	0.50	12.42	72.56	0.09	2.82	1.70	1.04	3.98	98.43
3.58	0.48	12.49	72.56	0.10	2.89	1.85	0.59	4.31	98.85
4.22	0.37	12.47	72.92	0.13	3.39	1.58	0.94	3.94	99.95
3.66	0.48	12.80	73.18	0.14	2.76	1.58	0.78	4.57	99.95
3.40	0.49	12.72	73.26	0.04	3.09	1.50	1.07	4.29	99.86
4.41	0.45	12.16	73.55	0.13	2.89	1.60	1.16	3.99	100.35
BV-100796 volcanic ash of Karymsky									
5.68	0.56	11.95	70.78	0.01	1.06	2.24	1.63	5.65	99.54
5.74	0.40	13.37	71.20	0.04	1.05	2.53	1.06	3.68	99.05
4.91	0.13	14.42	71.37	0.15	2.58	2.30	0.76	2.64	99.28

Appendix 3 continued

Na_2O	MgO	Al_2O_3	SiO_2	Cl	K_2O	CaO	TiO_2	FeO*	Total
3.26	0.51	12.39	71.58	0.06	2.84	1.81	0.97	4.24	97.67
3.27	0.42	12.45	72.25	0.16	2.90	1.64	0.83	3.89	97.81
5.87	0.08	14.45	72.58	0.05	1.74	2.05	1.07	1.95	99.84
5.17	0.40	12.19	73.03	0.03	2.48	1.57	0.82	3.20	98.89
3.91	0.35	12.26	73.03	0.16	3.02	1.61	0.99	3.39	98.71
4.25	0.34	11.78	73.44	0.12	3.83	1.05	0.95	2.88	98.65
4.01	0.35	12.02	73.47	0.20	3.08	1.50	0.93	3.19	98.75
5.58	0.35	11.54	73.53	0.05	1.12	1.77	1.01	4.52	99.46
5.93	0.26	12.68	74.22	0.00	1.46	1.38	0.58	2.35	98.85
5.48	0.13	12.28	74.52	0.10	2.36	1.13	0.83	2.20	99.03
3.98	0.02	11.64	74.62	0.13	3.63	0.70	0.88	2.02	97.60
4.97	0.07	12.35	74.83	0.10	2.94	0.90	0.50	1.72	98.36
3.76	0.04	11.52	75.75	0.12	4.20	0.44	1.10	2.14	99.07
K-3/9 volcanic ash of Karymsky									
4.61	0.49	13.91	69.98	0.11	2.70	2.74	0.91	3.71	99.17
4.29	0.56	12.83	70.33	0.13	2.94	2.17	1.07	4.47	98.78
5.02	0.23	14.85	70.42	0.05	2.29	2.69	0.66	3.02	99.23
4.08	0.49	12.90	70.87	0.11	3.16	2.06	0.82	4.28	98.76
3.88	0.64	12.71	71.07	0.16	3.12	1.97	1.22	4.26	99.05
4.32	0.57	12.82	71.07	0.18	2.75	2.11	0.97	4.30	99.08
4.05	0.26	12.71	71.79	0.15	3.22	1.65	1.03	4.12	98.97
3.86	1.13	12.17	71.80	0.12	3.20	1.88	1.16	5.55	100.87
4.04	0.27	13.34	71.94	0.18	3.36	1.57	1.04	4.42	100.16
K-3/8 volcanic ash of Karymsky									
4.60	0.51	12.48	70.09	0.29	3.13	2.57	0.90	4.99	99.55
4.05	0.47	13.49	70.36	0.16	2.66	2.52	1.15	4.32	99.17
3.11	0.60	12.57	71.01	0.13	2.84	2.22	0.89	4.46	97.84
3.54	0.57	12.79	71.10	0.11	2.93	2.08	0.76	4.42	98.30

Appendix 3 continued

Na_2O	MgO	Al_2O_3	SiO_2	Cl	K_2O	CaO	TiO_2	FeO*	Total
4.08	0.35	12.88	71.55	0.07	3.49	1.73	1.12	4.40	99.68
4.81	0.38	12.56	71.91	0.04	2.10	2.49	1.18	4.11	99.59
3.99	0.27	12.44	71.92	0.08	3.17	1.68	0.93	4.32	98.80
4.85	0.28	13.35	72.11	0.07	2.71	2.21	0.79	3.55	99.92
4.78	0.19	12.71	72.25	0.15	3.09	1.33	1.10	3.73	99.31
4.53	0.21	13.59	72.40	0.13	2.80	1.85	0.92	3.48	99.91
4.94	0.17	12.97	72.91	0.20	2.37	1.90	0.92	3.43	99.81
K-3.7 volcanic ash of Karymsky									
4.31	0.21	12.33	72.06	0.14	3.33	1.37	0.87	3.80	98.42
3.99	0.38	12.34	71.74	0.18	3.15	1.80	0.87	3.87	98.31
3.98	0.15	12.32	72.31	0.13	3.29	1.83	0.93	3.93	98.88
4.41	0.29	12.10	73.17	0.11	3.26	1.23	1.02	3.99	99.59
3.94	0.37	12.80	71.85	0.13	3.20	1.67	0.95	4.03	98.92
4.24	0.33	12.60	72.05	0.14	3.11	1.62	1.01	4.15	99.27
3.93	0.55	12.71	71.62	0.08	3.21	1.63	0.84	4.23	98.80
3.47	0.51	13.15	70.80	0.15	2.83	2.14	0.95	4.23	98.23
3.13	0.49	12.79	71.40	0.16	2.87	2.03	0.95	4.25	98.07
3.88	0.37	11.82	72.54	0.14	3.16	1.49	0.97	4.28	98.65
3.91	0.40	12.64	72.02	0.19	3.15	1.66	1.01	4.37	99.35
3.07	0.51	12.82	71.77	0.11	2.96	1.99	1.04	4.41	98.67
3.26	0.50	12.69	71.70	0.14	2.94	2.04	1.01	4.42	98.70
3.95	0.47	12.45	72.12	0.15	3.11	1.77	0.94	4.45	99.39
3.90	0.49	12.72	71.26	0.17	3.01	1.89	0.76	4.47	98.65
4.70	0.32	12.07	71.92	0.14	2.69	1.55	1.32	4.49	99.18
4.04	0.34	12.33	71.76	0.19	3.25	1.62	0.88	4.53	98.94
4.18	0.36	12.64	72.33	0.11	3.33	1.49	1.11	4.59	100.14
4.10	0.42	12.15	70.81	0.15	3.28	2.18	1.11	4.66	98.85
4.46	0.49	12.45	71.12	0.13	2.89	1.91	1.18	4.78	99.41
4.83	0.50	12.69	70.96	0.11	1.96	2.16	0.88	4.87	98.97

Appendix 3 continued

Na_2O	MgO	Al_2O_3	SiO_2	Cl	K_2O	CaO	TiO_2	FeO*	Total
K-3/6 volcanic ash of Karymsky									
4.42	0.39	12.92	70.46	0.13	2.87	2.17	0.91	3.91	98.18
4.13	0.46	13.04	71.44	0.13	3.02	1.94	0.97	4.41	99.54
4.18	0.60	12.46	71.55	0.16	3.43	2.00	0.93	4.41	99.72
4.03	0.50	12.50	71.73	0.07	3.05	1.82	0.90	4.04	98.63
4.23	0.35	12.43	71.82	0.07	3.00	1.69	1.03	4.23	98.84
2.99	0.49	12.70	71.98	0.12	3.11	1.81	0.77	4.37	98.34
3.96	0.44	12.18	72.18	0.14	3.05	1.72	0.93	4.51	99.11
3.93	0.46	12.20	72.49	0.17	3.07	1.70	0.91	4.49	99.42
3.06	0.44	12.65	72.49	0.11	3.03	1.59	1.12	4.02	98.52
5.97	0.21	12.28	72.72	0.08	1.07	1.85	1.32	3.80	99.29
K-3/5 volcanic ash of Karymsky									
4.36	0.35	12.65	71.88	0.07	3.28	1.58	1.06	3.92	99.15
4.25	0.45	12.47	71.59	0.13	3.04	1.77	1.11	4.02	98.82
4.73	0.51	12.63	71.51	0.10	2.63	1.93	0.93	4.05	99.01
4.27	0.38	12.39	71.78	0.11	2.83	1.66	1.04	4.22	98.68
4.45	0.50	12.38	71.54	0.15	3.12	1.74	1.00	4.22	99.10
3.65	0.41	12.49	73.11	0.10	3.13	1.60	1.15	4.27	99.91
4.37	0.51	12.47	71.07	0.11	2.77	1.85	1.01	4.34	98.50
4.30	0.45	12.60	72.07	0.13	3.28	1.69	0.83	4.35	99.70
4.42	0.54	12.68	71.34	0.11	2.85	1.83	0.91	4.45	99.13
4.23	0.40	12.59	71.54	0.16	3.07	1.88	1.11	4.45	99.43
4.44	0.36	12.61	72.49	0.12	3.07	1.49	1.26	4.46	100.30
4.46	0.54	12.56	71.82	0.10	2.92	1.82	1.38	4.47	100.05
4.68	0.17	13.67	70.50	0.10	2.19	2.18	0.96	4.49	98.93
K-3/4 volcanic ash of Karymsky									
4.62	0.44	13.33	70.81	0.18	2.61	2.15	0.89	3.91	98.94
4.95	0.33	13.13	71.15	0.13	2.73	1.90	1.13	3.71	99.15

Appendix 3 continued

Na_2O	MgO	Al_2O_3	SiO_2	Cl	K_2O	CaO	TiO_2	FeO*	Total
4.93	0.20	13.74	71.51	0.08	2.57	1.87	1.10	3.51	99.50
4.46	0.30	12.51	71.81	0.12	2.97	1.56	1.42	4.41	99.55
4.02	0.34	12.78	71.83	0.13	2.85	1.77	0.97	4.33	99.03
4.28	0.39	12.40	71.90	0.10	3.43	1.17	0.86	4.44	98.96
4.31	0.30	12.59	71.93	0.11	2.91	1.71	0.91	4.15	98.93
3.96	0.46	12.33	72.28	0.13	3.06	1.73	0.93	4.04	98.92
3.92	0.33	12.46	72.30	0.16	2.91	1.64	0.86	4.14	98.73
5.14	0.39	12.74	72.38	0.09	2.50	1.60	1.06	3.94	99.83
4.35	0.59	11.95	72.39	0.16	2.91	1.50	1.01	4.33	99.19
4.08	0.50	12.22	72.45	0.11	2.98	1.58	1.07	4.37	99.36
4.17	0.20	12.43	73.08	0.21	3.29	1.16	0.97	3.55	99.06
4.47	0.12	12.74	73.11	0.11	2.80	1.44	0.82	3.18	98.78
K-3/3 volcanic ash of Karymsky									
3.72	0.20	12.40	74.09	0.11	3.28	1.16	0.92	3.58	99.44
5.95	0.39	12.17	73.75	0.08	1.01	1.95	0.97	3.77	100.03
5.37	0.38	11.89	73.39	0.14	2.26	1.25	0.73	3.80	99.21
3.82	0.26	12.49	73.34	0.14	3.22	1.40	0.89	4.08	99.63
4.06	0.31	12.18	73.10	0.10	3.04	1.37	0.83	4.21	99.20
4.32	0.38	12.22	72.85	0.12	3.03	1.61	1.01	4.25	99.79
4.22	0.45	12.34	72.77	0.09	3.02	1.66	0.84	4.28	99.67
4.26	0.32	12.66	71.24	0.15	2.81	1.86	1.10	4.33	98.72
4.15	0.46	12.19	72.59	0.11	3.06	1.81	1.45	4.39	100.20
4.32	0.43	12.50	71.19	0.15	3.24	2.48	0.72	4.42	99.45
3.97	0.45	12.40	72.45	0.17	3.19	1.76	0.93	4.51	99.82
K-3/2 volcanic ash of Karymsky									
4.79	0.21	13.59	71.56	0.08	2.49	2.10	0.97	3.09	98.88
5.56	0.42	12.70	71.62	0.11	1.84	2.17	0.80	4.03	99.24
5.23	0.31	13.44	71.97	0.11	2.50	2.04	0.87	3.09	99.54

Appendix 3 continued

Na_2O	MgO	Al_2O_3	SiO_2	Cl	K_2O	CaO	TiO_2	FeO*	Total
4.87	0.38	12.65	72.09	0.10	2.42	1.83	1.18	4.24	99.74
3.62	0.44	12.58	72.34	0.16	2.87	1.77	0.90	4.21	98.88
4.46	0.34	12.19	72.37	0.07	2.96	1.47	0.97	3.96	98.78
4.23	0.38	12.21	72.59	0.13	3.05	1.49	0.96	4.26	99.30
3.99	0.45	11.53	72.69	0.08	3.66	1.37	0.90	4.19	98.86
4.66	0.36	12.09	72.85	0.10	2.68	1.63	0.79	3.90	99.05
4.63	0.30	12.57	72.96	0.10	2.96	1.45	1.00	3.68	99.65
5.20	0.37	12.24	72.98	0.14	2.37	1.64	0.65	3.89	99.47
5.09	0.38	12.14	72.99	0.10	2.28	1.67	1.01	3.87	99.52
5.18	0.37	12.07	73.17	0.13	2.62	1.56	0.89	4.09	100.06
4.88	0.27	12.33	73.31	0.12	2.40	1.65	0.73	3.50	99.19
4.16	0.37	12.31	73.31	0.07	3.04	1.49	0.89	3.97	99.59
4.19	0.22	11.60	73.57	0.12	3.04	1.22	0.94	3.51	98.41
K-3/1 volcanic ash of Karymsky									
3.96	0.57	12.45	71.28	0.11	3.01	1.76	0.97	4.10	98.21
4.93	0.85	12.73	71.30	0.19	2.69	1.82	0.99	3.84	99.34
4.26	0.59	12.67	71.50	0.05	3.06	1.57	0.99	4.12	98.81
4.62	0.46	12.96	71.63	0.07	2.63	2.07	1.01	4.00	99.43
4.13	0.37	12.27	72.08	0.10	2.79	1.77	0.80	3.98	98.29
4.28	0.30	12.18	72.23	0.13	2.84	1.60	0.85	4.17	98.58
4.64	0.34	12.41	72.34	0.13	2.74	1.55	0.89	3.79	98.81
4.40	0.39	12.17	72.47	0.13	3.01	1.54	0.81	4.22	99.14
4.56	0.44	12.24	72.63	0.15	3.03	1.30	1.10	4.17	99.64
4.82	0.14	13.61	72.82	0.00	2.24	2.01	1.05	2.74	99.44
BV-030497 volcanic ash of Karymsky									
3.83	0.33	12.42	71.44	0.18	3.49	1.73	1.14	4.00	98.56
3.49	0.50	12.92	71.57	0.11	2.79	1.78	0.76	4.03	97.96
3.98	0.39	12.46	71.59	0.11	3.63	1.65	0.94	4.34	99.09

Appendix 3 continued

Na_2O	MgO	Al_2O_3	SiO_2	Cl	K_2O	CaO	TiO_2	FeO*	Total
4.30	0.29	12.31	71.66	0.15	3.03	1.39	1.12	4.53	98.79
5.66	0.23	13.15	71.69	0.15	1.94	1.86	0.97	3.51	99.16
4.31	0.25	12.38	71.75	0.15	3.29	1.34	0.90	3.79	98.14
4.12	0.36	12.26	71.81	0.08	3.23	1.50	1.01	4.33	98.69
3.13	0.56	12.03	71.94	0.16	2.84	1.60	0.90	4.23	97.40
4.03	0.31	12.11	72.19	0.20	3.00	1.67	1.04	4.21	98.76
4.68	0.30	12.34	72.22	0.08	2.61	1.56	1.13	4.09	99.01
3.26	0.52	12.33	72.30	0.21	2.83	1.82	0.87	3.96	98.10
4.23	0.18	13.00	72.30	0.17	3.07	1.24	0.97	3.51	98.66
4.15	0.41	12.14	72.55	0.19	3.29	1.11	1.10	4.53	99.46
98IPE34 volcanic ash of Karymsky									
4.25	0.22	11.92	72.79	0.12	3.21	0.96	0.80	3.55	97.82
4.21	0.36	12.34	72.46	0.14	3.36	1.24	0.91	3.64	98.66
4.24	0.40	12.52	72.21	0.11	3.26	1.28	0.63	3.66	98.30
4.70	0.36	12.35	72.17	0.10	3.07	1.30	0.95	3.72	98.71
4.44	0.39	12.53	72.52	0.07	2.93	1.31	0.97	3.73	98.88
4.03	0.29	12.50	72.75	0.13	3.09	1.40	0.95	3.96	99.10
4.13	0.33	12.21	72.12	0.16	3.34	1.38	0.91	3.97	98.55
4.12	0.34	12.41	72.51	0.05	3.19	1.33	0.88	4.03	98.86
4.29	0.41	12.37	71.67	0.09	3.01	1.62	0.91	4.11	98.48
4.29	0.40	12.48	70.97	0.10	3.08	1.55	0.80	4.28	97.95
4.06	0.41	12.11	71.98	0.11	3.32	1.71	1.04	4.32	99.06
4.28	0.46	11.86	72.28	0.09	2.94	1.40	0.91	4.38	98.60
M-2113 volcanic ash of Karymsky									
4.25	0.54	12.65	71.11	0.15	2.78	1.66	1.25	4.58	98.96
3.28	0.54	12.79	71.41	0.10	2.74	1.75	1.00	4.17	97.77
3.34	0.50	12.50	71.46	0.16	2.61	2.31	1.01	4.56	98.44
5.84	0.38	12.55	71.56	0.02	0.84	2.07	0.90	3.86	98.00

Appendix 3 continued

Na_2O	MgO	Al_2O_3	SiO_2	Cl	K_2O	CaO	TiO_2	FeO*	Total
4.14	0.37	12.15	71.57	0.17	3.01	1.70	1.15	4.04	98.29
4.22	0.48	12.35	71.58	0.16	3.16	1.78	1.00	4.00	98.72
4.18	0.47	12.15	71.78	0.14	2.81	1.63	0.72	3.99	97.86
4.14	0.51	12.09	71.78	0.13	3.11	1.70	0.86	4.07	98.38
3.66	0.52	12.64	71.80	0.11	2.63	1.77	0.93	4.46	98.50
4.13	0.48	12.37	72.10	0.13	2.86	1.81	0.83	4.21	98.91
98IPE22a volcanic bomb of 1996 Academy Nauk eruption									
4.57	0.53	12.41	64.36	0.31	2.19	3.30	2.11	9.54	99.32
5.30	0.52	13.35	65.43	0.29	1.74	3.51	1.70	8.17	100.02
5.05	0.42	14.22	65.67	0.22	2.35	3.30	1.43	6.88	99.53
5.71	0.51	14.13	65.92	0.22	1.60	3.23	1.22	7.02	99.56
4.53	0.32	13.87	66.49	0.36	2.54	3.75	1.77	5.75	99.37
4.70	0.39	13.30	67.05	0.34	2.61	2.86	1.71	7.24	100.19
98IPE24 lava flow of Karymsky volcano									
4.02	0.03	11.96	76.15	0.18	4.32	0.59	0.77	1.89	99.90
3.90	0.02	11.71	76.79	0.22	4.24	0.67	0.67	1.61	99.82
3.39	0.05	11.26	76.81	0.19	4.68	0.83	0.85	1.86	99.90
3.39	0.08	11.88	76.93	0.23	4.73	0.33	0.75	1.49	99.81
3.27	0.23	10.96	77.26	0.17	4.75	0.53	0.65	1.86	99.69
3.63	0.02	11.88	77.57	0.23	4.94	0.34	0.71	1.95	101.25
3.29	0.00	11.19	77.62	0.26	4.49	0.33	0.89	1.78	99.85
3.53	0.03	11.38	77.73	0.24	4.66	0.40	0.82	1.73	100.52
3.52	0.03	11.18	77.74	0.13	4.34	0.40	0.92	1.45	99.71
3.33	0.04	11.45	77.74	0.22	4.64	0.50	1.06	1.80	100.78
98IPE25 lava flow of Karymsky volcano									
3.79	0.09	11.51	74.49	0.18	3.69	0.97	1.31	4.87	100.90
3.99	0.20	12.21	75.00	0.14	4.40	0.79	0.76	2.13	99.61
3.72	0.58	12.23	75.06	0.23	4.20	0.98	0.76	2.32	100.06

Appendix 3 continued

Na_2O	MgO	Al_2O_3	SiO_2	Cl	K_2O	CaO	TiO_2	FeO*	Total
3.90	0.37	12.42	75.27	0.11	4.56	0.76	0.89	2.08	100.38
3.78	0.20	11.67	75.45	0.17	4.05	0.78	1.10	2.54	99.73
4.11	0.03	12.53	75.85	0.15	4.47	0.71	1.18	2.04	101.07
5.50	0.10	12.04	76.00	0.13	2.23	1.22	1.10	2.95	101.28
3.91	0.06	11.96	76.55	0.16	3.87	0.65	1.18	2.78	101.12
98IPE26 lava flow of Karymsky volcano									
5.28	0.15	13.89	73.88	0.14	2.84	1.43	0.89	2.36	100.86
4.27	0.19	11.76	75.09	0.20	3.53	0.91	1.20	3.26	100.41
4.04	0.20	11.32	75.89	0.17	3.43	0.86	1.14	3.22	100.27
3.95	0.17	11.98	75.90	0.14	3.68	0.77	0.90	2.82	100.31
4.02	0.14	11.83	76.14	0.18	3.63	0.91	1.01	2.92	100.77
4.03	0.16	11.65	76.18	0.11	3.77	0.99	1.07	3.00	100.96
4.21	0.10	12.03	76.31	0.11	3.76	0.71	0.87	2.74	100.84
3.79	0.12	11.31	76.44	0.15	3.67	0.91	1.11	2.92	100.41
98IPE27 lava flow of Karymsky volcano									
4.39	0.13	12.48	75.08	0.15	3.15	1.32	0.85	2.63	100.18
4.17	0.16	12.24	75.08	0.14	3.83	0.89	0.98	2.87	100.34
4.27	0.13	12.45	75.28	0.12	3.18	1.35	0.89	2.91	100.58
4.06	0.10	11.83	75.35	0.15	3.52	1.05	0.79	3.15	100.00
4.54	0.07	12.22	75.49	0.13	3.24	0.98	0.85	2.47	99.99
3.88	0.12	11.65	75.75	0.14	3.58	0.80	1.25	3.01	100.17
4.25	0.08	12.31	76.09	0.18	3.64	0.76	0.96	2.63	100.90
98IPE28 lava flow of Karymsky volcano									
5.29	0.05	13.78	73.56	0.11	2.84	1.50	0.75	1.48	99.35
5.12	0.05	13.81	74.09	0.10	2.77	1.51	0.55	1.82	99.81
4.32	0.02	12.21	75.48	0.15	3.45	1.18	0.91	1.72	99.45
3.97	0.03	11.89	75.60	0.16	3.74	0.59	0.87	1.88	98.73
3.94	0.03	11.72	75.94	0.24	4.02	0.52	0.70	1.94	99.05

Appendix 3 continued

Na_2O	MgO	Al_2O_3	SiO_2	Cl	K_2O	CaO	TiO_2	FeO*	Total
3.83	0.07	11.60	76.10	0.16	3.96	0.87	0.81	1.82	99.22
3.87	0.08	11.58	76.12	0.16	3.90	0.50	0.77	2.05	99.02
3.71	0.06	11.31	76.22	0.16	3.89	0.50	1.26	2.31	99.41
3.80	0.03	11.45	76.42	0.20	3.93	0.63	0.77	2.06	99.30
98IPE29 lava flow of Karymsky volcano									
5.64	0.01	13.29	73.16	0.18	3.25	1.03	0.75	1.72	99.03
6.55	0.09	16.09	73.39	0.01	0.93	3.14	0.27	0.92	101.39
6.62	0.05	15.86	73.44	0.05	1.02	3.05	0.38	0.94	101.41
5.31	0.02	11.76	76.88	0.08	2.32	0.84	1.30	2.00	100.51
6.33	0.06	14.06	76.90	0.01	1.05	1.83	0.21	0.59	101.03
5.66	0.05	11.51	77.90	0.06	1.47	1.24	0.86	1.92	100.66
98IPE33 volcanic bomb of Karymsky volcano									
4.06	0.45	13.21	71.66	0.09	2.95	2.19	0.94	4.07	99.62
4.59	0.55	12.90	71.78	0.12	2.82	2.48	0.87	4.28	100.39
4.08	0.48	12.72	71.93	0.13	3.09	1.95	1.06	4.09	99.53
4.29	0.49	12.82	72.22	0.12	3.04	1.90	1.19	4.32	100.38
4.00	0.56	12.66	72.44	0.13	3.06	1.91	0.64	4.26	99.67
4.07	0.46	12.67	72.50	0.11	3.03	2.07	1.01	4.51	100.42
4.25	0.54	12.77	72.53	0.15	3.18	1.99	0.94	4.40	100.75
4.18	0.61	12.81	72.63	0.12	3.06	1.97	0.92	4.45	100.74
4.30	0.39	12.66	72.65	0.10	3.01	2.04	1.05	4.35	100.55
4.24	0.40	12.95	72.67	0.13	2.96	2.03	0.70	4.33	100.40
4.25	0.46	12.70	72.74	0.09	3.02	1.93	0.88	4.23	100.31
4.06	0.55	12.39	72.79	0.11	2.87	1.97	0.90	4.27	99.90
4.35	0.59	12.70	72.82	0.13	2.76	2.09	0.66	4.32	100.42
4.16	0.48	12.71	72.83	0.13	3.08	2.02	0.88	4.14	100.43
3.93	0.50	12.65	73.00	0.16	3.00	2.04	0.83	3.96	100.07
4.10	0.60	12.78	73.54	0.10	2.98	2.05	0.71	4.62	101.47

Appendix 3 continued

Na_2O	MgO	Al_2O_3	SiO_2	Cl	K_2O	CaO	TiO_2	FeO*	Total
BV-040496 volcanic bomb of Karymsky volcano									
3.81	0.22	11.40	74.56	0.20	3.55	2.59	1.12	2.59	100.04
4.84	0.25	14.45	72.09	0.07	2.57	2.45	0.92	2.63	100.27
4.23	0.24	12.04	75.58	0.18	3.35	1.16	0.68	2.79	100.24
4.06	0.74	11.36	74.40	0.12	3.54	1.11	0.78	2.92	99.04
BV-170296 lava flow of Karymsky volcano									
4.72	0.67	12.17	73.47	0.09	3.72	1.34	0.90	3.06	100.14
4.89	0.13	12.73	73.73	0.15	2.88	1.50	0.98	3.47	100.47
3.96	0.32	12.19	75.04	0.16	3.32	1.03	1.00	2.97	99.99
5.71	0.09	11.76	75.71	0.10	0.88	1.75	1.15	2.88	100.02
99IPE4 pumice of 7,900 yr. BP Karymsky caldera-forming eruption									
4.12	0.30	12.72	75.24	0.20	3.06	1.47	0.24	1.61	99.13
4.41	0.31	12.23	74.34	0.15	2.99	1.28	0.17	1.74	97.82
4.81	0.29	12.31	75.39	0.15	3.16	1.35	0.18	1.76	99.60
4.65	0.28	12.39	73.80	0.17	3.13	1.46	0.16	1.69	97.91
4.33	0.32	12.17	73.31	0.16	2.96	1.41	0.16	1.70	96.72
4.13	0.34	12.02	74.15	0.12	3.14	1.41	0.22	1.78	97.51
4.95	0.35	12.47	73.58	0.16	2.98	1.40	0.24	1.87	98.21
4.65	0.32	12.69	74.47	0.18	3.11	1.49	0.29	1.60	98.99
4.44	0.35	12.89	74.35	0.18	3.05	1.36	0.28	1.88	98.98
4.39	0.30	12.94	74.58	0.15	3.14	1.40	0.19	1.84	99.11
4.28	0.32	12.89	73.74	0.16	3.06	1.44	0.24	1.72	98.02
4.54	0.28	12.94	75.14	0.16	3.34	1.56	0.14	1.69	99.98
99IPE6 pumice of ca. 40,000 yr. BP Academy Nauk caldera-forming eruption									
5.01	0.31	13.69	72.92	0.20	3.10	1.50	0.16	1.74	98.84
4.74	0.39	13.39	71.31	0.14	2.87	1.85	0.16	1.82	96.87
4.79	0.32	13.35	72.57	0.16	3.00	1.61	0.26	1.81	98.08
5.03	0.33	12.87	72.46	0.17	2.88	1.70	0.22	1.74	97.60

Appendix 3 continued

Na_2O	MgO	Al_2O_3	SiO_2	Cl	K_2O	CaO	TiO_2	FeO*	Total
4.98	0.37	13.86	74.82	0.17	3.16	1.77	0.25	1.71	101.28
4.64	0.30	12.91	73.18	0.21	2.88	1.59	0.15	1.93	98.01
4.56	0.35	12.86	73.34	0.18	2.96	1.53	0.18	1.71	97.86
Glass inclusions in clinopyroxenes of Academy Nauk basalts									
5.09	0.74	18.01	62.26	0.11	1.51	6.78	0.64	2.20	97.32
4.78	0.59	19.75	61.47	0.11	1.02	5.32	0.23	2.30	95.58
4.75	0.95	18.17	61.65	0.12	0.99	7.60	0.53	3.28	98.04
4.43	0.99	17.67	60.75	0.11	1.05	7.45	0.93	3.57	96.95
4.18	0.82	18.46	58.42	0.11	0.62	9.43	1.33	4.22	97.60
4.34	0.70	19.25	59.38	0.12	1.06	6.83	0.64	4.30	96.61
4.71	0.83	17.76	60.58	0.12	1.25	6.22	1.50	4.55	97.52
4.17	1.97	17.44	58.25	0.09	1.18	8.07	1.09	5.41	97.67
4.79	0.72	16.84	60.48	0.12	1.32	4.85	1.29	5.70	96.12
3.58	1.66	18.67	55.69	0.10	0.81	10.48	0.94	5.82	97.76
3.82	2.16	18.80	55.50	0.13	0.92	7.86	0.88	6.54	96.59
5.35	1.21	18.51	56.65	0.08	0.98	8.44	1.26	6.69	99.16
4.79	1.75	14.76	61.35	0.17	1.07	5.73	1.47	8.31	99.40
4.06	1.52	13.85	58.62	0.19	2.01	7.80	1.93	8.71	98.69
4.37	1.72	16.64	57.04	0.09	1.23	6.83	1.33	8.79	98.06
4.02	1.89	14.55	60.03	0.18	1.53	6.42	1.40	9.49	99.51
4.48	1.78	14.37	60.04	0.16	1.38	5.67	1.60	9.72	99.19
4.35	1.81	13.81	60.49	0.15	1.19	5.69	1.22	9.83	98.54
4.40	1.88	14.36	59.36	0.14	1.23	5.49	1.36	10.25	98.47
2.59	4.88	8.77	59.08	0.17	2.67	4.14	1.59	10.33	94.20
3.08	5.80	10.86	54.26	0.12	1.21	6.83	1.61	11.58	95.34
4.70	3.60	14.31	56.67	0.13	1.44	6.24	1.11	11.81	100.02
3.02	6.28	11.63	56.33	0.09	1.06	7.44	1.18	11.88	98.90

Appendix 3 continued

Na_2O	MgO	Al_2O_3	SiO_2	Cl	K_2O	CaO	TiO_2	FeO*	Total
Glass inclusions in clinopyroxenes of Karymsky andesites									
4.96	1.31	14.20	65.26	0.16	2.65	3.27	1.02	4.87	97.70
5.22	1.39	14.28	65.37	0.22	2.74	3.36	0.82	4.97	98.36
5.21	1.29	13.99	65.07	0.18	2.69	3.39	1.20	5.12	98.14
5.01	1.25	14.69	65.38	0.24	2.75	3.21	0.70	4.84	98.07
5.01	1.17	15.09	65.54	0.17	2.66	3.12	0.64	4.54	97.93
4.04	0.34	12.51	73.50	0.11	3.08	1.51	0.98	4.14	100.20
4.23	0.39	12.82	73.18	0.10	2.80	1.83	0.84	3.81	100.00
Glass inclusions in pyroxenes of 7,900 yr. BP Karymsky dacite (99IPE4)									
4.21	0.32	13.11	73.17	0.23	3.11	1.37	0.41	1.64	97.76
4.56	0.25	13.07	73.28	0.18	3.06	1.33	0.31	1.63	97.86
4.55	0.34	12.60	72.01	0.19	2.79	1.51	0.35	1.60	96.12
4.23	0.30	12.88	73.65	0.24	3.05	1.34	0.29	1.67	97.84
4.34	0.28	12.75	73.20	0.16	3.05	1.32	0.44	1.51	97.24
4.34	0.27	12.75	73.43	0.18	2.90	1.41	0.36	1.70	97.53
4.07	0.24	12.36	72.63	0.13	3.05	1.41	0.28	1.62	95.97
3.88	0.28	12.32	72.64	0.17	3.44	1.32	0.44	1.31	95.92
4.30	0.30	12.13	72.69	0.14	3.16	1.31	0.20	1.45	95.84
3.83	0.27	12.16	72.47	0.19	3.24	1.41	0.36	1.36	95.43
4.07	0.25	12.38	72.45	0.16	2.88	1.32	0.27	1.23	95.15
3.89	0.23	12.29	72.37	0.18	2.96	1.35	0.28	1.24	94.92
Glass inclusions in pyroxenes of 40,000 yr. BP Academy Nauk dacite (99IPE6)									
3.45	0.23	12.80	72.13	0.20	3.63	1.22	0.28	1.65	95.76
3.75	0.29	13.38	71.56	0.16	3.49	1.23	0.16	2.38	96.67
3.59	0.26	12.49	72.60	0.16	3.53	1.10	0.30	2.15	96.42
3.71	0.29	12.85	71.50	0.19	3.18	1.39	0.34	2.34	96.06
3.47	0.65	12.49	72.18	0.19	3.81	1.05	0.20	2.42	96.72
3.70	0.22	12.75	72.12	0.23	3.65	1.16	0.08	2.28	96.45

Appendix 3 continued

Na_2O	MgO	Al_2O_3	SiO_2	Cl	K_2O	CaO	TiO_2	FeO*	Total
3.64	0.28	12.90	71.28	0.18	3.13	1.48	0.43	2.65	96.25
3.70	0.37	14.33	69.06	0.18	2.76	2.22	0.76	2.51	96.16
3.83	0.39	14.12	68.92	0.18	2.66	2.35	0.41	2.46	95.59

Appendix 4: Representative electron microprobe analyses of feldspars in natural samples

All samples were polished and carbon-coated to a thickness of ca. 250 Å. Plagioclase phenocrysts were analyzed for major elements at the University of Alaska Fairbanks using a Cameca SX-50 electron microprobe, which is equipped with four wavelength-dispersive and one energy-dispersive spectrometers. A 15 keV, 10 nA, 1-3-μm-diameter beam was used for all analyses. Major oxides are in wt.%, with all Fe reported as FeO. Anorthite content is reported in molar %. Relative distance between analyzed points is reported in microns. Details about counting times, standards, and analytical errors are summarized below.

Element	Counting Time		Standard	Typical Analytical Error (wt.%, 1 sigma)*
	Peak (sec.)	Background (sec.)		
Na	30	5	Anorthoclase (USNM 133868)	0.169
Al	10	5	Labradorite (USNM 115900)	0.216
Si	10	5	Tiburon albite	0.413
K	10	5	Orthoclase (CM Taylor)	0.094
Ca	10	5	Labradorite (USNM 115900)	0.049
Fe	30	5	Orthoclase (CM Taylor)	0.027

* Typical analytical errors for a representative sample calculated after Scott et al. (1995).

Appendix 4 continued

Relative microns	SiO_2	Al_2O_3	Na_2O	K_2O	CaO	FeO*	Total	An, mol. %
Plagioclase phenocryst in 1996 Academy Nauk basalt (Fig. 2.4c, rim to core)								
0	51.80	30.74	3.19	0.02	14.11	0.91	100.77	71
7	48.54	33.19	1.90	0.04	16.76	0.64	101.07	83
14	48.03	33.79	1.62	0.00	16.97	0.71	101.12	85
22	47.74	33.61	1.62	0.03	17.26	0.77	101.04	85
29	47.33	34.14	1.53	0.04	17.79	0.89	101.72	86
36	47.55	34.15	1.42	0.03	17.72	0.74	101.61	87
43	49.15	32.93	2.06	0.04	16.06	0.85	101.09	81
50	48.17	33.92	1.57	0.01	17.55	0.72	101.94	86
57	46.82	34.19	1.34	0.06	17.75	0.77	100.94	88
65	46.92	34.27	1.40	0.00	17.66	0.66	100.91	87
72	47.41	33.77	1.57	0.01	17.73	0.74	101.23	86
79	47.96	33.86	1.56	0.00	17.42	0.68	101.48	86
86	47.73	33.61	1.66	0.01	17.37	0.56	100.94	85
93	47.99	33.40	1.91	0.06	17.25	0.78	101.38	83
101	48.37	33.25	1.83	0.00	17.03	0.84	101.31	84
108	48.67	32.73	2.17	0.05	16.08	0.72	100.42	80
115	47.89	32.70	2.19	0.05	15.94	0.77	99.53	80
122	47.76	33.45	1.65	0.04	17.01	0.81	100.72	85
129	46.71	34.79	1.18	0.04	17.74	0.75	101.21	89
137	47.04	34.24	1.39	0.02	17.85	0.78	101.31	88
172	49.07	32.11	1.52	0.03	17.57	0.69	100.99	86
180	48.57	33.93	1.68	0.01	17.13	0.81	102.14	85
187	48.99	33.17	2.06	0.06	16.75	0.67	101.70	82
194	47.30	33.93	1.64	0.00	17.54	0.74	101.14	86
201	47.00	34.46	1.30	0.02	17.92	0.75	101.45	88
208	47.95	33.67	1.62	0.05	17.37	0.55	101.20	85
216	48.94	32.87	2.01	0.02	16.30	0.74	100.87	82

Appendix 4 continued

Relative microns	SiO_2	Al_2O_3	Na_2O	K_2O	CaO	FeO*	Total	An, mol. %
223	48.78	32.74	2.17	0.05	15.99	0.69	100.42	80
230	48.87	32.80	2.00	0.03	16.41	0.84	100.96	82
237	48.64	33.01	2.14	0.03	16.62	0.82	101.25	81
244	47.21	34.18	1.46	0.02	17.44	0.78	101.08	87
251	47.21	33.49	1.48	0.04	17.25	0.72	100.20	86
259	48.68	33.19	1.97	0.00	16.81	0.85	101.51	82
266	48.67	33.21	1.86	0.02	16.59	0.70	101.05	83
273	48.27	33.74	1.76	0.05	17.24	0.74	101.80	84
300	46.61	34.45	1.21	0.03	17.44	0.82	100.55	89
325	47.00	34.43	1.35	0.02	17.61	0.79	101.21	88
340	48.29	33.59	1.83	0.03	16.91	0.85	101.50	83
350	47.53	33.89	1.60	0.05	17.05	0.75	100.87	85
Oscillatory-zoned plagioclase phenocryst in Karymsky andesite (Fig. 3.2b, core to rim)								
0	55.05	28.87	5.05	0.17	10.92	0.73	100.79	54
11	54.81	28.37	5.22	0.15	10.79	0.51	99.85	53
22	54.28	29.42	4.72	0.15	11.80	0.64	101.00	58
32	52.32	30.32	4.18	0.10	12.27	0.58	99.76	61
43	53.62	30.32	4.28	0.12	12.55	0.63	101.52	61
54	53.82	29.54	4.94	0.13	11.50	0.56	100.49	56
65	53.61	29.51	4.45	0.13	12.09	0.63	100.40	60
76	55.16	28.45	5.21	0.15	11.08	0.65	100.70	54
87	55.84	28.50	5.15	0.15	10.66	0.62	100.92	53
97	55.04	29.21	4.58	0.12	11.27	0.64	100.86	57
108	55.66	28.75	4.87	0.17	11.23	0.66	101.35	55
119	55.19	28.57	5.14	0.14	10.60	0.65	100.29	53
130	55.19	28.64	5.26	0.15	10.62	0.63	100.51	52
141	55.65	28.62	5.08	0.13	11.07	0.71	101.26	54
151	55.22	28.48	5.30	0.15	10.54	0.56	100.24	52

Appendix 4 continued

Relative microns	SiO_2	Al_2O_3	Na_2O	K_2O	CaO	FeO*	Total	An, mol. %
162	54.90	29.11	4.76	0.13	11.00	0.65	100.56	56
173	54.36	29.42	4.59	0.12	11.56	0.62	100.67	58
184	54.75	29.15	4.98	0.11	11.61	0.64	101.23	56
195	54.83	29.01	4.85	0.18	11.16	0.63	100.66	55
206	54.31	29.23	4.67	0.07	11.47	0.65	100.41	57
216	54.50	29.35	4.48	0.06	11.77	0.61	100.77	59
227	54.58	29.29	5.01	0.14	11.44	0.61	101.07	55
238	53.07	29.32	4.62	0.13	11.64	0.62	99.40	58
249	54.73	29.02	4.93	0.16	11.57	0.55	100.95	56
260	55.17	28.72	4.90	0.16	11.17	0.50	100.62	55
270	55.41	28.78	5.21	0.16	11.09	0.70	101.36	54
281	55.58	28.58	5.13	0.19	10.91	0.56	100.95	53
292	54.71	28.55	4.98	0.15	11.03	0.69	100.10	55
303	55.47	28.72	4.96	0.13	11.20	0.55	101.03	55
314	55.32	28.40	5.08	0.17	10.61	0.61	100.19	53
325	55.01	28.69	4.98	0.18	11.02	0.66	100.54	54
335	55.36	28.39	5.14	0.16	10.97	0.49	100.52	54
346	54.15	28.46	5.20	0.19	10.75	0.73	99.48	53
357	54.63	28.71	5.08	0.17	10.86	0.71	100.16	54
368	55.54	28.48	5.01	0.21	11.01	0.61	100.85	54
379	55.29	28.73	5.05	0.14	11.07	0.69	100.96	54
389	55.80	28.63	5.41	0.14	10.98	0.73	101.70	52
400	55.71	28.40	5.24	0.16	11.07	0.59	101.17	53
411	55.57	28.48	5.36	0.15	10.96	0.61	101.13	53
422	55.77	28.52	5.05	0.17	10.42	0.60	100.52	53
433	55.68	28.37	5.25	0.16	10.59	0.74	100.80	52
443	55.95	28.54	5.22	0.16	10.96	0.54	101.36	53
454	55.80	28.58	5.10	0.17	10.86	0.68	101.18	54

Appendix 4 continued

Relative microns	SiO_2	Al_2O_3	Na_2O	K_2O	CaO	FeO*	Total	An, mol. %
465	56.01	28.44	5.43	0.11	10.74	0.56	101.29	52
476	55.71	28.48	5.36	0.16	10.73	0.61	101.05	52
487	56.47	28.29	5.32	0.14	10.59	0.61	101.42	52
498	55.83	28.14	5.48	0.14	10.59	0.54	100.72	51
508	55.88	28.51	5.33	0.18	10.90	0.64	101.43	53
519	56.11	28.28	5.56	0.17	10.60	0.67	101.39	51
530	56.61	28.20	5.30	0.18	10.69	0.58	101.56	52
541	56.04	28.43	5.21	0.18	10.59	0.56	101.00	52
552	55.60	28.25	5.45	0.15	10.42	0.49	100.36	51
562	56.29	28.17	5.46	0.20	10.29	0.61	101.01	50
573	56.19	27.90	5.43	0.18	10.61	0.66	100.97	51
584	56.33	28.06	5.28	0.16	10.84	0.54	101.22	53
595	57.21	27.94	5.64	0.18	10.25	0.66	101.88	50
606	56.35	27.97	5.70	0.19	9.96	0.63	100.79	49
617	56.44	27.75	5.44	0.13	10.16	0.57	100.49	50
627	57.04	27.48	5.67	0.16	10.13	0.61	101.08	49
638	57.67	27.48	5.73	0.23	9.80	0.63	101.54	48
649	56.60	27.34	5.84	0.24	10.10	0.67	100.78	48
660	57.42	27.59	5.79	0.17	9.75	0.69	101.42	48
671	56.59	28.13	5.37	0.18	10.46	0.64	101.36	51
681	56.72	27.96	5.52	0.21	10.53	0.51	101.45	51
692	55.20	27.88	5.51	0.16	10.17	0.66	99.57	50
725	56.11	27.93	5.12	0.17	11.07	0.68	101.08	54
Rimmed plagioclase phenocryst in Karymsky andesite (Fig. 3.2c, rim to core)								
0	56.74	27.97	5.64	0.21	10.66	0.67	101.89	50
11	56.43	28.01	5.36	0.17	10.47	0.51	100.96	51
19	56.52	27.65	5.57	0.19	10.45	0.66	101.03	50
27	56.59	27.60	5.84	0.23	10.07	0.64	100.98	48

Appendix 4 continued

Relative microns	SiO_2	Al_2O_3	Na_2O	K_2O	CaO	FeO*	Total	An, mol. %
34	55.39	26.63	5.74	0.17	9.82	0.67	98.41	48
42	54.61	26.94	5.24	0.15	10.16	0.67	97.77	51
50	56.99	27.32	5.80	0.21	9.97	0.57	100.86	48
57	57.03	27.08	5.88	0.19	9.84	0.71	100.74	47
65	57.18	27.35	5.86	0.27	9.85	0.65	101.16	47
73	56.55	27.64	5.69	0.23	10.32	0.72	101.14	49
80	56.65	27.96	5.44	0.21	10.45	0.78	101.49	51
87	56.31	27.53	5.48	0.19	10.63	0.61	100.75	51
96	56.90	27.66	5.56	0.22	10.39	0.78	101.51	50
103	56.28	28.10	5.62	0.21	10.41	0.71	101.33	50
110	56.22	27.69	5.63	0.23	10.31	0.60	100.68	50
118	56.79	27.55	5.58	0.20	10.49	0.52	101.13	50
126	56.69	27.73	5.77	0.14	10.40	0.64	101.36	49
133	56.83	27.64	4.98	0.20	10.52	0.50	100.67	53
141	56.79	28.01	5.40	0.20	10.65	0.52	101.57	52
148	55.79	27.91	5.30	0.23	10.98	0.63	100.84	53
156	57.28	27.35	5.76	0.24	9.89	0.58	101.12	48
164	55.74	27.97	5.38	0.17	10.78	0.67	100.71	52
171	56.21	28.12	5.35	0.19	10.55	0.73	101.15	52
179	56.14	28.19	5.44	0.14	10.62	0.61	101.14	51
187	55.77	28.12	5.65	0.20	10.54	0.60	100.89	50
194	55.96	28.22	5.36	0.19	11.07	0.55	101.36	53
201	56.00	28.23	5.21	0.17	11.07	0.72	101.40	53
210	48.29	33.00	1.99	0.05	16.37	0.68	100.38	82
217	47.80	33.30	2.08	0.05	16.45	0.80	100.48	81
224	48.18	33.55	1.94	0.04	16.86	0.87	101.46	83
232	47.21	33.77	1.72	0.07	17.29	0.72	100.78	84
240	48.06	33.00	2.02	0.06	16.60	0.70	100.45	82

Appendix 4 continued

Relative microns	SiO_2	Al_2O_3	Na_2O	K_2O	CaO	FeO*	Total	An. mol. %
247	48.10	32.98	2.15	0.05	16.66	0.75	100.70	81
255	47.22	32.74	2.11	0.04	15.93	0.73	98.76	80
263	48.13	32.95	2.05	0.04	16.34	0.69	100.20	81
270	47.72	32.60	2.18	0.08	16.23	0.67	99.48	80
278	47.43	33.57	1.89	0.05	16.37	0.86	100.18	82
285	47.71	33.06	2.08	0.05	15.82	0.71	99.43	81
293	47.48	32.27	2.16	0.07	15.95	0.71	98.64	80
301	48.14	32.71	2.25	0.05	16.07	0.70	99.91	80
308	48.42	33.26	2.07	0.06	16.63	0.65	101.08	81
315	48.50	32.77	2.26	0.09	16.25	0.72	100.60	79
324	48.68	32.95	2.11	0.03	16.41	0.67	100.84	81
331	48.87	32.84	2.43	0.05	16.02	0.67	100.86	78
338	48.52	33.05	2.28	0.09	16.33	0.72	100.99	79
346	48.79	32.88	2.18	0.07	16.43	0.75	101.11	80
354	48.58	33.00	2.20	0.06	16.64	0.83	101.31	80
361	47.98	33.39	1.93	0.06	16.78	0.74	100.89	82
369	47.95	33.35	1.98	0.04	16.68	0.76	100.76	82
377	47.89	33.34	2.09	0.07	16.67	0.71	100.78	81
384	47.66	33.24	1.99	0.01	16.64	0.65	100.18	82
392	47.69	33.05	1.99	0.05	16.63	0.73	100.14	82
399	48.26	33.15	2.02	0.07	16.54	0.73	100.78	82
407	48.13	33.38	2.22	0.04	16.45	0.77	100.99	80
415	48.35	32.56	2.48	0.07	15.78	0.71	99.95	78
422	49.14	32.46	2.58	0.08	15.71	0.71	100.67	77
429	48.82	32.75	2.45	0.04	16.18	0.73	100.97	78
438	48.75	32.76	2.42	0.04	15.80	0.79	100.56	78
445	48.94	32.79	2.43	0.07	16.13	0.73	101.09	78
452	49.20	32.90	2.25	0.08	15.95	0.72	101.10	79

Appendix 4 continued

Relative microns	SiO_2	Al_2O_3	Na_2O	K_2O	CaO	FeO*	Total	An, mol. %
460	48.44	32.69	2.43	0.06	15.97	0.63	100.23	78
468	49.71	31.89	2.88	0.07	15.03	0.80	100.38	74
475	49.37	32.23	2.57	0.06	15.58	0.71	100.51	77
483	49.50	32.30	2.85	0.05	15.75	0.69	101.15	75
491	49.21	32.75	2.30	0.08	15.95	0.75	101.03	79
498	48.57	33.10	2.02	0.06	16.56	0.67	100.98	82
506	48.43	33.03	2.09	0.08	16.37	0.70	100.70	81
513	47.77	33.59	2.01	0.08	16.88	0.89	101.23	82
521	49.60	32.46	2.65	0.06	15.39	0.79	100.95	76
529	48.83	32.98	2.23	0.05	16.70	0.72	101.51	80
536	48.24	32.92	2.13	0.05	16.15	0.72	100.20	81
Plagioclase phenocrysts in 7,900 yr. BP Karymsky dacite (99IPE4)								
Rim	56.73	26.63	6.27	0.25	8.75	0.46	99.10	44
Rim	56.08	26.95	6.17	0.24	8.83	0.41	98.67	44
Rim	56.76	26.79	6.29	0.27	8.86	0.53	99.49	44
Rim	55.97	27.02	6.18	0.26	8.88	0.49	98.80	44
Rim	56.51	26.47	6.32	0.29	8.88	0.52	99.00	44
Rim	55.72	26.75	6.26	0.26	8.89	0.49	98.38	44
Rim	56.56	26.69	6.42	0.27	8.71	0.39	99.04	43
Rim	56.15	26.80	6.26	0.23	9.06	0.43	98.93	44
Rim	56.54	26.46	6.32	0.28	8.97	0.52	99.09	44
Rim	55.94	26.55	6.28	0.27	9.10	0.45	98.60	44
Rim	56.35	26.67	6.46	0.28	8.64	0.43	98.82	43
Rim	55.99	26.64	6.43	0.28	8.90	0.44	98.67	43
Rim	56.93	26.49	6.64	0.27	8.58	0.33	99.25	42
Core	56.08	26.95	6.17	0.24	8.83	0.41	98.67	44
Core	56.15	26.80	6.26	0.23	9.06	0.43	98.93	44
Core	55.94	26.55	6.28	0.27	9.10	0.45	98.60	44

Appendix 4 continued

Relative microns	SiO_2	Al_2O_3	Na_2O	K_2O	CaO	FeO*	Total	An, mol. %
Core	56.41	27.80	5.51	0.25	9.01	0.49	99.46	47
Core	56.15	28.37	5.40	0.16	9.60	0.36	100.05	50
Plagioclase phenocrysts in 40,000 yr. BP Academy Nauk dacite (99IPE6)								
Rim	57.66	25.77	5.47	0.37	8.82	0.65	98.74	47
Rim	56.07	27.56	5.92	0.27	9.47	0.51	99.80	47
Rim	55.47	27.46	5.83	0.24	9.57	0.58	99.15	48
Rim	55.44	27.70	5.90	0.17	9.42	0.38	99.02	47
Rim	55.98	27.57	5.82	0.21	9.56	0.43	99.57	48
Rim	56.25	27.11	6.28	0.24	9.16	0.43	99.46	45
Rim	55.86	27.09	5.91	0.18	9.51	0.41	98.96	47
Rim	55.90	27.50	5.91	0.21	9.79	0.39	99.71	48
Core	51.49	29.83	4.30	0.15	12.47	0.49	98.74	62
Core	50.93	30.32	4.22	0.11	13.10	0.50	99.19	63
Core	51.24	30.44	4.31	0.12	12.87	0.44	99.43	62
Core	52.53	29.36	4.66	0.14	11.98	0.52	99.20	59
Core	51.90	29.36	4.58	0.11	11.76	0.43	98.13	59
Core	52.31	29.92	4.44	0.15	12.06	0.42	99.29	60
Core	52.53	29.73	4.49	0.12	12.31	0.52	99.70	60
Core	52.63	29.69	4.49	0.13	12.33	0.44	99.76	60
Plagioclase phenocrysts in granophyre xenolith (99IPE7)								
Rim	63.22	23.57	8.67	0.55	3.77	0.22	99.99	19
Rim	61.38	24.64	7.73	0.53	5.31	0.22	99.80	27
Rim	61.39	25.02	7.80	0.37	5.42	0.23	100.23	27
Rim	60.34	25.03	7.77	0.36	5.40	0.24	99.13	27
Rim	60.03	25.64	7.47	0.40	5.85	0.22	99.60	29
Rim	59.41	26.07	6.88	0.29	6.09	0.41	99.15	32
Rim	59.99	26.10	7.17	0.36	6.49	0.31	100.42	33
Rim	60.02	25.55	7.14	0.39	6.60	0.46	100.15	33

Appendix 4 continued

Relative microns	SiO_2	Al_2O_3	Na_2O	K_2O	CaO	FeO*	Total	An, mol. %
Rim	59.72	25.99	7.17	0.37	6.63	0.17	100.04	33
Core	58.93	25.82	6.76	0.34	6.79	0.36	98.99	35
Core	58.39	26.86	6.95	0.30	7.18	0.51	100.19	36
Core	58.22	26.87	6.54	0.32	7.54	0.43	99.93	38
Core	57.42	27.53	6.19	0.27	8.02	0.44	99.87	41
Core	57.17	27.58	6.00	0.28	8.50	0.36	99.89	43
Orthoclase in granophyre xenolith (99IPE7)								
	66.83	19.17	4.33	9.26	0.17	0.28	100.04	
	66.78	19.32	4.58	9.26	0.21	0.10	100.25	
	66.46	19.32	4.77	8.87	0.18	0.00	99.60	
	66.87	18.80	4.53	8.87	0.16	0.06	99.29	
	65.73	19.06	4.86	8.25	0.12	0.19	98.20	
	66.07	19.32	4.56	8.89	0.16	0.16	99.16	

Appendix 5: Representative electron microprobe analyses of pyroxenes in natural samples

All samples were polished and carbon-coated to a thickness of 250 Å. Pyroxene phenocrysts were analyzed for major elements at the University of Alaska Fairbanks using a Cameca SX-50 electron microprobe, which is equipped with four wavelength-dispersive and one energy-dispersive spectrometers. A 15 keV, 10 nA, 1-3-μm-diameter beam was used for all analyses. Major oxides are in wt.%, with all Fe reported as FeO; n.d. - not detected. Although Cr was analyzed, in most cases it was below detection limits and thus has not been used in the statistical analysis. Details about counting times, standards, and analytical errors are summarized below.

Element	Counting Time		Standard	Typical Analytical Error (wt.%, 1 sigma)*
	Peak (sec.)	Background (sec.)		
Si	10	5	Kyanite (CM Taylor)	0.151
Mn	20	10	Spessartine (CM Taylor)	0.022
Ti	10	5	Sphene (CM Taylor)	0.033
Na	10	5	Tiburon albite	0.022
Mg	10	5	Hypersthene (USNM 746)	0.124
Ca	20	10	Diopside (CM Taylor)	0.031
Al	10	5	Kyanite (CM Taylor)	0.026
Fe	10	5	Fayalite (USNM 85276)	0.256

* Typical analytical errors for a representative sample calculated after Scott et al. (1995).

Appendix 5 continued

SiO_2	TiO_2	Al_2O_3	FeO*	MnO	MgO	CaO	Na_2O	Total
Clinopyroxene phenocrysts in Academy Nauk basalt (98IPE22a)								
51.69	0.46	3.16	6.80	0.09	15.91	21.60	0.20	99.90
51.98	0.43	2.96	7.46	0.09	15.57	21.99	0.21	100.68
51.88	0.37	3.15	6.74	0.11	15.91	22.07	0.22	100.45
52.12	0.50	3.26	6.97	0.21	15.30	21.88	0.27	100.51
52.18	0.41	3.06	6.79	0.16	15.83	21.90	0.27	100.59
51.72	0.41	2.91	7.60	0.12	15.42	21.84	0.25	100.25
51.69	0.46	3.16	6.80	0.09	15.91	21.60	0.20	99.90
51.98	0.43	2.96	7.46	0.09	15.57	21.99	0.21	100.68
51.88	0.37	3.15	6.74	0.11	15.91	22.07	0.22	100.45
52.12	0.50	3.26	6.97	0.21	15.30	21.88	0.27	100.51
52.18	0.41	3.06	6.79	0.16	15.83	21.90	0.27	100.59
51.72	0.41	2.91	7.60	0.12	15.42	21.84	0.25	100.25
Clinopyroxene phenocrysts in Academy Nauk basalt (97IPE3)								
51.12	0.54	2.86	7.50	0.31	15.58	21.06	0.33	99.29
50.94	0.50	3.23	7.85	0.18	15.68	21.18	0.29	99.85
51.24	0.56	3.22	6.96	0.10	15.53	20.94	0.28	98.82
51.06	0.58	3.32	7.59	0.17	15.97	21.35	0.27	100.31
51.10	0.45	2.72	7.44	0.20	16.17	21.38	0.29	99.75
51.33	0.50	2.70	7.28	0.21	16.11	21.22	0.31	99.66
51.07	0.51	2.87	7.64	0.21	15.98	21.62	0.29	100.18
50.49	0.68	3.04	8.90	0.18	14.85	20.54	0.34	99.01
51.16	0.52	3.15	7.98	0.13	15.50	21.46	0.39	100.29
51.26	0.50	2.86	7.85	0.16	15.84	21.43	0.28	100.17
51.30	0.49	2.76	7.40	0.31	15.90	21.59	0.31	100.05
51.11	0.55	2.85	7.85	0.23	15.56	21.00	0.29	99.43
50.62	0.48	3.00	7.91	0.29	15.47	21.41	0.31	99.48

Appendix 5 continued

SiO_2	TiO_2	Al_2O_3	FeO*	MnO	MgO	CaO	Na_2O	Total
Clinopyroxene phenocrysts in Karymsky andesite (BV-170296, core)								
52.07	0.46	2.00	10.05	0.41	14.19	20.33	0.28	99.80
51.24	0.48	1.69	9.69	0.42	14.17	20.67	0.35	98.71
51.32	0.54	1.95	10.19	0.53	14.32	20.69	0.31	99.85
51.64	0.48	1.78	10.05	0.45	14.56	20.64	0.36	99.96
51.58	0.46	1.81	9.53	0.51	14.32	20.54	0.38	99.14
51.59	0.56	2.00	9.57	0.53	14.55	20.75	0.31	99.86
52.29	0.36	1.48	9.60	0.50	14.98	20.13	0.34	99.67
52.15	0.41	1.33	9.90	0.33	15.13	19.56	0.27	99.07
Clinopyroxene phenocrysts in Karymsky andesite (BV-170296, rim)								
51.78	0.62	2.20	10.62	0.50	14.72	19.17	0.36	99.98
51.45	0.57	2.14	9.55	0.47	14.40	19.79	0.34	98.72
51.93	0.44	1.92	9.71	0.49	14.89	20.02	0.29	99.67
51.23	0.60	2.21	9.99	0.29	14.54	20.11	0.27	99.24
51.16	0.63	2.03	9.92	0.50	14.53	20.08	0.37	99.21
51.91	0.55	1.97	10.31	0.45	14.66	20.10	0.36	100.32
52.20	0.59	1.90	9.04	0.44	14.66	20.65	0.40	99.88
51.34	0.56	2.10	9.90	0.32	14.48	19.99	0.42	99.10
Clinopyroxene phenocrysts in Karymsky andesite (BV-170296, core)								
50.71	0.80	3.19	11.34	0.32	13.82	19.62	0.36	100.16
52.56	0.43	1.91	9.67	0.36	14.74	20.41	0.29	100.38
52.95	0.49	1.73	9.54	0.33	14.86	20.76	0.30	100.97
52.22	0.60	1.78	9.79	0.43	14.88	20.46	0.29	100.46
51.43	0.72	3.16	9.84	0.33	14.62	20.34	0.34	100.78
51.73	0.57	2.87	9.51	0.39	14.60	20.65	0.31	100.64
51.56	0.59	2.58	9.56	0.54	14.83	20.13	0.30	100.09
51.90	0.61	2.51	9.37	0.45	14.87	20.43	0.40	100.53
51.69	0.73	2.33	9.77	0.29	14.10	20.93	0.31	100.16
53.22	0.60	1.82	9.14	0.30	14.38	21.09	0.33	100.88

Appendix 5 continued

SiO_2 [a]	TiO_2	Al_2O_3	FeO*	MnO	MgO	CaO	Na_2O	Total
52.33	0.62	1.77	10.78	0.42	14.45	19.72	0.32	100.41
52.48	0.45	1.60	10.22	0.34	15.00	19.91	0.34	100.34
52.05	0.50	2.30	9.70	0.36	15.00	20.38	0.38	100.65
52.08	0.52	1.59	9.58	0.54	14.59	19.70	0.29	98.89
52.59	0.60	1.81	9.75	0.38	14.62	20.02	0.35	100.13
52.46	0.43	1.62	10.02	0.36	14.63	20.09	0.29	99.90
51.48	0.68	2.48	10.24	0.36	13.80	20.32	0.31	99.68
52.31	0.57	2.05	10.15	0.46	14.91	20.16	0.36	100.97
51.60	0.59	2.54	10.04	0.30	15.24	20.02	0.33	100.67
51.61	0.52	2.14	9.39	0.43	14.48	20.69	0.39	99.63
52.78	0.41	1.61	10.02	0.55	14.60	20.73	0.27	100.98
52.48	0.51	1.55	9.67	0.49	14.54	20.03	0.32	99.59
50.77	0.62	4.09	9.03	0.27	14.45	20.72	0.30	100.26
51.80	0.58	3.31	8.27	0.22	14.80	21.70	0.26	100.94
51.77	0.49	3.15	8.06	0.10	14.61	21.48	0.18	99.85
51.19	0.55	4.36	8.93	0.09	14.33	21.20	0.31	100.96
50.90	0.63	3.57	8.25	0.16	14.84	21.48	0.23	100.06
51.32	0.49	2.87	8.00	0.19	14.84	21.54	0.28	99.53
52.29	0.45	1.63	9.19	0.33	15.30	20.34	0.23	99.76
52.43	0.49	1.67	10.45	0.45	14.68	19.76	0.30	100.24
52.10	0.50	2.15	9.50	0.53	14.99	20.67	0.33	100.76
53.32	0.46	1.64	9.89	0.40	14.59	20.31	0.37	100.98
51.20	0.58	3.92	8.84	0.34	14.44	20.81	0.27	100.41
51.53	0.65	3.14	8.85	0.26	15.09	20.81	0.28	100.60
50.39	0.98	4.33	10.57	0.29	14.44	18.95	0.35	100.28
50.28	0.83	3.99	10.92	0.26	14.09	19.40	0.39	100.15
50.25	0.81	3.67	10.38	0.20	14.68	19.31	0.31	99.61
52.45	0.49	1.80	9.26	0.23	15.90	19.73	0.23	100.08

Appendix 5 continued

SiO_2	TiO_2	Al_2O_3	FeO*	MnO	MgO	CaO	Na_2O	Total
52.63	0.44	1.87	9.07	0.33	15.35	20.30	0.37	100.37
51.94	0.53	1.81	9.37	0.36	15.16	19.86	0.38	99.42
52.25	0.39	1.88	9.26	0.47	15.16	20.75	0.28	100.44
52.21	0.51	1.80	9.43	0.41	14.97	19.98	0.30	99.62
52.42	0.46	2.11	9.19	0.26	15.16	20.00	0.35	99.95
52.90	0.50	1.96	8.77	0.25	15.38	20.08	0.29	100.13
52.35	0.48	2.37	9.05	0.34	15.60	20.25	0.32	100.76
52.47	0.42	1.88	8.86	0.26	15.79	20.82	0.21	100.72
52.69	0.47	1.83	8.65	0.35	15.77	19.58	0.25	99.57
Clinopyroxene phenocrysts in Karymsky andesite (98IPE28, core)								
52.47	0.45	1.59	10.91	0.29	15.05	19.92	0.28	100.97
52.21	0.47	1.53	9.71	0.29	15.02	19.13	0.28	98.65
52.49	0.47	1.64	10.29	0.39	15.21	19.55	0.26	100.29
51.87	0.52	1.98	10.71	0.40	14.85	19.43	0.36	100.12
50.88	0.80	3.01	10.50	0.45	14.08	19.90	0.39	100.01
51.18	0.66	2.78	10.46	0.42	14.50	20.15	0.37	100.51
51.49	0.59	2.22	10.32	0.47	14.19	20.17	0.41	99.84
51.23	0.59	2.32	10.02	0.34	14.32	20.31	0.33	99.47
52.20	0.52	1.76	9.26	0.23	14.57	21.29	0.28	100.10
51.13	0.79	2.84	10.79	0.33	14.74	18.83	0.34	99.80
51.70	0.53	2.15	9.89	0.51	14.84	20.35	0.34	100.30
51.83	0.66	1.80	10.12	0.50	14.95	20.25	0.28	100.39
51.93	0.61	2.11	10.55	0.38	14.63	19.35	0.38	99.94
51.90	0.63	2.01	9.70	0.36	14.59	20.95	0.34	100.47
51.71	0.66	2.12	9.77	0.29	14.57	20.64	0.22	99.99
51.24	0.73	2.99	9.63	0.26	14.60	20.57	0.40	100.42
50.60	0.72	3.10	10.07	0.38	14.68	19.96	0.39	99.89
51.80	0.73	2.65	9.46	0.42	14.76	20.38	0.25	100.45

Appendix 5 continued

SiO_2	TiO_2	Al_2O_3	FeO*	MnO	MgO	CaO	Na_2O	Total
51.18	0.73	2.70	9.32	0.39	14.72	20.57	0.26	99.86
52.03	0.66	2.04	9.15	0.43	14.82	20.74	0.28	100.14
51.40	0.65	2.26	10.14	0.49	14.75	20.17	0.37	100.23
51.44	0.74	2.33	10.73	0.30	14.57	20.22	0.34	100.67
51.79	0.70	2.41	10.31	0.29	14.34	20.36	0.34	100.53
51.26	0.67	2.49	10.41	0.37	14.29	20.86	0.34	100.71
51.72	0.53	1.84	9.53	0.48	14.88	20.59	0.32	99.88
52.16	0.60	1.86	9.90	0.36	15.03	20.45	0.38	100.73
51.68	0.61	2.09	9.83	0.41	14.69	20.77	0.32	100.39
51.69	0.68	2.12	10.06	0.43	14.65	20.84	0.39	100.86
Clinopyroxene phenocrysts in Karymsky andesite (97IPE4, core)								
52.23	0.58	2.02	9.54	0.48	14.86	20.33	0.28	100.31
52.36	0.51	1.38	9.84	0.59	15.69	20.07	0.29	100.73
52.47	0.46	1.56	9.44	0.54	15.44	20.55	0.33	100.78
51.90	0.53	1.64	10.65	0.56	14.48	20.41	0.31	100.47
52.03	0.44	1.54	9.90	0.42	15.15	20.56	0.34	100.38
52.14	0.51	1.67	9.72	0.65	15.06	20.47	0.32	100.53
51.85	0.53	1.50	10.00	0.42	15.43	20.13	0.29	100.15
51.88	0.59	1.75	9.14	0.57	15.26	19.79	0.34	99.32
51.71	0.50	1.62	10.38	0.51	15.80	20.10	0.30	100.92
51.76	0.48	1.62	9.55	0.52	15.76	19.89	0.30	99.86
Clinopyroxene phenocrysts in 7,900 yr. BP Karymsky dacite (99IPE4, rim)								
53.16	0.30	1.00	9.01	0.53	14.28	21.69	0.36	100.33
53.65	0.27	1.02	8.83	0.25	14.51	21.60	0.37	100.50
53.62	0.31	1.10	8.82	0.44	14.43	21.44	0.35	100.52
53.57	0.23	1.03	8.72	0.49	14.39	21.42	0.31	100.18
53.38	0.29	1.09	8.78	0.53	14.12	21.18	0.31	99.69
53.41	0.27	1.07	8.82	0.42	14.35	22.09	0.34	100.76

Appendix 5 continued

SiO_2	TiO_2	Al_2O_3	FeO*	MnO	MgO	CaO	Na_2O	Total
53.61	0.28	1.03	8.93	0.47	14.63	22.03	0.36	101.35
53.70	0.25	0.94	9.02	0.30	14.51	21.13	0.31	100.17
52.81	0.28	1.01	8.81	0.46	14.48	21.50	0.30	99.65
53.04	0.36	1.08	9.13	0.51	14.30	21.34	0.32	100.07
53.08	0.28	1.01	8.68	0.36	14.28	21.29	0.35	99.34
53.52	0.22	0.87	8.86	0.50	14.68	21.84	0.28	100.76
53.95	0.33	0.98	8.78	0.62	14.47	21.80	0.31	101.23
53.08	0.31	0.97	8.29	0.43	14.76	21.62	0.27	99.73
52.52	0.33	1.21	8.99	0.41	14.75	21.11	0.31	99.64
53.05	0.29	1.12	8.77	0.53	14.84	21.64	0.39	100.64
52.97	0.25	1.01	8.81	0.36	14.35	21.14	0.36	99.25
52.95	0.22	0.91	8.66	0.53	14.67	21.60	0.28	99.81
53.06	0.28	0.88	9.00	0.45	14.45	21.49	0.30	99.92
52.40	0.23	1.05	9.27	0.49	14.40	21.18	0.32	99.34
52.07	0.31	1.19	8.43	0.36	14.74	21.92	0.37	99.39
52.98	0.25	1.03	9.10	0.43	14.59	21.25	0.34	99.98
53.18	0.28	1.06	9.50	0.54	13.80	21.18	0.44	99.98
53.53	0.33	1.19	9.38	0.46	14.06	21.35	0.39	100.69
52.90	0.22	1.04	9.72	0.56	14.49	21.40	0.32	100.66
52.75	0.29	1.11	9.44	0.39	14.57	21.55	0.32	100.42
52.62	0.24	1.12	8.93	0.45	14.55	21.38	0.29	99.58
Clinopyroxene phenocrysts in 7,900 yr. BP Karymsky dacite (99IPE4, core)								
53.31	0.23	0.99	8.38	0.40	15.11	21.95	0.30	100.66
52.92	0.20	0.82	8.92	0.50	14.45	21.48	0.40	99.68
52.65	0.26	0.99	8.53	0.40	14.45	21.67	0.35	99.31
53.07	0.26	0.87	8.71	0.61	14.55	21.55	0.32	99.93
52.89	0.27	0.89	8.72	0.42	14.54	21.34	0.29	99.36
52.98	0.23	0.90	8.70	0.58	14.71	21.75	0.33	100.17

Appendix 5 continued

SiO_2	TiO_2	Al_2O_3	FeO*	MnO	MgO	CaO	Na_2O	Total
53.26	0.19	0.82	8.50	0.62	14.23	21.40	0.26	99.27
52.38	0.43	1.46	9.00	0.55	14.44	22.06	0.35	100.67
52.76	0.25	1.24	9.38	0.45	14.39	21.06	0.34	99.87
52.56	0.25	1.04	8.59	0.54	14.76	21.86	0.29	99.89
53.38	0.23	0.98	8.82	0.43	14.64	21.51	0.32	100.31
52.73	0.23	0.88	8.58	0.57	14.03	21.47	0.40	98.90
52.69	0.29	1.42	9.58	0.61	14.56	20.79	0.49	100.43
52.61	0.30	1.09	8.23	0.39	14.30	21.60	0.34	98.85
53.03	0.20	0.94	9.06	0.45	14.40	21.60	0.36	100.04
52.49	0.26	1.29	9.34	0.54	14.10	20.68	0.37	99.06
52.45	0.30	1.34	9.92	0.58	14.52	20.90	0.42	100.43
53.50	0.25	0.92	9.17	0.40	14.42	21.34	0.36	100.36
53.43	0.25	0.93	8.93	0.45	14.20	22.01	0.36	100.56
53.20	0.23	0.90	8.66	0.49	14.20	21.49	0.31	99.48
53.30	0.26	1.05	9.13	0.47	14.44	21.65	0.29	100.59
53.31	0.29	1.00	8.91	0.43	14.59	21.23	0.31	100.08
53.40	0.36	1.03	8.38	0.43	14.66	21.73	0.31	100.29
Clinopyroxene phenocrysts in 40,000 yr. BP Academy Nauk dacite (99IPE6, rim)								
52.59	0.26	1.17	8.60	0.50	15.04	21.37	0.30	99.82
51.31	0.46	1.86	8.88	0.48	14.45	21.00	0.38	98.83
52.12	0.25	1.42	9.41	0.52	14.98	21.36	0.34	100.41
52.92	0.28	1.26	8.70	0.50	15.28	21.09	0.33	100.34
50.91	0.46	1.96	9.11	0.55	14.52	21.02	0.36	98.89
51.92	0.46	1.97	9.61	0.52	14.81	21.44	0.29	101.02
Clinopyroxene inclusions in amphibole phenocrysts in the granophyre (97IPE7)								
52.20	0.31	1.04	11.22	0.50	13.82	20.92	0.31	100.33
52.10	0.24	0.88	11.24	0.51	14.00	21.09	0.34	100.40
51.99	0.25	0.88	10.57	0.59	14.10	21.23	0.32	99.93

Appendix 5 continued

SiO_2	TiO_2	Al_2O_3	FeO*	MnO	MgO	CaO	Na_2O	Total
52.31	0.23	0.84	11.21	0.59	13.65	20.85	0.34	100.02
52.22	0.30	0.95	11.54	0.34	13.83	21.26	0.38	100.83
52.00	0.17	0.91	10.87	0.31	13.74	20.77	0.39	99.16
52.27	0.28	0.90	11.61	0.43	13.93	21.22	0.31	100.95
52.12	0.32	0.84	10.76	0.46	13.98	21.15	0.39	100.02
51.64	0.31	0.88	11.35	0.34	13.91	20.99	0.35	99.76
52.52	0.26	0.91	10.87	0.49	13.93	21.03	0.32	100.32
52.60	0.18	0.86	9.74	0.52	14.55	22.01	0.32	100.79
52.40	0.21	0.93	9.41	0.49	14.60	21.85	0.26	100.14
52.93	0.22	0.86	9.38	0.35	15.09	22.19	0.34	101.35
52.74	0.27	0.85	9.46	0.60	14.78	21.98	0.35	101.02
52.21	0.19	0.85	9.77	0.47	14.55	21.75	0.35	100.15
52.28	0.29	0.91	9.52	0.39	14.04	22.04	0.29	99.76
52.03	0.22	0.84	9.93	0.51	14.35	21.84	0.25	99.97
Orthopyroxene phenocrysts in Karymsky andesite (98IPE28)								
53.35	0.31	0.78	18.99	0.81	24.25	1.62	0.01	100.11
53.64	0.22	0.76	18.91	0.78	24.46	1.77	0.04	100.58
53.81	0.34	0.81	18.83	0.87	24.23	1.58	0.01	100.48
53.54	0.28	0.84	19.38	0.80	24.16	1.58	n.d.	100.58
53.30	0.32	0.85	19.28	0.66	24.41	1.62	0.01	100.45
52.60	0.26	1.00	19.52	0.59	24.13	1.71	0.07	99.87
53.31	0.30	1.06	20.05	0.73	23.61	1.81	0.05	100.92
52.61	0.24	0.88	19.48	0.84	23.60	1.74	0.07	99.46
53.55	0.30	0.92	19.00	0.82	24.20	1.65	0.06	100.50
53.50	0.31	0.82	19.35	0.86	24.61	1.75	0.09	101.28
53.38	0.25	0.85	19.45	0.97	23.76	1.56	n.d.	100.21
53.54	0.26	1.02	18.21	0.99	24.91	1.74	0.03	100.71
53.44	0.25	0.84	18.66	1.14	24.40	1.53	0.02	100.28

Appendix 5 continued

SiO_2	TiO_2	Al_2O_3	FeO*	MnO	MgO	CaO	Na_2O	Total
Orthopyroxene phenocrysts in Karymsky andesite (BV-170296, rim)								
53.47	0.31	0.75	18.60	0.77	23.13	1.53	n.d.	98.56
53.60	0.24	0.77	19.32	0.61	23.51	1.50	0.03	99.57
Orthopyroxene phenocrysts in Karymsky andesite (BV-170296, core)								
53.88	0.33	0.92	19.14	0.72	24.12	1.60	n.d.	100.71
53.99	0.29	0.94	19.30	0.62	23.27	1.85	0.05	100.32
53.94	0.19	0.52	18.79	0.58	24.07	1.56	n.d.	99.63
53.86	0.28	0.77	18.73	0.71	23.67	1.62	0.05	99.68
53.19	0.36	1.04	20.23	0.80	22.73	1.63	0.03	100.00
53.64	0.26	0.99	19.82	0.77	23.26	1.67	n.d.	100.42
49.52	0.75	0.66	25.43	1.35	18.20	3.41	0.02	99.35
55.31	0.30	0.95	20.11	0.76	20.18	1.69	0.01	99.33
53.72	0.29	1.03	21.96	0.91	19.83	1.76	0.03	99.53
54.25	0.28	0.93	18.99	0.71	23.27	1.60	0.06	100.08
54.36	0.31	0.97	19.21	0.78	23.43	1.59	0.04	100.69
54.61	0.27	0.78	19.07	0.71	23.63	1.79	0.06	100.91
53.89	0.25	0.87	19.25	0.76	23.19	1.61	n.d.	99.82
53.02	0.39	0.55	22.89	1.28	20.17	1.81	0.07	100.18
54.57	0.27	0.84	18.65	0.90	22.92	1.79	0.01	99.94
53.16	0.22	0.87	18.71	0.91	23.34	1.69	0.03	98.92
53.69	0.25	0.75	19.63	0.77	23.28	1.75	n.d.	100.12
54.70	0.23	0.61	19.10	0.61	23.45	1.75	0.07	100.52
53.60	0.24	0.70	19.17	0.69	23.26	1.70	0.08	99.45
54.16	0.24	0.93	19.19	0.78	23.41	1.80	0.09	100.60
54.28	0.20	0.70	19.52	0.53	23.48	1.54	0.05	100.30
54.13	0.25	0.67	19.59	0.65	23.79	1.62	0.06	100.77
Orthopyroxene phenocrysts in Karymsky andesite (98IPE33, rim)								
52.95	0.30	0.85	19.36	0.52	23.40	1.40	n.d.	98.78
54.34	0.23	1.04	18.90	0.61	23.57	1.44	0.03	100.15

Appendix 5 continued

SiO_2	TiO_2	Al_2O_3	FeO*	MnO	MgO	CaO	Na_2O	Total
Orthopyroxene inclusion in olivine in 1996 AN basalt (98IPE22a)								
54.64	0.21	1.47	15.83	0.46	26.14	1.76	n.d.	100.51
53.87	0.27	1.51	15.34	0.39	25.71	1.88	0.04	99.01
54.41	0.23	1.47	14.91	0.32	26.19	1.60	0.05	99.18
53.73	0.23	1.71	15.97	0.30	26.04	1.76	0.07	99.79
Orthopyroxene phenocrysts in 7,900 yr. BP Karymsky dacite (99IPE4, rim)								
54.78	0.10	0.51	21.22	0.62	22.36	1.36	0.03	100.98
54.46	0.15	0.66	19.75	0.89	22.01	1.25	0.01	99.19
53.68	0.17	0.50	20.22	0.85	22.72	1.16	0.03	99.33
53.69	0.10	0.55	21.09	0.97	22.85	1.17	0.04	100.47
53.74	0.12	0.45	19.63	0.89	22.98	1.19	0.01	99.01
53.44	0.25	0.54	20.08	0.71	22.56	1.13	n.d.	98.71
54.03	0.21	0.54	19.97	0.91	22.53	1.08	0.04	99.32
53.73	0.12	0.54	20.01	1.06	22.78	1.21	0.03	99.49
53.58	0.18	0.56	19.75	1.02	22.52	1.23	n.d.	98.84
53.57	0.17	0.56	20.21	0.99	22.99	1.15	n.d.	99.63
54.64	0.14	0.37	19.25	0.82	22.63	1.25	0.03	99.13
54.84	0.18	0.43	19.99	0.85	22.60	1.16	n.d.	100.05
54.89	0.21	0.44	20.24	0.77	22.52	1.19	n.d.	100.26
54.58	0.16	0.39	20.08	0.98	22.88	1.11	n.d.	100.18
55.01	0.12	0.44	19.31	0.89	22.30	1.16	n.d.	99.23
54.51	0.18	0.47	20.02	0.96	22.45	1.16	n.d.	99.75
54.48	0.17	0.39	19.46	0.92	22.80	1.21	0.03	99.46
51.81	0.16	0.45	19.19	0.93	22.25	1.17	0.05	96.01
53.58	0.10	0.41	19.80	0.94	22.86	1.12	0.05	98.86
53.64	0.19	0.46	19.10	0.79	23.36	1.26	0.01	98.80
52.31	0.27	1.19	20.15	1.02	22.53	1.31	0.06	98.84
53.15	0.16	0.58	19.58	0.80	22.63	1.22	0.03	98.16
53.22	0.15	0.71	19.78	0.80	22.71	1.15	n.d.	98.53

Appendix 5 continued

SiO_2	TiO_2	Al_2O_3	FeO*	MnO	MgO	CaO	Na_2O	Total
Orthopyroxene phenocrysts in 7,900 yr. BP Karymsky dacite (99IPE4, core)								
53.80	0.20	0.49	20.29	1.12	22.42	1.17	n.d.	99.48
53.63	0.19	0.49	20.63	1.03	22.55	1.10	0.03	99.65
54.61	0.10	0.36	20.95	0.92	22.87	1.22	0.02	101.04
54.34	0.14	0.38	20.43	0.96	22.74	1.18	n.d.	100.18
53.68	0.13	0.43	19.62	0.79	22.22	1.05	0.02	97.95
53.71	0.13	0.58	20.68	1.02	22.47	1.15	0.03	99.77
54.07	0.12	0.35	20.41	0.90	22.47	1.19	0.02	99.52
53.38	0.17	0.64	20.92	1.18	22.73	1.22	0.05	100.28
53.03	0.17	0.63	20.84	0.91	22.31	1.21	0.03	99.13
53.79	0.14	0.33	19.95	1.01	22.80	1.16	0.02	99.19
53.88	0.16	0.35	20.02	1.09	22.60	1.10	0.04	99.23
53.84	0.20	0.48	20.75	0.95	22.46	1.17	n.d.	99.86
53.08	0.15	0.52	20.39	1.04	22.07	1.21	n.d.	98.45
53.57	0.14	0.47	21.26	0.87	22.24	1.18	0.01	99.74
53.66	0.23	0.55	19.80	1.04	22.06	1.20	0.05	98.59
53.53	0.14	0.46	20.22	0.99	22.06	1.24	0.02	98.66
53.79	0.12	0.47	20.63	0.92	22.18	1.11	n.d.	99.22
52.87	0.17	0.52	20.43	0.98	22.31	1.19	0.01	98.47
53.53	0.23	0.55	20.80	1.11	22.67	1.20	0.01	100.11
53.63	0.20	0.49	19.81	1.23	22.35	1.17	n.d.	98.88
54.07	0.15	0.58	20.53	1.02	22.56	1.26	0.01	100.17
54.34	0.11	0.45	19.71	0.77	22.85	1.28	n.d.	99.52
53.29	0.16	0.61	19.58	0.99	22.42	1.12	n.d.	98.17
54.00	0.23	0.73	20.17	1.04	22.77	1.13	0.04	100.12
53.77	0.17	0.49	19.81	1.15	22.68	1.19	0.04	99.30
53.64	0.17	0.45	19.83	0.99	22.66	1.01	n.d.	98.77

Appendix 6: Representative electron microprobe analyses of olivines in natural samples

All samples were polished and carbon-coated to a thickness of ca. 250 Å. Olivine phenocrysts were analyzed for major elements at the University of Alaska Fairbanks using a Cameca SX-50 electron microprobe, which is equipped with four wavelength-dispersive and one energy-dispersive spectrometers. A 15 keV, 10 nA, 1-3-μm-diameter beam was used for all analyses. Major oxides are in wt.%, with all Fe reported as FeO; n.d. – not detected. Details about counting times, standards, and analytical errors are summarized below.

Element	Counting Time		Standard	Typical Analytical Error (wt.%, 1 sigma)*
	Peak (sec.)	Background (sec.)		
Mn	20	10	Spessartine (CM Taylor)	0.044
Cr	40	10	Chromite (CM Taylor)	0.002
Ti	10	5	Sphene (CM Taylor)	0.001
Ca	20	10	Diopside (CM Taylor)	0.008
Fe	10	5	Fayalite (USNM 85276)	0.356
Mg	10	5	Olivine (USNM 1113127444)	0.203
Si	10	5	Diopside (CM Taylor)	0.195
Al	10	5	Kyanite (CM Taylor)	0.002

* Typical analytical errors for a representative sample calculated after Scott et al. (1995).

Appendix 6 continued

MnO	Cr_2O_3	TiO_2	CaO	FeO	MgO	SiO_2	Al_2O_3	Total
Olivine phenocrysts in 1996 Academy Nauk basalt (97IPE3)								
0.33	n.d.	n.d.	0.18	21.22	39.75	38.59	n.d.	100.06
0.28	0.02	0.01	0.17	20.50	39.79	38.66	0.03	99.46
0.29	0.02	n.d.	0.18	20.79	39.81	38.60	0.06	99.75
0.32	0.02	0.02	0.14	21.06	39.60	38.89	0.01	100.06
0.34	n.d.	0.05	0.16	21.01	39.79	39.04	0.04	100.43
0.46	0.01	0.01	0.16	20.94	39.44	38.15	0.02	99.18
0.39	n.d.	0.02	0.16	20.98	39.76	39.07	0.02	100.39
0.32	n.d.	n.d.	0.20	20.96	39.61	38.36	n.d.	99.46
0.35	n.d.	0.04	0.17	21.25	39.35	38.49	n.d.	99.65
0.39	n.d.	0.01	0.19	21.48	39.22	38.55	0.03	99.87
0.37	0.01	0.03	0.17	20.90	39.63	38.49	0.08	99.69
0.35	n.d.	0.02	0.16	20.47	40.38	38.92	0.01	100.30
0.25	0.03	0.04	0.20	19.54	39.90	38.84	0.01	98.81
0.32	0.01	0.01	0.16	20.14	40.64	38.88	n.d.	100.17
0.32	0.03	0.02	0.20	20.60	40.93	39.33	0.07	101.49
0.43	0.04	n.d.	0.14	24.53	36.87	37.88	0.01	99.88
0.45	0.01	0.04	0.15	24.53	36.90	38.14	0.03	100.24
0.44	0.01	0.02	0.18	24.70	36.62	38.25	n.d.	100.21
0.48	0.02	0.04	0.15	24.80	36.88	38.23	0.06	100.66
0.34	n.d.	n.d.	0.15	24.84	37.04	38.50	n.d.	100.86
0.49	0.02	0.01	0.17	24.54	36.96	37.98	n.d.	100.17
0.44	0.01	n.d.	0.15	24.22	36.75	37.85	0.01	99.43
0.39	0.03	0.03	0.15	25.12	37.29	37.93	0.05	100.98
0.35	n.d.	0.02	0.18	22.40	38.42	38.54	0.03	99.94
0.28	0.04	0.05	0.18	21.62	39.16	38.70	0.01	100.04
0.23	0.02	0.02	0.14	21.59	40.07	38.85	0.04	100.96
0.31	0.02	n.d.	0.17	20.72	39.67	38.64	0.03	99.56

Appendix 6 continued

MnO	Cr_2O_3	TiO_2	CaO	FeO	MgO	SiO_2	Al_2O_3	Total
0.29	0.01	0.03	0.17	20.82	40.10	38.56	0.01	99.99
0.38	n.d.	0.02	0.16	20.64	40.79	38.53	0.04	100.55
0.25	0.01	0.02	0.16	20.35	40.47	38.75	0.01	100.01
0.33	n.d.	0.01	0.13	20.38	40.50	38.78	0.08	100.23
0.28	0.04	0.01	0.18	20.21	40.56	38.64	0.03	99.96
0.30	0.01	0.01	0.15	19.99	40.69	38.86	0.04	100.05
Olivine xenocrysts in Karymsky andesite (98IPE27)								
0.34	n.d.	0.02	0.14	19.32	40.06	38.55	n.d.	98.43
0.42	n.d.	0.01	0.13	20.44	39.69	38.27	0.03	98.99
0.34	n.d.	0.04	0.15	20.58	40.01	38.22	n.d.	99.34
0.36	n.d.	n.d.	0.16	20.29	40.04	38.46	n.d.	99.30
0.40	0.02	0.03	0.15	20.68	40.51	38.33	0.03	100.14
0.26	0.02	0.02	0.17	20.69	40.27	38.33	n.d.	99.76
0.38	n.d.	n.d.	0.15	20.91	40.68	38.36	0.05	100.54
0.39	n.d.	0.03	0.20	20.57	40.16	38.54	n.d.	99.88
0.37	0.02	n.d.	0.20	20.58	40.30	38.15	0.05	99.67
0.34	0.04	n.d.	0.15	20.92	39.75	38.60	n.d.	99.80
0.36	0.02	n.d.	0.16	20.73	40.30	37.99	0.02	99.58
0.41	0.03	n.d.	0.19	19.74	39.41	38.32	0.04	98.15
0.42	n.d.	n.d.	0.15	20.99	39.45	38.14	n.d.	99.14
0.43	0.01	0.01	0.17	20.41	39.38	38.41	n.d.	98.83
0.38	0.02	0.02	0.17	20.72	39.54	38.84	n.d.	99.69
0.43	0.02	n.d.	0.16	20.91	39.71	37.91	n.d.	99.14
0.42	0.01	0.05	0.14	20.95	39.70	37.98	0.05	99.29
0.42	n.d.	0.02	0.17	21.22	39.00	38.02	0.02	98.86
0.42	0.01	n.d.	0.15	21.43	38.92	37.93	0.04	98.89
0.47	0.01	n.d.	0.18	21.75	38.93	38.01	0.02	99.38
0.42	0.03	n.d.	0.16	21.89	38.66	38.09	n.d.	99.25

Appendix 6 continued

MnO	Cr_2O_3	TiO_2	CaO	FeO	MgO	SiO_2	Al_2O_3	Total
0.47	0.03	n.d.	0.18	21.59	38.51	37.79	0.01	98.57
0.50	0.01	0.06	0.18	21.71	38.42	37.70	n.d.	98.57
0.47	0.01	0.01	0.13	22.43	38.46	37.38	0.02	98.92
0.51	0.01	0.03	0.17	23.00	37.69	37.45	0.04	98.90
0.65	0.04	0.02	0.14	27.49	34.36	37.02	0.04	99.75
0.70	0.02	0.01	0.12	27.62	34.42	37.01	0.02	99.93
0.68	n.d.	0.02	0.12	27.10	34.61	36.81	0.03	99.35
0.65	0.01	n.d.	0.13	27.22	34.72	36.97	n.d.	99.69
0.74	n.d.	0.03	0.13	27.65	34.37	37.12	0.03	100.06
0.76	n.d.	0.03	0.14	27.72	34.34	36.90	n.d.	99.89
0.75	n.d.	0.02	0.14	28.18	34.76	36.98	0.01	100.83
0.73	n.d.	n.d.	0.13	27.22	34.45	37.06	n.d.	99.59
0.67	n.d.	0.01	0.12	26.91	34.55	36.73	0.02	99.00
0.65	n.d.	n.d.	0.14	26.77	34.65	37.47	n.d.	99.68
0.65	n.d.	0.02	0.15	27.25	34.81	36.90	0.03	99.82
0.72	0.04	0.06	0.11	26.33	34.67	37.10	0.02	99.04
0.47	n.d.	0.03	0.12	25.11	35.49	37.08	n.d.	98.29
0.43	n.d.	n.d.	0.12	25.85	36.04	37.08	n.d.	99.51
0.45	n.d.	n.d.	0.11	25.52	35.88	37.36	0.02	99.34
0.44	0.03	0.02	0.13	25.99	35.83	37.49	0.03	99.95
0.50	0.02	n.d.	0.12	25.17	35.60	37.49	0.02	98.91
0.45	n.d.	0.04	0.12	25.79	35.51	36.81	0.03	98.75
0.54	0.01	n.d.	0.13	25.92	36.40	37.29	n.d.	100.29
0.50	0.02	0.01	0.10	25.36	35.39	37.28	0.03	98.69
0.49	n.d.	n.d.	0.13	25.59	35.53	37.22	n.d.	98.97
0.43	n.d.	n.d.	0.15	24.72	35.60	37.39	0.03	98.31
0.53	0.02	0.04	0.11	24.80	35.76	37.32	0.08	98.64
0.46	n.d.	n.d.	0.14	25.55	36.05	37.05	n.d.	99.25

Appendix 6 continued

MnO	Cr_2O_3	TiO_2	CaO	FeO	MgO	SiO_2	Al_2O_3	Total
0.50	0.01	n.d.	0.13	25.14	35.35	37.64	0.01	98.79
0.55	0.02	n.d.	0.13	25.83	35.61	36.92	0.04	99.09
0.45	n.d.	n.d.	0.15	25.26	35.82	36.96	0.05	98.69
0.50	n.d.	n.d.	0.10	25.22	36.30	37.12	n.d.	99.24
0.48	n.d.	n.d.	0.13	25.40	36.35	37.14	0.01	99.50
0.52	n.d.	0.02	0.10	25.03	35.69	37.35	0.03	98.74
0.46	n.d.	n.d.	0.14	25.26	36.07	37.13	0.02	99.08
0.44	n.d.	n.d.	0.17	24.77	36.31	37.48	n.d.	99.18
0.49	n.d.	n.d.	0.13	25.05	36.19	37.15	0.05	99.05
0.56	n.d.	0.01	0.12	24.72	35.63	36.85	0.03	97.92
0.44	n.d.	0.04	0.12	25.38	36.39	37.55	n.d.	99.92
0.49	n.d.	n.d.	0.16	25.63	36.75	37.51	n.d.	100.53
0.55	n.d.	0.03	0.17	25.40	36.34	37.22	n.d.	99.69
0.46	0.01	0.03	0.19	25.18	35.46	37.45	n.d.	98.78
0.45	n.d.	n.d.	0.15	25.24	36.35	37.50	0.01	99.70
0.49	n.d.	0.03	0.14	25.16	35.57	36.78	0.02	98.18
0.40	n.d.	0.01	0.14	24.91	35.67	37.23	n.d.	98.37
0.42	0.02	0.02	0.13	24.89	35.74	37.36	0.01	98.58

Appendix 7: Electron microprobe analyses of Fe-Ti oxides in natural samples

All samples were polished and carbon-coated to a thickness of ca. 250 Å. Magnetite and ilmenite phenocrysts were analyzed for major elements at the University of Alaska Fairbanks using a Cameca SX-50 electron microprobe, which is equipped with four wavelength-dispersive and one energy-dispersive spectrometers. A 15 keV, 10 nA, 1-3-μm-diameter beam was used for all analyses. Major oxides are in wt.%, with Fe_2O_3 and FeO calculated using the mineral formula calculation scheme of Stormer (1983); n.d. - not detected. Si was analyzed for monitoring purposes only; in all cases it was below detection limit and thus is not reported. Details about counting times, standards, and analytical errors are summarized below.

Element	Counting Time		Standard	Typical Analytical Error (wt.%, 1 sigma)*
	Peak (sec.)	Background (sec.)		
Mg	10	5	Chromite (USNM 117075)	0.083
Al	10	5	Chromite (USNM 117075)	0.014
Si	10	5	Quartz (USNM R17701)	0.003
Ti	10	5	Ilmenite (USNM 96189)	0.158
Cr	10	5	Chromite (USNM 117075)	0.002
Mn	10	5	Ilmenite (USNM 96189)	0.114
Fe	10	5	Ilmenite (USNM 96189)	1.115

* Typical analytical errors for a representative sample calculated after Scott et al. (1995).

Appendix 7 continued

FeO	Fe_2O_3	TiO_2	Al_2O_3	MgO	MnO	Cr_2O_3	Total
Magnetite grains in 1996 Academy Nauk basalts							
31.90	50.06	7.71	4.85	4.32	0.40	0.42	99.67
32.26	50.40	7.80	4.85	4.29	0.36	0.33	100.30
33.47	48.90	8.51	4.56	3.94	0.27	0.51	100.15
32.33	48.16	7.42	5.04	3.70	0.34	1.51	98.51
33.23	48.80	8.31	4.58	3.77	0.34	0.33	99.36
37.53	43.80	11.36	3.00	2.47	0.40	0.18	98.96
35.20	45.08	9.86	3.86	2.98	0.32	0.22	97.74
37.45	43.98	11.24	3.07	2.41	0.46	0.08	99.14
33.20	46.24	7.70	4.93	3.43	0.36	3.27	99.24
Magnetite grains in Karymsky andesite							
36.08	45.24	11.02	2.75	2.96	0.76	n.d.	98.97
37.61	44.79	11.28	2.76	2.38	0.55	0.05	99.49
37.17	44.71	11.38	2.81	2.74	0.51	0.01	99.44
37.90	45.90	11.13	2.68	2.26	0.64	0.04	100.69
36.87	45.90	11.07	2.83	2.84	0.66	0.10	100.39
37.04	46.31	11.13	2.80	2.98	0.49	0.06	100.95
36.64	45.98	10.99	2.73	2.76	0.86	0.12	100.16
37.31	46.44	11.32	2.77	2.99	0.59	0.08	101.57
37.48	45.88	11.40	2.77	2.86	0.54	0.05	101.06
38.68	44.58	11.77	2.54	2.24	0.38	0.08	100.45
38.29	43.53	11.91	2.65	2.21	0.66	0.06	99.45
37.10	45.28	11.42	2.76	2.92	0.57	0.05	100.20
36.51	45.29	11.11	2.82	3.07	0.39	0.07	99.36
37.97	44.65	11.45	2.66	2.29	0.54	0.08	99.73
37.47	45.71	11.31	2.67	2.70	0.55	0.13	100.58
36.99	44.60	11.23	2.83	2.61	0.62	0.04	98.98
37.54	44.01	11.44	2.67	2.52	0.27	0.09	98.58
37.03	45.62	11.18	2.67	2.68	0.73	0.06	100.02

Appendix 7 continued

FeO	Fe_2O_3	TiO_2	Al_2O_3	MgO	MnO	Cr_2O_3	Total
36.51	44.82	11.29	2.79	2.98	0.62	0.03	99.11
37.35	46.68	11.25	2.84	3.00	0.55	0.04	101.89
36.49	44.90	11.27	2.70	3.01	0.57	0.09	99.13
36.42	45.37	11.12	2.69	2.95	0.65	0.07	99.31
37.62	43.97	11.48	2.71	2.29	0.65	0.02	98.79
38.86	43.64	11.96	2.81	2.16	0.43	0.03	99.94
39.25	44.64	11.84	2.82	2.07	0.47	0.11	101.22
37.62	45.11	11.75	2.81	2.96	0.53	0.08	101.00
37.70	45.44	11.60	2.82	2.97	0.33	0.05	101.00
38.27	45.90	10.83	2.77	1.77	0.70	0.13	100.48
38.29	47.05	10.51	3.01	1.83	0.64	0.05	101.47
37.69	46.20	10.37	3.10	1.93	0.53	0.10	99.93
37.34	48.10	9.92	3.41	2.13	0.78	0.06	101.73
37.13	47.14	9.94	3.40	2.13	0.58	0.07	100.59
38.83	46.02	11.04	3.09	1.97	0.43	0.08	101.57
39.66	43.00	12.33	2.30	1.69	0.48	0.07	99.62
40.74	38.81	14.53	2.19	2.20	0.49	0.07	99.13
40.87	37.89	14.76	2.20	2.03	0.64	0.02	98.50
37.92	46.11	11.22	2.68	2.49	0.50	0.13	101.10
38.29	45.76	11.65	2.64	2.49	0.66	n.d.	101.59
40.21	40.02	13.92	2.25	2.11	0.68	0.04	99.23
40.99	38.26	14.69	2.08	2.01	0.55	0.05	98.63
42.08	36.69	16.03	1.84	2.16	0.72	0.04	99.57
38.30	43.96	11.70	2.67	2.08	0.70	0.01	99.42
42.00	38.03	15.48	1.97	2.04	0.72	0.08	100.33
41.52	39.47	14.77	2.04	1.99	0.73	0.08	100.59
40.33	41.38	13.45	2.21	1.90	0.67	0.04	99.99
41.04	40.61	14.03	2.28	1.94	0.66	0.10	100.65
38.81	42.02	12.60	2.39	2.17	0.59	0.05	98.63

Appendix 7 continued

FeO	Fe_2O_3	TiO_2	Al_2O_3	MgO	MnO	Cr_2O_3	Total
40.22	39.74	14.05	2.24	2.18	0.62	n.d.	99.05
39.77	40.87	13.13	2.40	1.90	0.58	0.07	98.71
38.86	44.41	11.86	2.45	1.97	0.70	0.07	100.32
38.37	43.93	12.00	2.63	2.39	0.59	0.06	100.05
Magnetite grains in 7,900 yr. BP Karymsky dacite							
37.09	48.62	9.63	1.98	1.60	0.67	0.07	99.65
36.01	48.59	9.17	1.95	1.70	0.70	0.06	98.17
37.20	49.80	9.41	2.06	1.66	0.65	0.08	100.87
37.25	50.76	8.99	2.12	1.55	0.53	0.10	101.29
36.85	49.83	9.36	1.97	1.77	0.68	0.07	100.54
35.88	49.68	8.95	1.95	1.85	0.68	0.08	99.07
36.68	49.52	9.30	1.94	1.72	0.63	0.02	99.82
37.00	50.53	9.11	2.08	1.65	0.71	0.14	101.21
37.16	50.49	9.22	2.08	1.75	0.49	0.01	101.21
37.16	50.27	9.41	1.90	1.78	0.58	0.08	101.19
36.90	49.40	9.25	2.06	1.65	0.50	0.08	99.84
Ilmenite grains in 7,900 yr. BP Karymsky dacite							
32.62	20.05	42.63	0.27	2.72	0.85	0.05	99.19
31.71	22.84	41.59	0.24	2.81	0.69	0.03	99.90
32.82	21.07	42.52	0.26	2.65	0.69	0.02	100.04
32.38	21.77	42.29	0.21	2.70	0.82	0.08	100.27
32.03	22.31	41.69	0.28	2.66	0.71	n.d.	99.69
32.52	21.66	42.32	0.26	2.79	0.56	0.01	100.12
32.45	22.41	42.33	0.23	2.74	0.72	0.02	100.90
32.31	21.36	42.28	0.25	2.72	0.86	0.03	99.81
31.99	22.49	41.77	0.19	2.73	0.71	n.d.	99.88
32.12	21.58	42.23	0.25	2.83	0.82	n.d.	99.83
32.12	21.35	42.14	0.27	2.83	0.72	0.02	99.46
32.72	21.72	42.51	0.23	2.67	0.76	n.d.	100.59

Appendix 7 continued

FeO	Fe_2O_3	TiO_2	Al_2O_3	MgO	MnO	Cr_2O_3	Total
32.72	21.00	42.60	0.22	2.63	0.89	0.05	100.11
32.10	21.63	42.09	0.29	2.76	0.82	0.04	99.74
32.81	21.22	42.47	0.27	2.63	0.70	0.01	100.11
33.68	19.57	43.47	0.26	2.81	0.41	n.d.	100.20
32.71	21.79	42.77	0.20	2.76	0.83	0.05	101.11
32.92	19.56	42.79	0.28	2.70	0.74	0.09	99.08
32.23	22.42	42.01	0.29	2.61	0.90	0.05	100.50
33.52	21.12	43.08	0.27	2.52	0.72	n.d.	101.23
Magnetite grains in 40,000 yr. BP Academy Nauk dacite							
36.42	49.93	9.21	1.92	1.86	0.70	0.10	100.13
36.73	50.76	9.20	1.88	1.79	0.79	n.d.	101.14
36.42	50.46	9.12	1.95	1.85	0.76	0.02	100.58
36.05	49.17	9.20	1.87	1.92	0.56	0.08	98.84
36.99	50.22	9.27	2.00	1.74	0.66	0.13	101.01
36.39	48.55	9.47	1.97	1.80	0.71	0.07	98.94
36.08	50.26	8.99	2.04	1.92	0.76	0.11	100.15
35.64	49.04	8.88	1.98	1.82	0.58	0.09	98.02
36.07	49.37	9.21	1.94	1.96	0.62	0.08	99.25
Ilmenite grains in 40,000 yr. BP Academy Nauk dacite							
31.78	24.56	40.97	0.23	2.55	0.52	n.d.	100.62
31.09	23.92	40.64	0.24	2.79	0.48	0.04	99.19
31.09	25.56	40.80	0.25	2.75	0.69	0.02	101.17
30.48	25.71	40.19	0.23	2.87	0.54	0.03	100.05
30.14	26.68	39.58	0.27	2.71	0.61	0.05	100.04
31.04	23.61	40.29	0.26	2.61	0.54	n.d.	98.35
30.41	26.08	40.08	0.27	2.70	0.82	n.d.	100.36
31.04	25.28	40.64	0.22	2.73	0.63	0.01	100.55
31.09	24.57	40.86	0.31	2.76	0.73	0.06	100.38
30.46	25.31	39.59	0.29	2.56	0.57	0.01	98.80

Appendix 8: Electron microprobe analyses of amphibole and biotite in granophyre xenoliths

All samples were polished and carbon-coated to a thickness of ca. 250 Å. Amphibole and biotite phenocrysts were analyzed for major elements at the University of Alaska Fairbanks using a Cameca SX-50 electron microprobe, which is equipped with four wavelength-dispersive and one energy-dispersive spectrometers. A 15 keV, 10 nA, 1-3-μm-diameter beam was used for all analyses. Major oxides are in wt.%, with all Fe reported as FeO. Details about counting times, standards, and analytical errors are summarized below.

Element	Counting Time		Standard	Typical Analytical Error (wt.%, 1 sigma)*
	Peak (sec.)	Background (sec.)		
Na	10	5	Hornblende (USNM 143965)	0.029
Mg	10	5	Hypersthene (USNM 746)	0.098
Al	20	5	Augite (USNM 122142)	0.128
Si	20	5	Orthoclase (CM Taylor)	0.207
K	10	5	Orthoclase (CM Taylor)	0.012
Ca	10	5	Sphene (CM Taylor)	0.000
Ti	10	5	Sphene (CM Taylor)	0.066
Fe	10	5	Synthetic almandine	0.396
Mn	10	5	Willimite (CM Taylor)	0.029
F	10	5	Fluorite (CM Taylor)	0.100
Cl	10	5	Scapolite (USNM R6600-1)	0.005

* Typical analytical errors for a representative sample calculated after Scott et al. (1995).

Appendix 8 continued

Na_2O	MgO	Al_2O_3	SiO_2	K_2O	CaO	TiO_2	FeO*	MnO	F	Cl	Total
Amphibole phenocrysts in granophyre xenoliths											
1.64	14.32	5.73	49.20	0.43	10.89	1.49	11.41	1.08	0.30	0.12	96.61
1.54	14.13	4.88	49.92	0.32	10.51	0.94	12.11	0.67	0.50	0.14	95.67
1.80	13.01	6.40	47.75	0.36	11.01	1.61	12.66	0.43	0.25	0.12	95.40
1.89	12.60	6.54	47.31	0.38	11.02	1.40	12.92	0.48	0.38	0.14	95.04
1.56	13.41	6.54	47.97	0.29	10.95	1.63	12.68	0.49	0.00	0.08	95.61
1.45	13.40	6.43	48.40	0.38	10.95	1.72	12.20	0.36	0.30	0.12	95.69
1.46	13.23	6.33	48.11	0.50	10.01	1.46	13.71	0.62	0.33	0.13	95.90
1.49	13.13	6.00	48.19	0.39	10.85	1.34	13.51	0.40	0.91	0.18	96.39
1.52	13.56	5.92	48.38	0.39	10.95	1.40	12.77	0.36	0.29	0.14	95.70
1.49	13.16	6.06	48.06	0.47	10.99	1.27	13.55	0.36	0.21	0.14	95.78
1.63	13.65	7.03	47.45	0.32	11.11	2.24	12.06	0.41	0.30	0.08	96.28
1.41	13.43	6.44	47.72	0.35	11.13	1.68	12.21	0.30	0.34	0.12	95.11
1.48	13.70	6.47	48.21	0.36	11.17	1.30	12.78	0.50	0.55	0.09	96.61
1.48	13.85	6.08	47.77	0.43	10.54	1.44	13.82	0.49	0.71	0.15	96.74
1.62	13.28	6.52	47.04	0.54	11.17	1.40	13.34	0.50	0.34	0.15	95.90
1.54	14.09	6.89	46.92	0.39	11.36	1.99	12.93	0.59	0.59	0.13	97.42
1.69	14.02	6.75	46.53	0.36	11.20	1.30	12.11	0.52	0.17	0.11	94.75
1.57	13.75	6.91	47.32	0.42	10.51	1.82	12.30	0.47	0.84	0.12	96.03
Biotite in granophyre xenoliths											
0.28	17.00	12.72	39.85	8.93	0.10	3.66	13.40	0.20	0.57	0.19	96.89
0.31	15.35	12.66	39.49	8.47	0.17	4.83	15.17	0.33	0.47	0.29	97.53
0.32	18.04	12.29	40.55	7.87	0.18	2.62	11.98	0.29	1.81	0.20	96.16
0.29	15.45	12.76	39.14	8.50	0.13	4.03	15.48	0.24	0.47	0.36	96.84
0.31	15.85	12.36	39.82	8.11	0.15	3.67	14.06	0.36	1.03	0.25	95.97
0.30	16.40	12.44	40.07	8.08	0.13	4.14	13.53	0.41	1.03	0.29	96.81
0.30	15.17	13.07	39.40	8.60	0.08	4.61	14.22	0.20	0.98	0.33	96.96
0.26	15.34	13.02	39.25	8.43	0.09	4.36	14.63	0.15	1.27	0.31	97.10

Appendix 9: Laser ablation inductively coupled plasma mass spectrometer analyses of plagioclase phenocrysts

All samples were polished and cleaned with ethanol. Sr and Ba contents in multiple spots along microprobe traverses of representative plagioclase phenocrysts were analyzed by using a Micromass &Plasma ICP-MS coupled with a Cetac LSX 200 laser-ablation system at Michigan State University. The 266 nm Nd:YAG laser was focused to 25 μm spot size and propagated into the sample at a rate of 3 μm/s. The concentrations of Sr and Ba were calculated from peak intensities of ^{88}Sr, ^{138}Ba, and ^{44}Ca, calibrated against NIST 612 glass standard and electron microprobe determinations of Ca in analyzed points as outlined in Norman et al. (1996). The typical analytical error is 1 ppm for Ba and 14 ppm for Sr, as suggested by repetitive analyses of homogeneous representative samples.

Sample identification numbers consist of the sample number, phenocryst number, and point number. Hence, 98IPE22a-N2-1 is the first point analysis of plagioclase grain number two in sample 98IPE22a. Types of plagioclases are (1) plagioclase phenocrysts in Academy Nauk basalt, and plagioclase phenocrysts in Karymsky andesites: (2) oscillatory zoned, (3) sodic rims, (4) calcic cores, (5) rim-core boundaries, and (6) patches in calcic cores.

Appendix 9 continued

Sample	Type	An, mol. %	Ca, wt.%	^{44}Ca, c/sec	^{88}Sr, c/sec	^{138}Ba, c/sec	Ba, ppm	Sr, ppm	Sr/Ba
98IPE22a-N2-1	1	87	12.70	874400	119900	10730	40	498	12.3
98IPE22a-N2-2	1	87	12.70	869800	111600	10000	38	466	12.3
98IPE22a-N2-3	1	87	12.70	856300	111600	9982	38	473	12.3
98IPE22a-N2-4	1	87	12.70	833900	109600	10250	41	477	11.8
98IPE22a-N1-1	1	89	12.90	822500	97300	10210	42	436	10.5
98IPE22a-N1-2	1	89	13.00	933200	130100	14780	53	518	9.7
98IPE22a-N1-3	1	89	13.00	815300	93450	10500	43	426	9.8
98IPE22a-N1-4	1	82	11.90	840700	132800	12180	45	537	12.0
98IPE22a-N1-5	1	83	12.10	849800	129500	11740	43	527	12.2
BV-170296-N2-1	2	58	8.30	850300	147300	27430	70	411	5.9
BV-170296-N2-2	2	55	7.91	822300	150300	31220	78	413	5.3
BV-170296-N2-3	2	54	7.68	829900	168600	33860	81	446	5.5
BV-170296-N2-4	2	57	8.18	820200	163800	29960	78	467	6.0
BV-170296-N2-5	2	58	8.25	844100	164400	30390	77	460	6.0
BV-170296-N2-6	2	55	7.87	828800	167100	32240	79	454	5.7
BV-170296-N2-7	2	55	7.77	819000	166100	32710	81	450	5.6
BV-170296-N2-8	2	55	7.81	790700	155400	29660	76	439	5.8
BV-170296-N2-9	2	54	7.73	796100	161900	31030	78	450	5.7
BV-170296-N2-10	2	54	7.76	792400	172900	32260	82	484	5.9
BV-170296-N2-11	2	54	7.65	800600	165200	34590	86	451	5.3
BV-170296-N2-12	2	53	7.55	782200	163800	33850	85	452	5.3
BV-170296-N2-13	2	53	7.55	790600	175200	39930	99	479	4.8
BV-170296-N2-14	2	51	7.17	786300	174600	39060	92	455	4.9
BV-170296-N2-14-r	2	51	7.17	856400	232500	50940	111	556	5.0
BV-170296-N2-15	2	52	7.32	781500	178100	44120	107	477	4.4
BV-170296-N2-16	2	55	7.91	789200	176800	39480	103	507	4.9
BV-170296-N2-17	2	55	7.85	790400	159200	29230	75	452	6.0
BV-170296-N2-18	2	53	7.60	764900	141800	25170	65	403	6.2

Appendix 9 continued

Sample	Type	An, mol. %	Ca, wt.%	^{44}Ca, c/sec	^{88}Sr, c/sec	^{138}Ba, c/sec	Ba, ppm	Sr, ppm	Sr/Ba
BV-170296-N2-19	2	53	7.60	790300	152700	22770	57	420	7.4
BV-170296-N2-20	2	51	7.24	750700	150300	35670	89	414	4.6
98IPE26-N1-1	2	51	7.20	752800	180700	40730	101	494	4.9
98IPE26-N1-2	2	50	7.13	752000	179300	40090	99	486	4.9
98IPE26-N1-3	2	53	7.50	792000	217700	46920	115	589	5.1
98IPE26-N1-4	2	51	7.20	766800	204300	52160	127	549	4.3
98IPE26-N1-5	2	51	7.20	766800	204300	52160	127	549	4.3
98IPE26-N1-6	2	53	7.60	742500	197800	46140	123	579	4.7
98IPE26-N1-7	2	54	7.62	768200	207700	50540	130	589	4.5
98IPE26-N1-8	2	55	7.87	738500	183000	39890	110	558	5.1
98IPE26-N1-2r	2	55	7.80	821800	245500	52690	130	666	5.1
98IPE26-N1-5r	2	51	7.30	783100	231900	61860	150	618	4.1
99IPE8-N4-1	2	57	8.20	670500	134900	25660	81	472	5.8
99IPE8-N4-2	2	52	7.40	688200	163900	35940	100	504	5.0
99IPE8-N4-3	2	60	8.60	720000	151300	27880	86	517	6.0
99IPE8-N4-4	2	57	8.10	681600	132400	32430	100	450	4.5
BV-170296-N4-2	3	59	8.46	834100	203400	43990	116	590	5.1
BV-170296-N4-7	5	54	7.70	827200	142000	15760	38	378	9.9
BV-170296-N1-1	3	55	7.91	816800	177300	33150	83	491	5.9
98IPE26-N4-4	3	65	9.29	813300	181300	28360	84	592	7.0
98IPE26-N4-5	3	65	9.29	836200	173800	26160	75	552	7.3
98IPE26-N4-6	3	65	9.29	863400	208500	28920	81	641	7.9
98IPE26-N3-1	3	55	7.82	787700	182100	36340	94	517	5.5
98IPE26-N3-2	3	55	7.82	867800	234000	45770	107	603	5.6
98IPE26-N3-8	3	52	7.37	880200	215800	29300	64	517	8.1
98IPE26-N3-9	3	55	7.82	799800	203700	44310	112	569	5.1
98IPE25-N1-3	3	55	7.91	812700	228800	42570	108	637	5.9
98IPE25-N1-4	3	55	7.91	771100	196700	38230	102	577	5.7

Appendix 9 continued

Sample	Type	An, mol. %	Ca, wt.%	^{44}Ca, c/sec	^{88}Sr, c/sec	^{138}Ba, c/sec	Ba, ppm	Sr, ppm	Sr/Ba
98IPE25-N1-5	3	55	7.85	737600	188300	40810	113	573	5.1
98IPE25-N1-6	3	52	7.37	745500	193300	44800	115	546	4.8
98IPE25-N1-7	3	53	7.60	723800	177500	40110	109	533	4.9
98IPE25-N1-8	3	52	7.37	716100	161600	41090	110	476	4.3
98IPE25-N1-9	3	50	7.03	714300	168000	41220	105	473	4.5
98IPE25-N1-10	3	53	7.50	775800	186400	33720	85	515	6.1
98IPE25-N1-11	3	53	7.50	749900	189700	39020	101	542	5.4
98IPE25-N2-1	3	57	8.10	709400	150500	28020	83	491	5.9
98IPE25-N2-2	3	58	8.30	758200	163500	27090	77	512	6.6
98IPE25-N2-4	3	53	7.60	695900	132400	26300	75	413	5.5
98IPE25-N3-2	3	54	7.65	682600	138200	33870	99	443	4.5
98IPE25-N4-1	3	64	9.20	728600	140800	15070	49	508	10.3
98IPE25-N4-2	3	64	9.20	758800	165400	16140	51	573	11.3
99IPE8-N6-1	3	50	7.10	679400	142300	29360	80	425	5.3
99IPE8-N6-2	3	55	7.78	681600	146600	27840	82	478	5.8
99IPE8-N6-3	3	53	7.56	696300	167100	35770	101	519	5.1
99IPE8-N2-1	3	56	8.00	671100	142100	26850	83	484	5.8
99IPE8-N5-1	3	52	7.42	675600	158800	35390	101	499	4.9
99IPE8-N5-2	3	52	7.42	665000	158200	36080	105	505	4.8
99IPE8-N5-3	3	51	7.29	689000	172600	40160	110	522	4.7
99IPE8-N5-4	3	55	7.80	695400	163500	29540	86	524	6.1
BV-170296-N4-1	4	76	10.97	842800	142700	14970	51	531	10.5
BV-170296-N4-3	4	82	11.94	851300	116200	9863	36	466	13.0
BV-170296-N4-4	4	83	12.07	938800	152600	11860	40	561	14.2
BV-170296-N4-5	4	82	11.84	930200	157600	12000	40	574	14.5
BV-170296-N4-6	4	76	10.97	931500	170600	14570	45	574	12.9
98IPE26-N4-1	4	83	12.10	830700	108000	8918	34	450	13.3
98IPE26-N4-2	4	85	12.30	885400	135100	11520	42	537	12.9

Appendix 9 continued

Sample	Type	An, mol. %	Ca, wt.%	^{44}Ca, c/sec	^{88}Sr, c/sec	^{138}Ba, c/sec	Ba, ppm	Sr, ppm	Sr/Ba
98IPE26-N4-3	4	85	12.30	944300	163300	13560	46	608	13.3
98IPE26-N3-5	4	75	10.88	810000	135700	14130	49	521	10.6
98IPE26-N3-6	4	76	11.00	864800	156600	15520	51	570	11.1
98IPE25-N1-1	4	79	11.50	750300	107400	9801	39	471	12.1
98IPE25-N1-2	4	83	12.00	819400	139000	10970	42	582	14.0
98IPE25-N1-12	4	81	11.70	745500	107500	10560	43	482	11.2
98IPE25-N2-3	4	77	11.10	802100	140400	15710	56	556	9.8
98IPE25-N3-3	4	77	11.10	724700	103200	15620	62	452	7.3
98IPE25-N4-3	4	82	11.85	782100	123900	10050	40	537	13.6
98IPE25-N4-5	4	82	11.85	738400	106200	9887	41	487	11.8
99IPE8-N6-4	4	86	12.58	797400	126900	11370	47	572	12.3
99IPE8-N6-5	4	83	12.10	747300	95520	8859	37	442	11.9
99IPE8-N2-2	4	75	10.91	721900	110000	13020	51	475	9.3
99IPE8-N5-5	4	83	12.01	744000	121400	11280	47	560	11.9
99IPE8-N5-6	4	79	11.41	744100	129100	12200	49	566	11.7
BV-170296-N1-2	5	64	9.25	859500	174900	22240	62	538	8.7
BV-170296-N1-3	5	70	10.03	852600	134600	13300	41	453	11.1
98IPE26-N3-7	5	66	9.54	885700	191200	20600	58	589	10.2
98IPE26-N3-3	6	52	7.41	775500	180700	41400	103	494	4.8
98IPE26-N3-4	6	54	7.66	817200	195100	43470	106	523	4.9
98IPE25-N1-13	6	55	7.91	729100	151900	30400	86	471	5.5
98IPE25-N3-1	6	53	7.60	669100	114900	31790	94	373	4.0
98IPE25-N4-4	6	53	7.50	696800	148800	30820	86	458	5.3
99IPE8-N2-3	6	55	7.86	700400	150800	28160	82	484	5.9
99IPE8-N2-4	6	59	8.46	722900	162200	27660	84	543	6.5

Appendix 10: Electron microprobe analyses of residual melt in experimental runs

All samples were polished and carbon-coated to a thickness of ca. 250 Å. Matrix glasses in experimental runs were analyzed for major elements at the University of Alaska Fairbanks using a Cameca SX-50 electron microprobe, which is equipped with four wavelength-dispersive and one energy-dispersive spectrometers. A 15 keV, 10 nA, 10-μm-diameter beam was used for all analyses. In order to minimize Na migration during analysis, the count rate of Na was scanned through time and corrected using an automated procedure following Devine et al. (1995). Major oxides are in wt.%, with all Fe reported as FeO. Details about counting times, standards, and analytical errors are summarized below.

Element	Counting Time		Standard	Typical Analytical Error (wt.%, 1 sigma)*
	Peak (sec.)	Background (sec.)		
Na	10	5	Tiburon albite	0.078
Mg	10	5	Basaltic Glass (USNM 113498/1)	0.012
Al	10	5	Orthoclase (CM Taylor)	0.115
Si	30	15	Wollastonite (CM Taylor)	0.173
Cl	10	5	Scapolite (USNM R6600-1)	0.012
K	10	5	Orthoclase (CM Taylor)	0.108
Ca	10	5	Wollastonite (CM Taylor)	0.041
Ti	15	7.5	Basaltic Glass (USNM 113498/1)	0.031
Fe	15	7.5	Basaltic Glass (USNM 113498/1)	0.058

* Typical analytical errors for a representative sample calculated after Scott et al. (1995).

Appendix 10 continued

Na_2O	MgO	Al_2O_3	SiO_2	Cl	K_2O	CaO	TiO_2	FeO*	Total
Experimental run PI-1									
4.09	0.28	12.71	72.19	0.01	3.03	1.39	0.17	1.61	95.66
4.02	0.25	12.39	71.61	0.07	3.17	1.27	0.41	1.80	95.19
4.17	0.26	12.53	72.58	0.05	3.26	1.35	0.25	1.49	96.11
4.39	0.24	12.83	72.22	0.03	3.12	1.42	0.15	1.60	96.18
4.30	0.28	12.89	72.05	0.02	3.10	1.35	0.18	1.51	95.84
4.82	0.24	12.64	71.77	0.01	3.17	1.29	0.21	1.69	96.03
4.61	0.26	12.43	71.86	0.03	2.98	1.35	0.25	1.53	95.47
4.08	0.23	12.57	72.64	0.01	3.19	1.38	0.22	1.66	96.15
4.22	0.24	13.10	72.61	0.03	2.95	1.31	0.22	1.63	96.50
4.30	0.33	12.62	72.36	0.03	3.13	1.27	0.27	1.46	95.94
Experimental run PI-2									
3.89	0.40	12.86	71.38	0.09	2.92	1.82	0.45	2.02	96.05
3.84	0.34	12.66	71.75	0.10	2.78	1.61	0.39	2.00	95.69
4.03	0.39	13.13	70.96	0.09	3.09	1.84	0.21	1.85	95.79
4.14	0.31	12.81	71.91	0.09	2.88	1.58	0.21	1.92	96.07
4.45	0.34	13.11	71.19	0.13	2.78	1.73	0.22	1.92	96.08
Experimental run PI-3									
4.06	0.32	12.81	72.49	0.10	3.18	1.56	0.19	1.84	96.75
4.23	0.30	12.42	72.97	0.06	2.88	1.61	0.32	1.71	96.69
4.25	0.49	12.65	72.35	0.11	3.08	1.78	0.20	1.83	96.93
4.12	0.31	12.59	72.50	0.09	3.15	1.53	0.29	1.66	96.42
4.54	0.30	12.88	72.10	0.09	3.07	1.49	0.35	1.63	96.64
4.14	0.27	12.76	72.83	0.04	3.01	1.53	0.25	1.63	96.65
3.94	0.36	12.91	71.90	0.07	2.91	1.56	0.23	1.86	95.95
4.13	0.34	13.37	72.21	0.12	2.98	1.70	0.36	1.80	97.20
4.08	0.30	12.89	72.58	0.10	3.18	1.49	0.15	1.72	96.69
4.23	0.26	13.13	72.53	0.08	3.13	1.45	0.26	1.73	96.98

Appendix 10 continued

Na_2O	MgO	Al_2O_3	SiO_2	Cl	K_2O	CaO	TiO_2	FeO*	Total
4.52	0.33	12.82	72.36	0.04	2.77	1.49	0.20	1.67	96.39
4.56	0.29	12.72	72.30	0.04	3.01	1.50	0.17	1.57	96.34
4.45	0.32	12.63	71.42	0.11	2.85	1.57	0.24	1.78	95.56
4.18	0.34	12.72	72.82	0.08	2.89	1.69	0.17	1.76	96.84
4.31	0.32	12.84	72.56	0.05	3.13	1.50	0.25	1.77	96.92
Experimental run PI-4									
4.34	0.29	12.82	72.57	0.13	2.89	1.71	0.19	1.89	97.03
3.46	0.26	12.84	73.41	0.17	2.82	1.63	0.18	1.89	96.87
4.40	0.39	13.08	71.90	0.13	2.96	1.77	0.28	2.04	97.18
4.13	0.31	12.74	72.68	0.14	2.99	1.57	0.30	2.10	97.20
4.40	0.33	12.64	72.59	0.15	3.07	1.60	0.30	2.11	97.43
4.00	0.32	12.71	71.67	0.17	3.00	1.64	0.31	1.83	95.86
4.01	0.35	12.62	72.67	0.18	2.90	1.63	0.34	2.07	97.00
4.18	0.38	12.86	72.52	0.14	2.85	1.74	0.25	2.14	97.29
4.66	0.40	12.64	71.95	0.12	2.95	1.73	0.38	1.97	97.02
4.60	0.39	12.86	71.87	0.17	2.88	1.95	0.26	1.93	97.12
3.79	0.39	12.99	71.85	0.16	2.97	1.99	0.35	1.92	96.62
4.19	0.36	12.90	72.23	0.18	2.80	1.71	0.13	2.05	96.78
4.60	0.38	13.17	72.33	0.12	2.98	1.69	0.24	1.76	97.46
4.31	0.36	12.65	72.11	0.14	2.85	1.68	0.21	1.92	96.44
4.22	0.33	12.60	71.42	0.17	2.89	1.74	0.20	1.91	95.70
Experimental run PI-5									
4.25	0.16	12.04	74.97	0.08	3.33	1.08	0.32	1.60	98.02
3.84	0.16	11.69	75.32	0.11	3.30	0.96	0.19	1.72	97.50
4.50	0.17	13.39	74.02	0.07	3.18	1.71	0.16	1.58	98.95
4.00	0.17	11.77	75.99	0.07	3.56	0.99	0.04	1.54	98.29
3.88	0.24	11.94	75.15	0.07	3.30	0.95	0.33	1.68	97.73
4.57	0.18	13.21	73.98	0.06	2.98	1.56	0.20	1.81	98.76

Appendix 10 continued

Na_2O	MgO	Al_2O_3	SiO_2	Cl	K_2O	CaO	TiO_2	FeO*	Total
4.68	0.15	12.11	75.04	0.09	3.35	0.96	0.08	1.64	98.29
4.36	0.18	12.07	73.91	0.07	3.27	1.00	0.73	2.29	98.12
4.53	0.17	11.98	75.43	0.07	3.62	0.96	0.19	1.57	98.70
4.63	0.17	13.38	73.88	0.06	3.16	1.46	0.24	1.44	98.57
4.00	0.18	11.81	75.55	0.03	3.31	1.05	0.32	1.59	98.02
3.71	0.19	12.04	75.97	0.10	3.46	0.93	0.17	1.87	98.66
4.09	0.19	12.29	75.08	0.04	3.46	1.00	0.23	1.74	98.31
4.35	0.17	13.10	73.78	0.10	2.95	1.79	0.10	1.47	97.98
4.28	0.24	11.90	74.75	0.08	3.14	1.11	0.10	1.65	97.46
Experimental run PI-6									
4.36	0.31	12.53	74.16	0.17	3.15	1.29	0.22	1.95	98.36
4.02	0.28	12.68	74.08	0.18	3.07	1.17	0.21	1.77	97.66
4.21	0.27	12.78	74.02	0.12	3.19	1.19	0.44	2.02	98.47
4.14	0.24	12.37	74.50	0.18	3.07	1.02	0.28	1.99	98.01
3.97	0.71	12.36	73.06	0.12	3.07	1.73	0.43	2.46	98.17
4.19	0.48	12.61	73.58	0.15	3.00	1.55	0.14	1.92	97.83
4.69	0.33	12.77	74.55	0.15	3.18	1.72	0.08	1.88	99.55
4.51	0.34	11.96	75.62	0.17	3.24	1.07	0.28	1.89	99.28
4.14	0.24	11.98	75.57	0.13	3.16	1.16	0.22	1.92	98.73
3.75	0.41	12.01	74.99	0.10	3.06	1.34	0.27	1.90	98.04
4.38	0.23	13.52	73.32	0.14	2.79	1.93	0.36	1.74	98.61
4.17	0.27	12.06	75.46	0.14	3.20	1.30	0.15	1.64	98.56
4.19	0.22	12.31	74.50	0.16	3.10	1.31	0.16	1.89	98.05
4.05	0.34	12.27	73.89	0.16	3.10	1.41	0.31	1.78	97.52
4.38	0.20	12.68	74.38	0.18	3.00	1.45	0.26	1.73	98.44
4.25	0.28	13.15	73.91	0.13	3.34	1.42	0.26	1.83	98.78

Appendix 10 continued

Na_2O	MgO	Al_2O_3	SiO_2	Cl	K_2O	CaO	TiO_2	FeO*	Total
Experimental run PI-7									
4.09	0.45	12.63	71.66	0.14	2.70	1.89	0.22	2.12	96.14
3.91	0.41	12.98	71.80	0.14	2.82	1.80	0.32	2.02	96.42
4.43	0.42	12.89	71.15	0.12	2.89	1.76	0.10	1.79	95.77
3.60	0.34	12.84	72.07	0.13	2.76	1.76	0.25	1.89	95.86
4.37	0.36	12.58	71.52	0.08	2.75	1.78	0.32	1.94	95.92
4.33	0.42	12.75	72.08	0.12	2.86	1.60	0.15	1.86	96.38
4.19	0.39	12.48	70.93	0.14	2.55	1.78	0.32	1.96	94.98
4.23	0.43	12.77	71.40	0.13	2.78	1.79	0.18	1.81	95.70
4.13	0.47	13.10	71.66	0.08	2.80	1.77	0.31	1.83	96.35
4.17	0.38	12.73	71.23	0.10	2.85	1.69	0.21	2.15	95.75
4.28	0.38	13.26	71.09	0.12	2.81	1.80	0.26	1.92	96.15
4.27	0.47	13.03	70.89	0.10	3.03	1.66	0.37	1.78	95.80
4.43	0.39	12.89	70.04	0.12	2.81	1.86	0.12	1.94	94.80
Experimental run PI-8									
4.04	0.29	13.12	71.78	0.05	2.87	1.84	0.25	1.59	96.02
3.96	0.32	13.02	71.49	0.09	3.01	1.75	0.24	1.96	96.06
4.20	0.35	12.78	71.94	0.07	3.11	1.88	0.31	1.74	96.57
3.95	0.41	13.37	71.60	0.07	2.74	1.85	0.15	1.74	96.09
4.36	0.37	13.54	71.68	0.04	2.98	1.97	0.20	1.77	97.10
4.42	0.35	12.92	72.19	0.03	2.85	1.64	0.35	1.86	96.80
3.72	0.37	12.83	72.29	0.04	2.83	1.69	0.16	1.86	96.01
4.42	0.41	12.68	72.31	0.04	2.93	1.40	0.28	1.68	96.34
4.39	0.38	12.77	72.78	0.07	2.88	1.52	0.18	1.74	96.88
4.28	0.34	12.59	72.19	0.02	3.04	1.59	0.19	1.80	96.25
4.16	0.32	12.77	72.20	0.06	2.85	1.82	0.15	1.62	96.14
3.91	0.33	13.02	71.98	0.05	2.99	1.81	0.28	1.78	96.36

Appendix 10 continued

Na_2O	MgO	Al_2O_3	SiO_2	Cl	K_2O	CaO	TiO_2	FeO*	Total
Experimental run PI-10									
3.90	0.28	12.92	72.42	0.04	3.24	1.45	0.20	1.77	96.42
4.20	0.30	12.84	72.58	0.11	3.03	1.31	0.38	1.57	96.50
4.16	0.27	12.73	72.44	0.04	3.15	1.43	0.26	1.63	96.30
4.01	0.30	12.58	72.43	0.07	3.27	1.39	0.24	1.54	96.00
4.11	0.26	12.77	71.95	0.07	3.10	1.41	0.36	1.76	95.99
4.21	0.25	13.00	72.56	0.05	3.20	1.43	0.20	1.86	96.98
4.00	0.21	12.79	72.31	0.05	3.07	1.39	0.38	1.81	96.20
4.15	0.21	12.84	72.37	0.06	3.00	1.42	0.38	1.60	96.20
4.10	0.31	12.77	72.36	0.04	3.20	1.37	0.16	1.70	96.21
4.26	0.29	12.78	72.22	0.09	3.23	1.36	0.50	1.69	96.61
3.99	0.24	12.54	72.62	0.04	3.31	1.37	0.28	1.39	95.94
4.05	0.25	12.90	72.62	0.06	3.16	1.42	0.60	1.43	96.65
4.78	0.31	13.00	72.94	0.06	3.30	1.40	0.18	1.55	97.69
4.06	0.28	12.83	72.74	0.07	3.20	1.37	0.08	1.30	96.07
4.08	0.21	12.58	72.73	0.07	2.99	1.29	0.00	1.46	95.57
4.18	0.24	12.96	72.48	0.03	3.21	1.32	0.26	1.49	96.33
4.23	0.25	12.73	72.58	0.07	3.20	1.32	0.40	1.69	96.67
4.08	0.25	12.34	71.95	0.05	3.01	1.31	0.46	1.57	95.19
4.01	0.20	12.71	72.41	0.08	3.26	1.40	0.32	1.54	96.10
4.07	0.26	12.90	72.46	0.05	3.26	1.29	0.42	1.23	96.07
3.98	0.24	12.68	72.29	0.03	2.93	1.39	0.22	1.71	95.66
4.02	0.27	12.32	72.42	0.01	2.98	1.44	0.16	1.63	95.44
4.23	0.24	12.78	72.58	0.08	3.09	1.29	0.20	1.81	96.50
4.25	0.26	12.96	72.28	0.07	3.10	1.28	0.18	1.63	96.19
Experimental run PI-11									
4.12	0.27	12.70	71.88	0.16	3.09	1.31	0.34	1.73	95.80
4.28	0.33	12.76	71.93	0.11	2.88	1.51	0.40	1.81	96.21

Appendix 10 continued

Na_2O	MgO	Al_2O_3	SiO_2	Cl	K_2O	CaO	TiO_2	FeO*	Total
4.00	0.31	12.51	71.89	0.16	2.98	1.57	0.04	1.82	95.48
4.07	0.25	12.67	72.26	0.07	2.90	1.60	0.32	1.78	96.11
4.03	0.24	12.66	72.49	0.12	2.82	1.57	0.22	1.99	96.35
4.45	0.29	12.87	72.60	0.12	2.90	1.65	0.32	2.14	97.58
3.92	0.25	12.90	71.64	0.08	2.87	1.43	0.40	2.12	95.85
4.08	0.26	12.68	71.55	0.10	2.78	1.53	0.46	2.05	95.71
4.01	0.29	12.96	72.22	0.16	3.14	1.59	0.44	1.88	96.90
3.97	0.30	12.85	71.43	0.12	3.13	1.40	0.36	1.81	95.56
4.38	0.22	12.61	71.40	0.17	2.87	1.53	0.42	1.76	95.55
3.84	0.31	12.76	72.06	0.13	3.03	1.55	0.50	1.85	96.23
4.41	0.32	12.65	72.28	0.13	2.91	1.54	0.14	1.90	96.49
Experimental run PI-12									
3.56	0.25	12.48	70.84	0.13	3.10	1.21	0.30	1.50	93.53
3.93	0.27	12.19	71.15	0.15	2.99	1.25	0.48	1.59	94.15
4.09	0.21	12.27	71.55	0.12	2.88	1.45	0.32	1.71	94.79
4.21	0.22	12.34	71.20	0.17	3.12	1.24	0.20	1.45	94.32
4.12	0.22	12.31	70.93	0.13	3.00	1.29	0.54	1.67	94.38
3.94	0.24	12.33	70.51	0.14	2.91	1.30	1.08	2.07	94.75
4.06	0.26	12.29	70.99	0.16	2.98	1.32	0.42	1.52	94.18
3.81	0.19	12.31	71.01	0.17	3.11	1.30	0.20	1.50	93.77
4.15	0.19	12.45	71.46	0.15	3.03	1.33	0.70	1.57	95.22
3.87	0.20	12.48	70.89	0.13	2.95	1.35	0.36	1.51	93.91
4.01	0.26	12.32	70.80	0.15	3.09	1.31	0.60	1.49	94.19
4.10	0.54	12.31	69.74	0.13	2.89	1.75	0.38	1.92	93.97
3.76	0.26	12.12	70.74	0.13	3.12	1.32	0.22	1.37	93.19
3.84	0.26	12.58	70.73	0.15	2.99	1.17	0.30	1.68	93.89
3.52	0.23	12.43	70.81	0.14	3.05	1.28	0.34	1.45	93.40
3.78	0.22	12.23	71.34	0.17	3.06	1.24	0.10	1.42	93.71

Appendix 10 continued

Na_2O	MgO	Al_2O_3	SiO_2	Cl	K_2O	CaO	TiO_2	FeO*	Total
4.35	0.57	12.02	70.81	0.16	3.05	1.73	0.42	1.94	95.27
3.99	0.25	12.37	71.53	0.13	3.13	1.20	0.16	1.67	94.61
4.08	0.23	12.22	70.95	0.14	3.08	1.41	0.32	1.54	94.14
3.81	0.26	12.38	71.07	0.14	2.88	1.35	0.40	1.49	93.95
Experimental run PI-13									
3.58	0.27	12.19	69.83	0.14	2.76	1.50	0.46	1.71	92.62
3.63	0.20	12.20	69.80	0.14	2.83	1.40	0.30	1.39	92.05
4.13	0.22	12.55	70.20	0.11	2.85	1.53	0.10	1.59	93.46
3.61	0.25	12.39	69.90	0.11	2.94	1.62	0.18	1.34	92.48
3.91	0.27	12.38	69.80	0.11	2.78	1.56	0.18	1.39	92.53
4.14	0.25	12.74	69.97	0.13	2.91	1.53	0.40	1.34	93.56
3.75	0.26	12.00	69.93	0.14	2.60	1.60	0.44	1.55	92.44
3.69	0.22	12.64	70.03	0.14	2.91	1.56	0.10	1.50	92.97
3.67	0.29	12.40	68.80	0.11	2.82	1.60	0.10	1.30	91.23
3.62	0.28	13.02	68.78	0.09	2.88	1.72	0.20	1.68	92.46
3.84	0.36	12.92	69.19	0.09	2.77	1.67	0.36	1.57	92.95
4.08	0.31	13.20	68.27	0.14	2.91	1.85	0.28	1.61	92.81
3.66	0.28	12.46	68.98	0.14	2.87	1.59	0.08	1.35	91.56
3.71	0.22	12.70	69.14	0.13	2.87	1.59	0.16	1.49	92.17
3.87	0.24	12.72	69.37	0.15	3.00	1.57	0.30	1.43	92.81
3.89	0.22	12.72	69.24	0.11	2.78	1.65	0.44	1.53	92.75
3.74	0.31	12.80	69.34	0.10	2.84	1.63	0.26	1.33	92.49
4.09	0.33	13.25	67.63	0.14	2.83	1.84	0.10	1.59	91.97
3.81	0.27	12.59	69.99	0.13	2.71	1.58	0.18	1.64	93.07
Experimental run PI-14									
3.95	0.22	12.81	74.42	0.14	3.17	1.36	0.22	1.96	98.46
4.17	0.23	12.03	74.52	0.10	3.26	1.27	0.22	2.09	98.15
4.29	0.25	12.20	74.68	0.15	3.03	1.22	0.36	1.99	98.40

Appendix 10 continued

Na_2O	MgO	Al_2O_3	SiO_2	Cl	K_2O	CaO	TiO_2	FeO*	Total
4.07	0.26	11.72	74.03	0.16	3.16	1.17	0.18	1.77	96.70
4.48	0.17	11.88	74.73	0.14	3.27	1.16	0.21	2.07	98.34
4.18	0.21	12.08	73.89	0.14	3.39	1.36	0.21	1.84	97.49
4.39	0.26	12.01	74.41	0.19	3.12	1.29	0.22	1.70	97.78
4.10	0.26	12.00	74.26	0.11	3.15	1.16	0.18	1.82	97.25
4.05	0.21	11.90	74.12	0.17	3.34	1.22	0.23	1.99	97.47
4.57	0.21	11.61	74.13	0.16	3.26	1.23	0.19	1.89	97.47
4.04	0.26	11.48	74.51	0.10	3.17	1.30	0.27	1.83	97.17
Experimental run PI-15									
4.13	0.25	12.85	73.20	0.11	3.41	1.32	0.62	1.83	97.92
4.79	0.18	12.96	73.48	0.09	3.11	1.39	0.63	2.00	98.84
4.10	0.21	12.58	73.86	0.09	3.37	1.48	0.73	1.76	98.37
4.21	0.21	12.81	73.40	0.07	3.39	1.33	0.45	1.69	97.74
4.48	0.22	12.26	74.63	0.05	3.52	1.28	0.60	1.79	99.03
3.99	0.24	12.30	73.82	0.02	3.31	1.34	0.58	1.77	97.55
4.06	0.20	13.14	73.62	0.04	3.33	1.24	0.52	1.70	98.05
4.13	0.17	12.62	73.48	0.04	3.39	1.22	0.39	1.70	97.34
Experimental run PI-16									
3.92	0.09	11.94	72.03	0.12	3.38	0.99	0.97	1.31	94.90
3.70	0.11	11.67	72.76	0.12	3.42	1.06	0.24	1.15	94.35
3.53	0.08	11.51	72.10	0.14	3.43	1.09	0.37	1.15	93.54
3.79	0.07	12.06	73.32	0.15	3.45	0.96	0.19	1.00	95.09
4.44	0.08	11.93	74.18	0.08	3.19	1.08	0.39	1.04	96.54
3.86	0.07	11.25	74.21	0.11	3.35	0.82	0.02	0.91	94.70
3.87	0.14	11.93	72.88	0.11	3.47	1.06	0.19	1.03	94.79
3.75	0.10	11.59	73.12	0.16	3.26	0.89	0.36	1.20	94.56

Appendix 10 continued

Na_2O	MgO	Al_2O_3	SiO_2	Cl	K_2O	CaO	TiO_2	FeO*	Total
Experimental run PI-17									
4.10	0.14	11.95	69.65	0.08	2.77	1.40	0.36	1.27	91.86
3.18	0.16	11.83	69.63	0.08	2.82	1.34	0.13	1.48	90.80
3.48	0.12	11.97	70.18	0.07	2.75	1.40	0.34	1.44	91.91
3.65	0.14	12.72	70.00	0.07	2.85	1.57	0.22	1.31	92.68
3.84	0.13	12.18	69.11	0.13	2.75	1.53	0.34	1.34	91.49
4.15	0.18	12.54	69.58	0.11	2.95	1.53	0.19	1.41	92.78
3.78	0.15	12.17	70.06	0.07	3.01	1.44	0.24	1.18	92.24
4.00	0.15	12.34	69.48	0.08	2.68	1.52	0.41	1.40	92.21
Experimental run PI-20									
4.41	0.10	12.29	69.61	0.02	2.93	1.44	0.05	1.06	92.03
4.27	0.16	12.44	68.69	0.06	2.83	1.49	0.09	1.37	91.56
4.12	0.10	12.41	69.09	0.04	3.14	1.55	0.16	1.08	91.81
4.61	0.11	12.49	69.27	0.07	3.10	1.50	0.03	0.95	92.23
4.22	0.11	11.91	69.52	0.03	2.87	1.41	0.01	1.10	91.29
3.75	0.10	12.06	69.13	0.02	2.71	1.55	0.00	1.19	90.64
3.92	0.08	12.53	70.11	0.02	3.02	1.55	0.15	1.11	92.62
Experimental run PI-21									
3.98	0.08	12.04	70.02	0.09	2.68	1.44	0.07	0.92	91.43
4.40	0.09	11.92	70.15	0.01	2.77	1.42	0.19	1.08	92.16
3.88	0.08	11.69	70.75	0.07	2.80	1.33	0.09	0.86	91.65
4.36	0.07	11.51	70.31	0.10	2.95	1.36	0.02	1.01	91.81
3.55	0.07	11.67	70.82	0.05	2.87	1.35	0.08	0.82	91.36
Experimental run PI-22									
4.45	0.09	10.77	75.04	0.05	3.67	0.82	0.13	0.92	96.06
3.81	0.07	10.96	75.02	0.08	3.63	0.57	0.04	1.07	95.37
3.73	0.07	10.79	75.56	0.03	3.72	0.68	0.20	0.88	95.76
3.74	0.09	10.49	75.40	0.04	3.64	0.65	0.26	0.86	95.25

Appendix 10 continued

Na_2O	MgO	Al_2O_3	SiO_2	Cl	K_2O	CaO	TiO_2	FeO*	Total
3.83	0.10	10.63	74.78	0.04	3.49	0.76	0.01	0.80	94.53
3.94	0.09	10.91	75.66	0.08	3.65	0.68	0.10	0.82	96.00
3.70	0.07	10.83	75.51	0.07	3.68	0.69	0.10	0.91	95.66
Experimental run PI-23									
3.89	0.03	11.79	75.73	0.02	4.42	0.42	0.11	0.93	97.43
3.50	0.08	11.33	76.18	0.07	4.49	0.37	0.10	0.60	96.77
3.69	0.04	10.83	74.73	0.10	4.58	0.47	0.13	0.71	95.37
3.61	0.04	10.96	74.54	0.07	4.59	0.47	0.00	0.82	95.20
4.37	0.05	11.13	75.53	0.05	4.72	0.46	0.03	0.73	97.16
4.03	0.04	10.69	74.37	0.03	4.23	0.54	0.19	0.73	94.93
3.84	0.04	10.85	75.44	0.09	4.55	0.42	0.18	0.80	96.30
Experimental run PI-24									
3.69	0.07	11.38	72.59	0.07	3.31	0.89	0.01	0.84	92.94
4.30	0.06	11.24	71.84	0.09	3.12	0.87	0.12	0.84	92.57
4.06	0.05	11.71	73.10	0.09	3.48	0.91	0.00	0.72	94.19
3.92	0.05	12.43	72.64	0.04	3.51	0.98	0.05	0.78	94.49
4.16	0.06	12.55	71.97	0.11	3.51	0.96	0.15	0.71	94.24
4.21	0.06	11.96	72.92	0.02	3.41	0.84	0.09	0.72	94.31
3.38	0.07	12.03	72.38	0.06	3.36	0.93	0.00	0.61	92.90
Experimental run PI-26									
4.02	0.05	12.51	73.77	0.05	3.62	0.79	0.07	0.81	95.78
4.07	0.05	12.03	72.39	0.02	3.45	1.07	0.17	0.87	94.21
4.50	0.04	12.82	72.77	0.00	3.38	1.02	0.03	0.59	95.22
4.06	0.03	11.84	73.34	0.07	3.86	0.78	0.11	0.69	94.86
3.67	0.04	11.47	74.02	0.03	3.81	0.68	0.09	0.72	94.61
Experimental run PI-27									
3.84	0.06	12.82	72.69	0.00	3.29	0.80	0.07	0.94	94.62
3.79	0.05	12.04	72.31	0.04	3.12	0.81	0.14	0.79	93.18

Appendix 10 continued

Na_2O	MgO	Al_2O_3	SiO_2	Cl	K_2O	CaO	TiO_2	FeO*	Total
3.40	0.05	13.00	72.75	0.05	3.32	0.93	0.07	0.86	94.53
3.83	0.06	12.35	72.63	0.07	3.25	1.03	0.06	0.89	94.29
3.64	0.08	12.91	73.21	0.08	3.32	0.93	0.04	0.94	95.25
4.04	0.04	12.66	73.47	0.01	3.40	0.89	0.00	0.86	95.46
3.52	0.08	12.02	72.65	0.07	3.29	0.93	0.12	1.07	93.87
Experimental run PI-28									
3.23	0.05	11.30	75.60	0.15	4.02	0.49	0.06	0.73	95.72
3.18	0.19	10.98	74.52	0.08	4.04	0.63	0.12	1.49	95.39
3.48	0.03	11.12	75.78	0.10	3.84	0.44	0.12	0.82	95.84
2.99	0.06	11.19	74.65	0.09	4.14	0.44	0.18	0.79	94.62
3.57	0.05	11.22	75.24	0.12	4.12	0.46	0.05	0.93	95.87
3.32	0.03	10.56	75.02	0.15	4.24	0.46	0.01	0.59	94.46
3.35	0.06	9.99	75.19	0.10	4.17	0.44	0.13	0.85	94.37
3.51	0.03	10.59	75.76	0.09	4.19	0.55	0.05	0.82	95.67
Experimental run PI-29									
3.49	0.17	11.13	70.21	0.02	3.06	1.23	0.01	0.97	90.40
3.84	0.06	11.72	70.80	0.05	3.00	0.99	0.19	0.69	91.42
3.48	0.07	12.40	70.03	0.10	2.83	1.18	0.02	0.60	90.77
3.59	0.05	11.41	71.07	0.09	2.99	0.93	0.00	0.60	90.80
3.78	0.05	11.97	71.06	0.02	2.92	0.95	0.00	0.57	91.38
3.69	0.06	12.14	70.74	0.02	3.10	0.95	0.03	0.57	91.38
Experimental run PI-30									
3.49	0.07	11.01	70.49	0.03	4.37	0.78	0.00	0.49	90.79
4.19	0.18	12.05	70.90	0.05	3.41	1.35	0.06	1.31	93.65
3.72	0.11	10.96	69.99	0.03	4.35	0.88	0.13	0.94	91.22
3.06	0.07	10.82	71.41	0.05	4.19	0.78	0.10	0.58	91.12
3.41	0.08	11.69	70.36	0.02	3.58	1.45	0.02	1.02	91.74
3.75	0.07	11.08	70.30	0.06	3.95	0.80	0.00	0.61	90.66

Appendix 10 continued

Na_2O	MgO	Al_2O_3	SiO_2	Cl	K_2O	CaO	TiO_2	FeO*	Total
3.44	0.03	11.52	70.11	0.00	4.03	0.76	0.08	0.56	90.59
3.39	0.03	12.72	70.72	0.02	3.94	0.88	0.01	1.07	92.91
Experimental run PI-31									
4.64	0.17	12.97	72.38	0.10	2.71	1.65	0.18	2.32	97.37
3.55	0.24	13.21	72.38	0.12	3.07	1.71	0.33	2.40	97.26
3.85	0.20	13.25	72.52	0.05	2.80	1.60	0.30	2.04	96.83
4.21	0.18	13.06	72.79	0.10	2.95	1.58	0.18	2.13	97.42
3.95	0.19	13.26	72.40	0.08	3.02	1.58	0.24	1.96	96.90
4.46	0.21	13.18	72.60	0.07	2.98	1.61	0.18	2.07	97.59
3.92	0.22	12.77	72.63	0.10	2.95	1.85	0.18	2.12	96.97
Experimental run PI-32									
3.63	0.23	12.06	71.39	0.13	3.19	1.78	0.26	2.12	95.02
4.40	0.27	12.06	71.79	0.14	3.12	1.68	0.16	2.22	96.08
3.72	0.22	12.39	71.83	0.12	3.21	1.81	0.27	1.97	95.76
4.63	0.24	12.60	71.66	0.12	3.18	1.75	0.17	2.08	96.67
4.39	0.25	12.68	72.25	0.07	3.11	1.76	0.23	1.87	96.82
4.41	0.21	12.66	71.87	0.12	3.05	1.81	0.19	2.22	96.78
3.80	0.21	12.83	71.95	0.09	3.16	1.80	0.11	2.05	96.23
Experimental run PI-33									
4.54	0.13	12.36	73.62	0.15	3.38	1.26	0.19	1.92	97.76
3.84	0.14	12.18	73.61	0.18	3.27	1.12	0.12	1.71	96.36
4.23	0.14	11.97	74.27	0.15	3.29	1.28	0.17	1.61	97.28
4.64	0.14	12.25	73.65	0.19	3.08	1.26	0.25	1.73	97.38
3.87	0.17	12.11	73.25	0.10	3.42	1.29	0.18	1.62	96.19
4.54	0.13	12.33	73.70	0.15	3.35	1.23	0.23	1.53	97.37
Experimental run PI-34									
4.32	0.09	11.98	75.10	0.15	3.00	1.03	0.22	1.49	97.57
4.12	0.15	12.48	74.85	0.15	3.34	1.28	0.18	1.85	98.59

Appendix 10 continued

Na_2O	MgO	Al_2O_3	SiO_2	Cl	K_2O	CaO	TiO_2	FeO*	Total
4.17	0.15	12.04	74.09	0.15	3.32	1.20	0.11	1.62	97.03
4.26	0.14	13.04	74.13	0.11	3.38	1.32	0.15	1.66	98.37
3.75	0.13	13.04	74.07	0.15	3.06	1.36	0.20	1.59	97.52
Experimental run PI-35									
3.47	0.17	12.19	72.08	0.13	3.90	0.82	0.19	0.84	93.87
3.75	0.10	12.20	71.80	0.08	3.85	0.88	0.07	0.73	93.54
3.51	0.08	12.33	72.79	0.14	4.06	0.77	0.09	0.72	94.57
3.45	0.03	11.88	72.17	0.09	4.07	0.74	0.20	0.77	93.49
3.45	0.04	12.64	71.89	0.14	3.66	0.98	0.20	1.03	94.16
3.47	0.08	11.63	72.36	0.11	3.75	0.68	0.57	1.16	93.95
Experimental run PI-36									
4.02	0.02	11.63	73.92	0.00	3.43	0.67	0.04	0.77	94.57
3.48	0.03	11.37	73.22	0.02	3.68	0.65	0.04	0.66	93.21
3.68	0.10	11.38	73.00	0.03	3.39	0.78	0.54	1.10	94.12
3.18	0.05	10.97	73.56	0.00	3.55	0.63	0.10	0.51	92.61
3.43	0.10	11.34	73.52	0.00	3.66	0.62	0.15	0.56	93.45
3.56	0.04	11.31	73.52	0.00	3.51	0.75	0.17	0.63	93.57
3.60	0.08	11.23	73.49	0.00	3.60	0.70	0.16	0.53	93.45
3.92	0.06	11.16	73.50	0.01	3.34	0.76	0.14	0.82	93.80
3.66	0.05	11.36	73.75	0.01	3.68	0.73	0.14	0.64	94.09

Appendix 11: Electron microprobe analyses of plagioclase microlites in experimental runs

All samples were polished and carbon-coated to a thickness of ca. 250 Å. Plagioclase microlites were analyzed for major elements at the University of Alaska Fairbanks using a Cameca SX-50 electron microprobe, which is equipped with four wavelength-dispersive and one energy-dispersive spectrometers. A 15 keV, 10 nA, 1-3-μm-diameter beam was used for all analyses. Major oxides are in wt.%, with all Fe reported as FeO. Anorthite content is reported in molar %. Details about counting times, standards, and analytical errors are summarized below.

Element	Counting Time		Standard	Typical Analytical Error (wt.%, 1 sigma)*
	Peak (sec.)	Background (sec.)		
Na	30	5	Anorthoclase (USNM 133868)	0.129
Al	10	5	Labradorite (USNM 115900)	0.257
Si	10	5	Tiburon albite	0.401
K	10	5	Orthoclase (CM Taylor)	0.022
Ca	10	5	Labradorite (USNM 115900)	0.222
Fe	30	5	Orthoclase (CM Taylor)	0.032

* Typical analytical errors for a representative sample calculated after Scott et al. (1995).

Appendix 11 continued

SiO_2	Al_2O_3	Na_2O	K_2O	CaO	FeO*	Total	An, mol. %
Experimental run PI-1							
57.40	26.80	6.42	0.29	8.64	0.43	99.98	43
58.65	25.99	6.15	0.42	8.30	0.59	100.10	43
56.83	26.87	6.18	0.25	8.97	0.51	99.62	45
57.61	26.92	6.14	0.27	8.95	0.49	100.38	45
Experimental run PI-3							
58.26	25.90	6.25	0.32	8.40	0.57	99.69	43
57.19	26.49	6.27	0.31	8.74	0.58	99.58	44
57.63	26.67	6.28	0.31	8.60	0.42	99.92	43
Experimental run PI-4							
57.52	27.14	6.04	0.29	8.91	0.44	100.35	45
56.09	28.13	5.57	0.25	10.11	0.67	100.83	50
Experimental run PI-5							
59.33	25.36	7.26	0.44	6.72	0.44	99.55	34
60.10	24.66	7.16	0.43	6.77	0.60	99.71	34
Experimental run PI-6							
59.48	25.61	7.07	0.42	6.60	0.42	99.59	34
59.45	24.60	6.81	0.56	6.79	0.61	98.82	36
60.13	25.14	6.86	0.40	7.10	0.34	99.97	36
Experimental run PI-7							
56.75	26.76	6.03	0.27	8.78	0.52	99.11	45
56.16	26.95	6.02	0.24	8.80	0.51	98.68	45
56.68	26.71	6.16	0.31	8.85	0.49	99.19	44
Experimental run PI-10							
58.22	26.08	6.53	0.32	7.94	0.58	99.67	40
57.50	25.98	6.77	0.33	7.95	0.42	98.94	39
56.04	27.22	6.17	0.26	8.86	0.50	99.06	44
56.90	26.18	6.58	0.32	8.18	0.37	98.53	41

Appendix 11 continued

SiO_2	Al_2O_3	Na_2O	K_2O	CaO	FeO*	Total	An. mol. %
57.19	26.24	6.47	0.32	8.46	0.40	99.08	42
57.61	25.99	5.66	0.43	8.91	0.68	99.27	47
57.20	26.75	6.16	0.30	8.88	0.49	99.79	44
Experimental run PI-11							
56.40	26.93	6.11	0.31	8.97	0.44	99.17	45
56.03	27.32	5.82	0.26	9.30	0.56	99.28	47
57.88	26.35	6.20	0.34	8.27	0.44	99.48	42
56.79	27.36	5.91	0.25	9.11	0.47	99.89	46
Experimental run PI-12							
58.20	26.51	6.67	0.32	8.25	0.48	100.42	41
59.00	25.56	6.41	0.48	7.84	0.66	99.94	40
58.23	26.48	6.46	0.30	8.64	0.51	100.62	42
57.98	26.68	6.78	0.28	8.14	0.37	100.23	40
Experimental run PI-14							
57.32	26.80	6.43	0.28	8.54	0.47	99.84	42
57.80	26.26	6.55	0.31	7.98	0.52	99.43	40
57.78	26.61	6.47	0.31	8.29	0.52	99.99	41
58.90	26.60	6.34	0.35	8.37	0.55	101.10	42
58.70	25.76	6.18	0.45	8.18	0.50	99.77	42
Experimental run PI-15							
57.50	26.59	6.21	0.40	8.50	0.54	99.73	43
57.17	26.55	6.34	0.29	8.66	0.42	99.44	43
57.43	26.69	6.36	0.33	8.45	0.59	99.85	42
57.44	25.89	6.31	0.36	8.01	0.61	98.62	41
57.43	26.77	6.32	0.30	8.67	0.45	99.93	43
Experimental run PI-16							
59.19	24.12	7.44	0.43	6.37	0.71	98.25	32
60.03	24.02	7.81	0.45	5.91	0.69	98.91	29

Appendix 11 continued

SiO_2	Al_2O_3	Na_2O	K_2O	CaO	FeO*	Total	An. mol. %
58.20	25.16	7.13	0.34	6.66	0.44	97.94	34
59.30	25.22	7.08	0.34	7.14	0.44	99.53	36
56.90	25.90	6.72	0.27	7.90	0.45	98.15	39
58.12	25.44	6.96	0.30	7.45	0.39	98.67	37
57.76	26.08	6.71	0.28	7.81	0.23	98.88	39
Experimental run PI-17							
56.44	26.61	6.21	0.32	8.74	0.46	98.78	44
56.93	26.67	6.18	0.26	8.80	0.44	99.28	44
55.79	27.13	5.90	0.28	9.62	0.47	99.18	47
56.25	26.70	5.92	0.24	9.37	0.44	98.92	47
Experimental run PI-20							
57.02	26.70	6.48	0.29	8.58	0.44	99.51	42
55.79	26.52	6.06	0.23	8.90	0.53	98.02	45
56.47	26.71	6.15	0.27	8.65	0.57	98.81	44
58.70	25.93	6.11	0.36	8.16	0.48	99.75	42
Experimental run PI-21							
60.05	24.63	7.22	0.42	6.32	0.39	99.03	33
60.59	23.99	7.70	0.42	5.63	0.21	98.54	29
61.02	23.60	7.34	0.51	5.68	0.20	98.34	30
60.56	23.76	7.48	0.52	5.67	0.15	98.14	30
Experimental run PI-22							
60.75	24.46	7.93	0.43	5.82	0.21	99.60	29
57.78	24.87	6.43	0.57	8.06	0.40	98.09	41
57.50	26.35	6.69	0.32	8.37	0.43	99.67	41
58.52	24.77	7.36	0.43	6.93	0.41	98.42	34
61.52	23.75	7.80	0.44	5.69	0.32	99.52	29
59.26	24.87	7.13	0.45	6.83	0.50	99.03	35
59.22	25.27	7.14	0.42	6.96	0.43	99.43	35

Appendix 11 continued

SiO_2	Al_2O_3	Na_2O	K_2O	CaO	FeO*	Total	An, mol. %
Experimental run PI-24							
61.36	23.74	8.08	0.54	5.23	0.20	99.15	26
62.35	22.91	7.26	0.61	5.12	0.26	98.51	28
60.94	23.26	7.90	0.55	5.12	0.43	98.20	26
60.34	24.33	7.93	0.42	5.80	0.25	99.07	29
Experimental run PI-29							
58.83	25.54	6.78	0.36	7.78	0.43	99.72	39
61.89	23.37	7.49	0.47	5.81	0.35	99.39	30
59.64	23.55	7.50	0.48	5.45	0.73	97.35	29
Experimental run PI-30							
58.95	25.97	7.01	0.38	7.73	0.44	100.47	38
Experimental run PI-31							
56.58	27.46	6.12	0.29	9.07	0.43	99.95	45
57.40	26.79	6.09	0.27	9.22	0.49	100.26	46
57.74	26.26	6.69	0.33	8.29	0.54	99.86	41
57.35	26.42	6.47	0.29	8.72	0.51	99.75	43
Experimental run PI-33							
58.81	25.89	7.27	0.39	7.96	0.39	100.71	38
58.74	25.27	7.46	0.34	7.71	0.36	99.88	36
59.61	24.74	7.08	0.52	7.20	0.41	99.56	36
59.21	25.64	7.18	0.41	7.90	0.34	100.67	38
58.84	26.20	7.05	0.37	7.77	0.42	100.64	38
Experimental run PI-34							
57.11	26.89	6.71	0.26	8.80	0.47	100.25	42
57.19	26.56	6.57	0.34	8.94	0.46	100.06	43
57.40	26.28	6.76	0.28	8.62	0.30	99.64	41
56.84	26.73	6.71	0.31	9.23	0.43	100.25	43
57.49	26.67	6.70	0.31	8.52	0.38	100.08	41
57.85	26.55	6.79	0.32	8.55	0.33	100.39	41

References cited

Anders, E., and Grevesse, N., 1989. Abundances of the elements: meteoric and solar. *Geochimica and Cosmochimica Acta*, 53: 197-214.

Andersen, D.J., and Lindsley, D.H., 1988. Internally consistent solution models for Fe-Mg-Mn-Ti oxides: Fe-Ti oxides. *American Mineralogist*, 73(7-8): 714-726.

Ariskin, A.A., 1999. Phase equilibria modeling in igneous petrology: use of COMAGMAT model for simulating fractionation of ferro-basaltic magmas and the genesis of high-alumina basalt. *Journal of Volcanology and Geothermal Research*, 90(1-2): 115-162.

Bacon, C.R., and Hirschmann, M.M., 1988. Mg/Mn partitioning as a test for equilibrium between coexisting Fe-Ti oxides. *American Mineralogist*, 73(1-2): 57-61.

Balesta, S.T., 1991. Earth crust structure and magma chambers of the areas of present Kamchatka volcanism. In: S.A. Fedotov and Y.P. Masurenkov (Editors), *Active volcanoes of Kamchatka*. Nauka, Moscow, pp. 36-45.

Belousov, A., and Belousova, M., 2001. Eruptive process, effects and deposits of the 1996 and ancient basaltic phreatomagmatic eruptions in Karymskoye lake, Kamchatka, Russia. *Special Publication of the International Association of Sedimentologists*, 30: 35-60.

Bergantz, G.W., and Breidenthal, R.E., 2001. Non-stationary entrainment and tunneling eruptions; a dynamic link between eruption processes and magma mixing. *Geophysical Research Letters*, 28: 3075-3078.

Bindeman, I.N., and Bailey, J.C., 1999. Trace elements in anorthite megacrysts from the Kurile island arc: a window to across-arc geochemical variations in magma compositions. *Earth and Planetary Science Letters*, 169: 209-226.

Blundy, J., and Wood, B., 1991. Crystal-chemical controls on the partitioning of Sr and Ba between plagioclase feldspar, silicate melts, and hydrothermal solutions. *Geochimica et Cosmochimica Acta*, 55: 193-209.

Blundy, J., and Cashman, K., 2001. Ascent-driven crystallization of dacite magmas at Mount St Helens, 1980-1986. *Contributions to Mineralogy and Petrology*, 140(6): 631-650.

Braitseva, O.A., 1998. Phreatomagmatic eruption in Lake Karymskoe (East Kamchatka) ~6500 ^{14}C years BP and Holocene episodes of basalt magma injection under the Karymsky area. *Volcanology and Seismology*, 19(5): 685-692.

Braitseva, O.A., and Melekestsev I.V., M., 1989. Karymsky Volcano: History of formation, dynamics of activity and long-term prediction. *Volcanology and Seismology*, 2: 14-31 (in Russian).

Braitseva, O.A., and Melekestsev, I.V., 1991. Eruptive history of Karymsky Volcano, Kamchatka, USSR, based on tephra stratigraphy and ^{14}C dating. *Bulletin of Volcanology*, 53(3): 195-206.

Coombs, M.L., Eichelberger, J.C., and Rutherford, M.J., 2000. Magma storage and mixing conditions for the 1953-1974 eruptions of Southwest Trident volcano, Katmai National Park, Alaska. *Contributions to Mineralogy and Petrology*, 140(1): 99-118.

Davidson, J., Tepley, F.III, Palacz, Z., and Meffan-Main, S., 2001. Magma recharge, contamination and residence times revealed by in situ laser ablation isotopic analysis of feldspar in volcanic rocks. *Earth and Planetary Science Letters*, 184: 427–442.

Devine, J.D., Gardner, J.E., Brack, H.P., Layne, G.D., and Rutherford, M.J., 1995. Comparison of microanalytical methods for estimating H_2O contents of silicic volcanic glasses. *American Mineralogist*, 80(3-4): 319-328.

Eichelberger, J.C., 1975. Origin of andesite and dacite: evidence of mixing at Glass Mountain in California and at other circum-pacific volcanoes. *Geological Society of America Bulletin*, 86: 1381-1391.

Eichelberger, J.C., 1978. Andesitic volcanism and crustal evolution. *Nature (London)*, 275(5675): 21-27.

Eichelberger, J.C., and Izbekov, P.E., 2000. Eruption of andesite triggered by dyke injection; contrasting cases at Karymsky Volcano, Kamchatka and Mt Katmai, Alaska. *Philosophical Transactions of the Royal Society of London: Mathematical, Physical and Engineering Sciences*, 358(1770): 1465-1485.

Fedotov, S.A., 1998. Study and mechanism of the simultaneous 1996 Karymsky volcano and Academy Nauk caldera eruptions in Kamchatka. *Volcanology and Seismology*, 19(5): 521-524.

Gardner, J.E., Rutherford, M., Carey, S., and Sigurdsson, H., 1995. Experimental constraints on pre-eruptive water contents and changing magma storage prior to

explosive eruptions of Mount St Helens Volcano. *Bulletin of Volcanology*, 57(1): 1-17.

Gardner, J.E., Hilton, M., and Carroll, M.R., 1999. Experimental constraints on degassing of magma; isothermal bubble growth during continuous decompression from high pressure. *Earth and Planetary Science Letters*, 168(1-2): 201-218.

Gardner, J.E., Layer P.W., and Rutherford, J.M., 2002. Phenocrysts versus xenocrysts in the youngest Toba Tuff: Implications for the petrogenesis of 2800 km^3 of magma. *Geology (Boulder)*, 30: 347-350.

Geschwind, C.-H., and Rutherford, M.J., 1992. Cummingtonite and the evolution of the Mount St. Helens (Washington) magma system: an experimental study. *Geology (Boulder)*, 20(11): 1011-1014.

Gorbatov, A., Kostoglodov, V., Suarez, G., and Gordeev, E., 1997. Seismicity and structure of the Kamchatka subduction zone. *Journal of Geophysical Research*, B, 102(8): 17,883-17,898.

Gordeev, E.I., Droznin, D.V., Kasahara, M., Levina, V.I., Leonov, V.L., Miyamachi, H., Okayama, M., Saltykov, V.A., Sinitsyn, V.I., and Chebrov, V.N., 1998. Seismic events associated with the 1996 volcanic eruptions in the Karymsky volcanic center. *Volcanology and Seismology*, 19(5): 713-735.

Grib, E.N., 1998. Petrology of ejecta from the Akademiya Nauk caldera eruption of January 2-3, 1996. *Volcanology and Seismology*, 19(5): 605-636.

Grove, T.L., Baker, M.B., and Kinzler, R.J., 1984. Coupled CaAl-NaSi diffusion in plagioclase feldspar: Experiments and applications to cooling rate speedometry. *Geochimica et Cosmochimica Acta*, 48: 2113–2121.

Hammer, J.E., and Rutherford, M.J., 2002. An experimental study of the kinetics of decompression-induced crystallization in silicic melt. *Journal of Geophysical Research*, 107(B1): ECV 8-1 – 8-24.

Huppert, H.E., and Sparks, R.S.J., 1988. The generation of granitic magmas by intrusion of basalt into continental crust. *Journal of Petrology*, 29(3): 599-624.

Ivanov, B.V., 1970. Eruption of Karymsky volcano during 1962-65 and the Karymsky volcanic group. Nauka, Moscow, 135 pp (in Russian).

Ivanov, B.V., 1996. Petrologic and geochemical peculiarities of the Karymsky volcano andesites: indicators of eruption types. *Volcanology and Seismology*, 17: 461-470.

Ivanov, B.V., Braitseva, O.A. and Zubin, M.I., 1991. Karymsky volcano. In: S.A. Fedotov and Y.P. Masurenkov (Editors), *Active volcanoes of Kamchatka*. Nauka, Moscow, pp. 181-203.

Izbekov, P.E., Eichelberger, J.C., Patino, L.C., Vogel, T.A., and Ivanov, B.V., 2002. Calcic cores of plagioclase phenocrysts in andesite from Karymsky volcano: Evidence for rapid introduction by basaltic replenishment. *Geology (Boulder)*, 30(9): 799–802.

Izbekov, P.E., Gardner, J.E., and Eichelberger, J.C., Comagmatic granophyre and dacite from Karymsky volcanic center, Kamchatka: experimental constraints for magma

storage conditions. Submitted to the Journal of Volcanology and Geothermal Research in October 2002.

Johannes, W., Koepke, J., and Behrens, H., 1994. Partial melting reactions of plagioclases and plagioclase-bearing systems. In: *Feldspars and their reactions*, Edinburgh, United Kingdom, pp. 161-194.

Johnson, J.B., Lees, J., M., and Gordeev, E.I., 1998. Degassing Explosions at Karymsky Volcano, Kamchatka. *Geophysical Research Letters*, 25(21): 3999-4002.

Johnson, M.C., and Rutherford, M.J., 1989. Experimentally determined conditions in the Fish Canyon Tuff, Colorado, magma chamber. *Journal of Petrology*, 30(3): 711-737.

Kadik, A.A., Rozenkhauer, M., and Lukanin, O.A., 1989. Experimental study of effect of pressure on crystallization of high-Mg and high-Al basalts of Kamchatka. *Russian Geochemistry*, 1989(12): 1748-1762 (in Russian).

Koyaguchi, T., and Kaneko, K., 2000. Thermal evolution of silicic magma chambers after basalt replenishments. *Transactions of the Royal Society of Edinburgh*: Earth Sciences, 91: 47-60.

Leonov, V.L., 1998. Ground surface breaks produced by an earthquake and volcanic eruptions in the Karymsky volcanic center on January 1–2, 1996. *Volcanology and Seismology*, 19(5): 655–674.

Lipman, P.W., 1967. Mineral and chemical variations within an ash-flow sheet from Aso Caldera, southwestern Japan. *Contributions to Mineralogy and Petrology*, 16: 300-327.

Lipman, P.W., Dungan, M.A., and Bachmann, O., 1997. Comagmatic granophyric granite in the Fish Canyon Tuff, Colorado: implications for magma-chamber processes during a large ash-flow eruption. *Geology (Boulder)*, 25(10): 915-918.

Lowenstern, J.B., Clynne, M.A., and Bullen, T.D., 1997. Comagmatic A-type granophyre and rhyolite from the Alid volcanic center, Eritrea, Northeast Africa. *Journal of Petrology*, 38(12): 1707-1721.

Maguskin, M.A., Fedotov, S.A., Levin, V.E., and Bakhtiarov, B.F., 1998. Ground surface deformation caused by seismic and volcanic activity in the Karymsky Volcanic Center during January 1996. *Volcanology and Seismology*, 19(5): 637-654.

Mastin, L.G., and Ghiorso, M.S., 2000. A numerical program for steady-state flow of magma-gas mixtures through vertical eruptive conduits. Open-File Report - U. S. Geological Survey, 0196-1497, 53 pp.

Masurenkov, Y.P., 1980. Volcanic centers: formation, dynamics, properties (Karymsky Structure). Nauka, Moscow, 300 pp (in Russian).

Miller, T.P., Chertkoff, D.G., Eichelberger, J.C., and Coombs, M.L., 1999. Mount Dutton Volcano, Alaska; Aleutian Arc analog to Unzen Volcano, Japan. *Journal of Volcanology and Geothermal Research*, 89(1-4): 275-301.

Muravyev, Y.D., Fedotov, S.A., Budnikov, V.A., Ozerov, A.Y., Maguskin, M.A., Dvigalo, V.N., Andreyev, V.I., Ivanov, V.V., Kartasheva, L.A., and Markov, I.A., 1998. Volcanic activity in the Karymsky center in 1996: Summit eruption at Karymsky and phreatomagmatic eruption in the Akademii Nauk Caldera. *Volcanology and Seismology*, v. 19(5): 567–604.

Murphy, M.D., Sparks, R.S.J., Barclay, J., Carroll, M.R., and Brewer, T.S., 2000. Remobilization of Andesite Magma by Intrusion of Mafic Magma at the Soufriere Hills Volcano, Montserrat, West Indies. *Journal of Petrology*, 41(1): 21-42.

Nakamura, M., 1995. Continuous mixing of crystal mush and replenished magma in the ongoing Unzen eruption. *Geology (Boulder)*, 23(9): 807-810.

Nelson, S.T., and Montana, A., 1992. Sieve-textured plagioclase in volcanic rocks produced by rapid decompression. *American Mineralogist*, 77(11-12): 1242-1249.

Norman, M.D., Pearson, N.J., Sharma, A., and Griffin, W.L., 1996. Quantitative analysis of trace elements in geological materials by laser ablation ICPMS: Instrumental operating conditions and calibration values of NIST glasses. *Geostandards Newsletter*, 20(2): 247-261.

Nye, C.J., Swanson, S.E., Avery, V.F., and Miller, T.P., 1994. Geochemistry of the 1989-1990 eruption of Redoubt Volcano; Part I, Whole-rock major- and trace-element chemistry. *Journal of Volcanology and Geothermal Research*, 62(1-4): 429-452.

Pallister, J.S., Hoblitt, R.P., Meeker, G.P., Knight, R.J., and Siems, D.F., 1996. Magma mixing at Mount Pinatubo: petrographic and chemical evidence from the 1991 deposits. In Newhall, C.G., and Punongbayan, R.S. (Editors), *Fire and mud: eruptions and lahars of Mount Pinatubo, Philippines*. Seattle, WA, University of Washington Press, pp. 687-731.

Rutherford, M.J., Sigurdsson, H., Carey, S., and Davis, A., 1985. The May 18, 1980, eruption of Mount St. Helens: 1. Melt composition and experimental phase equilibria. *Journal of Geophysical Research*. B, 90(4): 2929-2947.

Scott, V.D., Love, G., and Reed, S.J.B. 1995. Quantitative Electron-Probe Analysis. Ellis Horwood Limited, Hemel Hempstead, Hertfordshire, England, 311 pp.

Shirokov, V.A., Ivanov, V.V., and Stepanov, V.V., 1988. Deep structure of the Karymsky Volcano and characteristics of its seismicity based on data from a local network. *Volcanology and Seismology*, 1988(3): 71-80 (in Russian).

Snyder, D., and Tait, S., 1996. Magma mixing by convective entrainment. *Nature* (London), 379(6565): 529-531.

Singer, B.S., Dungan, M.A., and Layne, G.D., 1995. Textures and Sr, Ba, Mg, Fe, K and Ti compositional profiles in volcanic plagioclase: Clues to the dynamics of calc-alkaline magma chambers. *American Mineralogist*, 80: 776-798.

Sparks, R.S.J., and Marshall, L.A., 1986. Thermal and mechanical constraints on mixing between mafic and silicic magmas. *Journal of Volcanology and Geothermal Research*, 29(1-4): 99-124.

Sparks, R.S.J., Huppert, H.E., Wilson, C.J.N., Halliday, A.N., and Mahood, G.A., 1990. Evidence for long residence times of rhyolitic magma in the Long Valley magmatic system; the isotopic record in precaldera lavas of Glass Mountain; discussion and replies. *Earth and Planetary Science Letters*, 99(4): 387-399.

Stormer, J.C., Jr., 1983. The effects of recalculation on estimates of temperature and oxygen fugacity from analyses of multicomponent iron-titanium oxides. *American Mineralogist*, 68(5-6): 586-594.

Streck, M.J., Dungan, M.A., Malavassi, E., Reagan, M.K., and Bussy, F., 2002. The role of basalt replenishment in the generation of basaltic andesites of the ongoing

activity at Arenal volcano, Costa Rica: evidence from clinopyroxene and spinel. *Bulletin of Volcanology*, 64: 316-327.

Sugrobov, V.M., and Yanovsky, F.A., 1991. Geothermal field of Kamchatka, heatlosses by volcanoes and hydrotherms. In: S.A. Fedotov and Y.P. Masurenkov (Editors), *Active volcanoes of Kamchatka*. Nauka, Moscow, pp. 58-71.

Sutton, A.N., Blake, S., and Wilson, C.J.N., 1995. An outline geochemistry of rhyolite eruptives from Taupo volcanic centre, New Zealand. *Journal of Volcanology and Geothermal Research*, 68(1-3): 153-175.

Tokarev, P.I., 1989. Eruption and seismicity of Karymsky volcano in 1965-1986. *Volcanology and Seismology*, 2: 3-13 (in Russian).

Ushakov, S.V., and Fazlullin, S.M., 1998. Morphometric characteristics of Lake Karymskoye after an underwater eruption. *Volcanology and Seismology*, 19(5): 675-684.

Vance, J.A., 1965. Zoning in igneous plagioclase: patchy zoning. *Journal of Geology*, 73(4): 636-651.

Volynets, O.N., Ponomareva, V.V., Braitseva, O.A., Melekestsev, I.V., and Chen, C.H., 1999. Holocene eruptive history of Ksudach volcanic massif, South Kamchatka; evolution of a large magmatic chamber. *Journal of Volcanology and Geothermal Research*, 91(1): 23-42.

Wohletz, K., Civetta, L., and Orsi, G., 1999. Thermal evolution of the Phlegraean magmatic system. *Journal of Volcanology and Geothermal Research*, 91(2-4): 381-414.

Zobin, V.M., and Levina, V.I., 1998. Rupture history of the January 1, 1996, Ms 6.6 volcanic earthquake preceding the simultaneous eruption of Karymsky and Akademia Nauk volcanoes in Kamchatka, Russia. *Journal of Geophysical Research*, B. 103(8): 18,315-18,324.